Valorization of deinking sludges from wastepaper recycling: Biogas production and calcium carbonate recovery

Vom Promotionsausschuss der

Technischen Universität Hamburg

zur Erlangung des akademischen Grades

Doktor-Ingenieur (Dr.-Ing.)

genehmigte Dissertation

von

Moses Kolade Ogun

aus

Lagos, Nigeria

2024

Gutachter:

- PD Dr.-Ing. habil. Ina Körner
- Prof. Dr.-Ing. Frank Schmidt-Döhl

Tag der mündlichen Prüfung:

- 26. April 2023

ORCID iD: 0009-0007-0459-6058

DOI: https://doi.org/10.15480/882.9454

Handle: https://hdl.handle.net/11420/46877

ACKNOWLEDGEMENTS

The author is deeply grateful to PD Dr.-Ing. habil. Ina Körner, his primary reviewer, for her invaluable assistance, guidance and unwavering encouragement throughout the entire research period. The funding provided by her significantly contributed to the success of this dissertation.

Thanks is also extendend to Prof. Dr.-Ing. Frank Schmidt-Döhl, the head of the Institute of Materials, Physics, Chemistry of Buildings at the Hamburg University of Technology, for his commendable support as a co-reviewer and for facilitating various chemical analyses on the ash samples used in the research.

This study received financial support from the "Zentrales Innovationprogramm Mittelstand" (ZIM), Germany and a doctoral scholarship from the Rosaluxemburg Foundation, Germany. The generous support from these entities is sincerely acknowledged. Special appreciation is extended to the wastepaper recycling company in Germany, which provided the deinking sludge samples used for the experiments in this study.

The majority of the research was conducted in the laboratories of the Institute of Water and Wastewater at the Hamburg University of Technology (AWW) and the author extends heartfelt thanks to Prof. Dr.-Ing. Ralf Otterpohl, the head of the institute, for this privilege.

The author would like to thank colleagues who assisted with the construction of the automatically fed bioreactors used for the experiments in this study: Frank Sokolinski and Dirk Manning from the research workshop at the Hamburg University of Technology and Stefan Deegener from AWW.

Acknowledgment is extended to the author's colleagues at AWW, both staff members and graduate students, for their diverse support. Special thanks go to Susanne Eggers and Binnur Kuscu for their assistance with laboratory analyses. Importantly, the author recognizes the contribution of the following students: Dagnachew Amare, Ahmed Abass, Ke Wang, Shruthi Meenakshisundaram, Didier Nguetsop, Kostiantyn Hnennyi, Bastian Büning, Ge Wang, Folarin Sadiku, Xiaobai Xue, Yehia Abdo, Jan Willruth and Naga Sai Tejaswi Uppuluri, who worked as assistants, bachelor, project or master's thesis students. Their trust in the research hypothesis and dedicated conduct of experiments and analyses greatly contributed to the success of this work.

Above all, the author wishes to express gratitude to God Almighty, his wife Adeola and his children, whose unwavering encouragement and support were pivotal throughout this journey.

ABSTRACT

Deinking sludges are residues generated from deinking operation during wastepaper recycling. The common treatment option in Europe includes dewatering steps followed by incineration. Incineration of deinking sludge is capital intensive and not sustainable hence it was investigated if it can be valorized energetically by anaerobic digestion and materially by calcium carbonate recovery. Investigations were carried out by characterisation of substrates and execution of experiments.

The dry matter of deinking sludges depends on the dewatering stage in treatment plant and is in the range of 2 to 40% fresh mass. The pre-dewatered deinking sludge has a dry matter content of 5 - 16% fresh mass. The organic dry matter of deinking sludges is in the range of 29 to 33% DM. Calcium carbonate and ash contents have the highest fraction of dry matter in deinking sludges and are 47 - 52% DM and 67 - 71% DM respectively. Deinking sludges showed good digestibility with common inocula and their biogas yield was observed to be about half of that of cellulose under similar anaerobic conditions. Pre-dewatered deinking sludge from the mixture of high and medium wastepaper grades showed the highest specific biogas yield (417 ± 0 NL/kg·oDM) followed by those with a mixture of medium wastepaper grades (275 ± 14 NL /kg·oDM) and lastly those from ordinary wastepaper grades (250 ± 21 NL /kg·oDM). A carbon to nitrogen ratio in the range of 29 and 34 is recommended to improve the efficiency of a semi-continuously operated anaerobic digestion of deinking sludge.

Within the scope of this study, a hydraulic retention time of 19 days which corresponds to an organic loading rate of 1.6 ± 0.42 kg oDM/m^3·d was observed as optimal for anaerobic digestion of deinking sludge using a semi-continuous system. Deinking sludge settles quickly in bioreactors, hence an efficient mixing mechanism during semi-continuous process is recommended. The two-step first order kinetics showed the best fitting for the anaerobic digestion of raw and pre-dewatered deinking sludges from ordinary wastepaper grades. The modified Gompertz model showed the best fit for pre-dewatered deinking sludges from high and medium wastepaper grades. The ashes of deinking sludges and its digestates are rich in calcium carbonate and contain some elements found in portland cement but in different proportion. The ashes contribute to flexural and compressive strength which make them suitable as supplementary building materials. Results obtained from the study show that biogas production from deinking sludges combined with calcium carbonate recovery is a sustainable approach.

Key words: wastepaper, recycling, deinking sludge, biogas, digestate, calcium carbonate

TABLE OF CONTENTS

LIST OF FIGURES

LIST OF TABLES

LIST OF APPENDICES

ABBREVIATIONS

AD	Anaerobic digestion
ADM1	Anaerobic digestion model 1
AIK	Akaike information criterion
BC	Before Christ
BIC	Bayesian information criterion
BL	Biosludge fraction of filtrate from main dewatering
BOD	Biological oxygen demand
BS	Biosludge
C	Carbon
C/N	Carbon to nitrogen ratio
C_3S	Tricalcium silicate
CEM	Calcium-enriched mixture
CEN	European committee for standardization
CEPI	Confederation of european paper industries
CO_2	Carbon dioxide
COD	Chemical oxygen demand
C-S-H	Calcium silicate hydrate
CSTR	Continuous stirred tank reactor
d	Day
D10	The particle size at which 10% of the particles are finer
D50	The particle size at which 50% of the particles are finer
D90	The particle size at which 90% of the particles are finer
DL	Turbid water from pre-dewatering and clear water from microfiltration
DM	Dry matter content
DS	Deinking sludge
DS-digestate	The effluent of bioreactor after anaerobic digestion of deinking sludge
e	Euler's number 2.7183
EC	European Commission
EDTA/ DTPA	Ethylenediaminetetraacetic acid / Diethylenetriamine pentaacetate
EGSB	Expanded granular sludge blanket
FM	Fresh matter content

FTIR	Fourier transform infra-red spectroscopy
G	Gramme
GCC	Ground calcium carbonate
GJ	Giga joule
GUI	Graphical user interface
GW	Gigawatt
H	Hour
H_2	Hydrogen
HRT	Hydraulic retention time
IC	Internal circulation
IWA	International Water Association
K	Kelvin
k	Hydrolysis rate constant (1/day)
k_1	Hydrolysis rate constant of readily biodegradable organics (1/day)
k_2	Hydrolysis rate constant of less readily biodegradable organics (1/day)
kg	Kilogram
Kwh	kilowatt-hour
L	Litre
λ	Lag phase time (days)
Mg	Megagramme
Micrometre	Micrometre
MJ	Mega joule
mL	Millilitre
Model 1	One step first order kinetics
Model 2	Two steps first order kinetics
Model 3	Modified Gompertz
Model 4	Transfer function
Model 5	Logistic function
MS	Mixed sludge
N	Nitrogen
NA	Not available
ND	Not determined
NL	Normalized Litre

°C	degree Celsius
oDM	Organic dry matter
OLR	Organic loading rate
OCC	Old corrugated cardboard
PCC	Precipitated calcium carbonate
PfR	Paper for recycling or recovered wastepaper
ppm	Parts per million
R1A	100- L bioreactor with recirculation pump
R1B	100-L bioreactor with recirculation pump and highly inclined bottom
R2	100-L bioreactor with stirrer
R^2	Coefficient of determination
RCF	Recycled cellulose fibre
Rm	Maximum biogas production NL/(kg oDM day)
RMP	Residential mixed paper
RMSE	Root mean squared error
S	Sulphur
SC	Super calendared
SCC	Synthetic calcium carbonate
SEM	Scanning electron microscope
SO_4	Sulphate
SRB	Sulphate reducing bacteria
STP	Steinbeis paper company
TE	Trace elements
TOC	Total organic carbon
TC	Total carbon
TN	Total nitrogen
UASB	Upflow anaerobic sludge blanket
UN	United nations
VOA/TIC	Ratio of volatile acid to total alkalinity
w/c	Water to cement ratio
W70	Code for DS generated from ordinary wastepaper grades
W80	Code for DS generated from medium wastepaper grades
W90/100	Code for DS generated from a mixture of medium and high wastepaper grades

WC	Water content
WWTP	Wastewater treatment plant
XRD	X-ray diffraction
Y_1	Fraction of biogas by readily biodegradable organics
Y_2	Fraction of biogas not-readily biodegradable organics
Y_m	Maximum biogas yield NL/(kg oDM)
Y_t	Biogas yield at a particular time NL/(kg oDM)

CHAPTER 1 INTRODUCTION

The global pulp and paper industry reported an approximately 11% increase in the consumption of paper and board between the years 2009 and 2019 (CEPI, 2011, 2021b). This implies an average yearly growth of about 1% in this period. Despite the recent advancement in digitalization which promotes paperless means e.g. for e-learning and e-commerce (Chaffey, 2021; McCue, 2018) the industry continues to thrive in the production and sales of products for printing, writing, hygiene, decoration, packaging, and other paper and board applications. The industry is however affected by increasing economic and ecological constraints due to global competition and increasingly strict environmental legislation. It uses fibres and some non-fibre materials as input sources for production. In comparison with other industries, it is characterized by high consumption of water and energy (Jung & Pauly, 2011; Mongkhonsiri et al., 2018; Pokhrel & Viraraghavan, 2004). One of the progress of the industry in Europe in the contribution to sustainability is the promotion of recycled papers production which involves the use of recovered wastepapers as the main input source (CEPI, 2021b).

Wastepapers in paper production in recent years have become an imperative raw material in many countries countries (Bajpai, 2014b). This is consistent with United Nations (UN) sustainable development goal 12 (*responsible consumption and production)* (UN, 2019). The ecological and economic importance of the use of wastepaper for paper production can be illustrated with the following example: With 500 sheets of recycled A4 office paper, about 7.5 kg of wood, 19.3 kWh of energy, 108 L of water, and 1.6 kg of CO_2 is saved compared to paper produced from virgin fibre (STP, 2021). However, wastepaper recycling generates large amounts of residues, among which deinking sludges (DS) are quantitative of most concern. DS is generated in wastepaper recycling during a process aimed at removing the printing inks. According to Blanco et al. (2008) and Monte et al. (2009), 70% of the residues of the European pulp and paper industry are generated from the production of deinked recycled paper of which DS is an important fraction. In 2013 Germany produced 0.96 million Mg of DS (Jung et al., 2014).

A fresh DS discharged from a flotation cell during wastepaper recycling is a marshy-like liquid containing mainly water, but also considerable amounts of organic fines, fibres, and various inorganic compounds, with $CaCO_3$ having the highest share. Due to its organic dry matter content, the disposal of DS is prohibited in Germany and is gradually being reduced in other European countries under the Directive 2008/98 / EC. In Germany, a large fraction of DS is incinerated after dewatering (Jung et al., 2014). For the incineration of DS, considerable amounts of additional fuels are used due to its low calorific value caused by its high inorganic fraction.

In addition, the ashes are disposed of in landfills, where the inorganic portion of the DS also remains. The current disposal of DS is therefore very capital intensive and valuable inorganic components are also lost. Considering the challenges a more sustainable management approach is therefore required.

This dissertation, therefore, aims to answer the question as to whether the DS generated from wastepaper recycling can be valorized such that the capital intensive treatment option of incineration is avoided. It further intends to find out how the valorization options to be investigated can be appropriately applied in existing wastepaper treatment facilities for efficient use of the resource. The aspects of valorization investigated are energetic valorization by anaerobic digestion and material valorization by calcium carbonate recovery. The energetic valorization involves the anaerobic digestion of the organic content in DS which leads to the production of a renewable energy resource in the form of biogas. The biogas production fits into the UN sustainability goal 7 (*Affordable and Clean energy*) (UN, 2019), while the calcium carbonate recovery further advances the UN sustainability goal 12 (*responsible consumption and production)* of the industry.

This dissertation adopts an experimental approach to answer the research questions. The approach entails the determination of relevant physico-chemical properties of different substrates and careful design and execution of experiments following standard guidelines to investigate targeted properties that are the key to answer the research questions. The main experiments relevant to energetic valorization include the biodegradation of DS with common inocula, the biogas yields of different types of DS, the influence of dewatering degrees and water content on biogas production of DS, the influence of DS‘s high calcium carbonate on its biogas production, supplementation of nitrogen for nitrogen-limited conditions during AD of DS and the dewaterability of DS and DS’s digestate. The analysis and experiments relevant for material valorization include determination of particle size distribution, the chemical composition and mineralogy of ash from DS and DS’s digestate and the influence of ash from DS and DS’s digestate on flow value of mortar, density, flexural strength and compressive strength.

CHAPTER 2 PAPER AND WASTEPAPERS

This section discusses the development of paper consumption. It gives an overview of the paper value chain with a focus on wastepaper recycling which leads to the generation of deinking sludges. The chemicals, energy and calcium carbonate consumption of wastepaper recycling was also discussed.

2.1 Development of paper and paper consumption

Paper is a material used for multiple purposes such as writing, decoration, sanitary purposes and packaging. The word paper was derived from the Greek word Pápyros. Papyrus can be described as a specie of aquatic flowering plant that grows in a sunny climate, especially in swampy regions on lake areas all around Africa, Madagascar and the Mediterranean counties (Archer, 2004). Papyrus writing material is produced by pressing and drying plants (Mark, 2016), while paper is produced from fibres.

Papyrus plants were used in ancient Egypt and other Mediterranean societies for writing long before paper was discovered. The first paper making process is ascribed to China and the first organized paper production started there in 150 BC, where production of paper was done using raw materials such as macerated hemp fibres, old fishnets, plant bark and water (History of Paper, 2021). In the early times, the two main factors governing the location of a paper mill were the presence of raw materials and proximity to power and energy. Rags and used cloths were the major raw materials for paper production before the development of a process to free fibres out of wood with a grinding wheel (Bloom, 2017).

The discovery of the paper making process by the Chinese Cai Lun in 105 AD contributed to the success of early China due to ease in information documentation. This knowledge spread from China to Japan around 610 AD (History of Paper, 2021). In 751 AD, the Arabian acquired this knowledge from the Chinese people and further extended this knowledge to Egypt and North Africa. In the 11th century, the knowledge got to Europe due to the Arab invasion of Sicily and Spain (Cantavalle, 2019). The first paper mill in Germany was discovered in Nuremberg in 1389 (Salmons, 2012). In the quest for better raw material to substitute straw for papermaking, the wood-grinding machine which produced ground wood pulp suitable for paper making was invented by the German scientist Friedrich Gottlob in 1843 (CEPI, 2021a).

Today paper has become a very important commodity with huge global production, application and consumption (CEPI, 2021b). The early advancement in the printing press is one of the notable factors that influenced the spread of paper utilization globally.

The printing press is used for the mass production of uniform printed material, majorly text in the form of pamphlets, magazines, newspapers and books. The newspaper was first printed in Peking, China in 748 AD (History of Paper, 2021). The progress in printing technology resulted to the invention of the moveable type by Bi Scheng in 990-1051 AD. The printing press played and important role on civilization and advanced in Europe during the 15th century through the discovery of the Gutenberg press in 1439 (History, 2019). The printing industry enabled knowledge and idea sharing in an unusual scale using papers. It significantly contributed to the development of the Renaissance and the scientific revolution, creating the groundwork for the present knowledge-based economy (Bgiraudi, 2016).

Currently, paper and board are massively produced and consumed globally. With a global paper and board consumption of 413 million Mg in 2019, the global paper and board industry marked an increase of about 11% when compared to the statistics of 2009. A different trend is observed by the Confederation of European Paper Industries (CEPI) where a gradual decrease in the aforementioned time frame occurred. This is probably due to the significant impact of digitalization that occurred in Europe during this period. It is however pertinent to mention that digitalization influences majorly the printing and writing applications of papers and not the packaging, decorating and sanitary uses. Figure 2.1 shows the paper and board consumption globally from 2009 to 2020 as well as by the CEPI countries from 2009 to 2020.

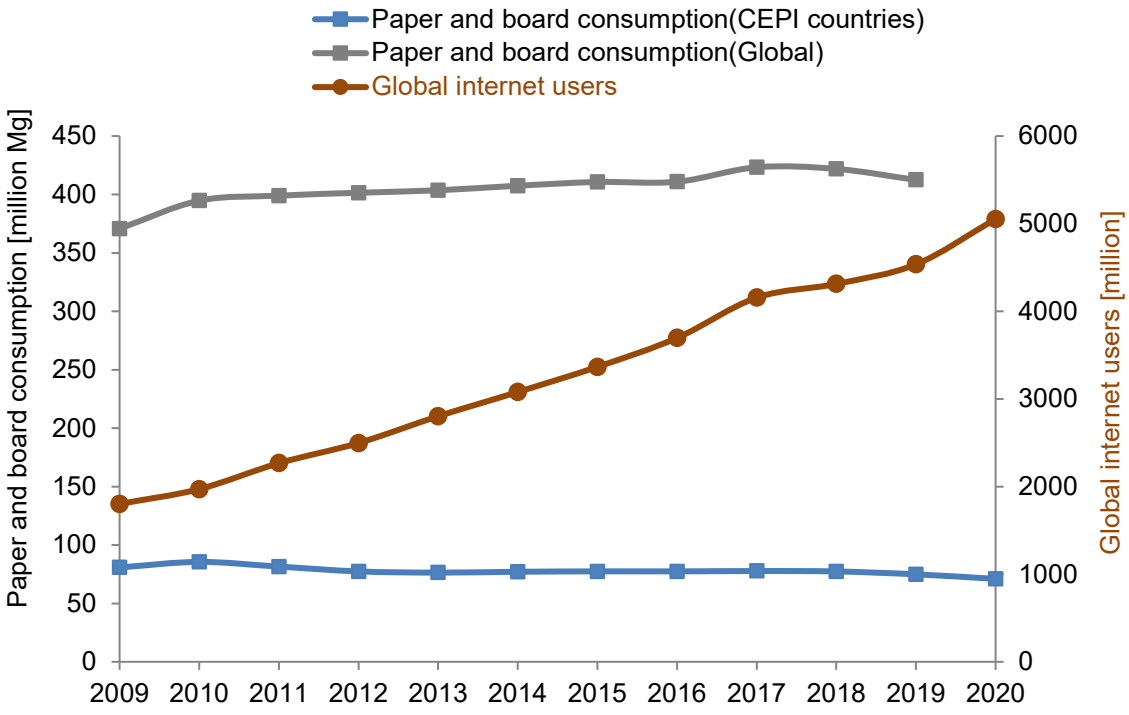

Figure 2.1 Paper and board consumption and global internet users (2009-2020) (drawn from CEPI (2021b) and IWS (2021))

It also gives information on the number of global internet users from 2009 to 2020. A high rate of continuous increase in the global internet user and a gradual decrease in the consumption of paper and board by CEPI countries is observable. This informs that paper and board production industry in Europe is faced with the challenge of a lower consumption with digitalization as one of the influencing factors. However, it is reported that the lower consumption applies more to graphic paper which is counter-balanced by the growth in packaging and hygiene papers (EC, 2021). The rate of increase in global paper and board consumption is also not that substantial, possibly due to the effect caused by continuous increasing global internet users. The efforts of the paper and board industries of the CEPI countries toward a circular economy are worth mentioning. In 2020, the rate of recycling of wastepapers has reached 74% in these countries (CEPI, 2021b). Figure 2.2 shows the trend of increase in recycling rate as well as consumption of fibrous (pulp) and non-fibrous materials by CEPI from 1991 to 2020.

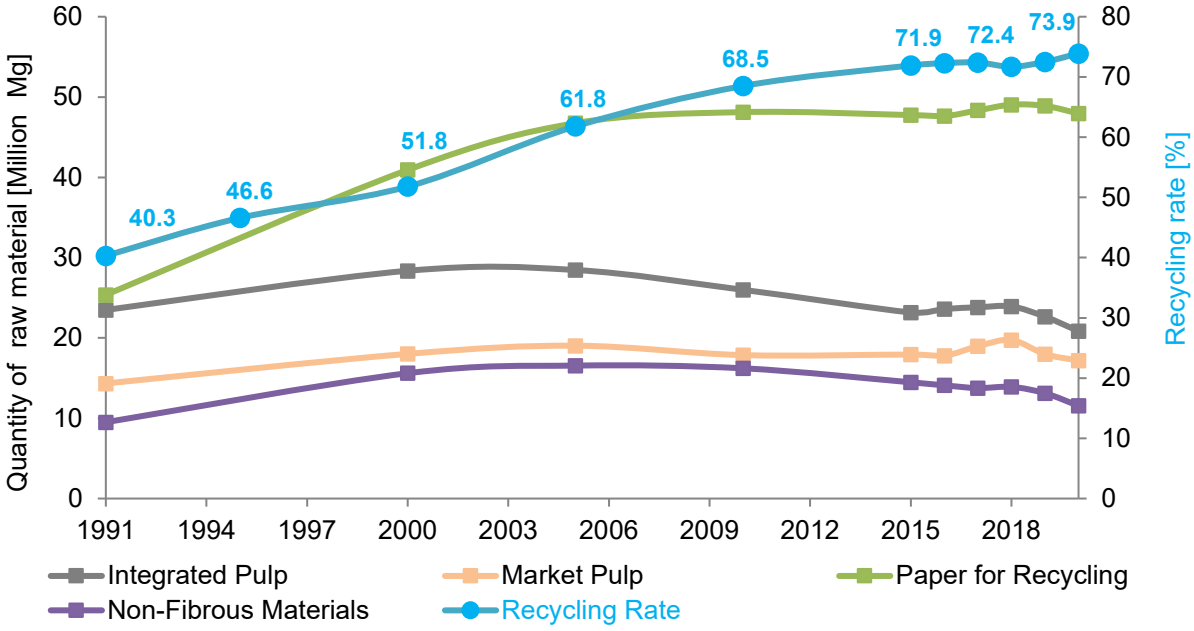

Figure 2.2 Quantities of raw materials consumed in the CEPI countries for paper and board production and wastepaper recycling rates from 1991 to 2020 (CEPI, 2021b)

Despite the very high recycling rate, the industry is still confronted with several challenges. They are lower consumption, trade barriers, raw material supply, recycling, energy prices and the EU environmental policies (EC, 2021).

On the aspect of recycling, they highlighted the fact that the 73.9% recycling rate reached is very close to the maximum possible recycling rate. The maximum possible wastepaper recycling rate as reported by CEPI is 78% (CEPI, 2017). Therefore other innovative concepts for improvement are expected. The report by European Commission (EC, 2021), listed separate collection systems, innovation in sorting as well as recycling technology as approaches to increase the quality and the availability of secondary raw materials. Essentially they identified two main opportunities for improvement which are resource efficiency and bioeconomy. In the aspect of resource efficiency, technologies that allow for optimal usage of raw material, water and energy are recommended. This also includes the efforts to reduce CO_2 emissions by up to 80% by the year 2050. In the aspect of bioeconomy, the production of novel materials from wood and wood fibres is recommended. The wastepaper recycling sector of the industry has huge potential. The valorization of the residues produced by the sector which allows for cascading use of resources can contribute further toward a circular economy and sustainability.

2.2 The paper value chain and residues

A paper value chain can be described as a set of activities that firms connected to the pulp and paper industry carry out to create and deliver valuable products. Figure 2.3 is a simplified paper value chain that considers the processes utilizing wood and wood related bioresources as input materials for production. The different outputs of the chain are categorized into high and low valued outputs. The goal of the chain is paper production. All downstream such as converting, printing and publishing and other utilizations are included in consumption. The chain includes processes starting from forestry up to wastepaper recycling. Figure 2.3 groups the bioresources in the paper value chain into primary, secondary, tertiary and quaternary categories according to their properties for valorization. A cascade utilization can be identified as wastepaper enters back into the main paper value chain again due to wastepaper recycling (Körner, 2015).

The paper chain produces some residues and other outputs which are of environmental concern (Monte et al., 2009; Suhr et al., 2015; Wang et al.,2016). This chapter discusses the bioresources of the different stages in the value chain and also lists the residues produced during the wastepaper recycling process.

Figure 2.3 A schematic diagram showing the transformation of different bioresources from forest to wastepaper (modified from Körner 2015

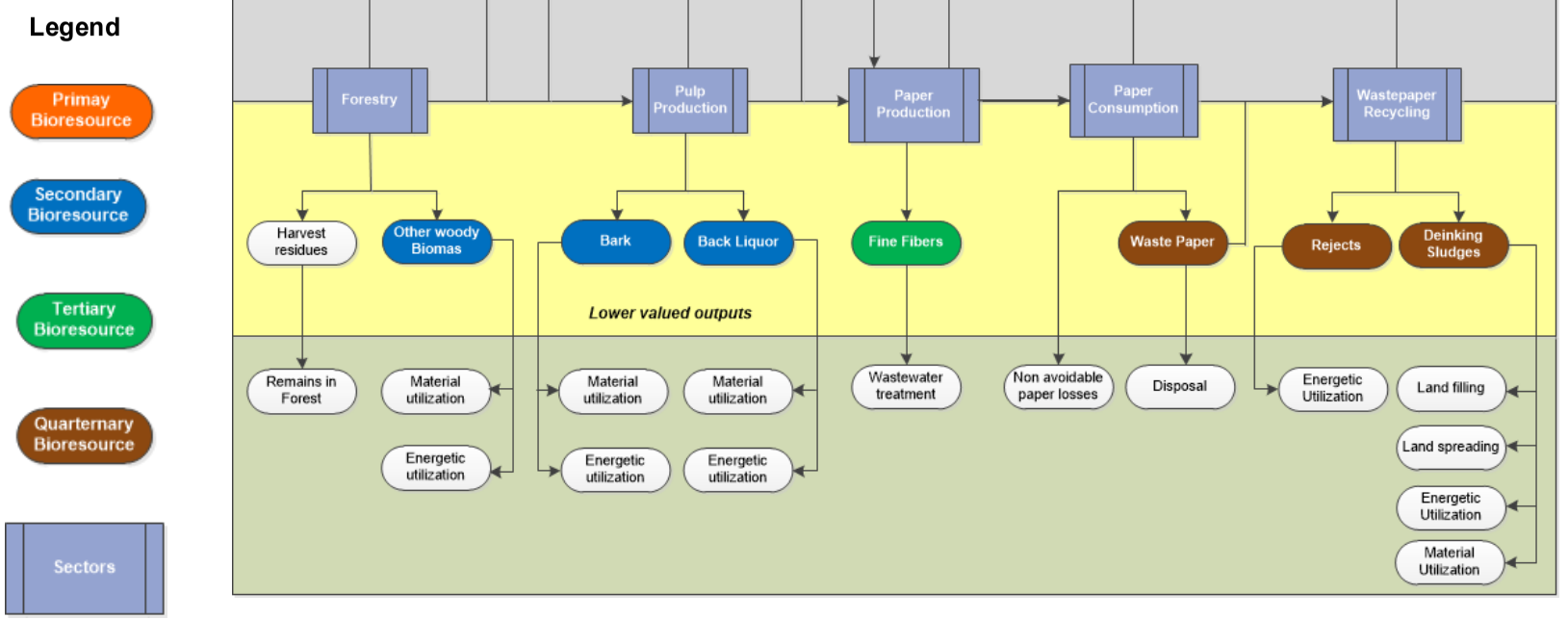

1.) Forestry

A forest is a complex ecological system where trees are the prevailing form of life (Schuck et al., 2002). Forestry is the industry that deals with forests and their resources such as wood. Wood is used for many purposes such as the building of houses, tools and furniture. It is also a raw material for pulp production and is categorized as a primary bioresource. The *by-products from a sawmill* and *other woody biomass* (output from forestry) due to their lower relevance and quantifiable benefits are classified as secondary bioresources. The *other woody biomass* such as twigs and branches can be utilized either as material such as soil amendments (Xie et al.), landscape material (Pilarski, 2020) or for energetic purposes (Tabata, 2018). Harvest residues remain in the forest.

2.) Pulp production

Different methods are used for making pulps and they are broadly classified into two main methods, the chemical and the mechanical methods (Cheremisinoff & Rosenfeld, 2010). These processes generally take in raw materials such as stem woods from forestry and by-products from sawmills. The *by-products from sawmills* are wood chips and shavings (Tabata, 2018). The main output is the pulp which is either marketed or used in its paper mill. Among the residues generated by a pulping process, the bark recovered before pulping and the black liquor are categorized as secondary bioresources which are of value either by material or energetic utilization. The barks have e.g. active ingredients such as antibiotics which make them relevant in medicine to cure diseases and they can also be formed into pellets for energy utilization (Pásztory et al., 2016). The black liquor which is a by-product of kraft pulping (chemical pulping) is majorly used for energetic purposes (Bajpai, 2014a). It can be used to make soil conditioners (González et al., 1992) as well as for wood preservatives (Durmaz et al., 2015).

3.) Paper production

Paper production utilizes either virgin pulp, recycled pulp, or a mixture of both for paper production. Aside from pulp, non-fibrous input materials such as calcium carbonate and starch may be used (CEPI, 2021b). The main outputs are paper products of different qualities used for different applications. Among the residues of paper production is the fibres fines which often flow into the wastewater treatment pathway.

4.) Paper consumption

Paper consumption involves paper utilization as an information transfer medium in printing, publishing, books and other uses such as packaging and hygienic purposes. The main output of paper consumption is often referred to as wastepaper. When they are collected they serve as the input source for wastepaper recycling and are termed recovered papers.

5.) Wastepaper recycling

The recovered papers are utilized in wastepaper recycling for paper production. The rejects and deinking sludges are important outputs of the deinking plant used for wastepaper recycling. The rejects which contain lumps of fibres, staples, sand, glass, plastic, and stickies are often used for an energetic purpose. The common treatment for deinking sludges according to Blanco et al. (2008) are landfilling, land spreading and incineration. In Germany, some fraction is used for building material purposes (Jung et al. 2014). The wastepaper recycling process is discussed in detail in section 2.3.

2.3 Wastepaper recycling process

This section describes the wastepaper recycling process and identifies an important challenge faced. It also describes the processes involved in wastepaper recycling and the generation of deinking sludge. It further discusses the consumptions such as chemical energy and calcium carbonate in wastepaper recycling.

2.3.1 Inputs and outputs of the wastepaper recycling process

Wastepaper recycling receives different streams of inputs and as well discharges different output streams. Figure 2.4 shows the main input raw materials which are recovered paper, calcium carbonate recovery and starch. Aside from these, energy, water, and chemical additives are used to achieve deinking. The main output is the paper product. The non-product outputs are noise and vibration, energy, wastewater, air emission and solid waste.

The solid wastes have different flow streams as shown in Figure 2.4. The ashes come from the possible installed steam power plant. The rejects and sludges are important fractions. The rejects are classified into coarse and fine sub-groups. They comprise impurities of different particle sizes from the wastepaper recycling process (section 2.3.2) which include a lump of fibres, staples, sand, glass, plastic, and stickies. The sludges can be broadly classified into deinking sludge, primary sludge, and secondary sludge. The DS is the direct output of the deinking operation (section 2.3.2). The derivatives of DS which are generated either by microfiltration or sedimentation are classified as primary sludges. They include sludge from process water clarification. The secondary sludge is a sludge generated from a biological wastewater treatment plant which is often installed in wastepaper recycling facilities. The biosludge is a typical example in this category.

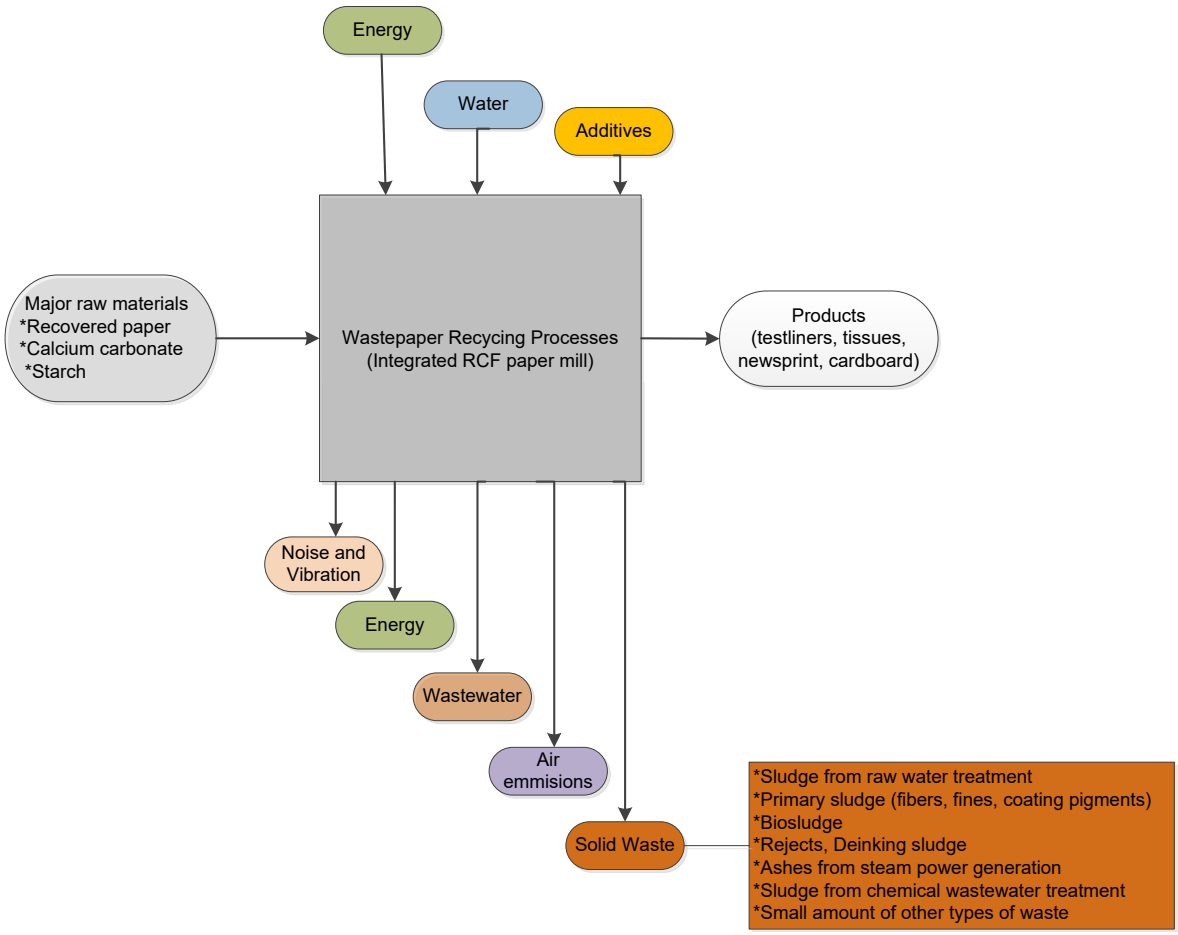

Figure 2.4 Input and output materials and emissions of a wastepaper recycling process (Suhr et al. 2015)

DS belong to the group of solid waste which are discharged from the wastepaper recycling process. The more the recovered paper, the more the recycled paper produced as well as the amount of generated DS (Berger et al., 2021; Suhr et al., 2015). The share of recovered paper as raw material consumed for paper and board production in CEPI countries in 2020 was stated as 49.2%. This implies an increase of 41% when compared to the 34.9% share in the year 1991. Also, the wastepaper recycling rate (section 2.3.2.1.(1)) as of 2020 in CEPI countries was stated as 73.9% (CEPI, 2021b).

Even with the high recycling rate, there is still a large potential for improvement of wastepaper recycling in the aspect of energy and material efficiency. Importantly, one of the drawbacks of wastepaper recycling involving deinking operation is the generation of DS. DS has been reported as an important residue generated by the European pulp and paper industry (Blanco et al., 2008). Environmental legislation in Europe prohibits the landfilling of DS and requires appropriate treatment methods. The consumption of wastepaper recycling is categorized into chemicals, energy and calcium carbonate are discussed in section 2.3.3.

2.3.2 Stages in wastepaper recycling and generation of deinking sludges

The wastepaper recycling process comprises a combination of different treatment steps. They are grouped into pre-deinking, deinking, and post-deinking steps (Figure 2.5).

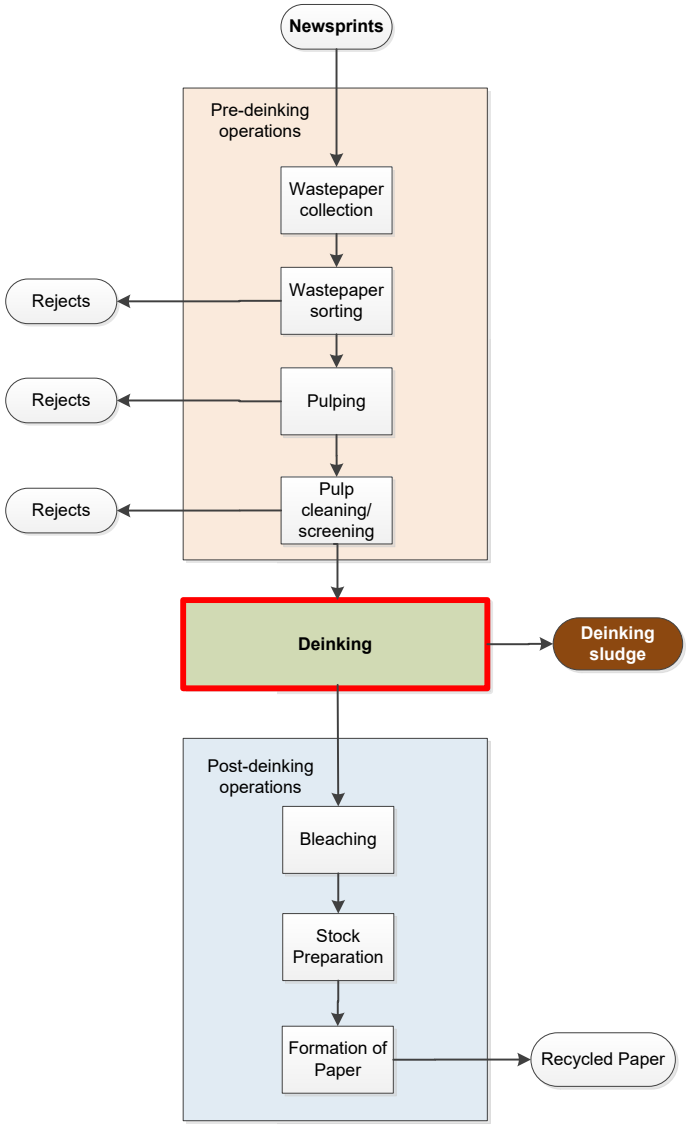

Figure 2.5 Process of deinking of newsprints for the production of recycled paper

The pre-deinking step begins with the disposal and collection of wastepapers. Collected waste papers are sorted to remove non-fibre-like materials. They are then pulped, followed by the removal of impurities terms cleaning/screening. After the removal of impurities, a deinking step is carried out. It is the deinking step that produces the deinking sludge. The deinked pulp which is then recovered pulp is further treated in the post-deinking steps. The possible process of the post-deinking step includes bleaching, stock preparation, and formation of the paper sheet. The individual steps of wastepaper recycling lead to the recovery of deinked fibre and recycled paper as shown in Figure 2.5.

Balwaik and Raut (2011) reported about 300 kg of sludge generation per Mg of recycled paper. The quantity however is dependent on the resulting wastepaper grade or pulp produced. The primary sludge and secondary sludge of the total sludge produced in a paper mill were reported as 70 and 30% respectively (Elliott & Mahmood, 2005, 2006; Krigstin & Sain, 2006). The amount of residues generated by a recycled paper mill in Europe based on Suhr et al. (2015) is presented in Appendix A.1. Sannigrahi (2018) also reported the ranges of solid waste production in wastepaper recycling which indicates that the higher the quality of recycled fibre required, the higher the amount of solid residues produced (Appendix A.2).

2.3.2.1 Pre-deinking stages

The pre-deinking stage involves all the steps taken to recover fibre from the wastepaper before the deinking stage. They include wastepaper collection, wastepaper sorting, pulping, and cleaning/screening.

1.) Wastepaper collection

Wastepapers are the major resources in wastepaper recycling, therefore they are first collected in the wastepaper recycling process. When papers such as newsprint, magazines, journals, writing or photocopy papers, or any other paper-like material are discarded as used or no longer fit for use, they are regarded as wastepapers. A detailed description of the collection systems of wastepapers and boards in Europe was reported by Levlin et al. (2010). They categorized them into household collection, industrial and business collection, and public collection. The different types of systems they mentioned and described were kerbside, blue bins, public containers, recycling yards, collection shops, recycling centres, and drop-off recycling parks. In Germany, wastepapers can be properly disposed of in containers as shown in Figure 2.6. There is also the possibility to take a very large quantity of wastepapers to the recycling centres (Stadtreinigung Hamburg, 2021). The wastepapers properly disposed of are collected by approved institutions and companies that pick them up from homes, companies, and institutions as well as public places. Some other wastepapers that are wrongly disposed of are also collected during community cleaning or sorting of other waste types.

Figure 2.6 Containers for the collection of wastepapers in Hamburg. At the left end is a blue bin for household-240 L (WERT, 2016), in the middle is a blue bin in commercial size-1100 L (WERT, 2016) and at the right end is a depot container to bring points - ca. 4100 L

According to CEPI (2021b), the wastepapers collected for recycling are termed paper for recycling (PfR). They consist of fibres but also include unusable non-paper components. The amount of non-paper components in the PfR depends on the wastepaper sorting efficiency (section 2.3.2.1.(2)) as required by the specific wastepaper grade and also varies based on country. The collection of wastepaper varies in different countries. Levlin et al. (2010) reported per capita paper and board production and environmental awareness as factors influencing paper collection. They explained that countries with a higher level in both tend to have a higher wastepaper collection and cited most European countries as an example of countries fitting into the higher collection group. The utilization rate of wastepaper for paper and board production according to CEPI is defined as the percentage of PfR utilized in comparison to the total paper and board production (Eq 2.1)

$$\text{Utilization rate (\%)} = \frac{PfR_{utilized}}{PB_{production}} \text{ x } 100\% \quad \text{.....Eq 2.1}$$

Where;

$PfR_{utilized}$ is the amount of collected wastepaper utilized in a year (Mg)

$PB_{production}$ is the total amount of paper and board production in a year (Mg)

According to CEPI (2021b), the utilization rate for members' states as of 2020 was stated as 56.3%. This implies an increase of 24.8% when compared to that of 2000. In Germany, the utilization of PfR increased by 36% between the years 2000 and 2018 amounting to a higher wastepaper utilization rate of 79% in 2020 (VDP, 2021). The recycling rate of wastepapers according to CEPI is defined as the percentage of PfR utilized plus the net trade for recycling in comparison to the paper and board consumption (Eq 2.2).

$$\text{Recycling rate (\%)} = \frac{PfR_{utilized} + PfR_{export} - PfR_{import}}{PB_{consumption}} \times 100\% \ldots\ldots\ldots\ldots \text{Eq 2.2}$$

Where;

PfR_{export} is the amount of collected wastepaper exported in a year (Mg)

PfR_{import} is the amount of wastepaper for recycling imported in a year (Mg)

$PfR_{utilized}$ is the same as in Eq 2.1

$PB_{consumption}$ is the total amount of paper and board consumed in a year (Mg)

The recycling rate as of 2020 in CEPI countries was stated as 73.9% (section 2.3.1), while in Germany it was stated as 79% (VDP, 2021). These values are about the theoretical maximum wastepaper recycling rate of 78% as reported by CEPI in 2017. The value is less than 100% because of the share of paper products that are non-collectable or non-recyclable which include coffee filters and hygiene papers (EPRC, 2017).

2.) Wastepaper sorting

Different qualities of wastepapers are used to produce different qualities of recycled papers. When wastepapers are recovered, they are often sorted into different categories before application in the recycling plant. The CEN (European Committee for standardization) therefore classify the wastepapers recovered to make recycled papers into different groups. According to the CEN EN 643, these different types of wastepapers were grouped into five different categories (CEN, 2002). The different groups are listed in Table 2.1. The ordinary grades are wastepapers which are made up of wood containing fibres with a high amount of lignin. They include groundwood or thermomechanical pulp. The medium and high-grade wastepapers contain a low amount of lignin and majorly comprise wastepapers from bleached chemical pulps (Steffen et al., 2017). The kraft grades consist of wastepapers that were made from kraft[1] or sulphate pulping. The special grades consist of wastepapers and boards which are recycled by unique or specific processes due to their possibility to bring about constraints to recycling in many instances.

[1] Kraft pulping is a method used to convert wood into pulp whereby pure cellulose fibres are treated with water, NaOH and Na_2S.

Table 2.1 Classification of wastepaper according to CEN EN 643 (CEN, 2002)

Group Nr.	Group Name	Example	Codes
1	Ordinary grades	Unsold magazine	1.01.00 – 1.11.00
2	Medium grades	Sorted office paper	2.01.00 – 2.12.00
3	High grades	White newsprint	3.01.00 – 3.19.00
4	Kraft grades	Unused corrugated kraft	4.01.00 – 4.08.00
5	Special Grades	Used liquid packaging board	5.01.00 – 5.07.00

The codes in Table 2.1 describe the different examples of wastepaper types used. Figure 2.7 shows the different positions of the codes. According to the classification, all grades have subgrades but not all subgrades have further categories. Figure 2.8 is a picture of sorted wastepaper delivered at a wastepaper recycling plant in Germany.

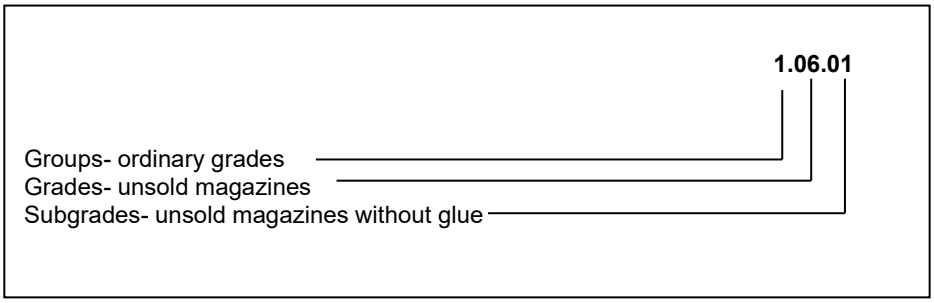

Figure 2.7 Code for describing the wastepaper grades used for recycling

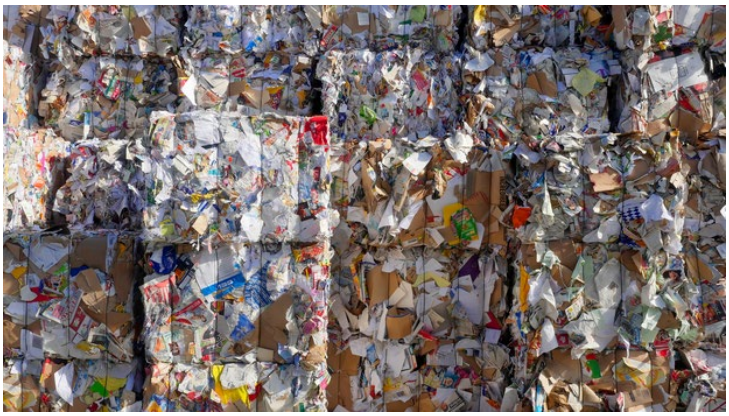

Figure 2.8 Sorted wastepaper for recycling in Germany (STP, 2021)

The heterogeneous nature of paper products is a possible challenge in the sorting efficiency of recovered papers. The use of different paper types for magazines and the use of plastic foils for packaging magazines and other commercial paper products are examples of sources of the challenges (Levlin et al., 2010). Göttsching et al. (2000) reported two main recovered sorting methods which are manual and automatic sorting. While the manual method utilizes personnel for the main sorting process, the main sorting process for automatic systems is done mechanically. The mechanical properties used for sorting are size, stiffness, or weight. For recycled paper production, different amounts of recovered paper are required. As shown in Table 2.2, the higher the quality of the targeted recycled paper the more the amount of wastepaper required. The tissue is made from high-quality pulp and marketable deinked pulps require a high quality as well. They are therefore produced from a high amount of wastepaper.

Table 2.2 Wastepaper required per Mg of recycled paper (Suhr et al., 2015)

Different recycled paper grade	**Wastepaper [kg/ Mg recycled paper]**
Case-making material (for corrugated medium)	1000
Newsprint	1 200 – 1 350
Tissue and market deinked pulp	2000

3.) Pulping

The pulping step involves the detachment of paper additives from fibres. Recovered papers are pulped by grinding them in water with the addition of some chemical additives. Typical chemicals added in the pulping of the recycled paper include sodium silicate or sodium hydroxide, hydrogen peroxide, calcium chloride, fatty acids, and soaps. A detailed overview of the chemicals and the typical quantity applied is presented in section 2.3.3. The pH is an important parameter during pulping. The ink collecting characteristics of fatty acids and soaps used in deinking are optimal in the alkaline pH range. The high pH resulting from the pulping process allows for the swelling of fibres which leads to ink detachment. However, the yellowing or darkening effect of lignin may be activated at higher pH of above 10 (Jiang & Ma, 2000). In recent years neutral pH pulping is getting more common due to more studies and also applications at an industrial scale as it allows the elimination of common wastepaper recycling chemicals (Mayeli & Talaeipour, 2015; Nicodimos & Haynes, 2011; Sulbarán-Rangel et al., 2016).

Different types of equipment are used for pulping namely low consistency pulpers, medium consistency pulpers, and drum pulpers. The application depends largely on the efficiency required. Desirability includes minimization of residual paper flakes, prevention of breaking up of contaminants, and efficient ink detachment.

4.) Pulp screening

The screening step involves the removal of impurities which are materials bigger than fibres. The materials which could not be removed by sorting are removed in this stage before the deinking stage. Particle size is the main property used for screening. Coarse or fine screens are used depending on the size of the impurities. Coarse screen size range from 1.3 - 2 mm while fine screen size range from 0.015 - 0.7 mm (Holik, 2006). During screening, pulps with desired size flow through the holes or slots on the screen and leave the screen through the accept port. The oversized impurities and the reject pulp do not pass through the screen but exit from the reject port of the screen (Hamelin et al., 2014). The different types of screens are closed and pressurized or basket screens. Performance of the screen is measured with parameters such as screen capacity, debris removal efficiency, mass reject ratio, fibre fractionation, and power consumption (Salem et al., 2013).

5.) Pulp cleaning

The impurities in the pulp which are denser than water can be removed by centrifugal cleaning or cyclones. They include staples, sand, plastic debris, etc. (Fricker et al., 2007; Holik, 2006). The cleaning step applies the principle of the centrifugal flow field to remove impurities. The working principle is such that the tangential inflow of materials into the cleaner produces a swirling motion. A centrifugal force is initiated through the swirling motion and causes particles heavier than the fibres to travel outside the cleaner while the lighter particles which include the fibres travel inward to the core of the vortex (Holik, 2006). Cleaners can be used to remove different plastic particles and melt adhesives. The efficiency parameter of cleaners is residence time, radial acceleration, and the diameter of the cleaner (Levlin et al., 2010). The impurities from the cleaner device are collected as reject.

2.3.2.2 Deinking stage

The deinking stage involves the removal of hydrophobic particles such as printing inks and micro stickies. The hydrophobic particles are removed employing flotation through the addition of additives such as surfactant, soaps, etc. Some methods of deinking include flotation deinking, wash deinking, and enzymatic deinking.

1.) Flotation deinking

The flotation step removes hydrophobic particles majorly ink particles. Ink particles in the range of 10 to 250 µm can be removed by flotation deinking (Suhr et al., 2015). The principle is explained as follows. Air is blown into the pulp slurry and the collector which includes chemicals like fatty acids and soaps that show affinity with ink particles and air bubbles. They cause the ink particles to attach to the bubbles. The air bubble takes the ink to the surface and forms a thick froth and can then be removed from the surface. An optimum process temperature of between 40 and 55 °C was reported for deinking floatation cells from a laboratory study by Mckinney (1995). While a higher temperature help to improve defibrization of wet strength paper, a lower temperature improves the removal of high stickies often on recovered papers such as magazines (Jiang & Ma, 2000). The flotation cells are often applied in series to improve the deinking efficiency. The thick froth which is the deinking sludge contains inks, fibres fines and some additive particles such as fillers and bleaching agents. A detailed list of the chemicals added is shown in section 2.3.3.1.

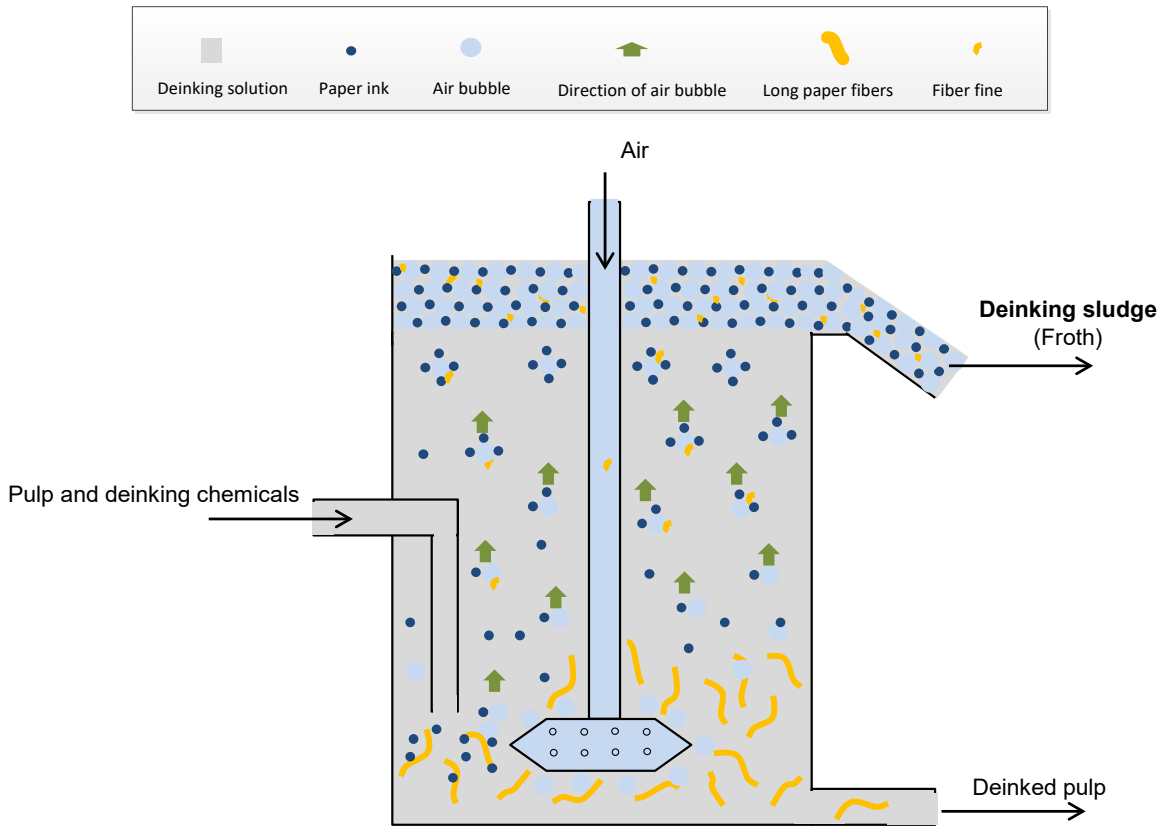

Figure 2.9 Diagram of a froth floatation cell showing fibre recovery and generation of deinking sludge (modified from Venditti et al. 2007).

2.) Wash deinking

In the process of wash deinking, the small particles in the pulp slurry are removed with water through a sieve, while the larger particles including the fibres remain on the sieve. This process is like a thickening technology and involves the use of a dispersant. The wash deinking removes particles in the size range of 10 μm and smaller (Fricker et al., 2007; Suhr et al., 2015). The different methods and mechanisms for wash deinking are displacement, dilution, extraction or diffusion. Rotary vacuum drums which are a type of displacement washer are the most common washers and operate at a paper stock consistency[2] range from 0.8 (inlet) to 18% (outlet) and have production capacity of 5 -12 moisture-free Mg/m^2 (Santos & Hart, 2014). Other washing devices require a higher inlet paper stock consistency making rotary vacuum drums preferably after a low paper stock consistency screening.

3.) Enzymatic deinking

Studies have shown that some enzymes alone or in combination with other chemicals can effectively remove or detach ink particles from wastepaper (Saxena & Chauhan, 2017; Wang et al., 2018). It is reported that the application of enzymatic deinking can reduce the expenses of the deinking process since it increases brightness and reduce the usage of bleaches. Even with the number of studies carried out to investigate the enzymatic deinking, they are not yet well applied due to some challenges as listed by Nathan and Rani (2019). The challenges amongst others include the high cost of pure enzymes, limitation of optimal temperature range, the problem with inhibitory conditions and high BOD load in effluent due to biological activity.

2.3.2.3 Post-deinking stages

The post deinking stages are steps taken to improve the quality of the deinked pulp and achieve desired property for the finished paper product. The desired properties include their mechanical properties such as strength and their physical properties such as brightness, colour, etc. The common steps for these are explained below;

1.) Bleaching

After deinking operation, the deinked pulp is often bleached to increase brightness and further remove dyes and colours (Bhardwaj & Nguyen, 2005). The bleaching agents may be added during the deinking stage or in a separate bleaching stage. The choice of the bleaching agent is largely dependent on the quality of the fibre which also includes the different impurities still present after deinking.

[2] Paper stock consistency (in percent) within the pulping and paper making industries is the dry solid content of a pulp slurry in water. It is calculated by dividing the fiber weight (in grams) by the sample volume used (in milliliters) times 100.

Bleaching of deinked pulp is carried out either by oxidizing or reducing agents. Due to environmental concerns resulting in strict legislation, chlorine-based bleaching chemicals are being replaced for bleaching deinked pulp. Hydrogen peroxide and sodium dithionite are widely used bleaching agents for all types of fibres (Fišerová et al., 2018). Hydrogen peroxide is an oxidizing agent while sodium dithionite is a reducing agent. Since Hydrogen peroxide is compatible with the environment as it decomposes to water and oxygen, it is reported as the most commonly used oxidizing bleaching chemical for deinked pulp (Petit, 1992).

2.) Stock preparation

A stock is referred to as the different types of pulp and their mixtures that are available for paper production. They often pass through treatment processes before they are finally used for paper production. This is because they are often available in the form of loose materials and suspensions with properties that are not yet satisfactory for paper production. The required treatment processes are dependent on the properties of the raw stock and the quality of the targeted recycled paper. Typical treatment processes include fibre disintegration, screening and fractionation, refining, and mixing (Holik, 2006; Suhr et al., 2015).

The fibre disintegration step removes the interlaced fibres and curls which are free in stock. The screening step involves the removal of smaller impurities and small isolated fibres which were not removed before pulping, while the fractionation step separates fibres according to different characteristics such as length, stiffness, and flexibility. The refining step helps through a mechanical process to improve the bonding ability of individual fibres thus increasing the strength of paper to be produced. In the mixing stage, different types of stocks are mixed based on the required proportion to achieve a desired recycled paper grade or quality. During stock preparation, some chemical additives are also used. The typical chemicals include resins, wet strength agents, colours, and filler (Holik, 2006; Suhr et al., 2015). The fillers are non-fibrous materials that are used to modify paper's structure, appearance, and other relevant properties that determine paper end-use performance and application. Typical fillers are calcium carbonate, kaolin, titanium dioxide, talc, and gypsum (Hubbe & Gill, 2016)

3.) Formation of paper

This step essentially involves the draining away of water from a dilute suspension of fibres and other chemical additives. The draining is carried out on a fine wire mesh; therefore, the mixture of the suspension and chemical additives is pumped uniformly on the mesh to achieve a uniform paper formation. During the formation of paper, a sizing or coating operation is optionally carried out (Lehtinen, 2000). The sizing operation can be wet-end or surface sizing.

In wet end sizing, starch or other sizing chemicals are added to a wet pulp at the wet end of the paper-making machine. This reduces the natural absorption capacity of paper, and it is beneficial for writing papers. The surface sizing involves the addition of a sizing agent on the surface of the paper at the dryer section of the paper machine.

It gives the paper the property such as prevention from dusting, especially for paper used for offset printing. Coating involves the application of different chemical additives on paper to create a desired surface property for paper such as colour, opacity, glossiness, brightness, and shade. They are added to the dryer section of the paper-making machine. The coating formulation for paper making typically comprises pigments, binders, and some chemical additives. The pigments carry the characteristic properties of the coating while the binders hold or glue the coating pigments to paper. The typical pigments are kaolin, clay, calcium carbonate (GCC & PCC), and titanium dioxide while the typical binders used are latex, starch, and polyvinyl alcohol (Özcan & Zelzele, 2017).

2.3.3 Consumptions in wastepaper recycling

This section discusses the chemicals and energy consumption of deinking operations. Additionally, calcium carbonate which is filler for papermaking is discussed.

2.3.3.1 Chemicals

To further discuss wastepaper recycling, this section list some common chemicals and their quantities as it applies to different recovered papers used for wastepaper recycling. A detailed report on typical chemicals used for wastepaper recycling has been given by Jiang and Ma (2000) and Suhr et al. (2015). They reported the quantities and functions of different a chemical as it applies to different recovered paper grades. The main purposes of chemicals during the pre-deinking (pulping) and deinking processes are for ink detachment, dispersion and removal. Chemicals are also used during post-deinking operations for operations such as bleaching, stock preparation and paper formation. Table 2.3 shows the quantities of some common chemicals used for wastepaper recycling from the pre-deinking step to the post-deinking step. The only post-deinking step considered in Table 2.3 is the bleaching step.

The chemicals listed are chemicals applicable to recovered papers such as newsprint, mechanical pulp-based computer printout, tissue paper and market pulp. Table 2.4 shows the quantity of some chemicals used during the paper production step (post-deinking operation) by a wastepaper recycling plant in Europe. The table identifies chemicals such as calcium carbonate, starch, binders, sizing agents and other colour additives. It is essential to note the high share of $CaCO_3$ among the chemicals added.

Table 2.3 Typical chemicals and their quantities used in wastepaper recycling

Wastepaper recycling stage	Process	Chemicals	Newsprint	Mechanical pulp-based computer print-out	Tissue Paper and Market pulp	Source
Pre-deinking	Pulping	H_2O_2	0.5 – 1.0% NA	NA 0.5 – 2.5%	0.0 – 1.0% NA	1 2
		NaOH	0.5 – 1.0% 0 – 5.0%	NA 0 – 5.0%	NA 0.0 – 5.0%	1 2
		Na_2SiO_3	1 – 2% NA	NA 0.5 – 5%	NA NA	1 2
		Na_2CO_3	NA	0.25 – 5%	NA	2
		$Na_2S_2O_4$	NA	0.25 – 5%	NA	2
		Ethoxylated alkyl phenol	0.1 – 2.0%	0.1 – 2.0%	0.1 – 2.0%	2
		EDTA/ DTPA	0 – 0.5%	0 – 0.5%	0 – 0.5%	2
		Sodium or Potassium phosphate	0.2 – 1.0%	0.2 – 1.0%	0.2 – 1.0%	2
		Hydrophilic polymers	0.1 – 0.5%	0.1 – 0.5%	0.1 – 0.5%	2
Deinking	Flotation	Soap	0.3 – 0.6% 0.2 – 0.4%	NA NA	0.3 – 0.6% NA	1 1*
			0.5 – 3.0%	0.5 – 3.0%	0.5 – 3.0%	2
		$CaCl_2^*$	NA	90 - 300 ppm	NA	NA
Post-deinking	Bleaching	H_2O_2	1.0 - 2.0%	NA	1.0 - 2.0%	1
		NaOH	0.5 – 1.2%	NA	0.5 – 1.2%	1
		$Na2SiO_3$	1.0 – 1.8%	NA	1.0 – 1.8%	1
		Dithionite	0.4 – 1.1%	NA	0.4 – 1.1%	1

[1] Suhr et al. 2015
[2] Jiang & Ma, 2000
NA- implies value not explicitly given by author
* Reported chemical and quantity for a second floatation step.

Table 2.4 Some chemicals used during post-deinking operation by a wastepaper recycling plant (Suhr et al., 2015)

Post deinking chemicals	Amount (kg/Mg of Input pulp)
Fillers ($CaCO_3$) - 73% DM	313
Coating pigment ($CaCO_3$, Kaolin) - 73% DM	7.0
Starch, dry	49
Binders, dry	0.3
Sizing agents - 20% DM	10.5
Other additives and dyes	57

2.3.3.2 Energy

Like every other manufacturing industry energy play a key role in production processes. The wastepaper recycling process which produces recycled paper utilizes energy in a different form for different purposes. Wastepaper recycling is more energy sustainable when compared with paper production from virgin pulp, in the sense that with 500 sheets of recycled A4 office paper about 19.3 kWh or 72% of energy is conserved when compared to paper produced from virgin paper (STP, 2021). The three main areas where energy is utilized in the wastepaper recycling process are:

- Heating energy - for heating of water, pulp, air and chemical additives to their required process temperature
- Electricity energy - for driving the machinery, pumping, vacuum, forming, ventilation and wastewater treatment
- Heat energy - for drying of paper in the paper machine

Most heat energies are produced on-site while electrical energy is brought or generated on-site (CEPI, 2021b). In the study of Laurijssen (2013) on the energy consumption of 23 different paper and board mills based in Europe, a report on the specific energy consumption (based on the actual energy consumption and not on installed power) of 7 different wastepaper recycling mills using at least 85% recovered papers was made as shown in Table 2.5. The process reported are deinking, dispersion, stock preparation, forming and press section and drying section. It was observable that drying paper consumes the highest amount of energy during wastepaper recycling.

Table 2.5 Energy consumption for wastepaper recycling in the Netherlands (drawn from Laurijssen 2013)

Wastepaper Recycling stage	Processes	Tissues [GJ/t pulp]	Other grades [GJ/t pulp]
Deinking	Dispersion	1.0 – 2.2	0.8 – 1.6
	Deinking	0.4 – 1.3	1.0 – 2.4
	Dispersion and deinking combined	2.6	2.3 – 3.0
Post Deinking	Stock preparation	1.7 – 2.3	0.4 – 1.7
	Forming and Press section	0.8 – 3.0	0.5 – 2.8
	Drying section	6.0 – 7.6	4.6 – 6.2

In Germany, the energy consumption from different types of recycled papers as reported by Suhr et al. (2015) is shown in Table 2.6.

Table 2.6 Specific energy consumption for wastepaper recycling in Germany (drawn from Suhr et al. (2015)

Paper grade manufactured	Total energy [GJ/t pulp]	Fibre supply
Newsprint, SC paper	7.5	100% RCF
Mainly newsprint	7.9	100% RCF
Newsprint	8.6[a]	85% RCF, 15% Ground wood
Newsprint, SC paper	10.2[a]	52% RCF, 42 RMP, 6% purchased chemical pulp
Tissue	9.4	75% RCF, 25% purchased chemical pulp

SC is an acronym for supercalendered. SC papers are primarily used for the production of magazines and advertising materials.

a - For recycled furnish (RCF) paper mills, the specific energy consumption is directly proportional to the portion and type of mechanical pulp in the furnish. Power consumption for refiner mechanical pulp (RMP) and groundwood is substantially higher than for RCF processing.

2.3.3.3 Calcium carbonate

Calcium carbonate improves paper opacity, strength and brightness in papers, also its usage to reduce paper production costs is a common practice (Chen et al., 2011; Doelle & Amaya, 2012; Han et al., 2020). Among the fillers known, calcium carbonate is the most widely used (Hubbe & Gill, 2016). Apart from production cost, another reason supporting the wide usage of calcium carbonate in the industry is due to the paradigm shift of the industry from acidic to neutral or alkaline sizing (Bajpai, 2015; Michael & Downs, 1996; Rende, 2015), where its application is a global industrial standard (John et al., 2007; Rende, 2015)

Figure 2.10 shows the use of non-fibrous material for paper production in the CEPI countries from 1991 to 2020. A continuous increase in the consumption of calcium carbonate is notable. In 2020 calcium carbonate account for about 56 % of the non-fibrous materials used for paper production in the CEPI countries (Figure 2.10). This amounts to an increase of about 49% in the consumption of calcium carbonate when compared with that of 1991. Its demand is expected to increase as the paper production industry grows.

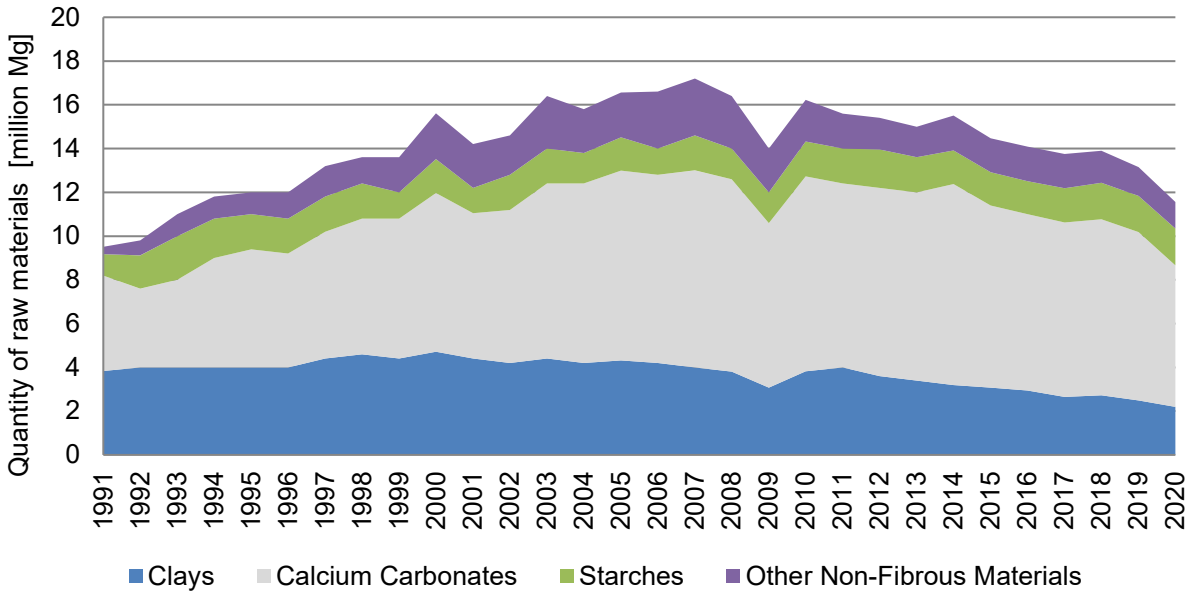

Figure 2.10 Consumption of non-fibrous materials for paper production in CEPI Countries (CEPI, 2021b)

Calcium carbonate in either the precipitated (PCC) or granulated form (GCC) are used extensively in the paper production industry and they are produced directly or indirectly from limestone (Durand & Pesaresi, 2007; Gaber, 2018). More on the description of PCC and GCC are available in section 3.4.1.

2.3.4 Residues of wastepaper recycling and deinking sludge in Germany

The residues of wastepaper recycling mills are a part of the residues generated in the pulp and paper mills. Jung et al. (2014) in their study identified some important residues in the German pulp and paper mills. They include the bark and wood waste, DS, waste from the dissolution of paper and cardboard waste, fibre waste and sludge, sludges from wastewater treatment, combustion residues and other waste. All these residues except bark and wood waste can be associated with wastepaper recycling. In 2013, DS amounted to about 20% of the residues generated in pulp and paper mills in Germany. It was second to fibre waste and sludge (Jung et al., 2014).

According to Blanco et al. (2008) and Monte et al. (2009), 70% of the residues of the European pulp and paper industry are generated from the production of deinked recycled paper of which DS is an important fraction. About 0.96 million Mg of DS was generated in the year 2013 in Germany according to Jung et al. (2014). Using PFR (paper for recycling) data and fractions of PFR used for deinking operation as reported by VDP (2021), the dried DS generated in Germany in 2015, 2019 and 2020 were estimated. It was assumed that the dry matter of DS as reported by Jung et al. (2014) is similar to that of pre-dewatered DS obtained in own study. The relationship between the amount of PFR and recycled paper produced as well as between the amount of dry DS generated and recycled paper produced was obtained from Suhr et al. (2015) and Berger et al. (2021) respectively. The estimated DS generated in Germany were 2.28 - 5.75 million Mg DS (2015), 2.60 - 6.54 million Mg DS (2019) and 2.36 - 5.91 million Mg DS (2020) (Appendix A.3). It can be observed that the 0.96 million Mg of DS reported by Jung et al. (2014) for the year 2013 is about 42% of the lower bound of the estimated range for the year 2015.

CHAPTER 3 VALORIZATION OF DEINKING SLUDGES

Valorization of deinking sludge implies increasing the value of DS from mere waste to a resourceful material with the possibility of applying it for economic or ecological beneficial purposes. The characteristics of DS, the current treatment approach and the application of anaerobic digestion as well as calcium carbonate recovery in wastepaper recycling are discussed.

3.1 Characteristics of deinking sludges

Some properties of DS have ben reported by some authors (Abubakr et al., 1995; Amare et al., 2019, 2020; Bienert et al., 2015; Krigstin & Sain, 2006; Kujala, 2012; Niessen, 2002; Steffen et al., 2017). The properties reported are often not detailed. Partly solid matter contents, ash contents, element contents (C, H, S, O, N) and/or heating values were reported. A pictorial view of DS and other substrates are shown in Appendix A.5. Generally, there exists a knowledge gap in the properties of the different types of DS respectively of sludges with constituents of DS (DS derivatives) and their impact on biogas production. Reports on the properties of the primary non-dewatered DS as a direct output of deinking are missing. DS undergoes several transformations in post-deinking processes (e.g. different dewatering steps) before it leaves the recycled paper mill as concentrated sludge. Table 3.1 show the DM, oDM and pH value of different DS samples as reported by different authors.

Table 3.1 Characteristics of deinking sludges (DS)

Sludge type (Dewatering)	Wastepaper-grade	DM [% FM]	oDM [% DM]	pH [-]	Source
Pre-dewatered DS	W70	14.3	29.3	7.3	Amare et al., 2019, 2020
Highly dewatered DS	NA	63.3*	32*	ND	Bienert et al., 2015
NA	NA	38 - 62	49	ND	Kujala, 2012
NA	NA	3 - 5	52.0	ND	Krigstin & Sain, 2006
NA	NA	ND	51.6	ND	Niessen, 2002
NA	NA	42.0	79.8	ND	Abubakr et al., 1995

*Computed from the average of minimum and maximum value.
NA- Not available
ND- Not determined

In this dissertation, a more detailed investigation of the physical-chemical properties of different DS and DS derivative types is carried out. The different types of DS due to different wastepaper grades and due to post deinking operations (dewatering) were investigated.

3.2 Current treatment of deinking sludges

DS generated as the output of the flotation steps in wastepaper recycling contains residual organics and a large amount of water. As practice, the DS is often mechanically dewatered internally to reduce to a great deal the sludge handling volume and incinerated externally. The common sludge handling approaches for DS are land spreading, landfilling and incineration (Blanco et al., 2008). The landfilling and land spreading of sludge have declined in some countries due to the ecological and economical aspects (Abubakr et al., 1995; Blanco et al., 2008; Monte et al., 2009). Jung et al. (2014) reported incineration as the most common treatment method applied for treating pulp and paper residues in Germany and it includes the treatment of DS. In 2013, incineration (external and internal combustion) had a treatment share of about 55% (Figure 3.1).

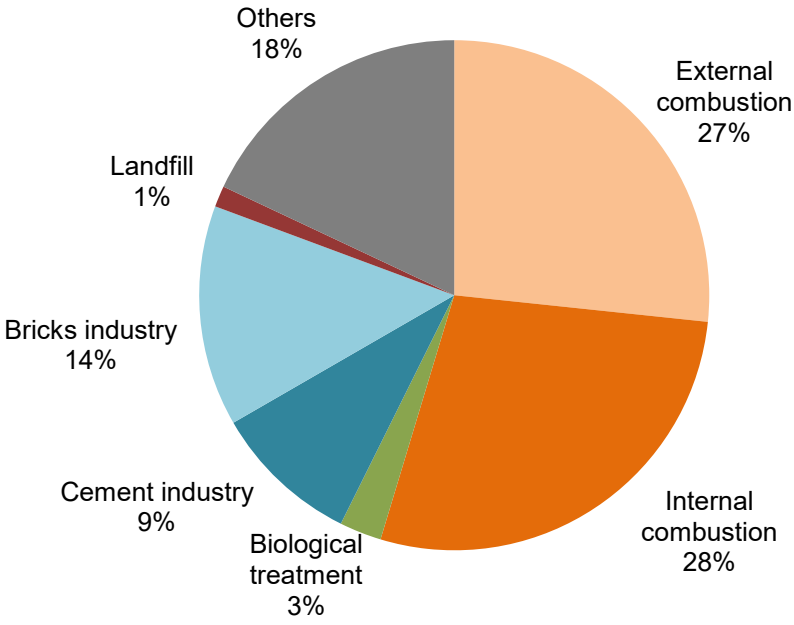

Figure 3.1 Treatment methods of pulp and paper residues in Germany (Jung et al. 2014)

Bousios (2016) and Bousios and Worrell (2017), have reported in detail, possible valorization options for residues in pulp and paper mills. Their options can be grouped into two categories, which are conversion into energy and energy carriers and the conversion into products.

The energetic conversion includes incineration, pyrolysis and anaerobic digestion. The substantial pathways include production of wood-plastic composite, nano-cellulose and building materials. This thesis however with a focus on DS, considers the application of AD coupled with recovery of calcium carbonate for building purposes as a more sustainable option compared to incineration.

3.2.1 Incineration

Waste incineration is the combustion of an organic fraction of waste for energy production (Porteous, 2001). Waste with high moisture content requires a fluidized bed incinerator for high efficiency (Patumsawad & Cliffe, 2002; Suksankraisorn et al., 2003), this is also applicable to DS. Although incineration has the highest share of treatment of residues generated in the German pulp and paper mills, it is arguably not economical and sustainable for the treatment of DS. DS has a low calorific value resulting from its high share of the inorganic compound and water content (Deviatkin et al., 2015). It therefore, requires a complementary fuel source for the energy efficiency of the incineration system. The treatment of flue gas which is required for incineration (Dong et al., 2020; Li et al., 2020) also increases the treatment cost of DS by incineration. A more sustainable pathway other than incineration of DS is therefore to be considered.

3.2.2 Application in the bricks and cement industry

The ability of DS to act as a supplementary building material in bricks and cement industry has been investigated by a few authors (Bousios, 2016; Deviatkin et al., 2015; Singh et al. 2018). It is explained to be due to the property of calcium carbonate to contribute to the strength of the material, especially when applied with cement. Though it is a promising valorization pathway its application is not common in Germany (Figure 3.1). The high treatment share of incineration also limits this application as the resulting ash from incineration gets contaminated with the constituents from other complementary fuel sources used for incineration. The biodegradation of the fines and fibres in DS to produce biogas as a by-product and further utilization of the ash content as a material for the construction industry is a treatment pathway that does not contaminate the calcium carbonate and allows for its efficient application as a supplementary building material.

3.3 Anaerobic digestion

The section begins with an overview of anaerobic digestion (AD) and identifies the substrates already used for AD in the pulp and paper industry as well as in the wastepaper recycling sector. It further discusses some important fundamentals of AD technology which include the kinetic modelling of the AD process.

3.3.1 Process overview

AD is a biochemical process carried out by the action of a microbial consortium that converts organic materials into biogas in the absence of oxygen. This process occurs naturally in bogs, moors, lake sediments, oceans, and digestive tracts of ruminants. Biogas comprises primarily of methane (CH_4) and carbon dioxide (CO_2). A description of the typical composition of biogas from AD facilities is shown in Table 3.2. Among the gases in biogas, the combustible component is the methane gas which has a calorific value of 50 - 55 MJ/kg (WNA, 2021). The biogas production from AD can be used as fuel for electricity, heat or steam generation and as well as automobile fuels (IRENA, 2018). Biogas substrates are mainly organic material that is either animal or plant-based. They include sewage or wastewater, manure, kitchen waste, energy crops and non-toxic biodegradable industrial wastes. Biogas is produced from non-fossil based material; therefore it is classified as a renewable form of energy. Its application helps in reducing the emission of the greenhouse gases such as CH_4, CO_2 and N_2O, thereby contributing to solving the problem of climate change. Other advantages of biogas production include the reduction of soil and water pollution, prevention of health problems and the generation of organic fertilizer (Abubaker et al., 2012; Paolini et al., 2018).

Table 3.2 Biogas composition and concentration range (Friehe et al., 2016b)

Component	Symbol	Concentration Range	Unit
Methane	CH_4	50 – 75	%Vol.
Carbon dioxide	CO_2	25 − 45	%Vol.
Water	H_2O	2 − 7 *	%Vol.
Hydrogen sulphide	H_2S	20 − 20000	ppm
Nitrogen	N_2	< 2	%Vol.
Oxygen	O_2	< 2	%Vol.
Hydrogen	H_2	< 2	%Vol.
* Vapour for temperature in the range of 20 - 40°C			

3.3.2 Substrates from the pulp and paper industry

The application of AD in the European pulp and paper industry is common (Ekstrand, 2019; Meyer & Edwards, 2014; Suhr et al., 2015; van Haandel & van der Lubbe, 2007). AD is often applied as a pre-treatment step in an anaerobic-aerobic treatment system in the industry.

The energetic utilization of organics present in pulp and paper mill effluents produces biogas which is beneficial in the energy-intensive process of the industry. One reason impairing the adoption of AD as a stand-alone treatment in the industry is the fact that the COD and BOD of AD effluents do not comply with the requirement set by EU legislation on environmental discharge (Suhr et al., 2015). Meyer and Edwards (2014) in their study also explained that the presence of lignocellulose, biosolids and associated complex organics limits the application of AD in the industry. This is because the hydrolysis of lignocellulosic materials is very slow and therefore limits their biodegradability (van Haandel & van der Lubbe, 2007).

AD is applied mainly for selected waste streams in the industry and is scarce for mill derived sludge. The waste stream identified as the input source for AD application in the pulp and paper industry in Europe is often the process water. The process water is generated in plants from various water-related operations (Hubbe et al., 2016; Suhr et al., 2015). Different process designs of AD are available in the European pulp and paper industry and include fixed bed reactor, up-flow anaerobic sludge blanket (UASB), expanded granular sludge blanket (EGSB) and internal circulation (IC) reactors (Suhr et al., 2015). The application of anaerobic-aerobic treatment for process waters in wastepaper recycling is common for plants without deinking operations since they often meet the COD requirement (1000 – 2000 mg/l) (Suhr et al., 2015). The residues and wastewater generated during wastepaper recycling are shown in Appendix A.1 and A.2.

DS in this study is different in terms of characteristics when compared with process water and also sludges from non-deinking pulp and paper plants. DS is not applied as feedstock for a known AD application. Also, studies on the AD of DS are not common in scientific reports. However, few studies using DS as a substrate for AD have been reported recently (Amare et al., 2019, 2020; Bienert et al., 2015). Table 3.3 shows that pulp and paper mill derived sludges are potential feedstock for biogas production. The biomethane yields of the deinking and non-deinking sludges fall in similar ranges. Detailed studies on the AD of DS are required to gain a deeper knowledge of its biogas yield. This includes studies on the different DS types with different characteristics, the influence of optimization measures such as nutrient supplementation as well as finding the optimal organic and hydraulic loading rate which is necessary for practical application.

Table 3.3 Methane yield from some pulp and paper mill derived sludges

Pulp and paper mills	Substrate type	Reactor type/process	Methane potential (NL/kg oDM)	Sources
Non- deinking plant	Biosludge	CSTR	130 - 200	Puhakka et al. (1992)
	Biosludge	CSTR	120	Karlsson et al. (2011)
	Primary sludge Primary sludge and biosludge	Thermophilic process	190 - 240 150 - 170	Bayr and Rintala (2012)
Deinking Plant	Highly dewatered DS	Batch/ mesophilic	160 - 180	Bienert et al. (2015)
	Pre-dewatered DS	Batch/ mesophilic	163	Amare et al. (2019)

3.3.3 Fundamentals of anaerobic digestion

Many different authors have reported the fundamentals of anaerobic digestion e.g. (Conrad et al., 2009; Gerardi, 2003; Leschine, 1995). This chapter is a summary of the generation of biogas, main milieu conditions in the anaerobic digester, inhibitors and some operation parameters of AD systems.

3.3.3.1 Phases

AD is a complex process involving four major phases. They include hydrolysis, acidogenesis, acetogenesis and methanogenesis. For an optimal production of biogas, these individual phases are expected to proceed at individual kinetics that leads to effective solubilisation of the biodegradable organic fraction, no accumulation of toxic substances for anaerobes and effective conversion of biogas precursors into biogas. The four biochemical phases (Figure 3.2) are described in more detail below.

1.) Hydrolysis

Hydrolysis involves the cleavage of a water molecule to polymeric biomolecules in the presence of hydrolytic enzymes, thereby breaking it down into parts (monomeric molecules). The polymeric biomolecules such as polysaccharides, proteins and lipids are broken down into monomeric molecules such as soluble sugar, amino acids and fatty acids respectively during hydrolysis. Hydrolysis is a relatively slow phase that can limit the rate of the AD process (van Haandel & van der Lubbe, 2007).

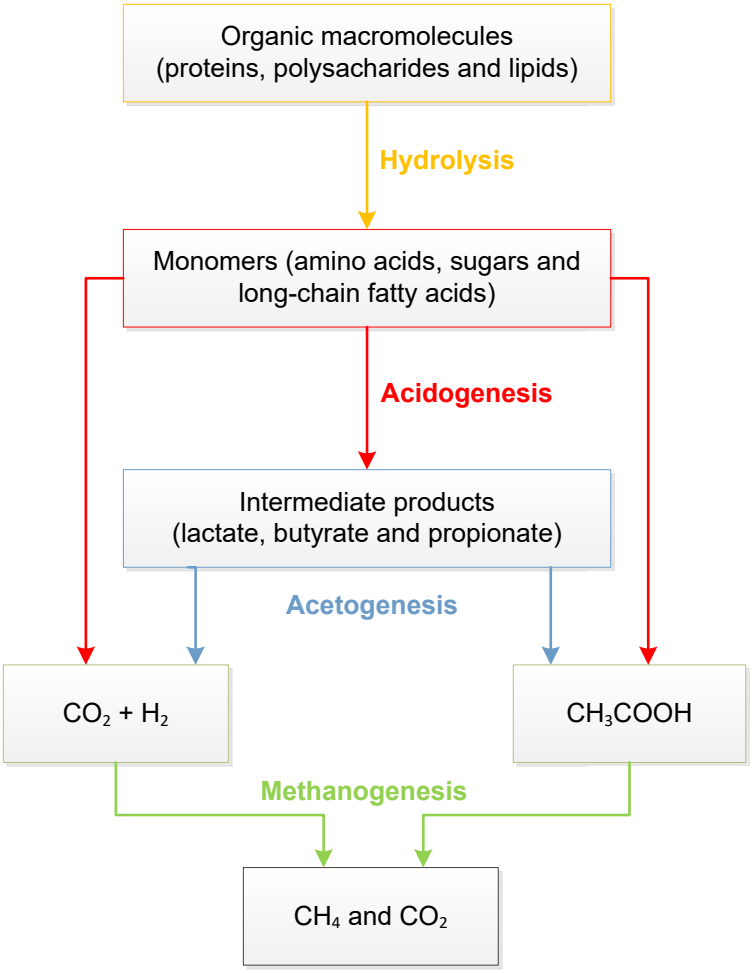

Figure 3.2 Anaerobic digestion phases showing the breaking down of organic macromolecule to the formation of biogas (modified from Abdelgadir et al. 2014)

Some hydrolytic enzymes include cellulases, amylases, proteases and lipases (Kashyap et al., 2003; Leschine, 1995). The majority of the hydrolytic enzymes are exoenzymes since they are released to the surface of the cell to induce contact with the substrate. The cellulose is hydrolysed by the activity of anaerobes such as *Clostridium lochhadii, Bacteroides succinogenes, Butyrivibrio fibrosolvens, Clostridium cellobioporus, Clostridium thermocellum, Ruminococcus flavefaciens, Clostridium stercorarium, Ruminococcus albus, and Micromonospora bispora* (Leschine, 1995; Lynd et al., 2002; Zhang & Lynd, 2004), while the hemicellulose by anaerobes such as *Ruminicola, Butyrivibrio fibrisolvens, Ruminococcus flavenfaciens and Roseovarius albus* (Andersen, 2007). The equation for hydrolysis is shown in Eq 3.1 (Anukam et al., 2019; Kamusoko et al., 2022). Figure 3.3 shows the breaking of the bond by hydrolysis to convert cellulose to glucose and hemicellulose to xylose. Deinking sludges are reported to contain a substantial amount of cellulose, hemicellulose and lignin (Steffen et al., 2017). The cellulose and hemicellulose fraction could be broken down and be beneficial for biogas production.

$$(C_6H_{10}O_5)n + n\ H_2O \quad \rightarrow \quad n\ C_6H_{12}O_6 \qquad \text{Eq 3.1}$$

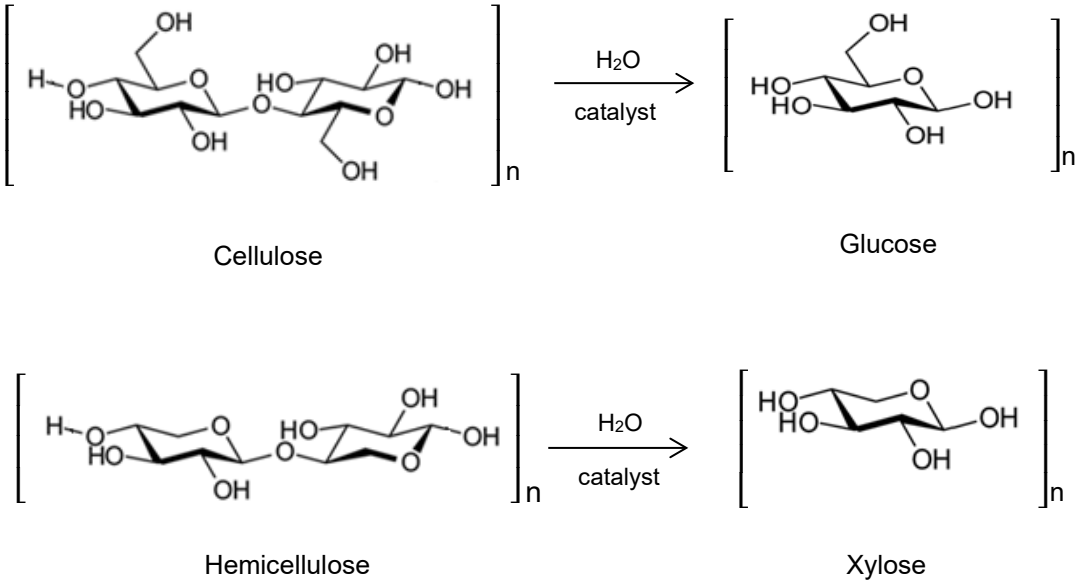

Figure 3.3 Diagram showing hydrolysis of cellulose and hemicellulose to glucose and xylose respectively (modified from (Kobayashi et al., 2016)

2.) Acidogenesis

The next step after hydrolysis is acidogenesis, which involves the further breaking down of monomeric molecules from hydrolysis. The microorganisms participating in acidogenesis produce acidic conditions due to the degradation of the monomers. Typical products of acidogenesis are carbon dioxide, hydrogen, ethanoic acid and shorter volatile fatty acids such as acetic acid, propionic acid, butyric acid, and ethanol. Some common acidogenic microorganisms are *Clostridium sp., Lactobacillus sp., Staphylococcus sp., Escherichia sp., Veillonella sp., Selemonas sp, Desulfobacter and Desulfomon* (Felchner-Zwirello, 2014). Equations of acidogenesis are shown in Eq 3.2 to 3.4 (Anukam et al., 2019; Kamusoko et al., 2022).

$$C_6H_{12}O_6 \quad \leftrightarrow \quad 2\ CH_3CH_2OH \ + 2\ CO_2 \qquad \text{Eq 3.2}$$

$$C_6H_{12}O_6 \ + 2\ H_2 \leftrightarrow \quad 2\ CH_3CH_2COOH \ + 2\ H_2O \qquad \text{Eq 3.3}$$

$$C_6H_{12}O_6 \quad \leftrightarrow \quad 3\ CH_3COOH \qquad \text{Eq 3.4}$$

3.) Acetogenesis

The acidogenesis step is followed by acetogenesis, which involves the formation of acetate from carbon with an energy source from the acetogenic microorganism. Many of the products of acidogenesis are broken down by acetogenic microorganisms into acetic acid, carbondioxide and hydrogen (Gerardi, 2003). The acetogenic microorganism are obligate H_2 producers. As hydrogen production increases, the partial pressure also increases in the AD system. These species of microorganisms are reported to survive only at very low H_2 concentration ranges (Gerardi, 2003). Therefore they carry out a symbiotic relationship with the microorganisms involved in the next step of AD, the methanogenesis. As the acetogenic microorganism produces H_2, the consumption of H_2 by the methanogenic microorganisms prevents the build-up of partial pressure to an undesirable value. Some common acetogenic microorganisms are *Clostridium sp., Syntrophomonas wolfei* and *Syntrophobacter wolinii* (Felchner-Zwirello, 2014). Equations of Acetogenesis are shown in Eq 3.5 to 3.7 (Anukam et al., 2019; Kamusoko et al., 2022).

$$CH_3CH_2COO^- + 3\,H_2O \leftrightarrow CH_3COO^- + H^+HCO_3^- + 3\,H_2 \quad \text{Eq 3.5}$$

$$C_6H_{12}O_6 + 2\,H_2O \leftrightarrow 2\,CH_3COOH + 2\,CO_2 + 4\,H_2 \quad \text{Eq 3.6}$$

$$CH_3CH_2OH + H_2O \leftrightarrow CH_3COO^- + 2\,H_2 + H^+ \quad \text{Eq 3.7}$$

4.) Methanogenesis

Methanogenesis is the final step which involves the formation of methane from the products of acetogenesis and intermediate products from hydrolysis and acidogenesis. There are three main pathways for methane formation during methanogenesis (Gerardi, 2003). One of which is the reduction of CO_2 by H_2 in the presence of hydrogenotrophic microorganisms to form methane and water (Eq 3.8) and the second is the cleavage of acetic acid by acetoclastic microorganisms to form methane and CO_2 (Eq 3.9). The methanogenic pathway by acetoclastic microorganisms is responsible for about 70 - 90% of the total methane produced in the AD of organic waste (Merlino et al., 2013; Morita et al., 2011). This can be explained to be because the hydrogenotrophic pathway requires four molecules of H_2 while the acetoclastic pathway requires only one molecule of acetate to form methane (Conrad et al., 2009). Sulphate reducing bacteria that have a high affinity for hydrogen could also be an explanation for limiting the hydrogenotrophic pathway. Microorganisms involved in methanogenesis are of the phylum Euryarchaeota and include *Methanobacteriales, Methanococcales, Methanomicrobiales, Methanopyrales and Methanosarcinales*.

The only acetoclastic methanogens among these microorganisms are the *Methanosarcinales*, example include *Methanosaeta and Methanosarcina* (Gerardi, 2003). Holmes and Smith (2016) described the third methanogenic pathway which is carried out by the action of acetoclastic *Methanosacrinales* and at least one member of the *Methanomicrobiales* on methanol or methylamines. This pathway is referred to as methylotrophic methanogenesis (Eq 3.10).

$$CO_2 + 4\,H_2 \rightarrow CH_4 + 2\,H_2O \qquad \text{Eq 3.8}$$

$$CH_3COOH \rightarrow CH_4 + CO_2 \qquad \text{Eq 3.9}$$

$$4\,CH_3OH \rightarrow 3\,CH_4 + CO_2 + 2\,H_2O \qquad \text{Eq 3.10}$$

A fourth pathway as described by Guyot and Brauman (1986) shows that formate could be converted to methane by interspecies hydrogen transfer between sulphate reducing bacteria and hydrogenophilic methanogens. Table 3.4 shows the Gibbs free energy for three different methanogenic pathways which indicate that methanogenesis is an exothermic process resulting in a yield of energy.

Table 3.4 Gibb's free energy (ΔGo) for three different methanogenic pathways (Thauer et al., 1977)

Methanogenic pathway	ΔG_o (kJ/mol substrate)
Hydrogenotrophic	- 135.5
Acetoclastic	- 32.3
Methylotrophic	- 79.9

3.3.3.2 Milieu conditions in the anaerobic digester

The milieu conditions refer to some important physico-chemical conditions within the reactor that influences the AD performance. The conditions discussed here are oxygen, water, temperature, pH and alkalinity as well as nutrient supply and inhibitors that may be encountered when DS is used as a biogas feedstock.

1.) Oxygen

AD proceeds in the presence of different microorganisms such as hydrolytic bacteria, acidogens, acetogens and methanogens. The hydrolytic acidogens and acetogens are facultative and obligate organisms that can live either in the presence or absence of oxygen.

The methanogens are strict anaerobes that can hardly survive in the presence of oxygen (Ueki et al., 1997). Whitman et al. (2006), reported that one species of *Methanosarcina* had a half time of survival of only 4 minutes in air equilibrated medium. The methanogens are the most important anaerobic species in the AD process since they produce the required methane. Therefore, the depletion of oxygen is favourable for the overall AD process. Conversely, some authors have reported that oxygen concentration at micro concentration improves hydrolysis (Jagadabhi et al., 2010; Johansen & Bakke, 2006) and oxidizes the sulphides to prevent unfavourable conditions (Duangmanee et al., 2007; van Pagel Zee et al., 2007; Zhou et al., 2007).

2.) Water

Water is important for living cells in the microbial consortiums which are responsible for the AD process. On a biological level, water helps cells with the transportation of molecules such as nutrients. It is also an important component in many biochemical reactions involving the building and breaking down of components of the cell (Gaur et al., 2014; Reuss, 2008; Watterson, 1988). The presence of sufficient water also allows the bioreactor's content to flow and allows for mixing. Wet and dry types of fermentation are discussed in section 3.3.3.4.(2).

3.) Temperature

The reaction rate of AD strongly depends on temperature. The temperature influences the growth rate and the activity of the anaerobic microorganisms which include the methanogens. Several authors have investigated and established the temperature dependency of AD processes (Bergland et al., 2015; Nielsen et al., 2017; Siggins et al., 2011; Wu et al., 2006). Depending on the temperature range of growth and metabolism, methanogens are classified into three groups. They include psychrophilic (< 20°C), mesophilic (25 - 45°C) and thermophilic (> 45°C) groups (Connaughton et al., 2006). With the psychrophilic methanogens, the AD process can be operated at ambient temperature without the need for external heat energy. The mesophilic and thermophilic methanogens require the input of heat energy for operation. While the mesophilic process requires a lower amount of heat, the thermophilic process requires a high amount of heat. The thermophilic process has the highest activity rate but requires very high external heat input. It has the advantage that during this temperature pathogenic organisms can be destroyed. However, it was reported that thermophiles do have lower diversity and they are very sensitive to changes in temperature and pH which therefore affect the stability of the AD process (Sivakumar et al., 2012).

4.) pH and alkalinity

pH is the negative common logarithm of the hydrogen ion activity (Baucke, 2002). It gives information on the acidity or alkalinity of an AD system. The alkalinity of a biochemical system such as AD is a measure of its buffer capacity, preventing a rapid change in pH. The acidogenesis phase of AD leads to the production of volatile acids which causes pH reduction (section 3.3.3.1.(2)). The volatile acids are taken up during the methanogenesis phase to produce alkalinity. Another source of alkalinity includes the degradation of organic-nitrogen compounds like proteins and ammonium as well as the CO_2 production from organic compounds (Gerardi, 2003). The produced alkalinity prevents the further drop in the pH of the system. Since the enzymatic activities of anaerobes are pH-dependent, an AD system requires sufficient alkalinity for stable conditions.

At pH values less than 6 or above 8.5, the system equilibrium favouring the built-up of biogas is distorted. Studies on AD have shown that an optimum pH value for the AD process is reported at about 7 (Diamantis et al., 2007; Gerardi, 2003). Considering the thermodynamics and kinetics of the AD system, the intermediates produced during acidogenesis could accumulate thereby limiting the further breaking down of organic matter. This accumulation also leads to the build-up of partial pressure of hydrogen. The high partial pressure of hydrogen negatively influences the biodegradation of propionic acid and butyric acid. On the other hand, sufficient hydrogen partial pressure is required by the hydrogenotrophic methanogenesis for the production of biogas. This leads to a narrow “Thermodynamic window “ within which the individual reactions proceed simultaneously.

Failure of an AD system can be monitored using the ratio of the volatile organic acid (VOA) and the alkalinity ratio termed VOA/TIC. Lili et al. (2011) reported that the AD system is at its maximum biogas production for a VOA/TIC ratio of 0.3 - 0.4. For pH and alkalinity adjustment in the AD system, a common chemical used is carbonate such as sodium bicarbonate and potassium bicarbonate since they release carbonate directly into the system (Lin et al., 2013). The uptake of soluble CO_2 by hydroxyl groups such as $Ca(OH)_2$ before the production of carbonate makes it not desirable for pH and alkalinity adjustment. The pH can also be regulated by reducing the organic loading rate or by stopping feeding for a while in a continuous AD system.

5.) Nutrient supply

Anaerobes involved in the AD process require the uptake of nutrients for survival, energy, growth and reproduction. These nutrients which are the basis of cellular metabolism are converted to energy and biosynthetic intermediates aiding cell maintenance and division (Blum et al., 2021; Wei et al., 2017). Based on the quantity needed by anaerobes, these nutrients can be classified into macronutrients and micronutrients.

Macronutrients are consumed in relatively large amounts, while micronutrients are needed in trace quantities. They are also referred to as trace elements (TEs). The macronutrients are used especially for growth and energy (Prentice, 2005). They include carbon, hydrogen, oxygen, nitrogen, phosphorus, sulphur, potassium, magnesium, sodium, calcium and iron. Among these, carbon assumes great importance as the main constituent of all organic cell materials and represents about 50% of the cell's dry weight (Loferer-Krössbacher et al., 1998; Romanova & Sazhin, 2010). The carbon requirement for synthesis by anaerobes can be derived from biodegradable organic matter such as DS, wastewater, food waste, energy crops and so on. As opposed to aerobic micro-organisms, anaerobes do not use molecular oxygen as a terminal electron acceptor during respiration, instead, molecules such as sulphate (SO_4^{2-}), nitrate (NO_3^-), or sulphur (S) are used (Michas et al., 2020).

The carbon-nitrogen (C/N) ratio is used to monitor the optimal operation of the AD process. In general, anaerobes are reported to consume carbon 25-30 times quicker than nitrogen (Samir et al., 2019). A C/N ratio in a similar fold in the AD mixtures may therefore enhance optimal biogas production. Too high C/N ratio may lead to poor uptake of carbon while too low uptake may lead to the build-up of ammonia which is not favourable for the AD process. C/N ratios reported for optimum biogas production are: 20 (Siddiqui et al., 2011), 25 - 30 (Wang et al., 2012) and 20-35 (Ceron-Vivas et al., 2019; Panichnumsin et al., 2012). This variation is largely dependent on the characteristics of feedstock. TEs have subtle biochemical and physiological roles in cellular processes. Examples are cobalt, copper, manganese, molybdenum, nickel, selenium, tungsten, vanadium and zinc. They are metals playing the role of cell catalysts and many of them play a structural role in various enzymes. A lack of these nutrients may result in a deficiency state that compromises the growth and reproduction of anaerobes (Ezebuiro, 2014; Khanal, 2008; Takashima et al., 1990). It is reported that supplementation of TEs in the AD process can lead to improved methanogenesis (Ezebuiro, 2014; Khanal, 2008; Takashima et al., 1990).

6.) Inhibitors

Inhibitors are substances that alter the optimal condition leading to the effective production of methane in an AD system. The main inhibitors in the AD process are ammonia, sulphate-reducing bacteria, hydrogen sulphide, heavy metals, long-chain fatty acids and salts (Akunna, 2018; Liu et al., 2018). The following inhibitors discussed are those relevant to the AD of DS.

a.) Sulphate

Sulphate reducing bacteria reduces sulphate (SO_4^{2-}) present in an AD system to sulphide. Sulphates are formed from sulphur in organic molecules like proteins. They also come from high sulphate rich substrates like some industrial wastewaters. The reduction of sulphate involves the usage of hydrogen, acetate and fatty acids. Since this reduction process competes for potential methane precursors, it leads to poor efficiency of biogas production. The production of sulphide is also reported to have a toxic effect on anaerobes (O'Flaherty et al., 1998). Depending on pH and other AD conditions, hydrogen sulphide in the range of 50 to 250 mg/L was reported inhibitory (Chen et al., 2008). With the application of air stripping the hydrogen sulphide concentration can be considerably reduced. By application of activated carbon or the use of Fe^{2+} and Fe^{3+} in the form of $FeCl_2$ or $FeSO_4$, the bioavailability of sulphur can be as well minimized (Petersson & Wellinger, 2007).

b.) Heavy metals

Heavy metals are micronutrients which include cobalt, molybdenum, selenium, titanium, copper, nickel (Briffa et al., 2020; Engwa et al., 2019). These nutrients play a key role in cell growth. The concentration of these metals beyond the tolerable range is toxic to anaerobes (Ezebuiro, 2014). The ink content of DS and wood source or paper are possible sources of heavy metals. The heavy metals present in the substrate can however be reduced e.g. adsorption, advanced oxidation processes, electrocoagulation, membranes (Qasem et al., 2021).

c.) Calcium

There are studies on calcium's possible inhibitory effect on AD. Ahn et al. (2006) reported an inhibitory effect due to calcium concentration in the range of 5 - 7 g/L for swine wastewater. On the contrary, Jackson-Moss et al. (1989) showed that calcium in the concentration of up 7 g/L does not inhibit AD in a UASB digester where a synthetic waste comprising glucose, urea and yeast was used as feedstock. This is relevant for DS since it has been reported to have a high fraction of calcium in the form of calcium carbonate (Amare et al., 2019, 2020; Steffen et al., 2017).

3.3.3.3 Operation and efficiency parameters

The main operational parameters of AD are the organic loading rate, the hydraulic retention time, the biodegradability, the biogas yield and the mixing types. These parameters which differentiate an AD process from another are described briefly as follows.

1.) Hydraulic retention time and organic loading rate

The hydraulic retention time (HRT) of an AD system is the amount of time it takes for the substrate to pass through the AD bioreactor. This operating parameter gives information on the quantity of substrate fed into the AD reactor per time. It is computed by dividing the volume of the AD reactor by the feeding rate as shown in Eq B.14 (Appendix B.9). HRT are reported in either hours or days. The HRT is dependent on the complexity of the organic component of the feedstock.

While a high HRT is needed for complex organics, a low HRT is sufficient for less complex ones. Many AD systems using wastewater as feedstock operate at an HRT of 15 - 30 days under mesophilic conditions (Alepu et al., 2016). AD relies on the activity of relatively slowly growing methanogenic bacteria which made it necessary that sufficient time is given for bacteria growth. A direct relationship exists between the HRT and the organic matter converted to biogas (Khanal, 2008). The organic loading rate (OLR) indicates the amount of organic matter fed into the digester each day. It is computed as shown in Eq B.15 (Appendix B.9). Ideal OLR rates to avoid the build-up of acids are reported as 0.5 - 3.0 kg oDM /($m^3 \cdot d$) (Deepenraj et al. 2014; Ramanathan et al., 2022).

The operating OLR depends on the type of wastes fed into the digester because different wastes have different biochemical characteristics (Babaei & Shayegan, 2011). If the digester is overfed, acids will accumulate, and methane production will be inhibited. Similarly, if the digester is underfed, the gas production will also be low.

2.) Biodegradability and biogas yield

The biodegradability in an AD process is determined by the fraction of organic matter from the total organic matter in the substrate fed that is biodegraded to form biogas by the action of anaerobes. The biodegradability indicates the efficiency of an AD system and it is also largely dependent on the characteristics of the substrate. Biodegradability can be computed by different methods. A common approach is to compute either the change in the mass of organic matter with Eq B.11 and B.12 (Appendix B.9) or the change in chemical oxygen demand (COD) due to biogas production. For semi-continuous bioreactor, it was computed with Eq B.13 (Appendix B.9).

The biogas yield is the cumulative optimum biogas formation from an AD substrate. The biogas yield of the different substrates varies depending on the nature of their organics. Substrates with organics that are readily biodegradable have a higher biogas yield. The biogas yield is reported either relating to the fresh mass (FM, NL biogas volume/kg) or relating to the organic dry matter (oDM, NL biogas volume/kg oDM).

3.) Mixing

Mixing refers to the homogenization of the content of an AD reactor. It is a key operating parameter for AD performance. Appropriate mixing of the AD system will foster an efficient distribution of the microbial consortium of nutrients and of the organics. This improves the bioavailability of substrates and the process efficiency of the system. For a continuously fed AD system, mixing helps in the inoculation of fresh feed, homogenizing the material and removing of end product of metabolism (Lindmark et al., 2014). Mixing in the AD process is required to ensure homogeneity of the reactor mixture to promote a uniform process condition such as temperature, pH and nutrients for anaerobes. In the comprehensive review of Kariyama et al. (2018) on the influence of mixing on AD efficiency in digesters, they reported in general three mixing methods used for AD processes which are gas recirculation, liquid/slurry recirculation and mechanical mixing. The gas recirculation involves the introduction of biogas at the bottom of the reactor in a recirculation form to cause a turbulent flow in the reactor mixture. In liquid/slurry recirculation, a pump is used to recirculate the reactor‘s content which also causes turbulent flow. The mechanical mixing involves the use of impellers or agitators (such as paddle, anchor, helical and propeller) which are driven by a motor to introduce a turbulent stream in the bioreactor‘s content.

An appropriate mixing method should be selected to ensure an efficient process with minimum power consumption. Different authors have studied the influence of mixing on AD. Based on the mixing energy level, the efficiency was ranked in the order: mechanical mixing followed by gas recirculation and then liquid /slurry recirculation (Wu, 2010). Trad et al. (2016) reported efficiency in a contrary order; starting with gas recirculation followed by liquid /slurry recirculation and then mechanical mixing. This difference in their position for mechanical mixing may be owed to the different types of equipment used by the two different authors. While Wu (2010) has used a lower power number impeller, Trad et al. (2016) used one with a higher power number which generates a higher shear rate.

It was reported that the hydrodynamic shear force which results from agitation is a pathway leading to cell damage in bioreactors and consequently to poor efficiency (Wang & Zhong, 2007). For the three mixing methods possible high-velocity zones which can damage cells are reported. In gas recirculation and liquid /slurry recirculation, high-velocity zones often occur at and near the inlet and injection nozzles, at locations of entrainment and at the surface where bubbles collapse. For mechanical mixing high-velocity zones are found at and close to the tip of impeller blades (Kariyama et al., 2018).

However, Wu (2010) reported that the possibility to achieve homogeneity using a lower mixing time, especially with a high organic loading rate in non-Newtonian fluids makes mechanical mixing a preferred option for optimization.

3.3.3.4 Reactor types

There are different AD reactor types used for the production of biogas. They can be grouped according to some operational criteria namely: mode of feeding, solid content matter treated, number of process phases of AD and the efficiency of the system.

1.) Mode of feeding operation

The feed in an AD system refers to the substrate containing the organic material that is converted to biogas. Regarding substrate feeding, there are three main types of reactors: batch, semi-continuous and continuous fed AD reactors (Slimane et al., 2016; Zhang et al., 2013). In a batch AD system, the AD mixture comprising the substrate and the inoculum is mixed and allowed to produce biogas until the end of the process without extra substrate addition. In a semi-continuous AD system substrates are added and removed from the reactor intermittently, for example once or twice daily. In a continuous AD system substrates are added continuously. The feeding system operates continuously during the AD process at a particular feeding rate. The semi-continuous and continuous systems have a high requirement for a pump to feed new substrate and take out effluent during operation. This sums up to a high energy input during the AD process. If DS suits as a good feedstock for biogas production it may be applied in all modes. This is however dependent on some factors which include storage space for DS in the plant, size of the digester and targeted biogas energy production.

2.) Solid matter content treated

The solid matter content in the reactor differentiates AD reactor types into wet or dry fermentation reactors. A wet fermentation reactor commonly operates with solid matter content of less than about 15% while a dry fermentation reactor with about 20 - 40% (Kusch-Brandt & Oechsner, 2005). Wet fermentation reactors are applied for e.g. wastewaters with low dry matter content while dry fermentation reactors for fibrous materials with high solid contents. Pumps can be applied in the feeding system for wet fermentation due to the low amount of solids but not in dry fermentation. The mixing ability of wet fermentation either through pumps or agitators gives it a high biogas production. The dry fermentation does not use or require a pump as critical equipment for operation (Marjolaine, 2021). DS is known to have a high or low dry matter content depending on dewatering. Those with the low dry matter may be suitable for wet fermentation and the others for dry fermentation provided they have sufficient organic matter in them.

3.) Process phase stages

When all the four phases of AD (section 3.3.3.1) are allowed to occur in a single reactor, this type of AD reactor is called a single-phase reactor. Due to the variation in the kinetics of the various AD phases the hydrolysis phase is very slow. It is also possible to operate a system where only the first two stages of biodegradation (hydrolysis and acidogenesis) take place in one reactor (Demirel & Yenigün, 2002). This is done by adjusting the pH to fairly acidic conditions so that the AD process does not proceed to acetogenesis and methanogenesis. After this, a second stage is carried out in a second reactor. A neutral pH condition is set for the effluent of the first stage. This allows the acetogenesis and methanogenesis to proceed leading to biogas formation. This type of system is referred to as a two-stage AD (Damayanti et al., 2019).

4.) Efficiency of the system

This classification type groups AD reactors according to their efficiency. The three groups are the passive, low rate and high rate systems. The passive system includes covered lagoons in which biogas production is carried out (McCabe et al., 2014). They do not involve temperature regulation and operate in the natural atmospheric temperature (Safley & Westerman, 1988).

Low rate systems are systems in which containers or vessels are used to contain AD mixtures. Temperature is regulated and leads to better biogas production when compared to passive systems. Low rate system AD reactors include also continuous stirred tank reactors (CSTR) (Boe & Angelidaki, 2009) and plug flow reactors (Teng et al., 2014).

In the high rate systems, the anaerobes are trapped in the AD reactor to increase efficiency either by recirculating anaerobes or allowing them to grow on surfaces immobilized in the reactor. High rate systems include fixed film digesters (Steinberg et al., 2017), up-flow anaerobic sludge blanket (UASB) digesters (Chong et al., 2012) and sequencing batch digesters (Elamin & Gasmelseed, 2018). UASB digesters are suitable for substrates with a high amount of suspended solids and a low amount of settleable solids. DS has a very high amount of settleable solids. It may not be suitable for DS. The CSTR, the fixed-film digester and the sequence batch reactor are options to be considered for the use of DS as a feedstock for biogas production.

3.3.4 Kinetic models for anaerobic digestion processes

A knowledge of the thermodynamics and kinetics of chemical and biochemical reactions can provide information on the course of AD processes. While thermodynamic properties are required to determine the reaction direction as well as energy and entropy changes, kinetics describe the speed at which a simple or complex chemical or biochemical reaction proceeds.

A biomethane yield test that involves the determination of the biomethane yield of substrates such as DS is a complex reaction that is costly and time-consuming during execution.

A kinetic model adapted to the AD of DS could be an alternative method to the biomethane yield test. It is also important in monitoring the kinetics of AD of DS in a continuous AD system. Kinetic modelling of AD processes was motivated by the need for efficient operation of anaerobic systems in the early 70s (Gavala et al., 2003). According to the review by Kythreotou et al. (2014) on AD models, a variety of models with varying purposes have been designed for the AD process. In their work, they identified and divided existing mathematical models for the AD process into three groups namely: models on theoretical biogas yield, models with reaction kinetics and the IWA anaerobic digestion model 1 (ADM1). The theoretical models determine gas composition through the chemical composition of the feedstock. The reaction kinetics models are centred on bacteria growth by using the Monod equation. Unlike the theoretical biogas yield and reaction kinetics models, the ADM1 includes multiple steps describing the biochemical and physicochemical processes of AD.

Velázquez-Martí et al. (2019) also worked on the review on models applied in the AD process. They grouped the models into 5 categories, namely exponential models, the Gompertz model, kinetic models, models based on the transfer function and the cone model. The exponential models are based on bacterial growth and fit the groups of models of reaction kinetics as reported by Kythreotou et al. (2014). The one and two steps first order kinetics, the modified Gompertz kinetics, the transfer function and the logistic function models are explained in section 4.8.2.1.

3.4 Calcium carbonate recovery

This section discusses the properties of calcium carbonate as a filler in paper and as a supplementary building material. It also discusses some material valorization options of calcium carbonate found in DS.

3.4.1 Calcium carbonate

Calcium carbonate is a substance with the chemical formula $CaCO_3$ and appears as a white, odourless powder or colourless crystal and it is sparingly soluble in water (Kim et al., 2019). It occurs in both biological and geological sources. The biological sources include eggshells, snail shells and also most seashells. The geological occurrences are in polymorphs. The three polymorphs of calcium carbonate are vaterite, aragonite and calcite. Based on structure, the polymorph with the highest thermodynamic stability is calcite. Also, it has the highest occurrence in nature and next is aragonite (Ni & Ratner, 2008).

The scratch hardness of calcite is 3, according to the Mohs scale of mineral hardness (William, 2000). Its density is 2.71 g/mL and its melting point is 1.339 °C (Al Omari et al., 2016).

Calcium carbonate exists in two main types, ground calcium carbonate (GCC) and precipitated calcium carbonate (PCC). The GCC is produced directly from the mining of limestone while the PCC which is a purer form of calcium carbonate produced industrially by the decomposition of limestone to calcium oxide and followed by a recarbonisation step (Kim et al., 2019). The PCC which is also termed synthetic calcium carbonate (SCC) can be produced from waste with high calcium carbonate content (Krigstin & Sain, 2006). Figure 3.4 shows the chemical structure of calcium carbonate. Calcium ion binds ionically with CO_3^{2-}. Also, a covalent bond exists between carbon and oxygen atoms in the carbonate ion. These properties of calcium carbonate allow it to be suitable for a wide range of use. It is the most extensively used filler in paper, paint, plastic, food, ceramic, cosmetic, and pharmaceutical industries (Erdogan & Eken, 2017; Khanna & Xanthos, 2010).

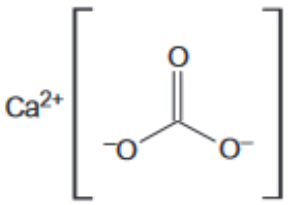

Figure 3.4 Structure of calcium carbonate (Al Omari et al., 2016)

It is also used in food additives and ingredients as well as a component of bone substitutes in medical science (Chen et al., 1999; He et al., 2015; Monchau et al., 2013). The properties of calcium carbonate discussed further as applicable to this study are its properties as filler for papers and properties as a supplementary building material.

3.4.2 Properties as fillers in paper

Fillers are particulate materials that are added to papers either to make them achieve the desired properties or to reduce cost or a combination of both (Dong et al., 2008; Hubbe & Gill, 2016). Calcium carbonate due to its physico-chemical properties is often used in paper as filler. Due to the varying characteristics and properties of different types of calcium carbonate, specific types are selected to meet desired qualities in a paper application (Ni & Ratner, 2008). The economical aspect of the use of calcium carbonate in paper production is becoming more important and its use in the European wastepaper recycling industry has continued to increase. The high demand for calcium carbonate in CEPI countries was mentioned in section 2.3.3.3.

3.4.3 Properties as supplementary building material

Calcium carbonate is widely known for its filling effect. It has been shown by some authors that calcium carbonate is not an entirely inert material. Its properties as a supplementary building material have been studied and reported by different authors (Kakali et al., 2000; Péra et al., 1999; Wang et al., 2012). Reports have shown that calcium carbonate promotes an accelerating crystallization effect on tricalcium silicate (C_3S) and cement hydration (Kakali et al., 2000; Péra et al., 1999). The C_3S and the C-S-H are the determinants of the strength of cementitious mortar. Cement hydration is the reaction process of cement and water that leads to the hardening of the cement. It is therefore worthwhile to investigate the suitability of the calcium carbonate present in DS to understand its suitability as a supplementrary building material.

Portland cement made from limestone and clay with some amount of gypsum is reported as the simpliest cement and is widely produced (Habert, 2013; Helmuth et al., 2000). Many authors have studied portland cement and have shown the influence of its particle size on the hydration and strength of hardened cement paste (Argiz et al., 2018; Osbaeck & Johansen, 1989; Zhang & Napier-Munn, 1995). Argiz et al. (2018) reported that for given water to cement ratio (w/c), the finer the portland cement is milled the better is its hydration rate and promotion of high early strengths.

3.4.4 Material recovery from deinking sludges

DS contain a large amount of calcium carbonate, which should be sustainably managed by recovery. Sustainable waste management broadly considers approaches such as energy utilization, material inertisation, and recycling or reuse.

The hierarchy of waste from Directive 2008/98/EC describes waste lifecycles towards a sustainable economy. Waste recycling was identified in the pyramid as an important option. The recycling approach essentially enhances a shift from the conventional linear economy to a circular economy. It does not only contribute to the reduction of raw material demand but also largely reduces the energy consumption and gaseous emissions resulting from the extraction and processing of raw materials.

Recycling of waste in the pulp and paper industry has been studied by different authors (Deviatkin et al., 2015; Kujala, 2012; Monte et al., 2009; Ochoa de Alda, 2008; Seyyedalipour et al., 2014; Sudarshan et al., 2017). The study of Deviatkin et al. (2015), was extensive in the sense that different pathways of material recovery from DS were identified. The pathways of material recovery include direct applications and the recovery of inorganics in DS for further application. These recovery approaches are geared towards the rich mineral composition of DS which is mainly determined by calcium carbonate.

Table 3.5 lists the different pathways as reported by Deviatkin et al. (2015). The direct application approach utilizes dried DS to either make cement-based or other types of products. The calcium carbonate of DS is as a supplementary material for the binders in the products. In the pathways which involve the conversion of DS into single products, DS is treated thermally to either remove unwanted material or to transform some essential components into a useable form. For DS to be suitable as a pozzolona as repoted by Deviatkin et al. 2015, it is expected that it contain sufficient amorphous siliceous or siliceous and aluminous material which react with calcium hydroxide in the presence of water to create cementitious hydration products such as calcium silicate hydrates and calcium silicate aluminate hydrates (Walker & Pavía, 2011).

Table 3.5 Different recovery pathways for DS from wastepaper recycling (*based on Deviatkin et al. (2015)*)

Direct application	Conversion into products
Cement and cement-based products	Carbonization
Ceramic products (bricks, lightweight aggregates, tiles)	Vitrification
Wood-based panels (fibreboards, particleboards, millboards, cement bound boards)	Supercritical water oxidation
Stone wool	Pozzolana
Plasterboards	Composite materials
	Animal bedding /litter
	Synthetic calcium carbonate

3.5 Research strategy

To answer the research questions (section 1.0), the strategic flow diagram drawn shows the hypothetical treatment of DS which is investigated in this study (Figure 3.5). The diagram considers DS as a resource flowing into a treatment scheme to produce renewable energy in the form of biogas and as well utilizing its high $CaCO_3$ content as a supplementary building material in a further process step. This energetic and material valorization of DS is expected to improve the sustainability of the wastepaper recycling industry.

Figure 3.5 considers the generation of raw DS, which is first dewatered to increase its dry matter content. The thickened sludge (pre-dewatered DS) then serves as an input into the AD process. The AD process produces the biogas which can be used, for example, to cushion the high heat demand of the industry. The effluent of the AD process (digestate) comprises water, hardly biodegradable organic solid fractions and the inorganic solid fractions.

The inorganic solid fraction which is the main component of interest in the digestate contains majorly $CaCO_3$. The digestate can be treated by drying and burning to remove the water and hardly biodegradable organic solid fractions.

This allows for the recovery of ash that is rich in $CaCO_3$ and can be used as a supplementary building material.

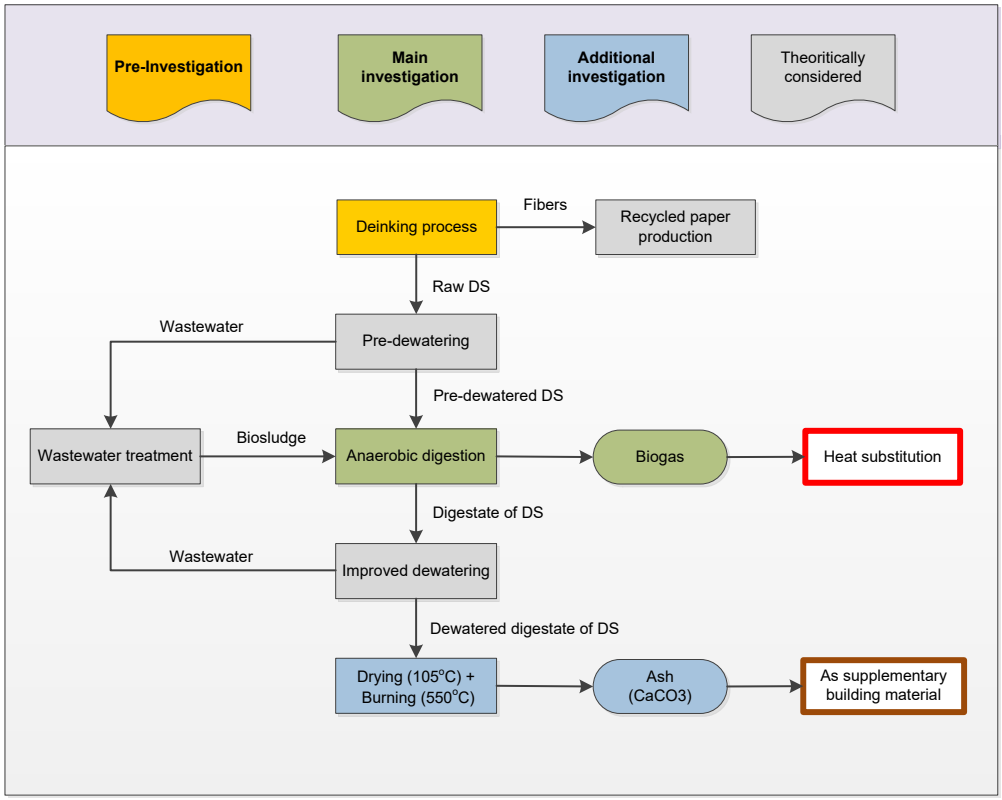

Figure 3.5 Strategy for the energetic and material valorization of deinking sludges

The six groups of substrate studied are:

1. DS
2. DS derivatives
3. Biosludge
4. DS-digestate
5. Ash of DS
6. Ash of DS-digestate

The DS and DS derivatives refer to the raw DS and other streams of DS generated by the partner wastepaper company due to the dewatering treatment process (Figure 4.1, Appendix A.6). The biosludge is an effluent of the biological wastewater treatment plant where DS and other wastewater types are fed as influents.

The DS, DS derivatives and biosludge were supplied by the partner wastepaper recycling company. The DS-digestate is an output of own anaerobic treatment studied. The ash of DS and DS digestate were generated by drying and incinerating their respective fresh samples.

Also, inoculum from different existing anaerobic digestion plants was investigated but these do not fall into the main category of the investigation. Pictures of DS, Digestate of DS, Ash of DS and Ash of Digestate of DS are shown in Appendix A.5.

CHAPTER 4 MATERIALS AND METHODS

The materials and methods begin with an overview of the research methods and the classification of the different types of DS and their derivatives in the partner wastepaper recycling company. This is followed by a detailed description of the methods used to investigate the valorization of DS. The chapter discusses the methods used to characterize the DS and its derivatives, the experimental approach to investigate the energetic and material valorization of DS, the dewaterability of DS and its digestate, modelling the AD of DS and the approach for the design of different treatment scenarios for DS.

4.1 Research methods

Table 4.1 gives an overview of the investigations and the parameters analysed. It also highlights the substrates investigated. It includes a comprehensive list of research methods, starting from sample characterization and various AD tests, followed by solid-liquid separation of DS and DS-digestate, an investigation of the properties of DS and DS-digestate ash as potential supplementary building materials, modeling of AD for DS, and finally, the design of different treatment scenarios for evaluating the novel DS treatment approach. These experimental investigations are also part of the research approach. The investigation also adopted a modelling approach for the AD of DS. The possible practical applications of the novel treatment approach for DS are discussed using process flow scenarios.

Table 4.1 Overview of investigations

Investigations			
1			Characteristics of DS, DS derivatives and inoculum: DM, oDM, ash content, $CaCO_3$, pH, TC, TN and TEs
2			Anaerobic digestion of DS & derivatives
	a.		Batch tests usng 1-L bioreactors
		i.	The adaptability of DS with common inocula
		ii.	Influence of high $CaCO_3$ on DS digestibility
		iii.	Influence of water content on DS digestibility
		iv.	Influence of wastepaper grades on DS digestibility
		v.	Influence of nitrogen supplementation
	b.		Semi-continuous tests using 100-L bioreactors
		i.	Studies on HRT and OLR
3			Modelling of AD of different DS streams
	a.		Model fitting for AD of DS
	b.		Model comparison and best model selection
4			Characteristics of DS-digestate: DM, oDM, ash content, $CaCO_3$, pH, TC, TN, COD
5			Solid-liquid separation of DS and DS-digestate
	a.		Wet sieve analysis
	b.		Sedimentation analysis
	c.		Centrifugation analysis
6			Characteristics of DS and DS-digestate ashes Particle size distribution, chemical composition and determination of phases
7			Material valorization of DS and DS-digestate by recovery of $CaCO_3$
	a.		Characterisation of ash of DS and DS-digestate
	b.		Test of density and flow value
	c.		Test of flexural and compressive strength
8			Mass flow scenarios of DS application for biogas in plants
	a.		Comparison of scenarios for the energetic and material valorization of DS
	b.		Estimation of biogas energy and calcium carbonate potentials of DS

4.2 Classification of wastepaper

The wastepaper types used are described in Table 4.2. The Table also gives information about the codes used for the DS samples in this study. They are based on the wastepaper used as input. The codes *W70*, *W80* and *W90/100* are used to describe the different categories of DS types generated by the partner's wastepaper recycling plant.

Table 4.2 Classification of DS samples with regard to wastepaper inputs and corresponding recycled paper qualities of partner wastepaper recycling company

Sample code in study	**Wastepaper**			**Recycled paper**
	Grading	*EN-643 Code*	*Types used in the facility*	*ISO-Brightness*
W70	Ordinary	1.06.00	Unsold magazines	70
		1.11.00	Sorted graphics for deinking	
W80	Medium	2.03.01	Lightly printed white shavings with or without glue	80
W90/100	Medium	2.05.00	Sorted office paper	90
	Medium	2.08.00	Coloured wood free magazines	
	High	3.10.00	Wood free, coated, lightly painted, free from wet-strength paper or paper coloured in the mass	100

The numbers behind the letter “W” in the sample code correspond to the ISO-brightness of the targeted recycled paper. The targeted ISO-brightness of recycled paper determines the quality of wastepaper required as input for wastepaper recycling. The DS samples with code *W70* were generated during the wastepaper recycling process that utilizes mainly two types of wastepaper grades “*1.06.00*” and “*1.11.00*”. They both belong to group 1 of the wastepaper grades termed ordinary grades as classified by CEN. DS samples with the code *W80* were generated from the use of medium (*2.03.01, 2.05.00*, *2.08.00*) and high grades (*3.10.00*) wastepapers. The DS samples with code *W90/100* as well, were generated from the use of medium and as well high-grade wastepapers. Although the DS from samples *W90* and *W100* have different wastepaper input and chemical additives, they have been grouped in this study due to chemical similarities and limited quantity produced.

4.3 Classification of deinking sludges and streams investigated

Figure 4.1 is a simplified flow, showing the treatment of DS in the partner’s wastepaper recycling company. The simplified flow is the basis of the analysis of the valorization of DS as investigated in this study. It is relevant to mention here that the treatment steps as shown in Figure 4.1 are not always the same with all deinking plants. The selected treatment of DS is from an award-winning wastepaper recycling company. The approach in the treatment of DS can therefore be considered a good practice.

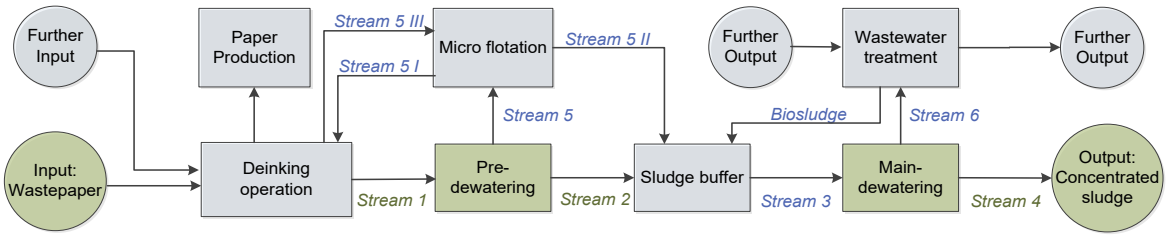

Figure 4.1 A simplified flow of DS with codes for the investigated streams

Figure 4.1 starts with the input of wastepaper as a resource into the deinking operation. Although the input into the deinking operation is preceded by some other wastepaper recycling steps as described in section 2.3.2, the simplified diagram has been drawn to visualize only the essential components for this study. The further inputs comprise mainly the process water and chemical additives used especially during the pulping stage. As the deinking operation leads to the generation of DS, the deinked pulps are further treated to produce recycled papers. Three main treatment processes specifically important to study after the generation of DS are dewatering, reuse of process water and wastewater from biological treatment.

The dewatering is done in three steps: pre-dewatering, microflotation and main dewatering. The pre-dewatering step takes in fresh or non-dewatered DS (*Stream 1*) as input into a dewatering device that operates by gravitation to produce a pre-dewatered sludge (*Stream 2*). The microflotation step involves the further removal of particles in the liquid fraction from the pre-dewatering (*Stream 5*). The main-dewatering step utilizes a winkle press to further dewater a mixed sludge (*Stream 3*) comprising *Streams 2, Stream 5 III and Biosludge* to produce a sludgy fraction *(Stream 4).* The reuse of process water is derived from the microflotation step which generates „clear water" that is further recycled into the deinking operation. The biological wastewater treatment step takes in the liquid fraction of the main-dewatering step (*Stream 6*) and chemical additives as further input and treats the containing organics by an aerobic process.

The output of the simplified flow of DS includes the concentrated DS derivative characterized by a high solid content and the discharged effluent from the wastewater treatment plant. The further treatment step of the concentrated DS adopted by the partner company is incineration (internal and external). The sludge is incinerated with the addition of RFD (refused derived fuel) due to the low calorific value of DS. The analysis of the incineration of the concentrated DS is beyond the scope of this study and therefore not included in the simplified diagram.

A further description of the different streams of the simplified flow which were used for the investigation as well as their codes in this study can be seen in Table 4.3.

Table 4.3 Description of DS and DS derivatives as obtained from partner wastepaper recycling company

Code	Sample characteristics	
	Type	**Description**
Stream 1	DS	Fresh, non-dewatered DS
Stream 2	DS	Pre-dewatered DS
Stream 3	DS + MS + BS	Pre-dewatered mixed sludge (DS with biosludge and micro flotation sludge)
Stream 4	DS + MS + BS	Highly dewatered mixed sludge (DS with biosludge and microflotation sludge)
Stream 5	DL	Turbid water from pre-dewatering
Stream 5 I	DL	Clear water from microflotation
Stream 5 II	MS	Microflotation sludge
Stream 5 III	DL	Turbid filtrate from disc filters of deinking operation
Stream 6	DL + BL	Filtrate from the main dewatering
Biosludge	BS	Sludge from biological wastewater treatment
DS-Deinking sludge; MS-Mixed sludge; BS-Biosludge; DL-Dewatering liquid; BL-Biosludge liquid		

The code for the various samples of DS and derivatives investigated in this study follows the below example designation (Figure 4.2).

Example of a designation

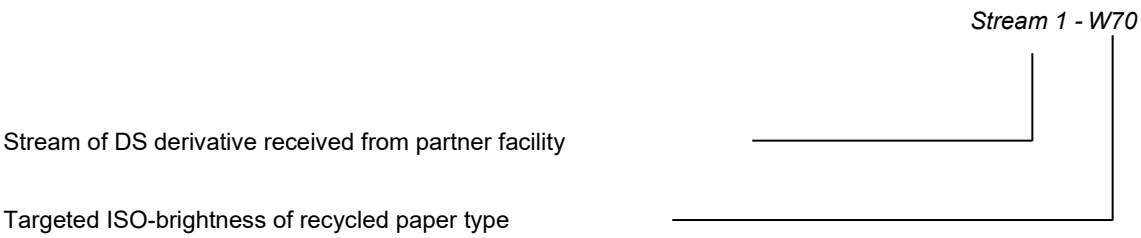

Figure 4.2 Example of code for describing different DS types investigated

The biosludge is a recycled stream from the wastewater treatment plant. It is generated from the mixture of different DS types and other process waters hence the biosludge sample is not denoted with a targeted ISO-brightness of recycled paper type.

4.4 Analytical methods

The physico-chemical properties of DS and its derivatives were determined to get information to assess the suitability for the production of biogas and for the use of the inorganic fraction which mainly consists of $CaCO_3$ as material for building reinforcement. The suitability for biogas generation was determined from the following properties: Dry matter content (DM), Water Content (WC), Organic dry matter content (oDM), C/N ratio, pH value, sulphur content as well as Trace element (TEs) content specifically Co, Ni, Se and Mo. The ash content and $CaCO_3$ content informs on the potential of usability as a supplementary building material. The overview of the analysed parameters is shown in Table 4.4.

Aside from the DS and the DS derivatives, the inoculum used for the AD test and the digestates generated were analysed for DM, oDM, ash, $CaCO_3$ and pH. Different equations were used to compute the different physico-chemical properties of DS and its derivatives into the units given in Table 4.4. The equations used are shown in Eq A.1 to A.9 (Appendix A.4). The various samples collected from the partner company and other sample types generated during this study are classified into three different groups as seen in Figure 4.3. The sludge comprises the DS and its derivatives as well as the inoculum used and the digestate generated. The gas category is the biogas generated during the anaerobic process while the solid category is the DS and DS-digestate ash which were used for the test for suitability as a supplementary building material. It further describes the different methods of sampling, sample storage and parameters analysed from the different samples collected and generated.

Table 4.4 Overview of analysed parameters with guidelines and equipment used for characterizing DS and its derivatives

Parameter	Unit	Guideline/ Equipment	Comments
Dry matter content (DM), Water content (WC)	% FM	DIN EN 12880: 2001-02 (2001)	15-20 mg fresh sample; drying at 105 °C overnight
Organic dry matter content (oDM)	% DM	DIN EN 12879:2001-02 (2001)	Samples analysed for DM were often used for oDM measurement
Ash content (Ash)	% DM		Computed from oDM value
$CaCO_3$	% DM	DIN EN 12880: 2001-02 (2001); DIN EN 12879:2001-02 (2001)	Samples analysed for oDM were often used for $CaCO_3$ measurement
C/N ratio	-	Centrate: C & N: Multi NC Analyzer Solid cake: C: ELTRA-Elemental Analyzer Fresh sample N: Buchi test	Centrifugation of fresh sample into centrate and solid cake Total C and Total N were computed by adding separately measured values of the individual phases A fresh sample was additionally analysed for N
COD	mg/L	Cuvette test by Hach Lange	Measurement range 15 -150 mg/L O_2
pH-value	-	pH-Meter [Model 323, WTW]	Liquid sample only analysed. The sample must be sufficient to submerge the pH sensor
TEs (Co,Ni,Se,Mo)	mg/kg DM	PE-Optima 700 DV OES with ICP and PE –Nexion ICP –MS	Samples are first dried at 105°C and analysed at the Central Laboratory of TUHH

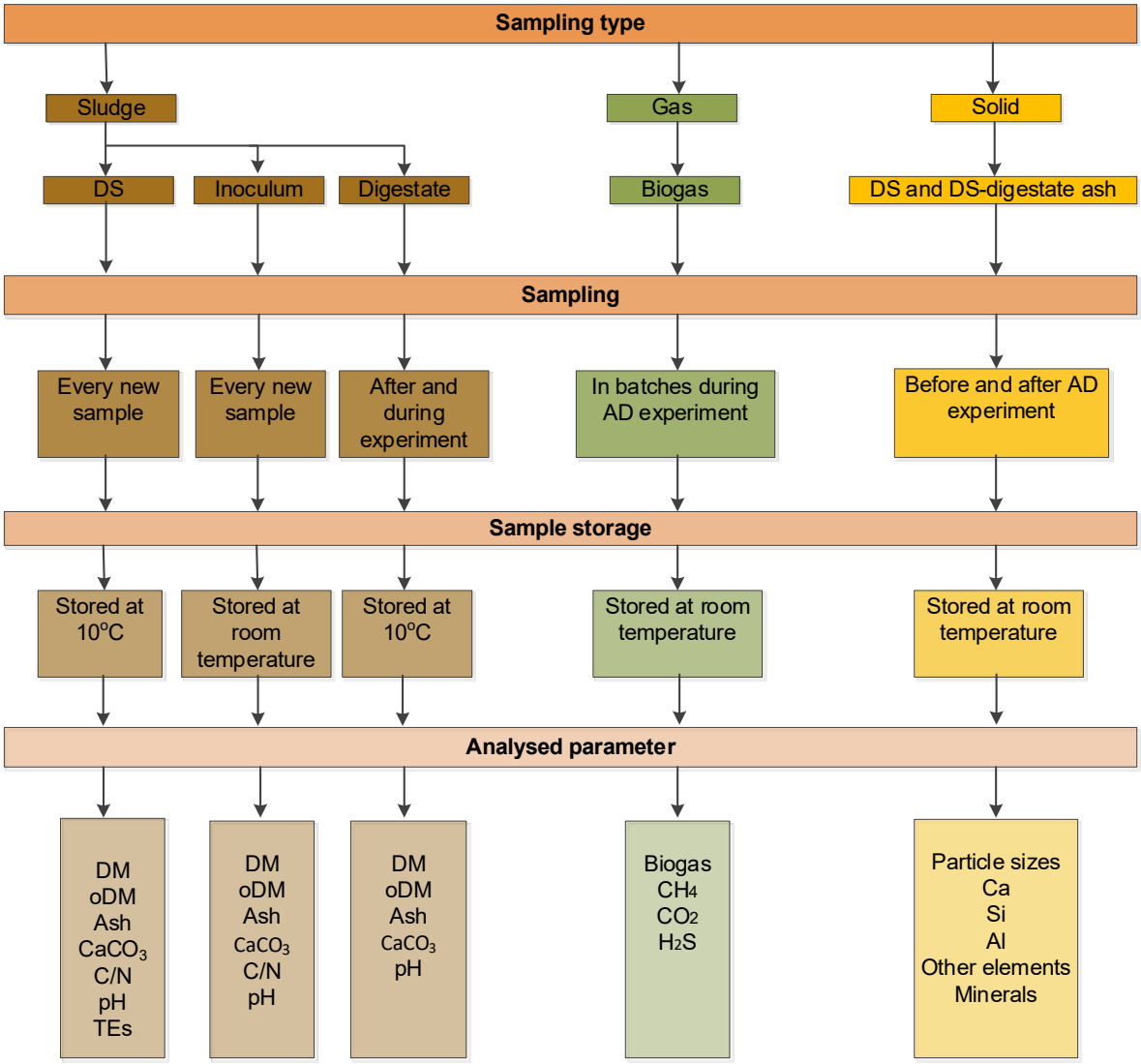

Figure 4.3 Overview of sample types

4.5 Energetic valorization of deinking sludge

The methods to investigate the energetic valorization of DS comprises the design of AD test systems, substrate characterisation, execution of AD experiments and the measurement of parameters required for AD process description.

4.5.1 Design of 1-L batch anaerobic digestion test system

The setup of the AD test system as shown in Figure 4.4 is a simplified diagram showing only one of the reactors. The system comprises an open rectangular shaped vessel (1), which seats on a metal frame (2). The vessel is filled with deionized water (3) which is heated and regulated at the desired temperature with the aid of a thermostat (4) and serves as the water bath. In the water bath, up to fifteen 1-L volume of Duran glass bottles were partly immersed.

The closed 1-Liter volume duran glass bottle (5) is the reactor that contains the AD mixture for an experiment. A seal is used between the cover of the glass bottle to allow for air and water tightness. The reactors are immersed in the water bath such that their content is submerged in the water to ensure a uniform distribution of heat in the AD mixture.

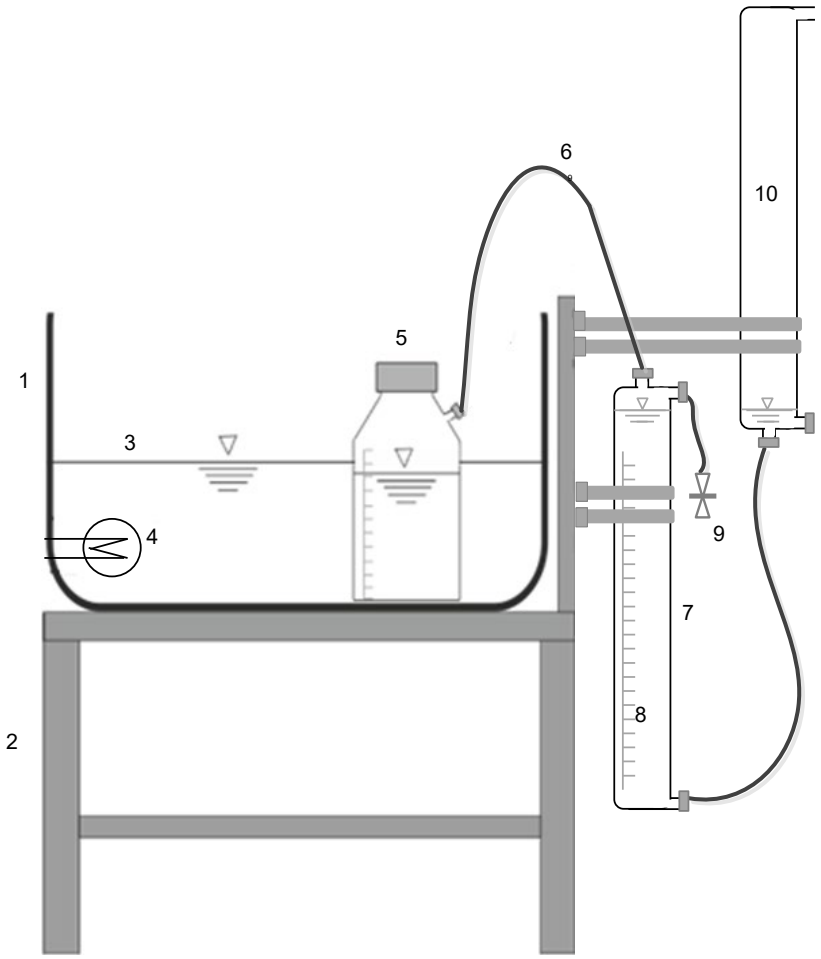

1.	Rectangular shaped vessel	6.	Gas tubing
2.	Metal frame	7.	Eudiometer
3.	Water	8.	Eudiometer liquid
4.	Heater with thermostat	9.	Coupler
5.	Reactor	10.	Barrier solution glass cylinder

Figure 4.4 Simplified diagram of the 1-L AD test system (not to scale)

For a better homogenization of the reactor content, the reactors were shaken manually daily. The reactors are connected via their gas outlet with gas tubing (6) to a graduated glass cylinder. The graduated cylinder is the eudiometer (7) which is filled with water that is saturated with salt and coloured with methyl orange (8).

The eudiometer indicates the volume of biogas produced. When the pressure of produced biogas builds up in the reactor it push the liquid into the graduated glass cylinder downwards. This change of gas volume represents the biogas volume produced in the specified period. To determine the quality of biogas produced, biogas samples are taken through the coupler (9) attached to the gas tubing and connected to the eudiometer. The content of the ungraduated glass cylinder (10) attached to the graduated glass cylinder is the same as the eudiometer liquid but serves as a barrier solution and opens to the atmosphere. The components of the 1-L AD test system and their suppliers are described in Appendix B.1. The pictorial view of the test system is also available in Appendix B.2.

4.5.2 Automatically fed 100-L anaerobic digestion test systems

This section discusses the design of the automatically fed 100-L AD system and the process control for the operation of the systems.

4.5.2.1 Design of 100-L anaerobic digestion test systems

Three AD test systems were designed to investigate the AD of DS in a semi-continuous process. Table 4.5 shows the difference between them and the operation parameters of the AD tests carried out with them.

Table 4.5 Difference in the three bioreactors designed and investigated

100-L bioreactor	Stirrer installed	Recirculation pump	Inclination of the bottom to the outlet	Operation parameter	
				HRT	Duration of operation
			[°]	[d]	[Weeks]
R1A	No	Yes 170 - 1000 L/ h	5	30, 25, 20, 15	50
R1B	No	Yes 100 - 3000 L/ h	45	19	6
R2	Yes	No	5	19	6

The design of the bioreactors considers the bioreactors in two groups: bioreactors with a recirculation pump (R1A and 1B) and with a stirrer (R2). The discussion is done based on the principal and attached components of bioreactors.

1.) Principal components of bioreactors

The designs of the bioreactors are shown in Figures 4.5 and 4.6. Their pictorial view is available in Appendix B.3 and further information on their components can be seen in Appendix B.6.

Aside from the difference in their mixing mechanisms, both systems were designed with several similar principal components. They are made up of a 100-L double jacket vessel (1). The outermost layer is made of stainless steel. The outermost layer and the first jacket consist of an insulator (2) to prevent heat loss due to conduction. The first jacket holds water which is heated and regulated by a thermostat (3) at the desired temperature.

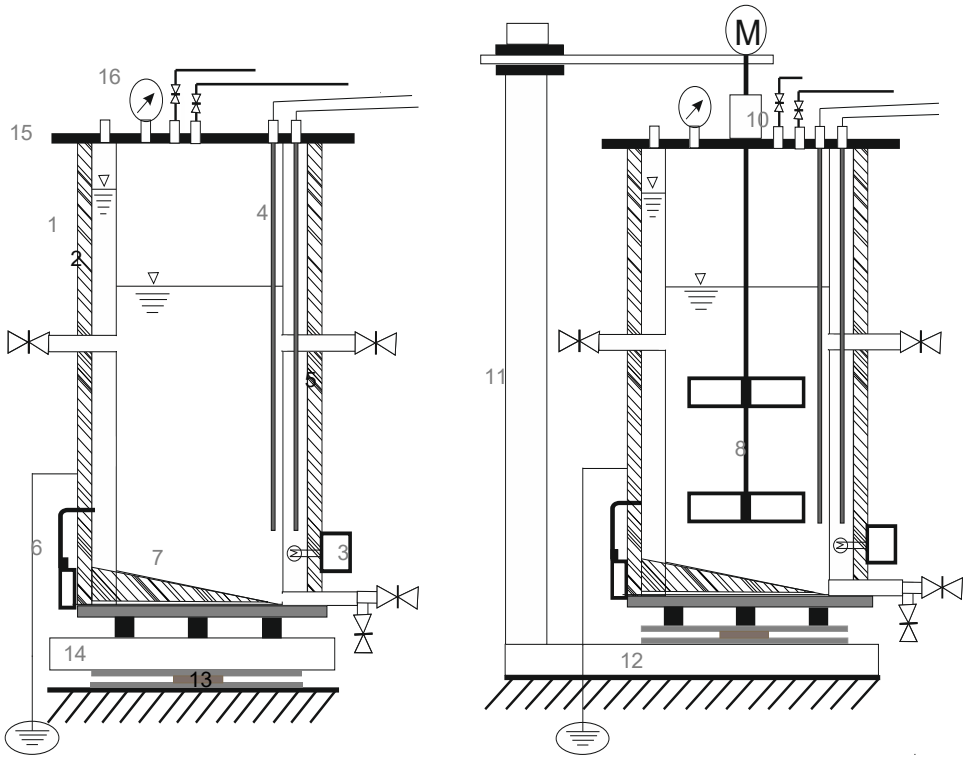

1.	Cross-section double jacketed reactor	9.	Electric motor
2.	Insulator	10.	Clutch
3.	Heater with thermostat	11.	Stand for electric motor
4.	Temperature sensor 1	12.	Metal platform
5.	Temperature sensor 2	13.	Weighing balance
6.	Recirculating water pump	14.	Pallet
7.	Inclined bottom	15.	Cover
8.	Paddle stirrer	16.	Bourdon gauge

Figure 4.5 Components of 100-L bioreactor R1A and R1B (left) and R2 (right) (not to scale)

The second or inner jacket holds the bioreactor content or the AD mixtures. The temperature of the bioreactor content and the water jacket are measured by a PT100 sensor (4 and 5). The content of the water jacket is recirculated with the aid of a small attached recirculating water pump (6) to allow for even heat distribution.

The cover of the bioreactor seats on a ring seal which is designed to make the bioreactors airtight. The R1A and R2 have a bottom inclined (7) at 5°, while R1B has an inclined bottom of 45°. The inclined bottom of R1B is made with a PVC material and padded with extruded polystyrene material. The R2 has an installed double paddled stirrer (8) attached to an electric motor (9) used for mixing. The motor is attached through a clutch (10) to the stirrer with a damping effect made from plastic material. The motor is held fixed by a stand (11) which is attached to a metal platform (12) to ensure the stability of the system required for weighing.

The entire bioreactor vessel seats on a weighing balance (13) to measure the bioreactor's content. For the R1A and R1B the weighing balance is placed on the floor via a plastic pallet (14) without fixing it. For R2, the metal platform carries the weighing balance. The cover (15) of the bioreactors has three main gas outlets. One outlet connects to the gas manometer (16) for measuring the pressure of gas in the bioreactor vessel.

2.) Attached components to 100-L bioreactors

The attached components refer to equipment that are not the main parts of the bioreactor but are attached externally to ensure the proper functionality of the AD system. They are similar for all bioreactors except for the pump-type attached. Beginning with the solenoid valve 1 (17) attached to the second outlet at the cover which is designed to open when feeding in the substrate to allow for pressure equalization in the reactor vessel. It connects to a gas bag filled with nitrogen (18). The third gas outlet connects the first to the second solenoid valve 2 (19) and then to a first gas scrubber (20) before a biogas flow meter (21). The first gas scrubber allows for the cooling of biogas to room temperature and possible removal of condensed water in biogas coming from the bioreactor. After the measurement of biogas volume by the biogas flowmeter, the biogas passes through a second and third scrubber (22) before being stored in a biogas bag (23). The second gas scrubber serves as a water trap for the third gas scrubber. The third gas scrubber is partly filled with water and serves as a pressure barrier to prevent the building up of negative pressure at this point. With this setup, the pressure of the system remains roughly at ambient atmospheric pressure. The biogas quality analyser (24) measures the main components of biogas which are methane and CO_2. The mixing of the bioreactors with the recirculation pump is carried out by a progressive cavity pump-1 (25). The R1A has a pump with a capacity of 170 - 1000 L/h while R1B has a capacity of 100 - 3000 L/h. The feed tank (26) of the bioreactors holds the influent which is kept homogeneous by a feed tank stirrer (27). The effluent tank (28) holds the digestate. The transport of substrate and effluent in and out of bioreactors is done with the combination of a pump and two ball valves (29 and 30).

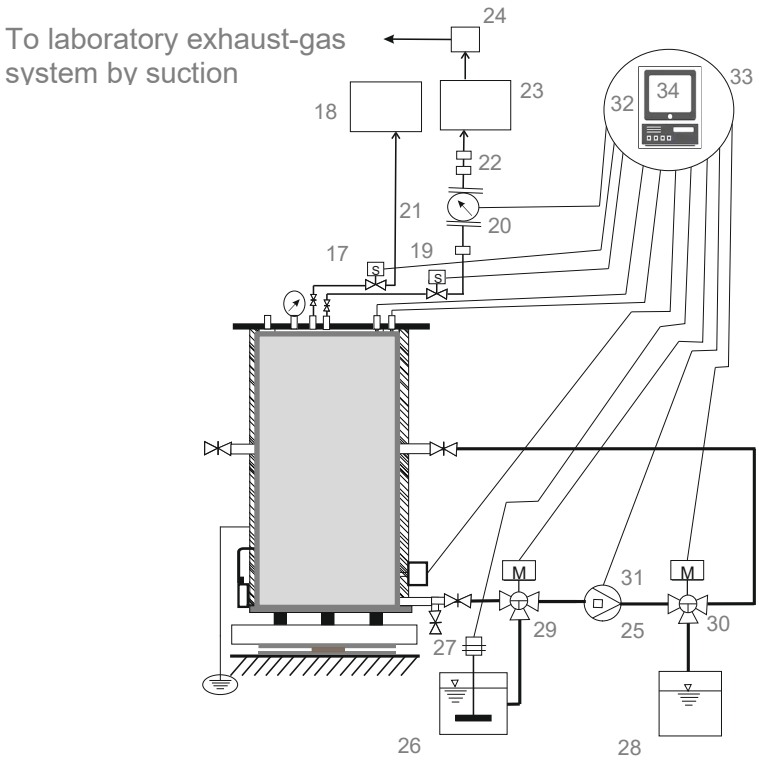

17.	Solenoid valve 1	26.	Feed tank
18.	Nitrogen gasbag	27.	Feed tank stirrer
19.	Solenoid valve 2	28.	Effluent tank
20.	Biogas scrubber 1	29.	Control ball valve 1
21.	Biogas flow meter	30.	Control ball valve 2
22.	Biogas scrubbers 2 and 3	31.	Progressive cavity pump-2
23.	Biogas storage bag	32.	Data logger
24.	Biogas quality analyser	33.	Control box
25.	Progressive cavity pump-1	34.	Computer

Figure 4.6 Components attached to the 100-L bioreactors (not to scale)

The R1A and R1B use the same progressive cavity pump-2 for mixing while the R2 uses a progressive cavity pump-2 with a capacity of 5 - 25 L/h (31). The systems have a data logger (32) which measures environmental parameters such as atmospheric temperature and pressure. The systems have a control box (33) and the computer (34) is used to run the LAB-VIEW program for process control. The process control of the 100-L automatically fed AD test system is further discussed in detail in section 4.5.2.2.

4.5.2.2 Process control system

The process of automatic operation and control of the 100-L AD test systems is explained in this section. It covers the description of the graphic user interface, the temperature measurement, the feeding and effluent removal as well as the biogas measurement.

4.5.2.2.1 Graphic user interface of the process control system

The process control systems of the automatically fed 100 L bioreactors were operated with the aid of the LabVIEW Software (2017). The LabVIEW software developed by National Instruments is a workbench for data acquisition, instrument control and industrial automation. The software allows the design of a graphic user interface (GUI) that aids the easy visualization and control of instruments. The design and the electrical works of the process control system were done through a collaborative effort with the electrical department of the research workshop of the TUHH. Figure 4.7 shows the GUI for the system with a stirrer. The menus and relevant sections of the GUIs are explained in the following. The words with "*" are translated. The original German words used in the LabVIEW GUI are shown in the foootnote.

1.) Reactor control[3]: This is the first menu from the left. It displays a pictorial representation of the bioreactor and components involved in the process flow of substrates and biogas. It indicates the operation mode which is either manual or automatic as well as notifies a batch or semi-continuous process. It also indicates the weight of the reactor content and the working mass. The working mass is a constant mass set for the bioreactor's content. It is stored in the initialization data of LabVIEW. Other important data indicated include biogas production, atmospheric pressure and room temperature.

2.) Graphical representation[4]: This menu displays the graph of temperature in the water jacket and in the reactor content versus time. It also shows the graph of biogas produced versus time and the cumulative biogas production with time.

3.) Time and stirrer system[5]: This menu displays the dialogue boxes where input values to set feeding operation parameters are entered. These main input values are feed mass of substrate, duration of a complete cycle, duration of recycling bioreactor's content (via pumping), duration of stirring reactors content and duration of pump idle state. The duration of stirring of the content of the feed tank before the feeding operation can also be entered here.

[3] Reaktorsteuerung
[4] Yt –Reaktor
[5] Zeiten & Rührwerke

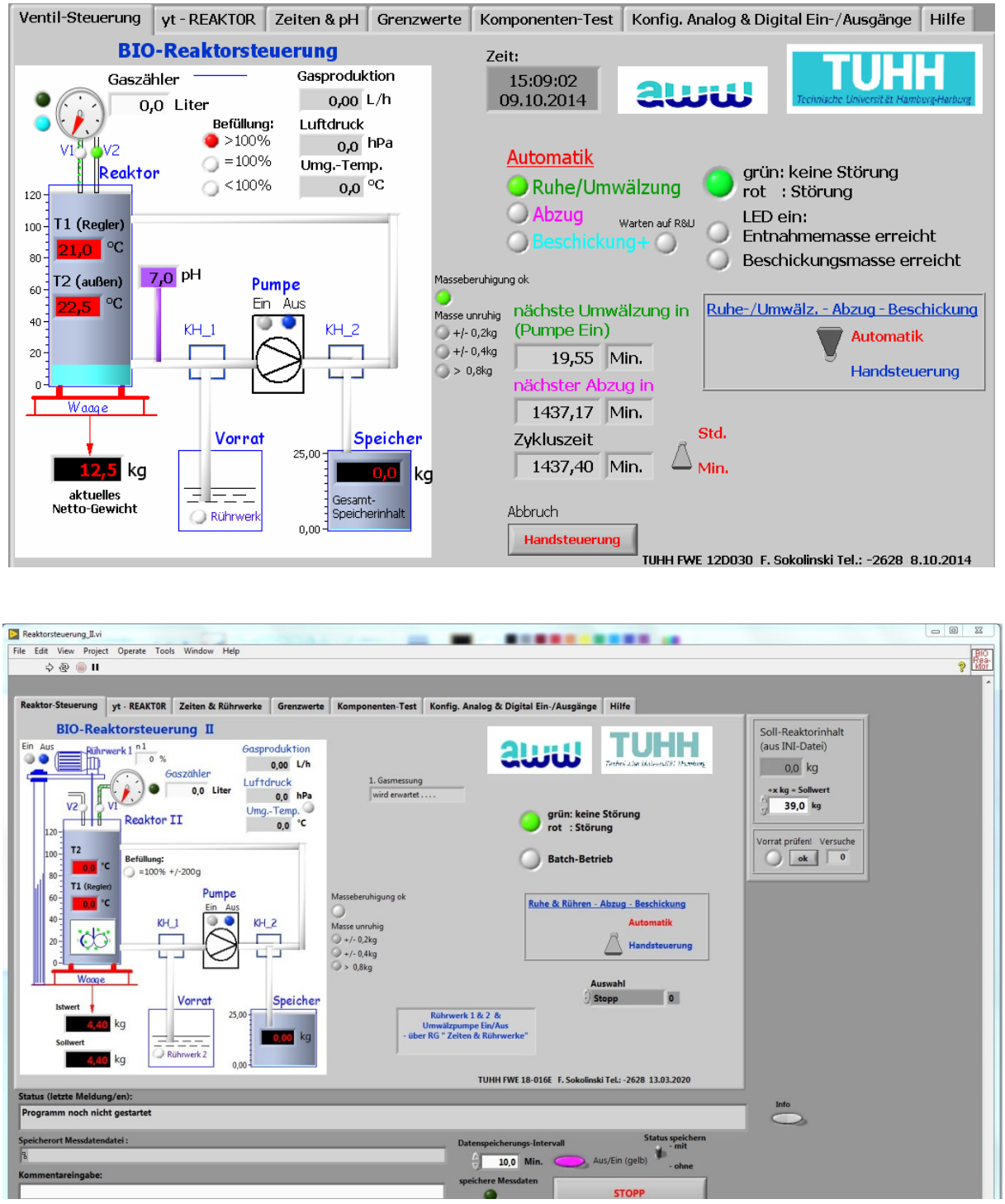

Figure 4.7 The LabVIEW graphic user interface for control of the 100-L bioreactors. Top: Bioreactor without a stirrer. Bottom: Bioreactor with a stirrer (Sokolinski, 2014, 2019).

4.) Limit values[6]: This menu allows the input of limit values necessary for operating the process within a tolerable range. It includes the maximum and minimum temperatures of the bioreactor's content and the maximum and minimum values of the weight balance. The amount of feed, effluent per cycle (day) and maximum volume of effluent container can be entered here.

5.) Component test[7]: This menu displays the location where some relevant components of the process control system can be tested for effective signal reception. This test is required when the system is started newly after being idle or not being in operation for a long-given period of time. The components that can be tested include the two ball valves for feeding, the two magnetic valves, the dataloger device (Extech SD70), the pump, the weight balance and the watchdog (digital communication detector).

6.) Configuration (analog & digital outputs and inputs)[8]: This menu displays the analogue input data from the temperature sensors and the weight balance. It also displays the reactor initialization data (mass of the empty reactor).

7.) Others status[9]: This is not a menu but is displayed on the GUI. It informs on the last error message and the location of data storage during the operation of the system. The error message helps for an early and quick reaction such as adjustment or repair where necessary.

4.5.2.2.2 Temperature control system

The main components of the temperature control system include two Pt 100 temperature sensors, a universal PID temperature controller (UR4848), a transmitter, a Labjack U12[10], a thermostat, a water jacket, a recirculation pump and the LabVIEW software. Figure 4.8 shows the signal flow within the temperature control system. The temperature sensor (Pt 100_1) is placed in the water jacket of the double jacket bioreactor while the temperature sensor (Pt 100_2) is placed in the inner jacket which contains the bioreactor's content. They are both placed below half of the height of the bioreactor. The heating element of the thermostat is placed in the water jacket while the recirculating pump helps to distribute heat within the water jacket. As seen in Figure 4.8, the UR4848 receives input data from the Pt 100_1 and controls the temperature based on the set value. The data from the UR4848 is sent to the LabVIEW via the Labjack U12.

---

[6] Grenzwerte
[7] Komponenten Test
[8] Konfig- Analog & Digital Ein /Ausgänge
[9] letzte Meldung/en und Speicherort Messdatetendatei
[10] Portable data acquisition and control system

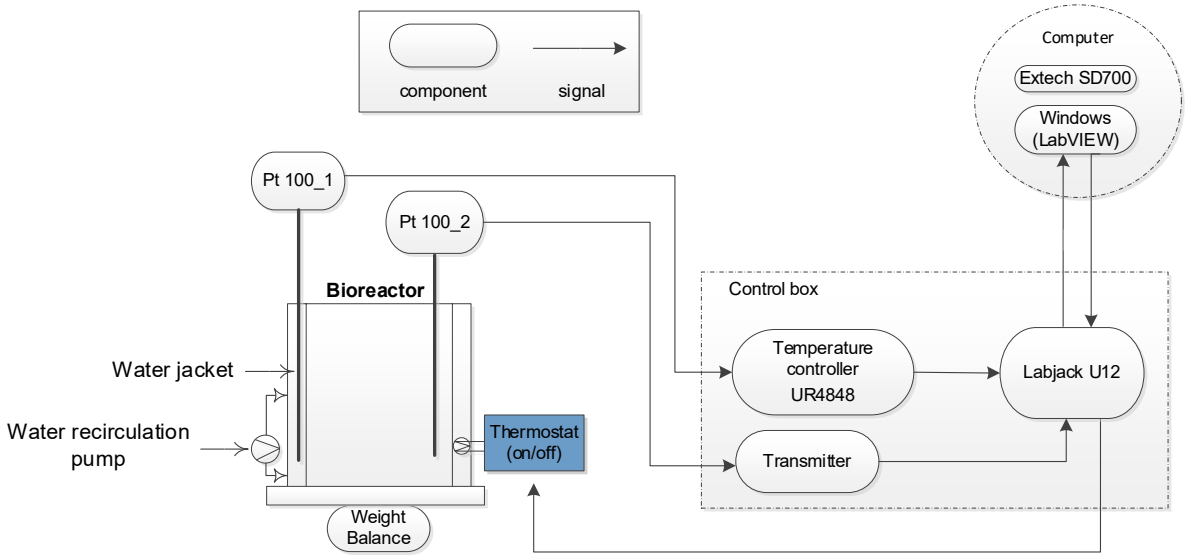

Figure 4.8 Components and flow of signals for temperature control

The control process of the UR4848 is achieved by comparing the set value (temperature) and the Pt 100_1 data (temperature) at any time. The Labjack then communicates this with the thermostat which leads to either putting the thermostat on or off depending on what is required. The data of the Pt 100_1 at any time is displayed on the UR4848 and also via LabVIEW. The temperature control is achieved with a deviation of ± 1 K. The input data from Pt 100_2 (temperature of the bioreactors' content) at any time is transmitted and sent to the Labjack U12 and displayed via LabVIEW. A detailed signal and temperature control diagram is available in the process control documents of bioreactors (Sokolinski, 2014, 2019).

4.5.2.2.3 Feed operation control

The feed operation is carried out with the combination of a weight balance, a measuring amplifier, the Labjack U12, the installed LabView software, two ball valves and a pump (feeding and discharge operation). As seen in Figure 4.9, analogue signals from the weight balance are first amplified and sent to the Labjack U12 in the control box. The LabVIEW displays the mass continuously. The ball valves and the pump are actuated by the Labjack U12 according to the instruction received from LabVIEW. The feed operation consists of discharging a quantity of reactor contents into the effluent vessel and then adding the same quantity of DS from the feed vessel to the reactor.

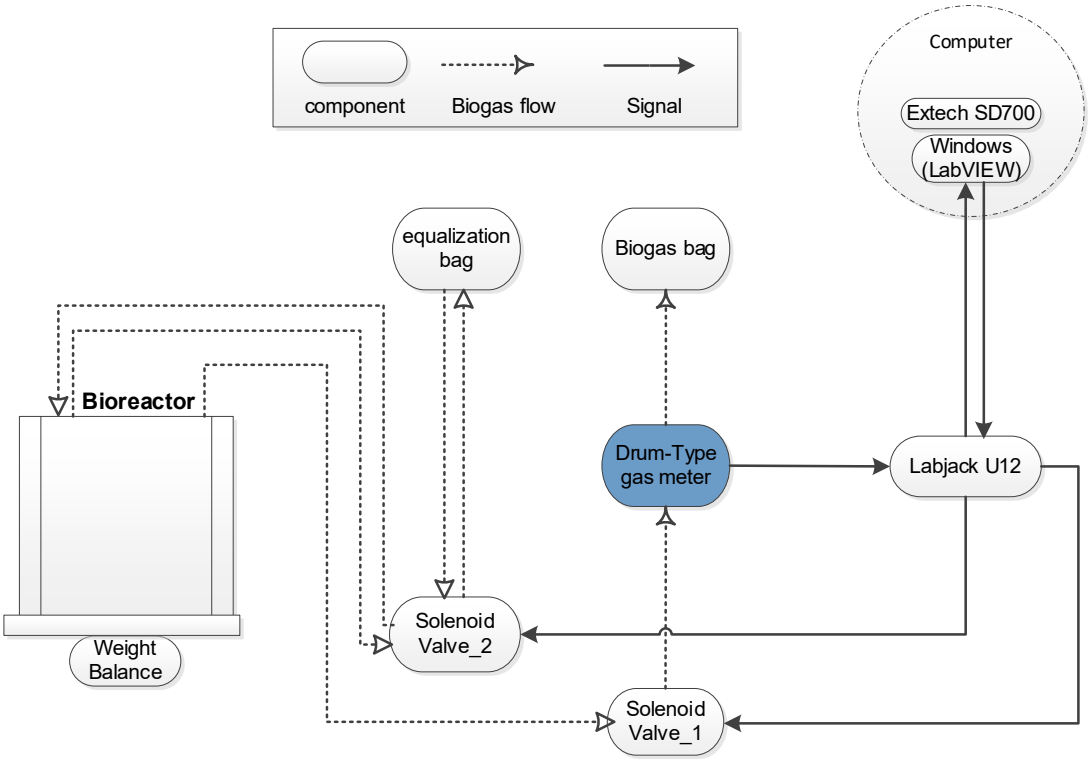

Figure 4.9 Components and flow of signals for feed operation

The pre-set duration of a cycle for the feeding operation (feeding and discharge) is 24 h. The operation of the main components of the feed control system which include the weight balance, the ball valves and the pump are described in the following:

1.) Weighting system

The weight balance has a squared shaped platform made of two metal plates one at the top and the other below. Between them lies a load cell that generates an analogue signal. It is displayed and used for weight control. The maximum load of the weight balance is 400 kg. The sensitivity of the balance is ± 0.2 kg. The working mass is the maximum mass of the AD mixture allowed in the bioreactor. The value is entered in the LabVIEW software. The initialization process of the control system records the empty mass of the reactor which includes the reactor vessel, its cover and all other attached components. This mass serves as a reference for subsequent measurements. The total mass of the bioreactor at any time (which is the sum of the empty bioreactor mass and the AD mixture) is measured continuously by the weight balance.

The mass displayed at a given time by the LabVIEW software is the difference between the total mass of the reactor and the reference mass of the bioreactor. This corresponds to the mass of the AD mixture or reactor's content. The system is designed so that the mass of the AD mixture at any time does not exceed the working mass which is entered as a pre-set value.

The required mass of AD substrate to be fed and the required time for feeding are inputed as variables into LabVIEW. The discharge of effluent precedes the feeding of the substrate. When it is time for taking out of effluent, the LabVIEW software subtracts the required mass of the sample to be fed from the mass of the bioreactor's content. This new mass or targeted mass is then compared with the working mass before the actuation of the ball valves.

2.) Ball valves

Two three-way electric actuated ball valves are used for the feeding operation. As soon as the ball valves receive digital signals for feeding operation, they switch to open any of the three pathways as shown in Figure 4.10. The pathway for recirculation is the ground state according to design. This occurs only when positions 1, 2, 4 and 5 are opened. For the feeding operation only positions 2, 3, 4 and 5 are opened, while for the discharge of effluent only positions 1, 2, 4 and 6. As soon as the required states or positions of the ball valves are reached, the pump is automatically switched on to carry out the operation.

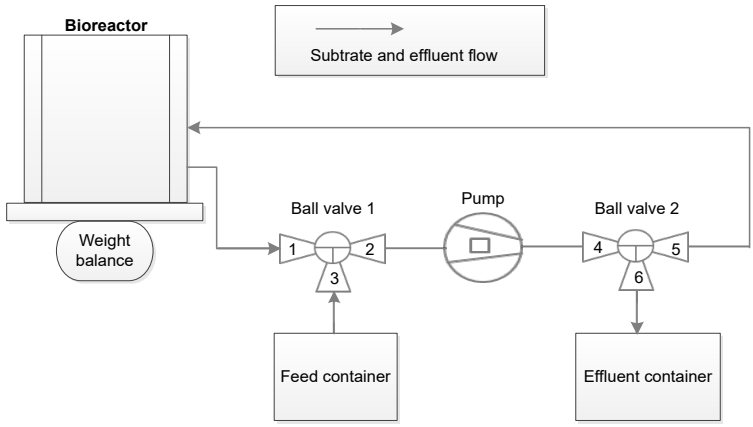

Figure 4.10 Diagram showing bioreactor components, substrates and effluent flow

3.) Pump

The two different pump types were used for the three 100-L AD bioreactors, a progressive cavity pump and a rotary positive displacement pump (section 4.5.2.1). While the progressive cavity pump transfers fluid utilizing the progressive rotating action of a sequence of small fixed shape discrete cavities, the rotary positive displacement pump uses the actions of rotating gears to transfer fluids. To be able to carry out an accurate feeding operation, the pumps are operated at a slow speed and in a batch form. Figure 4.11 shows the flow scheme for the feeding operation. Whenever an automatic feeding operation is about to start, the LabVIEW software follows the sequence as described in the logical flow scheme until the pump is actuated. The pump feeds intermittently until the targeted mass is reached and then stops.

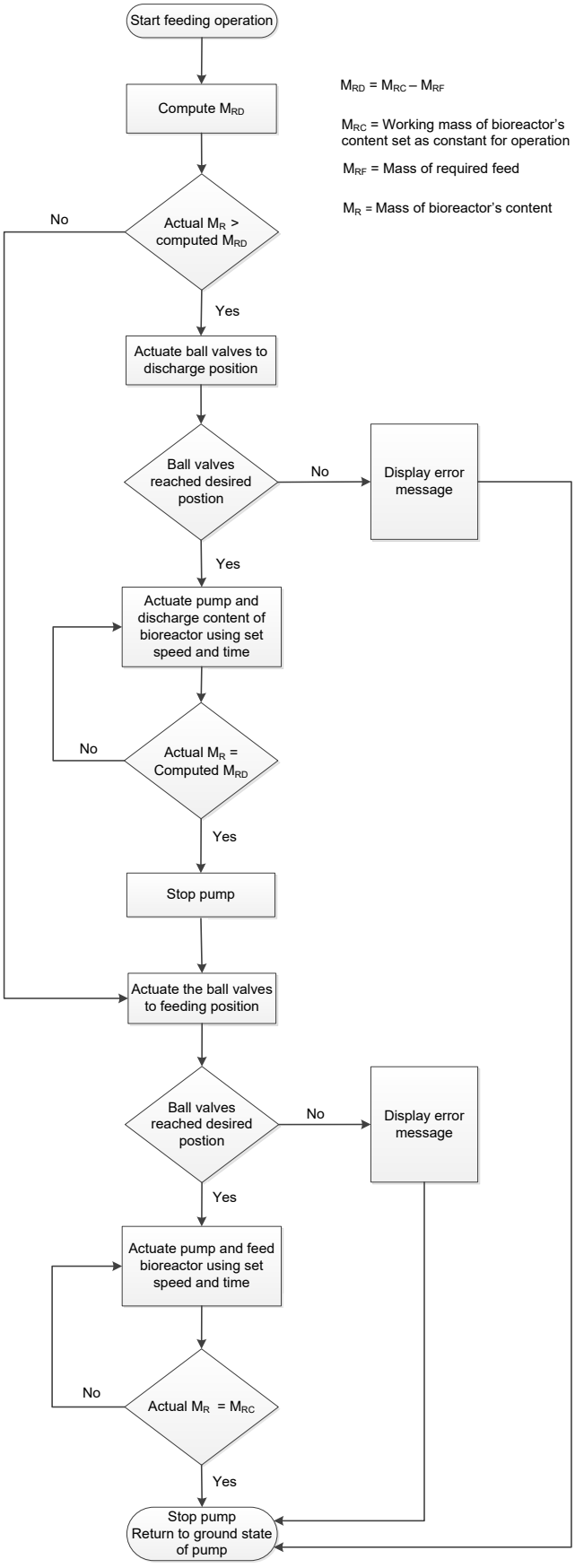

Figure 4.11 Algorithm for the automatic feeding operation of the 100-Liter AD system

4.5.2.2.4 Mixing operations

Two different mixing operations were carried out automatically. They are mixing of the substrate in the feed container and the mixing of the AD mixture in the bioreactor. For an effective AD process, both feed input and AD mixture must be properly mixed. The substrate in the feed container is mixed with anchor type stirrer (section 4.5.2.1). The stirrer is switched on by instruction from the LabVIEW software. The control system allows the input of the time for the start of the stirrer before the feeding operation begins. For this study, the time is often set at 5 minutes. The mixing of AD content of the 100-L AD system is carried out either by a stirrer or by a pump (section 4.5.2.1). The duration and the frequency of operation of the stirrer and the pump for a cycle (24 h) are input values in the LabVIEW control system.

4.5.2.2.5 Automatic biogas measurement

The automatic control of the biogas measurement is described in Figure 4.12. The main components are a drum-type gas meter, the Labjack U12, a computer with installed LabVIEW software and two solenoid valves. The drum-type gas meter sends digital signals to the Labjack U12 and this is displayed via LabVIEW. The gas meter is not continuously opened for reading. The two solenoid valves help to manage when biogas flows into the gas meter or the equalization bag. This helps to maintain a pressure balance in the bioreactor during feeding operation.

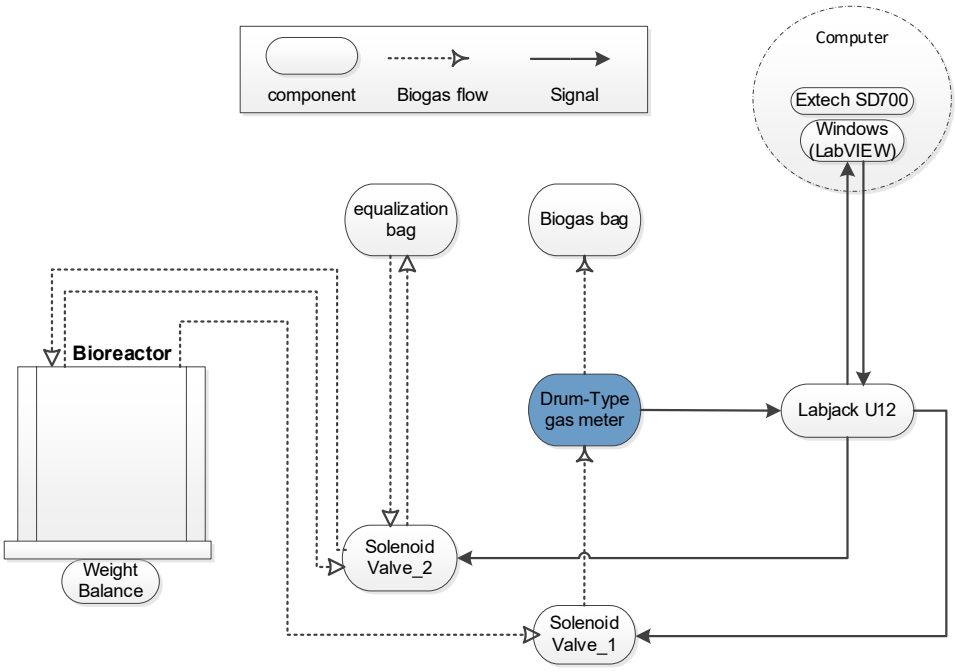

Figure 4.12 Components and flow of signals for biogas measurement

The gas meter works on the principle of positive displacement. A measuring drum is partly submerged in a barrier liquid. Two different biogas meters were used and they operate with different barrier liquids, one with tap water and the other with an aromatic free paraffinic oil (*Ondina 909*). The drum rotates as biogas flows into the system. The periodic filling and emptying of the rigid measuring chambers by the drum give information on the volume of flowing biogas. The magnitude is indicated by a magnetic coupling, a needle dial and a cumulating counter. The measuring accuracy of the gas meter is ± 0.2% or better at standard flow value and ± 0.5% across the full measurement range. The measuring range is from 1 to 18000 L biogas / h. More information on the components can be found in the product manual (Ritter, 2017).

In addition, the Extech SD700 data logger which measures atmospheric temperature, pressure and relative humidity is also attached to the system. It does not give any signal used for control but the provided data are used to compute normalized biogas (273 K,1 atm). The data of the Extech SD700 are displayed and stored via the LabVIEW software. The measurement range of atmospheric temperature, atmospheric pressure and relative humidities of the Extech SD700 Data logger are 0 - 50°C and 10 - 1100 hPa. Their respective accuracies are 0.8°C, 2 - 3 hPa and ~ 4%.

4.5.2.2.6 Data storage

Data storage is a key part of the process control system. The storage of data in the system can be classified into two groups, the static and the dynamic data. The static data are constants. They include the total bioreactor‘s reference mass and the working mass of bioreactors‘ content. The dynamic data are continuously changing and include time, the mass of the reactor content, the temperature of the water jacket, the temperature of the bioreactor’s content, the atmospheric temperature, the atmospheric pressure and comments. The possible comments include confirmation of feeding operation and process errors during feeding operation. The dynamic data are stored in Microsoft Excel compatible format and can be used for further processing.

4.5.3 Execution of anaerobic digestion experiments

This section consists of the description of substrates used for the AD experiments, the description of AD experiments carried out, the analysed parameters and the relevant equations.

4.5.3.1 Substrates and characterization

The substrates for the AD mixtures are feedstock and inoculum. The feedstock is the organic source while the inoculum is the microbial consortium containing active anaerobes.

The inocula were collected from AD plants in Germany. Different inocula were used in the course of this study. The sources of inocula used are reported when describing the experiment. The feedstocks used for the AD experiments were DS of different types collected from the partner wastepaper recycling company.

4.5.3.2 Description of anaerobic digestion tests with deinking sludges

This section describes the different AD experiments carried out using the 1-L AD test-system.

1.) Batch tests

This section describes the different experiments carried out as a batch process in the 1-L AD test system. They were all carried under mesophilic conditions and allowed to run for about 21 days. Cellulose was used as a control substrate. Each sample mixture was investigated in double fold. The goals and their AD mixtures are described in the following:

a.) Experiment 1: Biogas yield of *Stream 1-W70* and *Stream 2-W70*

The goal of this experiment is to determine the biogas yield of quantitatively most important DS *W70* and to determine the difference in the biogas yield of the two DS types differing in the dewatering degree. One sample of *Stream 1-W70* was used, while two different samples of *Stream 2-W70* differing by sample dates were used. The inoculum used was collected from the AD treatment plant Seevetal in Hamburg. Details of the AD mixtures and the experiment, in general, can be seen in Appendix C.1.

b.) Experiment 2: Influence of different inocula on DS biogas yields

The goal of this experiment is to determine how different common inocula from AD plants behave with DS as a feedstock. The DS sample used for this experiment was *Stream 2-W70.* The different inocula used were inoculum 1 (AD treatment plant-Herrling; input substrate: maize silage), inoculum 2 (AD treatment plant Seevetal; input substrate: sewage sludge), inoculum 3 (AD treatment plant Köhlbrandhöft; input substrate: sewage sludge and some grease trap residues) (Amare et al., 2019). The various masses of the reactor content are shown in Appendix C.2.

c.) Experiment 3: Influence of water content of DS on biogas yield

The goal of this experiment is to determine how different water contents (dewatering settings) resulting from the main-dewatering unit (winkle press) of the partner's company could affect the AD production of DS. The substrates used were mixtures of DS derivative *Stream 4-W70* and *Stream 6-W70*. They were mixed in proportion using Eq B.4 and B.5 (Appendix B9) to achieve different mixtures of targeted DM contents between 9 and 48% FM (Appendix C.3).

The maximum DM corresponds to the maximum DM obtainable by the winkle press. The inocula with the best performance in Experiment 2 (AD treatment plant Seevetal) were used but differed by sample dates.

d.) Experiment 4: Influence of wastepaper grades of DS on biogas yield

The goal of this experiment is to determine the biogas yields of further DS types with other wastepaper grades other than the W70 type (Experiment 1). The substrates used are *Stream 2-W80* and *Stream 2-W90/100*. The best performing inoculum from Experiment 2 (AD treatment plant Seevetal) was collected. The different masses of the feedstocks and inocula added are shown in Appendix C.4.

e.) Experiment 5: Influence of $CaCO_3$ on the AD of DS

The goal of this experiment is to determine if an inhibition exists in the AD production of DS due to its high $CaCO_3$ content. The feedstocks for the experiment were cellulose-$CaCO_3$ mixtures. The cellulose was used to simulate the oDM content of DS, while different masses of $CaCO_3$ were added to cover ranges of high and low $CaCO_3$ contents of DS. Appendix C.5 shows the masses of cellulose, $CaCO_3$ and inoculum for the AD mixtures for different bioreactors.

f.) Experiment 6: Influence of different C/N ratio on AD production of DS

The goal of this experiment is to determine the C/N range that is optimal for AD. The feedstock was *Stream 2-W70.* The inoculum used was a digestate taken from a semi-continuously operated AD of DS (*Stream 2-W70*). The inoculum was taken after 68 days of operation when biogas yield production was declining (Appendix C.6). An ammoniacal N (NH_3/NH_4^+-N) concentration of less than 20 mg/L was assumed as the limited nitrogen concentration for AD of DS. Therefore, experiments were conducted with AD mixtures of different C/N ratios to investigate the influence of limited nitrogen. Different masses of NH_4Cl were added to obtain C/N ratios of 24, 29, 34 and 44 (Appendix C.7)..

2.) Semi-continuous tests

The goal of this experiment was to investigate the semi-continuous AD of DS regarding OLR, HRT, inhibitions and possible operational problems. The three different 100-L automatic AD systems (section 4.5.2.1) were used for this investigation and were operated in a semi-continuous mode. The feed stock used is *Stream 2-W70* and the inoculum used was collected from the AD treatment plant Seevetal. The feeding patterns of the bioreactors are found in Appendix C.8.

4.5.3.3 Analysed parameters for anaerobic digestion

The basic parameters analysed are DM, oDM, ash and $CaCO_3$ content as well as pH (Table 4.4). Additional parameters analysed during the AD experiments are listed in Table 4.6

Table 4.6 Complementary parameters analysed for the AD experiments

Parameter	Unit	Guideline / Equipment (Appendix B.8)	Comments
VOA/TIC	% FM	FOS/TAC 2000 Pronova Analysentechnik GmbH	Sample: Digestate of DS
Kjeldahl nitrogen	mg/L	Buchi distillation unit K-350	Sample: Digestate of DS
Biogas Characterization (CH_4, CO_2, H_2S)	% Vol.	GEOTECH Biogas 500	A minimum of 250 mL of gas required

Different equations were used to compute the appropriate masses of substrate mixtures, biogas and methane potentials as well as DS fed into the semi-continuously operated AD process. The equations are shown in Eq B.4 to B.17 (Appendix B.9).

4.6 Solid-liquid separation of fresh and digested deinking sludges

This section discusses the method of sieve analysis, sedimentation and centrifugation. Selected DS substrates and DS-digestates were tested for their behaviour in solid-liquid separation. The different substrates used are shown in Appendix E.1. The parameters measured to analyse the influence of separation are DM, oDM and $CaCO_3$.

4.6.1 Preparation of deinking sludge digestate

DS used for sedimentation test was those generated from a semicontinuous operation of AD. A 10-L bioreactor (not described in this study) was operated mesophilically using pre-dewatered DS as substrate.

The effluent was used for the sieve analysis and sedimentation tests. The DS-digestate used for centrifugation was generated from one of the automatically fed 100-L bioreactors (R1A).

4.6.2 Sieve analysis

A wet sieving analysis was carried out to evaluate the particle size distribution of undissolved solids present in samples of DS and DS-digestates. The DS investigated was *Stream 2-W70* and the digestate investigated was the effluent of a 10-L bioreactor (Influent: *Stream 2-W70)*. The sieve seizes used for analysis and samples investigated are shown in Appendix E.1. The various sieves and the particles trapped in them were dried to compute the total mass of particles on each sieve. Photos of dried solids on the sieves were taken with the aid of a camera to get optical information on their structure.

To summarize the particle size distribution evaluation of the various particles detected were grouped into three different categories. They include less than 63 µm (very fine), 63 - 200 µm (fine) and greater than 200 µm (fibrous and lumpy).

4.6.3 Sedimentation analysis

The behaviour during sedimentation was compared between DS and DS-digestate (Appendix E.1) using imhoff cones of 1 L volume size. The settling property investigated was the settling time during sedimentation under gravity. The first sedimentation test was carried out by using the samples in an Imhoff cone and allowed to stay for 48 h. The solid matter content of DS-digestate was observed lower than that of DS due to the biodegradation of a fraction of the organic matter present in the solid matter.

Knowing that the total amount of solid matter content present in a sample during settling may influence the settling time, the second sedimentation was carried out. Samples of similar solid matter content for DS and DS-digestate were prepared. This allows for an appropriate comparison of the settling behaviour of the particles of the different samples without the impact of the number of particles. The preparation was done by diluting the DS sludge to the DM of the DS-digestate before sedimentation as shown in Appendix E.2. The Imhoff cones were kept uprightly in a stand and were filled to the 1 L mark with the respective samples after thorough mixing. The settling of the supernatant was observed optically and documented for a period of 12 h in the following sequence: 0.5 h, 1 h, 2 h, 4 h, 6 h and 12 h. After the last settling period the supernatant was decanted from the Imhoff cones. The dry mass of the supernatant and the sedimented fractions were measured and representative samples were taken from the different fractions for DM, oDM and $CaCO_3$ measurement.

4.6.4 Centrifugation analysis

The centrifugation experiments were carried out using an Haereus Multifuge X3 centrifuge from Thermo Fisher Scientific GmbH with samples shown in Appendix E.1. The samples were poured into 750 mL polypropylene bottles and placed in the sample points of the centrifuge following the suppliers' protocol. The centrifugation experiments were carried out at a rotation speed of 4500 rpm with an acceleration of 5 m/s^2 and deceleration of 9 m/s^2 for 30 min. After centrifugation, the centrate which is the supernatant liquid was decanted from the solid sludge (cake). The mass of the supernatant and the solid sludge were noted (see Appendix E.3. for the preparation of the samples for the centrifugation test).

4.7 Material valorization of deinking sludges and its digestate

The section explains the methods for the determination of particle size distribution, the process for the formation of mortar prism, the preparation of mortar prisms for flexural and compressive strength test, the analysed parameters and the relevant equations.

4.7.1 Preparation of ashes from deinking sludge and its digestate

Pre-dewatered DS of the *W70* type obtained from wastepaper recycling on 07.02.2017 and DS-digestate at the end of operation of the 100-L-bioreactor (R1A) were first dried at 105ºC and then burnt at 550 ºC to generate the ashes. Thereafter, they were homogenized and pulverised using a milling machine with a mesh size of 1 mm (see the image of ashes in Appendix A.5).

4.7.2 Preparation of mortar and formation of mortar prisms

The mixtures (mortar) for the rectangular prisms were made with and without ash of DS or DS digestate. The ones made without the ash of DS or DS digestate were termed Reference. The other mixtures were formed by increasing the addition of DS ash or DS-digestate ash as well as a simultaneous reduction in the cement fraction of the mixture (Appendix F.2). The water-cement ratio is an important factor that influences the strength of mortar. Therefore, the water-cement ratio was used as a factor to design the different ranges of applications. A standard mortar mixer according to DIN EN 196-1 was used. After mixtures were prepared, they were tested for flow consistency by using a flow table. This was followed by the formation of the rectangular mortar prisms by the use of a forming device from Toni Technik GmbH and a compacting device from AEG-Vibrationstechnik GmBH. The mortar prisms made had a cross-section of 40 mm x 40 mm and a length of 160 mm. Following the DIN EN 196-1, the steps in Figure 4.13 were followed from 1 to 10 to make the mortar which took about 4 minutes to complete.

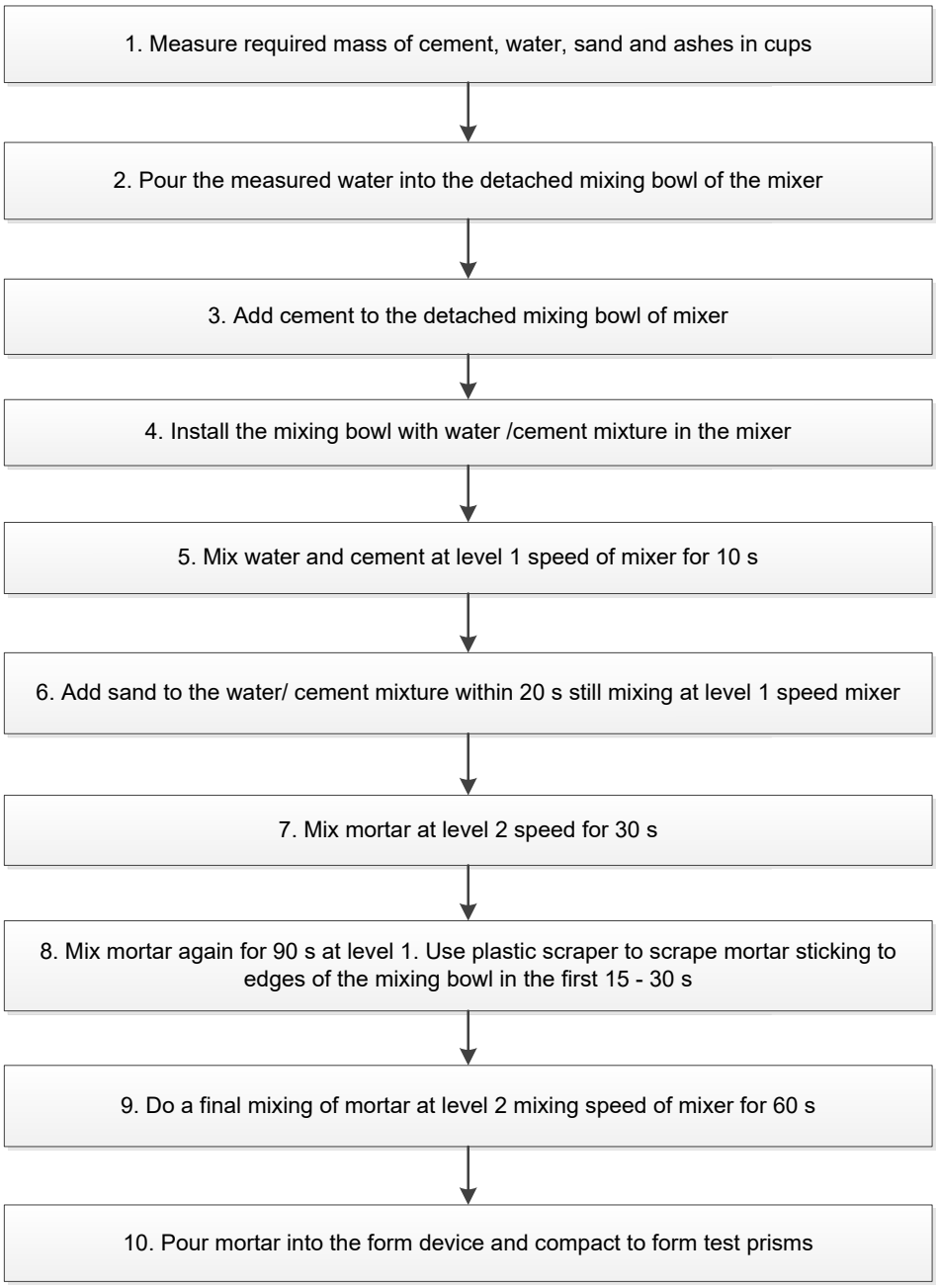

Figure 4.13 Preparation of mortar and formation of mortar prism (carried out at Institute of Materials, Physics and Chemistry of Buildings at TUHH)

4.7.3 Curing of mortar prisms

The mortar prisms were tested for density, flexural and compressive strength. After the formation of the mortar prisms, they were placed in a climate controlled chamber. The chamber regulates the temperature of the mortar prism at a set point of 20^{o}C with relative humidity ≥ 90% overnight. This was necessary to begin the curing process. It was followed by curing under water for 28 days ± 4 h (DIN EN 196-1: 2016-11, 2016). After curing the bulk density, flexural strength and compressive strength of the mortar prisms were determined.

4.7.4 Analytical methods

The parameters and the equipment used for the analysis of ashes of DS and DS-digestates, mortars and mortar prisms are presented in Table 4.7.

Table 4.7 Analysed methods, equipment and methods for ashes and mortar

Parameter	Units	Equipment/Method	Reference/ DIN Norm
Ash of DS and digestate			
Particle size[11]	µm	Mastersizer 3000 from Malvern Panalytical Ltd	Malvern (2013)
Ca and other elements[12]	% DM	X-ray fluorescence analysis	Schmidt-Döhl (2013)
Phases[12]	-	Fourier-Transform infrared spectroscopy (FTIR) and X-ray diffraction	Schmidt-Döhl (2013)
Mortar			
Flow value	mm	Flow table, truncated conical mould, tamper, trowel, palette knife and calliper	DIN EN 1015-3: 2007-05 (2007)
Mortar prism			
Density	kg/m^3	Vernier calliper and weight balance	-
Flexural strength	N/mm^2	Toni Technik compressive/flexural strength testing machine (TONI COMP III)	DIN EN 196-1: 2016-11 (2016)
Compressive strength	N/mm^2	Toni Technik compressive/ flexural strength testing machine (TONI COMP III)	DIN EN 196-1: 2016-11 (2016)

To compute the bulk density, flexural and compressive strength the equations as shown in Eq G.1 to G.3 (Appendix G.1) were used. The comparison based on determined parameters was carried out between reference mortar prisms, mortar prisms with DS ashes and mortar prisms with DS-digestate ash.

1.) Particle sizes in ashes

The particle sizes of materials have to be determined for the analysis of strength properties. The sand used for all mortar prisms was in accordance with the DIN EN 196-1 and has the particle size distribution corresponding to that shown in Appendix F.1. The cement used was a portland cement CEM I 42.5 R-NA (today CEM I 42.5 R (na)) according to DIN EN 196-1. The Mastersizer 3000 device from Malvern Panalytical Ltd was used (Malvern, 2013). It applies the technique of laser diffraction to determine particle size distributions. A laser beam is generated and passed through a dispersed particulate sample.

[11] Analysis by Institute of Advanced Ceramics at TUHH
[12] Analysis by Institute of Materials, Physics and Chemistry of Buildings at TUHH

The angular variation in the intensity of the scattered light is then measured. Since the angular variation is dependent on the particle sizes, it is therefore used as a parameter to calculate the size of particles resulting from the scattering based on the Fraunhofer theory of laser diffraction (Cyr & Tagnit-Hamou, 2001). The results are presented in a volume equivalent to sphere diameter.

2.) Determination of chemical composition and mineralogy of ashes

The application of X-ray fluorescence (XRF), X-ray diffraction analysis (XRD) and Fourier-transform infrared spectroscopy (FTIR) for the determination of the chemical properties of building materials has been reported by Schmidt-Döhl (2013). These three methods were used for the chemical analysis of DS and DS-digestate ash. All analysis were carried out by the laboratory of the Institute of Materials, Physics and Chemistry of Buildings at TUHH. The XRF is a method used for the determination of the elements present in materials. When a sample is activated by a main X-ray source, each element present in the sample emits a distinct set of recognizable fluorescent (or secondary) X-rays which is exclusive to it. An element is present when its distinct fluorescent is detected. The detailed principle and instrumentation of XRF is provided by Ait Bouh (2020). XRD is an analytical method typically employed for crystalline material phase identification. When monochromatic X-rays are incident to samples containing crystalline material they produce constructive interference (and or diffracted rays) at certain conditions (Bragg's Law). The diffracted rays are collected and analysed to determine the phases present in the sample. Detailed information on instrumentation and application of XRD is provided by Bunaciu et al. (2015). Lastly, the FTIR is a method used for the determination of the infrared spectrum of absorption or emission of a given material which is its characteristic property. This is achieved by exposing samples to infrared light (IR). The sample's capacity to absorb energy from infrared light at various wavelengths is examined to ascertain the molecular make-up and structure of the substance. Sufficient information on the principle of FTIR is provided by Schmitt and Flemming (1996).

3.) Determination of flow value of mortars

The mortar mixtures prepared (section 4.7.2), were tested for flow property according to the DIN EN 1015-3: 2007-05 (2007) before the formation of mortar prisms. The procedure entails putting a truncated conical mould filled with mortar samples at the centre of the flow table's disc. Compacting was done with the tamper for at least 10 short strokes and excess mortar was skimmed off. After about 15 seconds, slowly the mould was lifted vertically, and the flow table was shocked 15 times at a consistent frequency of roughly one per second. As a result, the mortar spreads on the flow table.

On the flow table, the diameter of the mortar was measured in two directions at right angles to each other and estimated to the nearest millimetre. The flow value was then calculated as the average of the two measurements. Each test was done twice, with the average as the actual flow value. If the individual flow results are 10% higher than the average flow value, the test is repeated.

4.) Determination of density of mortar prisms

Cured mortar prisms (section 4.7.3) were subjected to density determination. The length, height and width were measured with a vernier calliper to compute the volume. The weight was measured with a weight balance. The value of the volume and weight were then inputted into Eq G.1 (Appendix G.1) to determine the density.

The average density of three individual results determined on a set of three mortar prisms was calculated. The test with the set of three individual mortar prisms was done twice and their average was taken as the actual density.

5.) Determination of flexural and compressive strength of mortar prisms

The flexural and the compressive strengths were determined using the Toni COMP III from Toni Technik. The procedure as described in DIN EN 196-1 was used. For flexural strength, the three-point loading method was adopted, where a cured mortar prism was placed in the test machine such that one of its side-face is on the support rollers and the prism's longitudinal axis is perpendicular to the rollers. The load was applied perpendicularly to the other side of the prism with the load roller and increased consistently with a load increment of 50 ± 10 N/s until failure occurs. The load at the fracture point, the width of the mortar prism and the length of the support span were inputted into Eq G.2 (Appendix G.1) to determine the flexural strength. Each result was specified to be at least 0.1 N/mm^2. The average flexural strength of three individual results determined on a set of three mortar prisms was calculated. The test with the set of three individual mortar prisms was done twice and their average was taken as the actual flexural strength. The prism halves were covered with a damp cloth until the compressive strength was determined.

The compressive strength was conducted on cured mortar prism halves obtained during flexural strength testing. A half prism was placed on the machine's test plates, aligned laterally to within 0.5 mm and longitudinally so that the prism's end face protrudes about 10 mm beyond the plates. The load was increased consistently across the full loading range with a load increment of 2400 ± 200 N/s up to failure. To determine the compressive strength, the load at the fracture point and the cross-sectional area of the mortar prism half were entered into Eq G.3 (Appendix G.1).

Each individual result was specified to be at least 0.1 N/mm^2. The average compressive strength of three individual results determined on a set of three mortar prisms halves was computed. This was done twice and the average was taken as the actual compressive strength.

4.8 Statistics, modelling and material flow design

Appropriately modelling the AD process of DS allows for simulation of the biogas and methane production rate and also gives valuable information for the design and the efficiency evaluation of biogas plants.

4.8.1 Statistical methods

The characterization of DS samples and their derivatives generated a substantial amount of data which necessitated the use of a statistical tool to compute the minimum and maximum values, mean, median and standard deviations of means.

A double-sided t-test was used to determine if a significant difference existed in the properties of the different samples tested. The t-test provided t-statistic, degree of freedom and significance levels. Microsoft Excel (2010) was used for the determination of the statistic parameters and the t-statistics.

Normal distribution tests were carried out before the t-test, with the online statistical tool from Hemmerich (2018) to ascertain the normal distribution of data sets. The F-test was carried out by Microsoft Excel (2010) before the t-test. The purpose of the F-test is to determine if the data sets have equal or unequal variance. This is necessary as an input in Microsoft Excel (2010) for the t-statistics. For all the double-sided t-statistics, a null hypothesis was assumed and was rejected or accepted at a significance level (P) of 0.05.

4.8.2 Modelling of anaerobic digestion of deinking sludges

This section discusses the models used for the AD simulation of DS, the method of parameter estimation and the approach for model comparison.

4.8.2.1 Models investigated for anaerobic digestion of deinking sludges

Five different models for the AD process of DS were used. The predicted values with the different models were compared with values obtained from a laboratory experiment. The different models investigated are explained below;

1.) One-step first order kinetics model

The first order kinetic (one step) model is a simple model when compared to some other models used in AD such as Gompertz.

The model considers one of the AD process phases as a limiting step and the rate constant for the AD process is determined based on this step. Also, it considers a single rate constant for the degradation of readily and less biodegradable organics. The use of a one-step first order kinetics model for AD processes has been reported by many authors (Angelidaki et al., 2009; Deepanraj et al., 2015; Sánchez et al., 1996). It is represented as shown in Eq 4.1.

$$Y_t = Y_m * [1 - \exp(-kt)] \quad \text{Eq 4.1}$$

where,

Y_t Is the biogas yield (L/kg oDM) with respect to time (days)

Y_m is the maximum biogas yield of the substrate (L/kg oDM)

k is the hydrolysis rate constant (1/day)

t is the time (days)

2.) Two-steps first order kinetics model

The two steps first order kinetics is a model similar to the first order kinetics (one step). The difference is that it considers different degradation rate constants for the readily and less biodegradable organics. If a single or equal degradation rate constant is achieved, then the model suggests that a two steps kinetics can be disregarded. The two-step first order kinetics as reported by Luna-delRisco et al. (2011) is shown in Eq 4.2.

$$Y_t = Y_1 * [1 - \exp(-k_1 t)] + Y_2 * [1 - \exp(-k_2 t)] \quad \text{Eq 4.2}$$

where,

Y_1 is the biogas yield (L/kg oDM) associated with bioconversion of readily biodegradable organics

Y_2 Is the biogas yield (L/kg oDM) associated with bioconversion of less readily biodegradable organics

k_1 is the hydrolysis rate constant of Y_1 (1/day)

k_2 is the hydrolysis rate constant of Y_2 (1/day)

Y_t, and t have the same description as in Eq 4.1.

3.) Modified Gompertz model

The modified Gompertz model is based on the variable cell growth of microorganisms. The model describes the cell concentration at a certain time in the AD process. The model does not consider maximum cell growth.

The model as proposed by Velázquez-Martí et al. (2019) is shown in Eq 4.3.

$$Y_t = Y_m * \exp\left\{-\exp\left[\frac{R_m * e}{Y_m}(\lambda - t) + 1\right]\right\} \quad \text{Eq 4.3}$$

where,

R_m is the maximum biogas production rate (L/kg oDM day)

λ Is the lag phase time (days)

e is the Euler's number (2.7183)

Y_t, Y_m, and t have the same description as in Eq 4.3

4.) Transfer function model

The transfer function model is derived from the one-step first-order kinetic model. It considers the kinetic of the rate-limiting step not sufficient to model the AD process. It, therefore, substitutes this constant with the ratio between the maximum and medium methane production velocity. The model as described by Velázquez-Martí et al. (2019) is shown in Eq 4.4

$$Y_t = Y_m \left\{1 - \exp\left[-\frac{R_m(t - \lambda)}{Y_m}\right]\right\} \quad \text{Eq 4.4}$$

Where,

Y_t, Y_m, R_m, t and λ have the same description as in Eq 4.3

5.) Logistic function model

The logistic function model is based on biomass growth. Unlike monod kinetics, it is independent of substrate concentration. Its microbial growth rate is proportional to the biomass concentration and the difference between the maximum concentration of biomass and the actual biomass concentration. The modified logistic equation as reported by Donoso-Bravo et al. (2010) is shown in Eq 4.5

$$Y_t = \frac{Y_m}{1+\exp\left[4R_m\frac{\lambda - t}{Y_m} + 2\right]} \quad \text{Eq 4.5}$$

Where,

Y_t, Y_m, R_m, t and λ have the same description as in Eq 4.3.

4.8.2.2 Parameter estimation and comparison of models investigated

The estimation of parameters in the models is shown in Eq 4.6 to 4.9 and the prediction of biogas yield was determined by carrying out a nonlinear least-square regression analysis with the aid of Microsoft excel (2010) software. To identify and compare the accuracy of the different models investigated, the coefficient of determination (R^2), and root mean square (RMSE) were computed for each model. The R^2 informs about the goodness of a model fit while the RMSE is the standard of deviation between the predicted and measured values. The R^2 was computed using Microsoft excel (2010) while the RMSE was computed using the Eq 4.6 (Pramanik et al., 2019)

$$RMSE = \sqrt{\sum_{i=1}^{N}\frac{(PY_i - MY_i)^2}{N}} \quad \text{Eq 4.6}$$

Where,

PY_i is the predicted biogas yield

MY_i is the measured biogas yield

N is the number of measurements

The Bayesian Information Criterions (BIC) test and the Akaike Information Criterions (AIC) test were also carried out to evaluate and determine which model has the highest probability of correctness. BIC was computed with Eq 4.7 and 4.8 and AIC was computed with Eq 4.9 to 4.11 (Fabozzi et al., 2014; Pramanik et al., 2019).

$$BIC = N\ln\left(\frac{RSS}{N}\right) + K\ln(N) \quad \text{Eq 4.7}$$

$$\Delta BIC = BIC_1 - BIC_2 \quad \text{Eq 4.8}$$

$$AIC = N\ln\left(\frac{RSS}{N}\right) + 2K + \frac{2K(K+1)}{(N-K-1)}, \text{ when } \frac{N}{K} < 40 \quad \text{Eq 4.9}$$

$$AIC = N \ln\left(\frac{RSS}{N}\right) + 2K, \text{ when } \frac{N}{K} \geq 40 \qquad \text{Eq 4.10}$$

$$\Delta AIC = AIC_1 - AIC_2 \qquad \text{Eq 4.11}$$

Where,

N	is the number of measurements
K	is the number of parameters in the model
RSS	is the residual sum of square
ΔBIC	is the difference between the BIC of the best model and the candidate model compared
BIC_1	is the BIC of the best model
BIC_2	is the BIC of the candidate model compared to the best model
ΔAIC	is the difference between the BIC of the best model and the candidate model compared
AIC_1	is the AIC of the best model
AIC_2	is the AIC of the candidate model compared to the best model

4.8.3 Material flow design

The basis of the material flow design was according to the simplified flow diagram of DS in the partner treatment plant (Figure 4.1). The input comprises the annual fresh mass of wastepaper, process water and the output as concentrated sludge. The DM, oDM and $CaCO_3$ values obtained from sample analytics were used to compute mass flows. The design of the material flow was done with the aid of the STAN (subSTance flow Analysis) software, developed by the Vienna University of Technology (Cencic & Rechberger, 2008). With STAN a graphical representation of all material flows from the wastepaper raw material over its drainage to incineration and disposal of the residual materials were drawn for the example of the recycling company.

Novel treatment scenarios for DS, focusing on the production of biogas in partner's DS treatment facilities, were drawn using MS Visio software. This software facilitated the creation of detailed diagrams showing the flow of materials and processes within each scenario, particularly highlighting the integration of AD into the treatment process.

CHAPTER 5 RESULTS AND DISCUSSION

5.1 Characteristics of deinking sludges and their derivatives

The characteristics obtained can be used to make a contrast between the different DS and derivatives and to analyse their suitability for a targeted sludge treatment. They are used in this dissertation to discuss their suitability for biogas production.

5.1.1 Dry matter contents

The results of the dry matter content of different DS and DS derivatives streams without consideration of the wastepaper grades (*W70, W80, W90/100*) are shown in Figure 5.1. The dry matter content of biosludge streams is also shown in Figure 5.1. The corresponding data and other statistical indicators are shown in Appendix H.1 to H.7. The various streams were described in section 4.3.

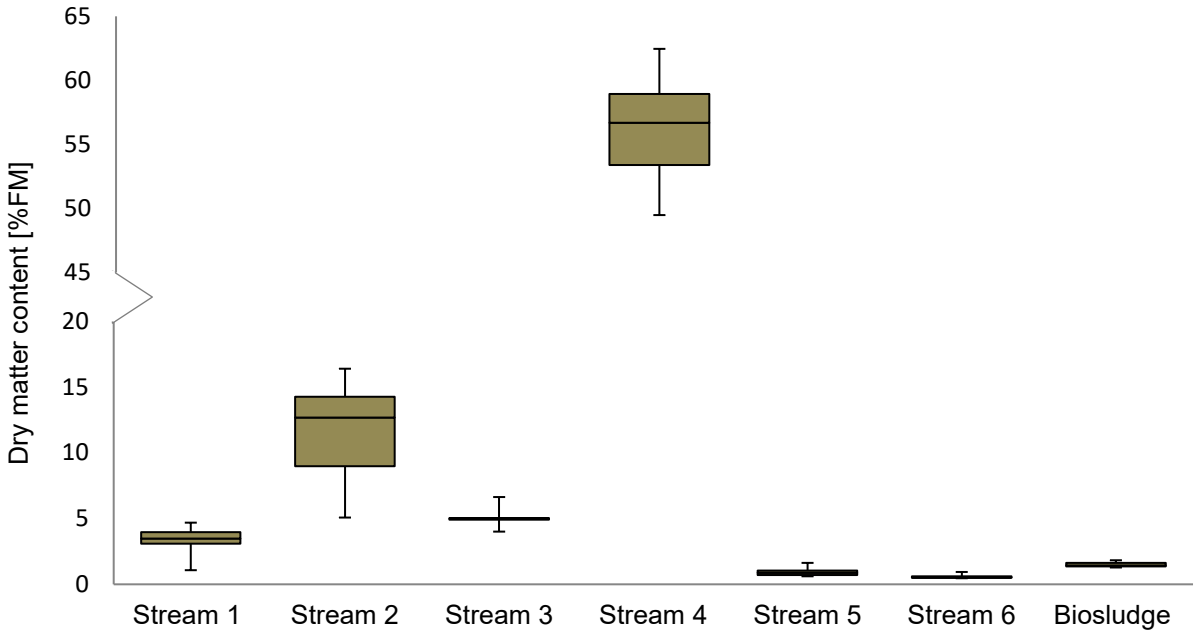

Figure 5.1 Minimum, median, maximum and interquartile range of dry matter contents (DM) of different DS and DS derivatives. (On the y-axis, the distance between 20% and 45% is not to scale)

Stream 1 which is the raw DS has a considerable amount of DM. The output of the pre-dewatering unit (*Stream 2*) shows distinctly more DM content when compared with *Stream 1*. The output of the sludge buffer (*Stream 3*) also has a considerable amount of DM.

This stream contains other flows such as microflotation sludge and biosludge. The output of the main-dewatering unit (*Stream 4*) contains a high amount of DM due to intense mechanical dewatering by the winklepress. This high DM of *Stream 4* informs that the sludge volume is reduced significantly by the application of both dewatering units due to water removal. The liquid phase of the pre-dewatering unit (*Stream 5*) contains a low amount of DM. It is recycled and used as process water to supply the huge water demand of the wastepaper recycling process. The output of the main-dewatering unit (*Stream 6*) and the biosludge also show little values of DM.

From a statistical point of view, the DM data obtained for the different DS and its derivatives streams showed slightly negative or positive skewed distributions (different mean and median values). For instance, a negative skew was observed in the DM boxplot of *Stream 2* and *Stream 4*, while the box plot of *Stream 1* shows a positive skew. The difference between means and medians ranged from 1% (*Stream 4*) to 12% (*Stream 6*). Normal distributions of DM data for all streams except *Stream 6* were ascertained through a test (Appendix H.1). The large difference in the DM of *Stream 6* can be attributed to the low number of samples. Since medians are preferred measures of central tendency for slightly skewed distribution, they are used for further discussion on the DM of DS and its derivatives.

1.) Streams of the pre-dewatering unit

The raw DS (*Stream 1*) which is discharged from floatation cells show low DM values (1.1-4.7% FM). This is because aside from deinking chemicals a large quantity of water is used to deink recovered wastepapers. The pre-dewatering unit receives the raw DS as an input and generates *Stream 2* (5.1 - 16.4% FM) which is about 3.7 higher in DM compared to *Stream 1*. *Stream 2* is categorized as medium DM sludge.

The DM difference between *Stream 1* and *Stream 2* denotes the significance of the pre-dewatering unit in the sludge handling cascade. The large range of the DM of *Stream 2* can be attributed to the DM variation of *Stream 1* and further to variable operation conditions of the pre-dewatering unit. The turbid water (*Stream 5*) as the second output from the pre-dewatering unit had DM below 1% FM and therefore grouped as a very low DM sludge. This stream is recycled via a microflotation unit.

The other streams which are not shown in Figure 5.1 are the turbid filtrate from the disc filter of deinking operation (*Stream 5III*) with DM of 1.8% FM, the clear water (*Stream 5I*) with DM of 1.8% FM and microflotation sludge (*Stream 5II*) with DM of 6.4% FM (see Figure 4.1 for flow diagram).

2.) Streams of the main-dewatering unit

The input of the main-dewatering unit is a mixed sludge from the sludge buffer consisting of pre-dewatered DS (*Stream 2*), microflotation sludge (*Stream 5 II*) and the *Biosludge* (Figure 4.1). The mixed sludge is characterized by a low DM (4.0 - 6.6% FM). It is highly dewatered to generate *Stream 4* (30.0 - 61.1% FM) sludge with an increase in DM by about 8.6 fold. The DM of *Stream 4* is notably about 4.2-fold that of *Stream 2*. *Stream 4* is grouped as a high DM sludge. The filtrate from the main-dewatering unit (*Stream 6*) had a very low DM of below 1% FM. It is transported to the biological wastewater treatment plant (WWTP) for further reduction of biological oxygen demand (BOD) before final discharge in the river. The biosludge generated from the WWTP has also a very low DM (less than 2%) and is recirculated into the sludge buffer.

The result of DM obtained for the DS and its derivatives in this study can be compared to those reported in the literature. It is not commonly described in the literature which post-deinking operations are carried out. DS in the range of 3 - 5% FM as reported by Krigstin and Sain (2006), fall into the category of low DM. These DS might be referred to as a raw DS (*Stream 1*) which is not yet dewatered. Other reported DM of DS in literature fit the high DM category: 42% FM (Abubakr et al., 1995), 38 - 62% DM (Kujala, 2012), and 64% FM (Bienert et al., 2015). They might be referred to as the highly dewatered DS (*Stream 4*).

5.1.2 Composition of the deinking sludges and their derivatives

The results regarding the oDM contents of different DS streams without consideration of the wastepaper grades (*W70, W80, W90/100*) can be seen in Figure 5.2. The corresponding data with statistical indicators are available in Appendix H.2. The dry matter composition was distinguished into organic matter and inorganic matter, whereas the last mentioned was composed of $CaCO_3$ and other compounds. T-test analyses were carried out to evaluate if significant differences exist in the oDM and $CaCO_3$ flow across the pre- and main-dewatering units. The summary of t-test results can be found in Appendix H.5.

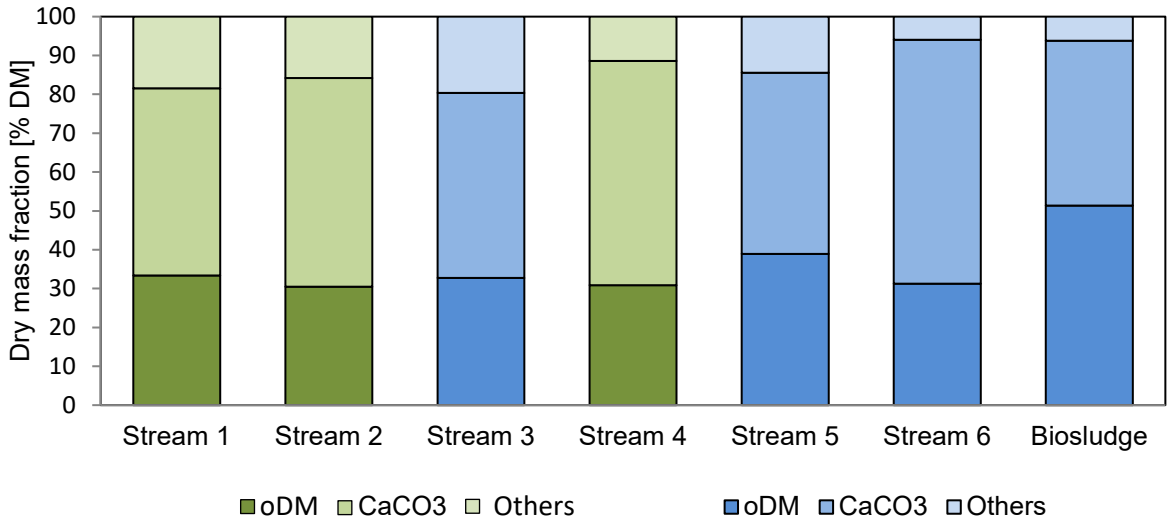

Figure 5.2 Mean values of organic dry matter (oDM) and calcium carbonate content ($CaCO_3$) of different DS and DS derivative types. "Others" refer to the fraction of ash other than $CaCO_3$. The green bars are the main DS streams while the blue bars are the DS derivatives.

1.) Organic dry matter content

Figure 5.2 confirms that organic dry matter is present in all the DS and DS-derivatives analysed. The oDM content of all samples ranged from 19.2 to 57.0% DM. However, the mean values of the oDM of *Stream 1* to *6* fall in a narrow range of 30.5 to 33.4% DM. The biosludge on the other hand is characterised by a higher oDM with a mean value of 51.3% DM and a range of 44 to 57% DM. The WWTP of the wastepaper recycling company receives also non-wastepaper recycling-related inputs which might have an impact on its oDM. Very few oDM contents of DS are reported in the literature. However, it is possible to compute oDM values from the few reported ash contents of DS. The oDM value of DS reported by Bienert et al. (2015) who investigated DS in a high DM category is 33% DM. It falls well in the range of the oDM obtained in this study. The oDM content from DS by other authors are 79.8% DM (Abubakr et al., 1995), 52.0% DM (Krigstin & Sain, 2006), 51.6% DM (Thompson et al., 2001), 49.9% DM (Niessen, 2002) and 49.0% DM (Kujala, 2012) (see Table 3.1 for more oDM values of DS reported).

2.) Ash and $CaCO_3$ Content

The ash content is the inorganic fraction left after the ignition of the organic matter in DS. Figure 5.2 shows that a substantial amount of $CaCO_3$ is present in the inorganic fraction of all the DS and DS derivatives analysed. It also denotes that $CaCO_3$ is the main component of the ash content of DS and its derivatives.

It is observable that excluding the biosludge all other DS and its derivatives have a higher ash and $CaCO_3$ as oDM content. $CaCO_3$ contents in the range of 21.4 - 76.7% dry matter and ash contents in the range of 43.0 - 71.4% dry matter were obtained for DS and its derivatives. Ash contents of DS have been reported in literature but the $CaCO_3$ contents are scarce to find. The ash contents of DS reported are 20% DM (Abubakr et al., 1995), 48% DM (Thompson et al., 2001), 48% DM (Krigstin & Sain, 2006), 50% DM (Niessen, 2002), 51% DM (Kujala, 2012) and 67% DM (Bienert et al., 2015). Most of the ash contents reported in the literature are similar to that obtained in the main DS streams (*Stream 1, 2, 4*) of this study which is in the range of 43 - 81% DM. The only report deviating from own ash contents of DS and derivatives is that of Abubakr et al. (1995) with a lower ash content. A lower amount of $CaCO_3$ (mean 42.5% DM) is observed for biosludge. This might be due to dilution caused by other different input wastewater streams into the WWTP. These results inform that ash and $CaCO_3$ content are significant components of DS and should be as well recovered for other practical applications.

3.) oDM and $CaCO_3$ flow across the pre- and main dewatering units

The dewatering units distribute DM present in input streams into two categories of streams (Figure 4.1). One with low DM and the other with high DM. The DM of the two streams also corresponds to their low and high oDM and $CaCO_3$ in the fresh matter. This section used a t-test to investigate if oDM or $CaCO_3$ present in DM of streams are influenced by the action of any of the dewatering units.

For the pre-dewatering unit, t-test result showed that the mean oDM value of *Stream 1* (33.4% DM) is significantly different from *Stream 2* (30.5% DM) (Appendix H.3). Some oDM fraction of *Stream 1* probably flows into the liquid phase (*Stream 5*) which results in a higher oDM value of *Stream 5* (39.0% DM) compared to *Stream 2*. It is possible to infer that there may be some finer particles that are non-fibre like that make up the organic fraction of the DM in *Stream 1*. These possible flow into *Stream 5* due to the influence of the pre-dewatering unit. A further t-test between the oDM of *Stream 1* and *Stream 5* showed no significant difference and suggest that the organics in *Stream 1* and *Stream 5* are similar. This result suggests that during the process of pre-dewatering, some amount of organic fraction from the *Stream 1* may be lost. The t-test comparing *Stream 1* and *Stream 2* regarding $CaCO_3$ indicated no significant difference. This suggests that the pre-dewatering unit does not influence the flow of $CaCO_3$ components in the DM of the flowing streams significantly.

For the sludge buffer, t-tests were carried out to compare the oDM and $CaCO_3$ contents of streams across the sludge buffer (Appendix H.3). The result obtained suggests that the oDM and $CaCO_3$ in the DM of flowing streams are not influenced by the sludge buffer.

*For the main-dewatering unit, d*ifferent t-tests carried out to compare the oDM and $CaCO_3$ across the main-dewatering unit all showed no significant difference (Appendix H.3). It suggests that the main-dewatering unit does not influence the oDM or the $CaCO_3$ in the DM of flowing streams. In comparison with the t-test obtained for the pre-dewatering, the lack of influence on oDM might imply that the amount of the non-fibre like organic fine particle presumably in *Stream 1* has reduced significantly before input into the main-dewatering unit.

In summary, the results obtained inform that DS and derivatives contain a substantial amount of oDM but the $CaCO_3$ content is the most significant fraction of the DM. The pre-dewatering unit of raw DS could lead to a loss of oDM but not $CaCO_3$ in the DM of raw DS. The main-dewatering unit does not impact the oDM or $CaCO_3$ present in the DM of flowing DS streams. These characteristics of DS and derivative are required for application in biogas modelling from DS and also for mass balance computation.

5.1.3 Comparisons based on wastepaper grades

Figure 5.3 compares the main DS streams (*Stream 1, 2, 4*) regarding DM, oDM and $CaCO_3$ content with consideration of wastepaper grades (*W70, W80, W90/100*) used in deinking. The corresponding data with statistical indicators are available in Appendix H.4 and H.5.

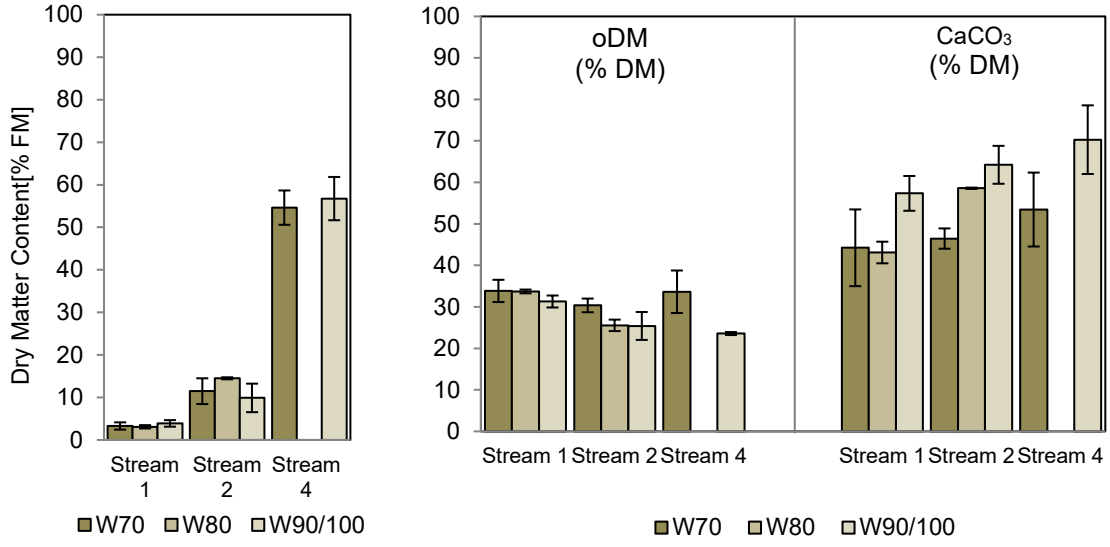

Figure 5.3 Mean values with standard deviation of the dry matter (DM), organic dry matter (oDM) and $CaCO_3$ contents from *Stream 1*, *2* and *4* samples for different wastepaper types

1.) Dry matter content

The t-test between the DM of the different *Stream 1(*raw DS*) types* showed no significant difference due to the difference in wastepaper grades (Appendix H.5). Also, the t-tests between the DM of different *Stream 2 (*pre-dewatered DS*)* did not show any difference due to difference in wastepaper grades except that between the mean DM of *Stream 2-W80* (14.5% DM) and the mean DM of *Stream 2-W70* (11.5% DM) (Appendix H.5). The difference suggests that the DM of pre-dewatered DS from *W80* is significantly higher than that from *W70*, but this is inconclusive due to the very low sample size of DM values of *Stream 2-W80* and the fact that the DM values of *Stream 2-W70* were not normally distributed (Appendix H.4). It can be concluded from the results of the t-test that DM of DS is similar for the different *Streams 1, 2* and *4* irrespective of their wastepaper grades.

2.) Organic dry matter

For *Stream 1*, a significant difference was observed in the t-test between the mean oDM of *W80* (33.7% DM) and *W90/100* (31.3% DM) (Appendix H.5). For *Stream 2*, a significant difference was also observed in the t-test between the mean oDM of *W70* (30.4% DM) and *W80* (25.6% DM) as well as between the mean oDM of *W70* (30.4% DM) and *W90/100* (25.4% DM) (Appendix H.5). The results suggest that the oDM of raw DS from *W80* (medium wastepaper grades) is greater than that of *W90/100* (medium/high wastepaper grades). It also suggests that the oDM of pre-dewatered DS from *W70* is greater than other pre-dewatered DS from *W80* and *W90/100*. The oDM of raw DS from *W70* and *W80* are not significantly different as observed by their pre-dewatered DS. It may be assumed that the pre-dewatering unit impacts on the oDM of raw DS from *W80* due to a high fraction of non fibrous fine organic particles contained in its DM (section 5.1.2.3). The distinct lower oDM of DS from *W90/100* compared to those from other wastepaper grades may be due to its high $CaCO_3$ content (Steffen et al., 2017). The results inform that the oDM of raw and pre-dewatered DS may vary due to the wastepaper grades used for recycling. DS from *W70* tends to have a higher amount of organics compared to those from *W80* and *W90/100*.

3.) $CaCO_3$ contents

For *Stream 1*, a significant difference was observed in a t-test between the mean $CaCO_3$ contents of *W70* (44.2% DM) and *W90/100* (57.4% DM) as well as between the mean $CaCO_3$ of *W80* (43.1% DM) and *W90/100* (57.4% DM) (Appendix H.5). For *Stream 2*, a significant difference was also observed in the t-test between the means of *W70* (30.4% DM) and *W80* (25.6% DM) as well as between the means of *W70* (30.4% DM) and *W90/100* (25.4% DM) (Appendix H.5).

The results suggest that DS from *W90/100* is significantly higher in $CaCO_3$ when compared to those from other wastepaper grades. This corresponds to the lower oDM as observed for DS from *W90/100* in section 5.1.3.2.

5.1.4 Comparison of deinking sludges with common biogas feedstocks

The DM categories of DS and its derivatives which are very low, low, medium and high using their median values as described in section 5.1.1 were used as the basis to assign them in Table 5.1. Table 5.1 also lists common biogas feedstocks which corresponds to DS and its derivatives using the same DM categories. The DM of DS and its derivatives can be compared with the DM of various common biogas feedstocks as shown in Table 5.1. Blackwater from vacuum toilets has very low DM, which can be placed at the lower boundary of the very low DM category of the DS derivatives.

Table 5.1 Assignment of DS and DS derivatives to dry matter (DM) categories of common biogas feedstocks (numbers in brackets exceed / fall below assigned category)

DS and DS derivative					**Common biogas feedstock**			
Dry matter category		**DM and oDM content**						
Type	**Range [% FM]**	**Type**	**DM [% FM] Median value**	**oDM [% DM] Median value**	**Type**	**DM [% FM]**	**oDM [% DM]**	**Source**
Very low	>0.4 – 2	*Stream 5* *Stream 6* *Biosludge*	*0.9* *0.5* *1.4*	*39.1* *29.1* *53.4*	Blackwater from vacuum toilets	0.4 – 0.5 – 0.9[a]	56	1
Low	>2 – 7	*Stream 1* *Stream 3*	*3.5* *5.0*	*33.4* *29.5*	Sewage sludge Greasy water Pig manure	4 – 8[a] 2 – 3 – (10)[a] 6[b]	60-80 82 80	2 1 3
Medium	>7 – 20	*Stream 2*	*12.7*	*31.0*	Liquid cow manure	10[b]	80	3
High	>20	*Stream 4*	*54.1*	*31.2*	Food waste Solid cow manure Chicken manure Green waste Lawn cuttings	23 ± 10[c] 25[b] 40[b] 45[b] 14 – 67[a]	88 80 75 NA 83	4 3 3 5 1

[a] minimum–mean–maximum value; [b] literature standard value, [c] mean value ± standard deviation,

NA- not available by Author

1- Hertel et al., 2015 ; 2- Olivia et al., 2009 ; 3- Friehe et al., 2016a ; 4- Fisgativa et al., 2016 ; 5- Richter et al., 2017

The oDM fraction of about 56% DM of blackwater from vacuum toilets allows it to fit as a co-substrate for biogas even with its very low DM (Hertel et al., 2015). The biosludge in the very low DM category has similar oDM to black water from vacuum toilets and might also be suitable as a biogas co-substrate. *Stream 5* (liquid fraction of the pre-dewatering step) and *Stream 6* (liquid fraction of the main-dewatering step) have lower oDM values compared to blackwater from vacuum toilets. The lower oDM might impair their suitability as a biogas co-substrate.

The DS and its derivatives in the category of low DM (*Stream 1 and 3*) correspond to sewage sludge, greasy water and pig manure. However, these common biogas feedstocks in the low DM category show about 2.0 fold higher oDM when compared to that of DS and its derivatives in a similar category (Table 5.1). This implies that though the DS and its derivative might be suitable for biogas production, they might also have a lower biogas yield compared to the common biogas feedstock in the low DM category. The DS in the category of medium DM (*Stream 2*) also corresponds to liquid cow manure while that in the high DM (*Stream 4*) category corresponds to food waste, solid cow manure, chicken cow manure, green waste and lawn cuttings (Table 5.1). The oDM of DS is also lower compared to that obtainable in the medium and low DM category of common biogas substrate. However, their sufficiently high DS and substantial oDM make the potential substrate suitable for biogas production. Though a lower biogas yield might be envisaged when compared to a common biogas substrate, it is also dependent on the biodegradability of the organic fraction contained in the substrate.

5.1.5 Other relevant characteristics of deinking sludges

Aside from the oDM, ash and $CaCO_3$ component of DS other relevant characteristics that may impact its suitability for biogas production include, chemical oxygen demand (COD), C/N ratio, Trace elements and pH. They are discussed as follows:

1.) Chemical Oxygen Demand

The chemical oxygen demand of raw and pre-dewatered DS types was analysed with the method as shown in Table 4.4. Figure 5.4 shows the COD of the different DS types. The raw DS has COD in the range 20197 - 21785 mg/L. The pre-dewatered DS has COD in the range of 44613 - 82427 mg/L, which is about the 2 - 4 folds of the raw DS. This further explains that the pre-dewatering unit concentrates the organic fraction of its inputs (raw DS) resulting in the pre-dewatered DS. The COD of the raw DS shows similar values irrespective of the wastepaper grades.

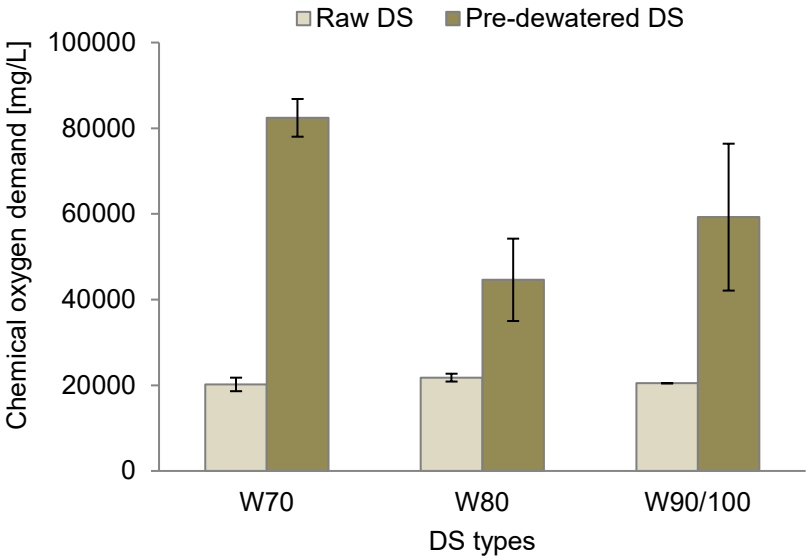

Figure 5.4 Chemical oxygen demand of different DS-types

For the pre-dewatered DS, the *W70* had the highest COD value while the *W80* has the lowest. The COD comprise both biodegradable and non-biodegradable organics. It does not alone give information on the biogas yield of the substrate except when information about the biodegraded fraction is known. The COD value is similar to the oDM. Figure 5.3 (oDM) and Figure 5.4 (COD) identifies *W70* as the highest in term of organics. While Figure 5.3 (oDM) shows a similar organic for *W80* and *W90*, Figure 5.4 (COD) suggest some difference in magnitude of organics between *W80* and *W90*.

2.) C/N ratio

The results of the C/N ratios of DS are shown in Appendix H.6. The average C/N ratios of *Streams 1* and *2* were 93 ± 24 and 82 ± 51 respectively. *Stream 4* had a significantly higher average C/N ratio of 178 ± 7. Bienert et al. (2015) and Fierro et al. (1997) reported a C/N ratio of 240 and 114 respectively for a highly dewatered DS. The fibres and fines in DS emanate from wood which is known to be characterized by high C content but a relatively low N content, hence resulting in their high C/N ratio (Chen, 2014). It is reported that there is the possibility that wood N varies by more than 14 fold in different tree species (Martin et al., 2014; Martius, 1992). There may be also influence due to variations in chemical types and quantities used for the deinking process. Also, the N-rich ink in wastepaper may be present. These explain the wide variation between own results and that reported by Bienert et al. (2015) and Fierro et al. (1997). The C/N ratio of a sludge influences the biodegradability by anaerobic microorganisms and a range of between 20 and 35 is recommended for an optimal process (section 3.3.3.2.(5)).

The C/N of DS are higher than the recommended range. It implies that the high C/N ratio of DS might not support an optimal uptake of carbon and may necessitate a N supplementation for the optimal application of DS streams for biogas production (section 5.2.1.6).

3.) Heavy metals

Heavy metals are metals with a density of more than 5 g/cm^3. They include cadmium, cobalt, chromium, copper, iron, lead, manganese, molybdenum, nickel, selenium (Briffa et al., 2020; Engwa et al., 2019). Some of these heavy metals are required by living organisms in trace quantities (very low concentration). Therefore, they are referred to as trace elements (TEs). The result obtained for selected DS were presented in Table 5.2. Some authors have reported the influences of TEs on the AD process (Ezebuiro, 2014; Gonzalez & Stres, 2019). The main sources of TEs in DS are pigment colourant and driers in printing inks used on wastepaper. Due to toxicity concerns, the European Printing Ink Association restricts the use of some TE-based pigment colours (EuPIA, 2020). This may explain to a large extent why the TEs of DS are low. TEs are also present in the wood from which the fibres are made (Harju et al., 1997; Tejada et al., 2020). The TEs of DS analysed in this study were those investigated by Ezebuiro (2014). The optimal ranges he suggested for AD as follows: Co (96.2 - 184.0 mg/kg DM), Ni (35.0 - 94.0 mg/kg DM), Se (0.0 - 23.1 mg/kg DM) and Mo (0.0 - 70.4 mg/kg DM) for mesophilic AD process. Supplementation of AD of DS with TE (Co, Ni, Mo and Se) have been reported to improve methane yield (Amare et al., 2020).

Table 5.2 Trace elements in raw DS, pre-dewatered DS and inoculum (Amare et al., 2019b)

Sample	Sample Date	Fe (g/kg DM)	Co (mg/kg DM)	Ni (mg/kg DM)	Se (mg/kg DM)	Mo (mg/kg DM)
Stream 1-W70	02.12.2013	1.01	2.67	10.50	< 0.52	1.66
Stream 2-W70	02.12.2013	1.14	3.18	11.50	< 0.51	2.46
Stream 2-W70	05.11.2013	0.57	1.53	10.10	< 0.50	1.00
Stream 2-W70	24.04.2014	NA	2.11	12.00	< 0.51	1.70
Inoculum 1	15.01.2014	56.4	4.72	98.50	1.92	9.63
Inoculum 2	30.04.2014	NA	5.64	27.50	1.23	7.88
NA- not available						

The values of TEs obtained from DS do not fall well in the range of values recommended by Ezebuiro (2014). AD mixture consists also of inoculum which might contain TEs and may compensate for the deficiency in the DS. However for a long time AD process, TEs concentration might run below the recommended values due to low TEs of DS and this might require optimization for an optimal biomethane production (Amare et al., 2020).

4.) pH value

Most biological reactions are pH-sensitive. Biogas production proceeds optimally in the pH range of 6.5-7.5 (Cioabla et al., 2012; Malina & Pohland, 1992; Reungsang et al., 2012). The statistical evaluation of the pH values from this study is shown in Appendix H.7. The pHs obtained are in the range of 6.0 - 8.0. This establishes that the pH of DS streams falls well in the suitable pH range for optimal biogas production. The high amount of $CaCO_3$ in DS could serve as a pH buffer which allows for a relatively stable pH in the biological process during biogas production.

5.1.6 Key findings on characteristics of deinking sludges for valorization

The following are the key findings of the investigation for the energetic valorization of DS by AD.

1.) Different DS types are possible in a wastepaper recycling company. They differ based on wastepaper grades used for recycling, deinking chemicals used and the treatment carried out within the plant.

2.) The dry matter content of DS and its derivatives can be compared with that of common biogas feedstocks. The raw DS (3.5% FM), pre-dewatered DS (12.7% FM), mixed sludge (5.0% FM) and main dewatered DS (54% FM) can be grouped into categories of low to high DM.

3.) DS contain organic matter originating from fibres, inks and soap amounting to about 29 to 33% DM. The largest fraction of its dry matter content is calcium carbonate with about 46 to 73% DM.

4.) DS generated from high wastepaper grade contain less lignin. They also contain a substantial amount of calcium carbonate.

5.) DS has a high C/N ratio which may result in a biogas process limitation due to low N content for a semi-continuous process in a long run.

5.2 Biogas production from deinking sludges

This section discusses the results obtained from the various experiments carried out on the AD of DS using the 1-L test system and the 100-L automatically fed test system.

5.2.1 Results from 1-L bioreactor batch tests

The results obtained in the investigation of biogas yields of DS using a 1-L test system (section 4.5.3) are discussed in the section. An overview of the AD tests carried out is shown in Table 4.1 (section 4.1). All experiments were described in section 4.5.3.2.

5.2.1.1 Influence of inocula on biogas production

Three inocula of different sources were tested with pre-dewatered DS of *W70* type (section 4.5.3.2.(1)). Cellulose is microcrystalline and using cellulose as a control experiment helped to ascertain the activity of the microbial consortia and to compare the biogas yield with that of DS. The biogas yields reported were obtained by subtracting biogas produced by the inoculum from that produced by DS and inoculum mixture. The influence of inocula on the biogas yield of DS is discussed by considering the biogas formation, the specific biogas yields and the methane content in biogas.

1.) Specific biogas yield

The specific biogas yield is a cumulative value of the biogas produced throughout the retention period. The yields of the two feedstocks are seen in Figure 5.5. The specific biogas yield of a substrate is its characteristic property within a set of defined operational AD conditions. Both graphs describe a sigmoid curve of bacterial growth. They both denote lag phases, with the DS feedstock upto 1 day and the cellulose feedstock upto 3 days for the different inocula investigated. It is pertinent to restate here, that this difference may be due to the existence of hydrolysed chemical compounds such as fatty acid from soaps present in the DS as compared to the pure cellulose feedstock. For the DS feedstock, a rapid biogas production rate began from day 1 and peaks on day 6 with cumulative specific biogas yields in the range 185 - 245 NL/kg oDM for the different inocula.

For the cellulose feedstock, the rapid phase began between days 2 and 3 and peaks are days 7 and 8 with cumulative specific biogas yields in the range of 495 - 501 NL/kg oDM for the different inocula. The biogas production rate continues to decrease for both feedstocks and peaks at the 22 day retention time with the DS feedstock reaching a biogas yield in the range of 243 - 286 NL/kg oDM and the cellulose feedstock in the range of 585 - 588 NL/kg oDM. Although the DS feedstock had a lower or almost negligible lag phase when compared to cellulose feedstock, a substantially higher biogas yield was observable for the cellulose feedstock.

This cellulose specific biogas yield at the peak of this phase is about 2 folds of that of DS. This explains that the components leading to a shorter lag phase for DS (supposedly fatty acids) are not the major components for bioconversion into biogas. DS contain a substantial amount of fibres and fines aside from the deinking chemicals added during wastepaper recycling. A study on three different DS samples from 2 different wastepaper recycling mills identifies the presence of total carbohydrates in the range of 12.7 – 59.3% DM and lignin of 5.5 - 11.8% DM. Lignin in DS was reported to originate from wood wastepaper grades and fibres. Wood can contain up to 19% lignin (Steffen et al., 2018). The total carbohydrate include cellulose and hemicellulose which have varying biodegradability. The lignin reported is an organic polymers that is known to be hardly biodegradable. It informs that the lower biogas yield of DS as compared to cellulose might be due to the lignocellulosic components of DS (*W70* type).

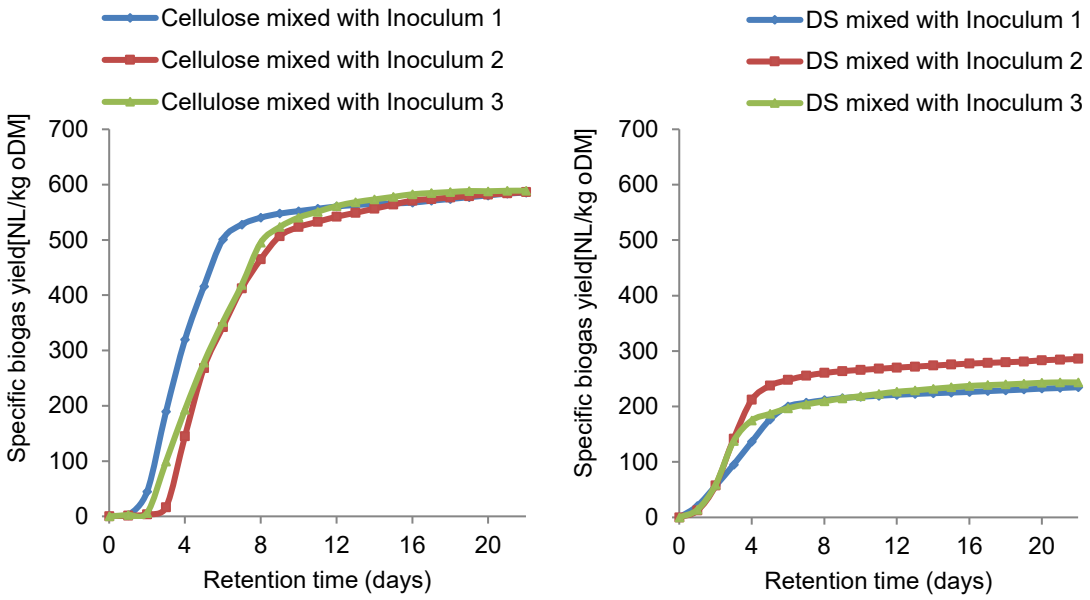

Figure 5.5 Specific biogas yields of DS and cellulose with three different inocula for 22 days (drawn from Amare et al. 2018)

Aside from the difference in the biogas yields due to the feedstock, Figure 5.5 also suggests a difference in the bioactivity or performance of the three different inocula used. For DS as feedstock, a significantly higher biogas yield is observable by inoculum 2 having a final cumulative biogas yield of 286 NL/kg oDM at end of the retention time. This is however not the case when using cellulose as a feedstock. Instead of inoculum 2, inoculum 1 showed a faster biogas production rate during the rapid phase but culminates in a relatively equal biogas yield with the other inocula.

With regard to the performance of inoculum 2 with the DS feedstock, it is necessary to mention that there are likely characteristic properties of the inocula that contribute to such distinct performance. This is discussed in a later subsection of this section. Conclusively, Figure 5.5 confirms the biodegradability of DS for biogas production with common inocula and does not suggest an inhibitory characteristic of DS components towards the production of biogas.

2.) Biomethane content in biogas

The building up of biomethane content for the two different feedstocks and three different inocula is shown in Figure 5.6. The AD with DS as feedstock attained a maximum production of methane content at about 4 days. This increasing trend was similar for the three different inocula used. On the other hand, the AD of cellulose showed a delay in attaining maximum methane content which was in about day 10. This may be owed to the quicker adaptability of methanogens to the characteristics property of the DS. However in the long run similar methane content was observable for both feedstock and both culminated as well at a similar final biomethane content of 71 ± 1% (for DS) and 69 ± 2% (for cellulose).

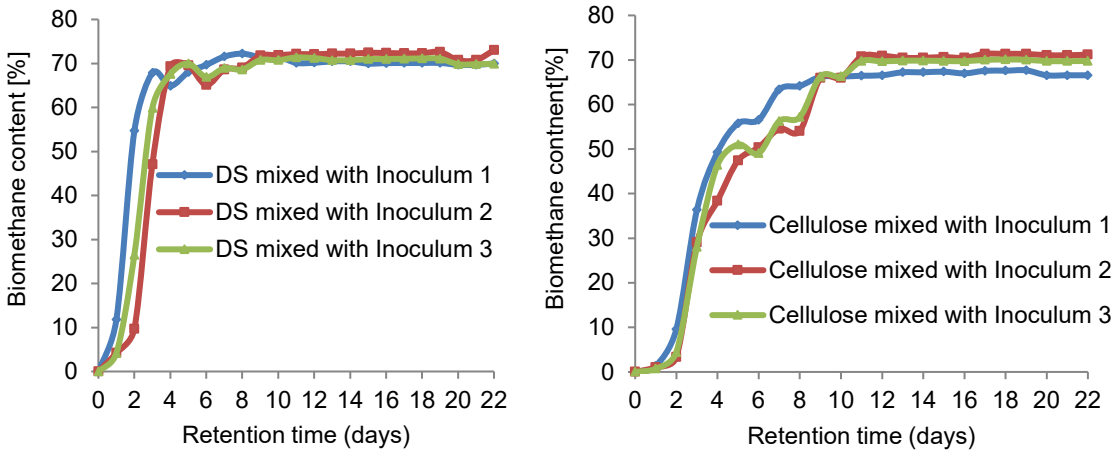

Figure 5.6 Biomethane content in biogas generated during AD batch test of two different feedstocks

3.) Comparison of inocula based on characteristics

The variations in the biogas and biomethane yield are often due to the characteristics of substrates as well as the operational conditions. The operational conditions for the two feedstocks and the three different inocula were kept constant, therefore the observed differences are largely due to their characteristics.

Appendix I.1 shows the C/N ratio and the VOA/TIC of the individual substrate inoculum mixtures prepared for the AD process and corresponding biogas yield and biodegradability. The TN_{liq} and C/N_{liq} were computed from the liquid phase of the sample. Appendix I.1 shows that the macronutrient N which is required for microbial activity is in the descending order starting from reactors with inoculum 1 followed by inoculum 3 and then inoculum 2. However, the N concentration alone does not give sufficient information as compared to the C/N ratio which is a performance indicator for a biogas producing AD process.

The C/N_{liq} was computed only for the reactors with DS as feedstock and the variations from 26.7 to 229 were obtained. When compared to the 20 - 35 optimum C/N ratio for the AD process (section 3.3.3.2.(5)), reactors with inoculum 1 and 3 having a C/N ratio of 52.2 and 229 respectively might have conditions of lower uptake of carbon. The reactors with inoculum 2 fall into the reported range for optimum AD process and hence its considerably higher biogas yield during the biodegradation of DS when compared to the other two inocula. The biodegradability of inoculum 2 (26% oDM) for DS as feedstock is also the highest when compared to other inocula. This further establishes why inoculum 2 had a higher biogas yield with DS as feedstock. The strains of microbial consortium present in inoculum 2 might also have influenced the result obtained. But the analysis of microbial consortium was beyond the scope of this study. Also, inoculum 2 does not show a distinctly higher performance in terms of biodegradability or biogas yield when cellulose was used as feedstock. This concludes that although common inocula types, especially those tested in this study all could produce biogas from DS. The inoculum 2 from a sewage sludge treatment plant happens to perform better possibly due to the optimum C/N ratio in its DS-inoculum mixture or the strains of microbial consortium present in it. The inocula used for further studies on AD of DS in this study were similar to inocula 2 as they were collected from the same source.

5.2.1.2 Influence of high calcium carbonate on biogas production

The influence of high $CaCO_3$ on the biogas yield of DS was carried out as described in section 4.5.3.2.(1). The result of the biogas test for the different samples of cellulose-$CaCO_3$ mixtures are shown in Table 5.3. Table 5.3 shows the corresponding biogas yield, biomethane yield and hydrolysis constants for the different cellulose-$CaCO_3$ mixtures. The results showed that a possible negative influence of $CaCO_3$ in AD is not observable. The negative influence of $CaCO_3$ in AD as reported by van Langerak et al. (1998) are: the limitation of the mass transfer due to highly scaled biomass and the growth of thin biofilms of biomass on the surface of precipitates.

It is therefore arguable that for cellulose-$CaCO_3$ mixturse with a $CaCO_3$ content in the range of 0 - 40% DM, there is no inhibitory effect on the AD process. The cellulose-$CaCO_3$ mixtures can be compared to the oDM-$CaCO_3$ content of the DS sample produced in the highest proportion by the partner wastepaper recycling company (*W70*). The median value of the $CaCO_3$ content in this DS type for raw sludge is 42% DM and for pre-dewatered sludge, it is 47% DM. These values are at the upper boundary of the range of $CaCO_3$ content investigated, other authors have reported that the high $CaCO_3$ content of DS has no negative influence on the AD of DS due to any form of chemical interaction (Steffen et al., 2017). A reason might be that the concentration of $CaCO_3$ in DS is not sufficiently high to initiate an inhibition in the AD process. The experiment of van Langerak et al. (1998), where inhibition was observed, was operated at $CaCO_3$ of 4000 mg/L using a UASB, whereas the concentration of $CaCO_3$ in pre-dewatered DS of all types is between 24.2 - 132.4 mg/L. This concludes that the presence of high calcium carbonate in DS is not too high to lead to an inhibitory effect.

Table 5.3 $CaCO_3$ share in the cellulose-$CaCO_3$ mixture, biogas and biomethane yield and hydrolysis constant for cellulose $CaCO_3$ AD test

Sample number	$CaCO_3$ added to cellulose	Specific yield		Hydrolysis constant	
		Biogas	Biomethane		
	[% DM*]	[NL /kg oDM]	[NL /kg oDM]	k	R^2
1	0	654 ± 2.0	273 ± 1.3	0.430	0.9808
2	12	667 ± 2.7	277 ± 0.7	0.407	0.9874
3	22	662 ± 0.6	273 ± 0.5	0.418	0.9872
4	40	656 ± 10.7	271 ± 4.6	0.367	0.9831
*Refer to the total dry matter in a mixture that includes both the $CaCO_3$ and the cellulose					

5.2.1.3 Influence of wastepaper grades on biogas yields

The influence of wastepaper grades on the biogas yield of DS was investigated as described in section 4.5.3.2.(1). DS samples discussed are shown in Appendix C.1, C.2 and C.4. This section discusses differences in biogas yield of the samples regarding absolute and specific biogas, biomethane yields as well as on biodegradability of DS.

1.) Absolute biogas and biomethane yield

The absolute biogas yield is a cumulative value which refers to the biogas (or biomethane) produced regarding its fresh mass. It is the volume of biogas (or biomethane) in normalized Litre that 1 kilogram of a fresh DS will produce under an AD process. The fresh mass of a DS sample includes its water as well as organic and inorganic components. Figure 5.7 shows the absolute biogas and methane yield of three different DS samples which differ in terms of different wastepaper grades. The samples investigated were all pre-dewatered DS *(Stream 2).* For all experiments, inocula from the same source as inoculum 2 were used. Figure 5.7 shows some variations in the biogas and biomethane yield of the different DS samples.

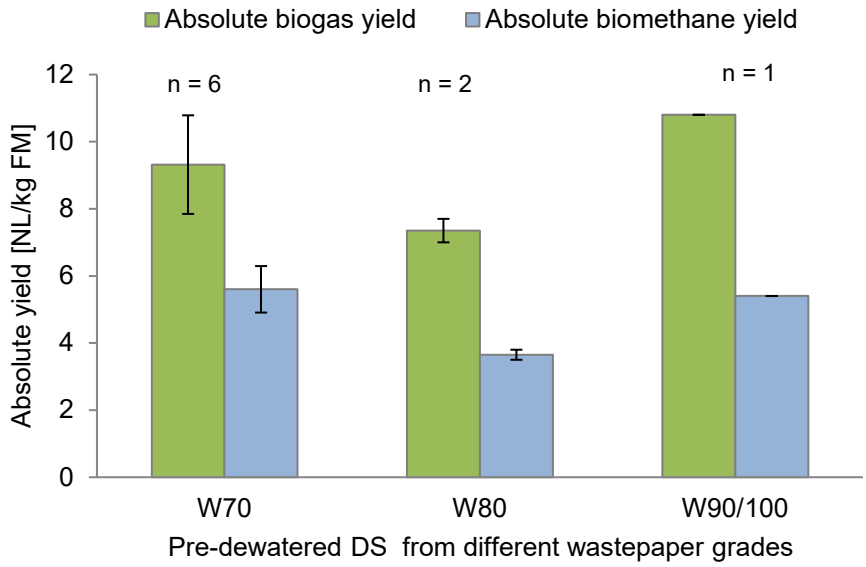

Figure 5.7 Absolute biogas and biomethane yields of different pre-dewatered DS which differ by wastepaper grades. n is the number of samples.

The absolute biogas yield for these three categories of DS samples investigated was in the range between 7.0 and 12 NL/kg FM. The minimum value of 7.0 NL/kg was observed for *W80*, while the maximum value of 12.0 NL/kg FM was observed for *W70*. According to the average values obtained, their absolute biogas yields are 9.3 NL/kg FM (*W70*), 7.4 NL/kg FM (*W80*) and 10.8 NL/kg FM (*W90/100*). The average values according to Figure 5.7 present *W90/100* as the highest followed by *W70* and then *W80*. The high standard deviation of *W70* is notably. It occurred due to variation in a large number of samples tested. On the other hand, *W90/100* had a limited amount of samples.

The biogas produced by all DS from different wastepaper grades contains a substantial amount of biomethane. In terms of average values, their absolute biomethane ranged between 3.7 and 5.4 NL/kg FM. Provided all other AD process conditions are kept constant, the main property of AD substrate that leads to differences in absolute biogas yield is the amount and nature of the organic components in the dry matter. If the nature or types of organic components is the same for different AD substrates, then their absolute biogas yield should have a direct relationship with their organic content in fresh mass.

The mean organic content in the fresh mass of the different pre-dewatered DS investigated are; *W70* (3.8% FM), *W80* (2.7% FM) and *W90/100* (2.6% FM). The trend described by the absolute biogas yield of *W70* and *W80* has a direct relationship with their respective oDM in fresh mass. This is not the case with the *W90/100*. It might imply that the organics in *W70* and *W80* have similarities, but they are both different from those present in *W90/100*. The difference like the organics in *W90/100* might be the reason for its higher absolute biogas yield when compared to the other DS samples from other wastepaper grades. They are generated from the deinking process which involves high quality recovered wastepapers (section 4.2).

A study on the total carbohydrate and lignin characteristics of different DS samples which differ based on wastepaper grades has been reported by (Steffen et al., 2017). The samples investigated were collected from a laboratory deinking process. They reported the total carbohydrate content of raw DS in the order *W100* > *W90* > *W80* > *W70*. The lignin content of raw DS in the order *W100* < *W90* < *W80* < *W70*. The highest biomethane yield was observed for *W100.* This implies that the high amount of carbohydrate and low lignin content of *W90/100* might be the reason for a higher absolute biogas yield when compared to the DS from the other wastepaper grades. Based on carbohydrate and lignin content the *W80* is expected to be better than *W70*, but this is not the case as can be observed in Figure 5.7. An explanation for this might be due to the substantially higher oDM of *W70* with more yield than the influence of the better organic type reportedly present in *W80*. The influence of the different organics present in different DS on biogas production can further be established in section 5.2.1.3.(2) which discusses differences in the specific biogas and biomethane yield of DS from different wastepaper grades.

2.) Specific biogas and biomethane yield

The specific biogas and biomethane yield of different DS types is given in Figure 5.8. It shows similar values for *W70* and *W80* but different for *W90/100*, which *had the highest* specific biogas yield with a value of 417 NL/kg oDM.

The specific biogas yield describes the biogas generation related to the organics present. Although *W80* has less lignin and a higher carbohydrate than *W70*, the difference of 22 NL/kg oDM in specific biogas observed in favour of *W80* is not high. They can therefore be grouped into the same category in terms of biogas generation. The higher specific biomethane yield of *W90/100* is shown in Figure 5.8. corresponds to the report of Steffen et al. (2017). Biomethane content of biogas were also obtained for the different DS types and are *W70* (72%), *W80* (63%) and *W90/100* (66%).

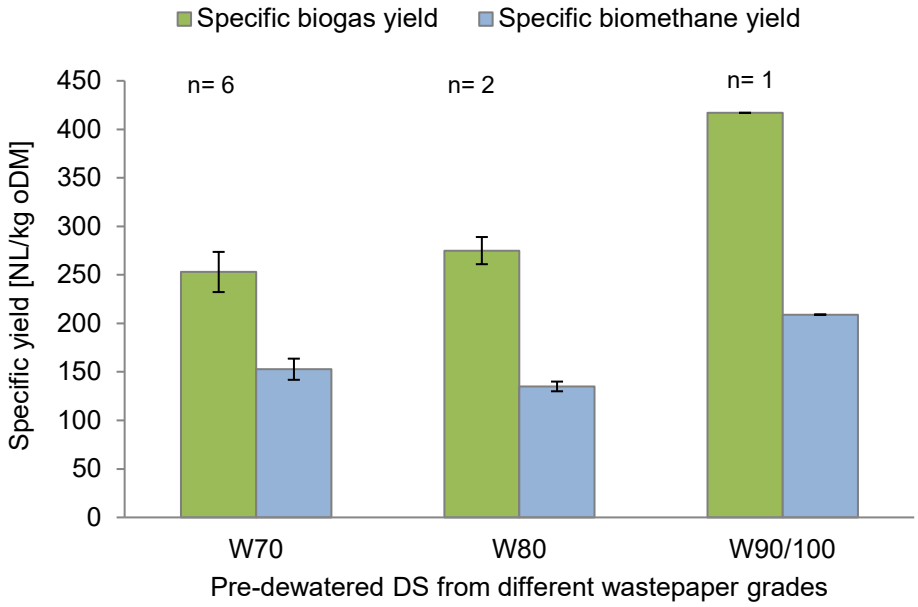

Figure 5.8 Specific biogas and biomethane yields of pre-dewatered DS differing by wastepaper grades

3.) Biodegradability

The biodegradability of different DS samples was computed using Eq B.11 and B.12 (Appendix B.9). The mean biodegradabilities of pre-dewatered DS obtained were 23% oDM (*W70)*, 26% oDM (*W80)* and 39% oDM (*W90/100)*. These values correspond to the specific biogas and biomethane yields. The biodegradability of *W90/100 was* significantly higher compared to the other two DS samples. The biodegradability of *W70* and *W80* are similar.

5.2.1.4 Influence of pre-dewatering on biogas yield

This section compares the input of the pre-dewatering unit (raw DS) with its output stream (pre-dewatered DS). It discusses the variations in the biogas yield of the different streams. The selected samples were DS of *W70* type. Figure 5.9 depicts the absolute and specific biogas and biomethane yields of the two different DS types. Also, their biodegradabilities are shown on the plot. The average absolute biogas yield of the pre-dewatered DS is about 2.2 times higher than that of the raw DS. The ratio of oDM in the fresh mass of pre-dewatered DS to raw DS is approximately 3.2 of that of raw DS. Since their oDM ratio in fresh mass (pre-dewatered to raw DS: 3.2) is not similar to the ratio of their absolute biogas yield (pre-dewatered to raw DS: 2.2), it may imply that the two samples possibly have different organic matter composition. Organic matter composition here refers to the proportions of the different organic types present. It suggests that a proportion of a more readily biodegradable organic fraction from raw DS finds its way into the liquid phase (*Stream 5*) during the pre-dewatering process.

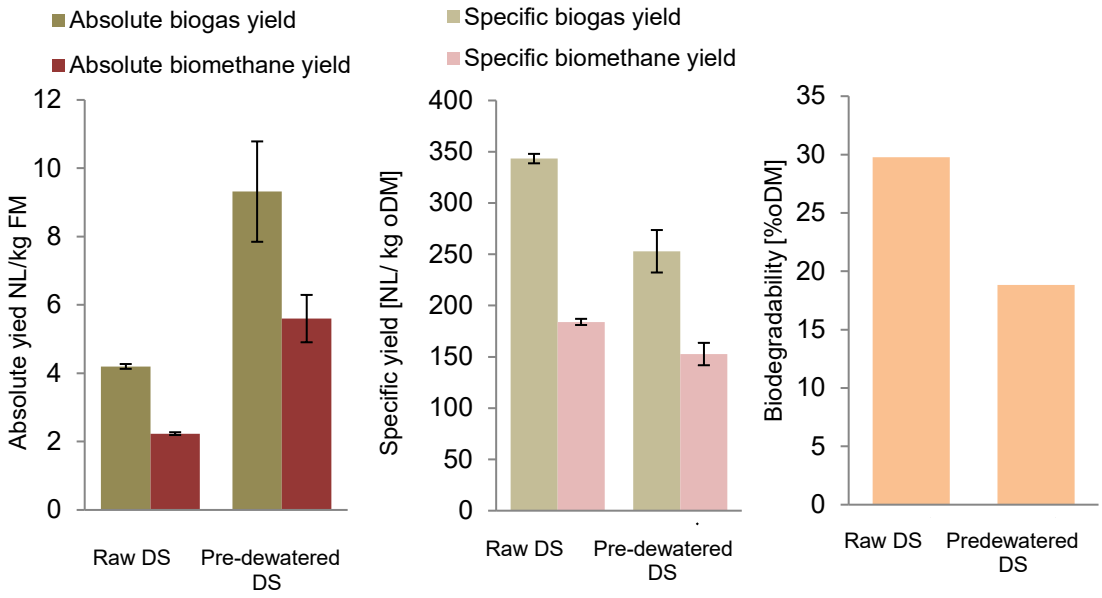

Figure 5.9 Absolute and specific biogas yields and biomethane of raw and pre-dewatered DS samples from wastepaper grade *W70* as well as biodegradability

The sources of organics in raw DS other than fibres and fines include soaps originating from deinking chemicals (section 2.3.3.1) or detached printing ink from wastepaper. They have finer particles (dissolved) when compared to fibres and fines. They may also be readily biodegradable depending on their nature and composition.

Soap (alkaline salt of fatty acids) for example has been reported with biodegradability of 80% in anaerobic treatment (Prats et al., 1999). The result suggests that the loss of these fractions of biodegradable organic matter in raw DS resulted in a negative impact on the absolute biogas yield of pre-dewatered DS of *W70* type. The 2.2-fold of absolute biogas yield obtained for pre-dewatered DS in comparison to raw DS is a beneficial impact of the pre-dewatering operation on biogas production. However, the specific biogas yield of *Stream 2-W70* is seen to be lower than that of *Stream 1-W70* (Figure 5.9). This establishes further that the nature of the total organics present in raw DS is more biodegradable than those in pre-dewatered DS.

This is also confirmed by the biodegradability plot (Figure 5.9). Also, the biomethane concentration of the two DS types increased was different, 67% (raw DS) and 72% (pre-dewatered DS). The influence of the water content of DS on biogas yield is further discussed in section 5.2.1.5.

5.2.1.5 Influence of water content on biogas of deinking sludge

In this section, the impact of water content on the biogas yields of DS was investigated. To generate a range of DS samples with varying DM contents, a highly dewatered DS (*Stream 4-W70)* and the corresponding filtrates (*Stream 6-W70*) were mixed in different proportions (Appendix C.3). The equations used for calculating the required substrate for mixing are Eq B.4 and B.5 (Appendix B.9). The water contents (WC) of DS mixtures were 55, 64, 71, 80 and 91%. A raw DS is similar to the DS mixture with a WC of 91%, a pre-dewatered DS is similar to a WC of 80% and a highly-dewatered DS to that with a WC of 55%. Figure 5.10 shows the absolute and specific cumulative biogas yields at different times for the different DS mixtures. All samples had a similar starting pattern, characterised by little lag phases (1 - 2 days). The mixtures with the WC of 91 and 80% completed their rapid phase and reached the declining phase within the 21days period. The other DS mixtures were still in their rapid phase after 21 days. They require more time to reach the declining phase.

In terms of absolute biogas yields, the DS mixtures within the WC range of 55 - 71% showed similar high performance on day 21, followed by the DS mixture with WC of 80%, while the least was DS mixture with WC of 91%. When the specific biogas yields are considered, a different order was observed. The DS mixtures in the WC range of 71 - 91% showed the best performance followed by the DS mixture with a WC of 64% and the DS mixture with a WC of 55% as the least.

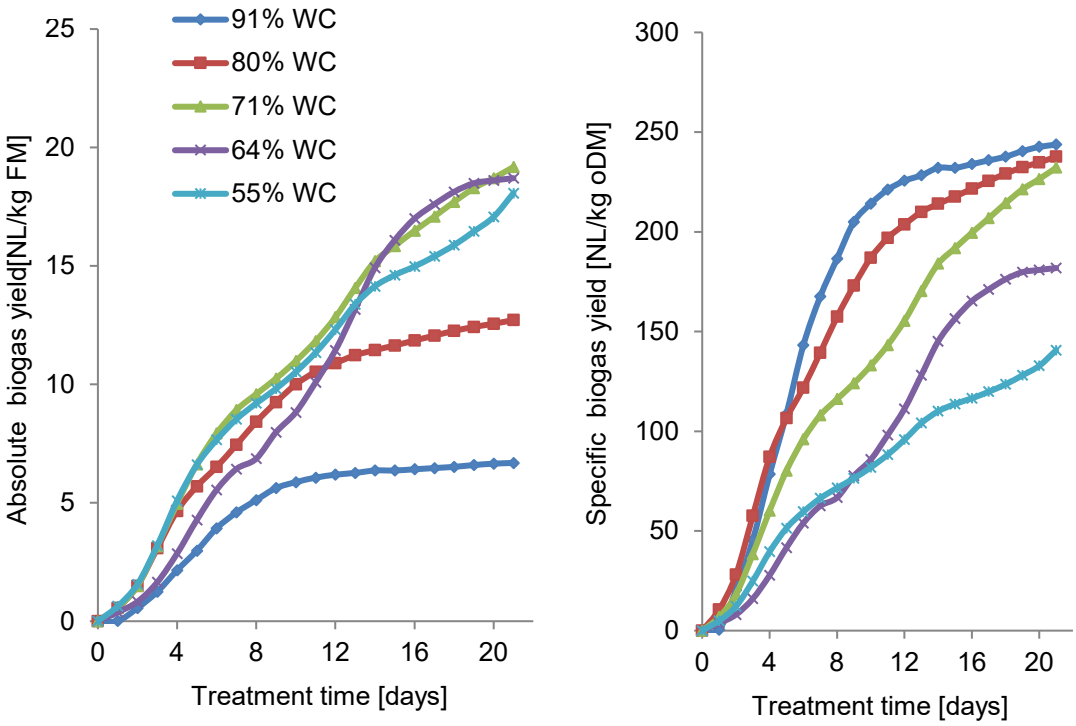

Figure 5.10 Absolute and specific biogas yields of different DS mixtures (*Stream 4-W70* and *Stream 6-W70*).

The results revealed that for DS with higher WCs (91 - 80%), the final absolute biogas yields were lower, but they had improved biodegradability since their specific biogas yields showed that more biogas was produced per kg of oDM when compared to the DS mixtures with lower WC (55 - 64%). The lower biodegradability of DS mixtures with lower WC observed during the period might have been caused by poor mixing efficiency due to higher solid contents.

Using the result obtained as a basis for the comparison of different DS types based on water content, it can be inferred that the degree of dewatering of DS types may influence their application for biogas production. In a real application, a highly dewatered DS requires a lower size of the bioreactor to achieve a desired biogas production but it will as well require a longer retention time to reduce the oDM fraction considerably. A raw or less dewatered DS requires a larger bioreactor size to achieve a similar desired biogas due to lower oDM in fresh mass but results in an improved reduction in its oDM fraction. It is therefore necessary to find a point of compromise that is optimum for biogas production.

The point should depict a dewatering degree for DS to achieve desired biogas yield within a rather small bioreactor and for which retention time may also not be too long. Figure 5.11 shows the intersection of the trend lines describing the absolute and specific biogas yields of the DS mixtures regarding their various water contents. The two trend lines are polynomials with sequence 3.

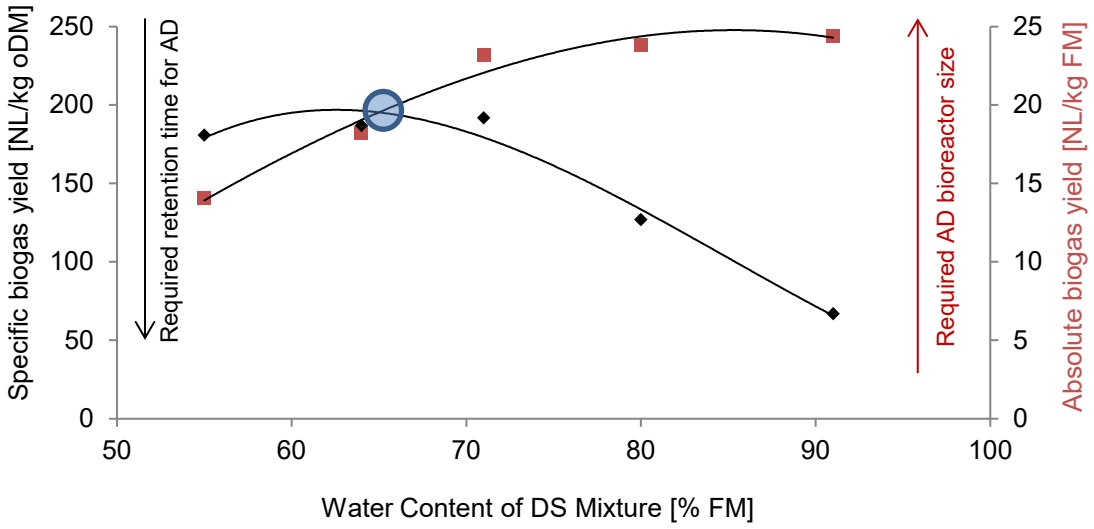

Figure 5.11 Trend lines and point of intersections between the specific and absolute biogas yield of DS mixtures with different water contents

Their intersection denotes the point of compromise for bioreactor size and retention time. It coincides with a WC of about 65%. Raw DS had WC in the range of 95 to 99%, which is not optimal for biogas production with consideration of bioreactor size and retention time. Therefore for an optimal application in this regard, dewatering of raw DS might be beneficial. The main-dewatering unit results in DS with WC in the range of 38 - 51% DM which is too thick for biogas production, especially in the wet fermentation process. A different set of dewatering units to yield DS with WC of about 65% is recommended. It is however also important to consider the energy balance as to whether the energy expended in dewatering is compensated for by the resultant surplus biogas energy output.

5.2.1.6 Influence of nitrogen supplementation

The influence of nitrogen (N) supplementation on the AD of DS was studied. Ammoniacal N was used for the study. Inocula with low N concentration and pre-dewatered DS of type *W70* were mixed and spiked with ammonium chloride to achieve samples of different N-contents (section 4.5.3.2.(1), Appendix C.7). The C/N ratio of the DS mixtures obtained were 44, 34, 29 and 24. The different DS mixtures began biogas production without a lag phase but showed partly differences in their rapid phases (Figure 5.12).

At the end of the batch test, they culminated in a similar cumulative biogas yield. The mixtures with C/N ratios of 34, 29 and 24 showed a higher biogas production rate in the rapid phase and described well-shaped biogas production curves. The mixtures with a C/N ratio of 44 had a lower biogas production rate during the rapid phase, indicating a suboptimal condition in the biogas production process, which may be connected to a longer lag phase of adaptation of the microorganism in the particular mixture. It is thought to be as a result of an N limitation as other variables of sample mixtures as well as AD conditions were considered constant.

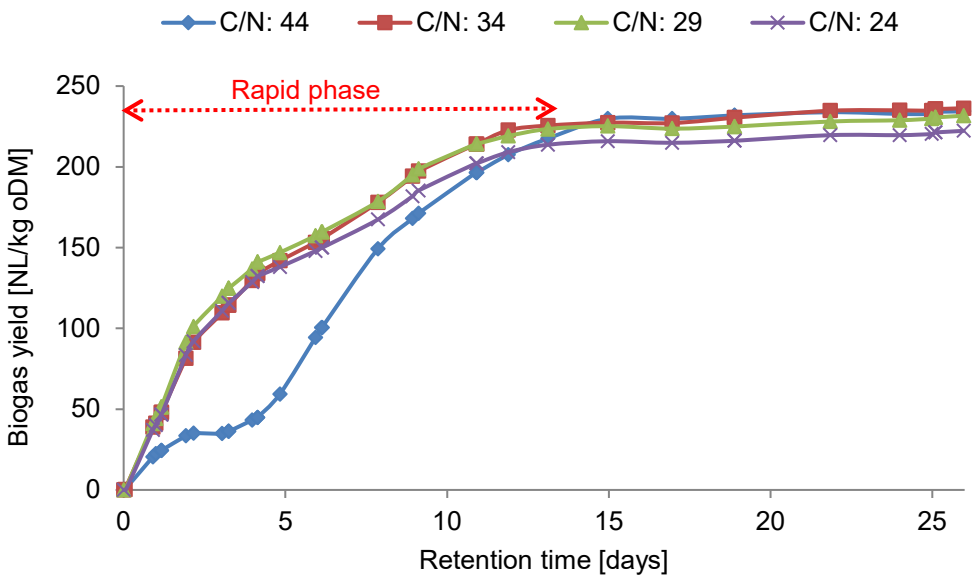

Figure 5.12 Biogas yields of different samples with the same masses of DS and inoculum mixture but varying C/N ratios. The C/N ratio was varied with the addition of ammonium chloride.

The C/N ratio of inoculum and DS used for the AD test are 34 and 49 respectively (Appendix C.7). This shows that the nitrogen concentration in the inoculum used is higher than that in the DS used. In comparison to the inoculum, the mixture with a C/N ratio of 44 represents a condition of depleted N, which can occur during a long run of a semi-continuously operated AD process. Nevertheless, this nitrogen depletion condition does not suggest a process concern for a batch AD, since in the long run it eventually yielded similar biogas to the other AD mixtures. However, when the process is operated semi-continuously a high yield in the rapid phase is desirable. Also on further consideration, the C/N ratio of 44 is beyond the reported optimal range of 20 to 35 for the AD processes (Ceron-Vivas et al., 2019; Panichnumsin et al., 2012; Siddiqui et al., 2011; Wang et al. 2012).

The result obtained suggests that for a semi-continuously operated AD using DS as substrate, the AD mixture set with a C/N ratio of about 44 and above may be disadvantageous. Conditions of N depletion can be corrected by the addition of synthetic nitrogen chemical sources such as NH_4Cl or NH_4OH or the use of co-substrate rich in nitrogen such as urine, pig or cow manure (Samir et al., 2019) as well as grass silage (Dickson et al., 1991; Hertel et al., 2015).

It concludes that in a long run, a semi-continuously or continuously operated AD of DS may encounter impaired process efficiency possibly due to nitrogen depletion, which can lead to reduced biogas production rate in the rapid phase. For conditions of this kind, N supplementation by the use of a synthetic N source or co-substrate is recommended to bring the C/N ratio in the range of 24 and 34 to improve the productivity of AD of DS.

5.2.1.7 Comparison of deinking sludge with common biogas feedstocks

The study on batch and semicontinuous AD using different types of DS as substrate showed that DS are biodegradable and can be used for the production of biogas. The biogas yields of common biogas feedstocks (section 5.1.4) were compared to the biogas produced from DS in the 1-L batch test. As shown in Table 5.4 the blackwater from vacuum toilets which has the same DM category as *Stream 5*, *Stream 6* and *Biosludge* has very low absolute biogas yields owing to the very low DM content. The low DM category of common biogas substrates which include the sewage sludge, greasy water and pig manure have absolute biogas yield in the range of 15 - 30 NL/kg FM. Their specific biogas yield is also in the range of 525 - 1066 NL/ kg oDM. The *W70 Stream 1* which belongs to the same low DM category showed absolute and specific biogas yields below these ranges. This low value may be owed to the lignin content in the *W70 DS sample* as discussed in section 5.2.1.3.

The liquid cow manure which belongs to the medium DM category has absolute and specific biogas yields of 25 NL/kg FM and 312 NL/kg oDM respectively. The *Stream 2* DS samples belonging to the medium DM category showed varying biogas yields. Their absolute biogas yield is lower with DS samples from *W90/100* having about half of the liquid cow manure. Although the specific biogas yield of DS from *W70* and *W80* DS types are also lower than that of liquid cow manure, that of *W90/100* is sufficiently higher. The biogas feedstock in the high DM category has absolute biogas yield in the range of 50 - 411 NL/kg FM. The DS sample of *Stream 4* which belong to the same category may have biogas of about this range as well due to sufficient oDM in the fresh mass.

The comparison of the biogas production from DS *Stream 1 and 2* with common biogas feedstock showed that although they might be lower they are as well biodegradable and produce a substantial amount of biogas that can be beneficial for the wastepaper recycling industry.

Table 5.4 Comparison of biogas yield of deinking sludge with that of common biogas Feedstocks

DS and DS derivative					**Common biogas feedstock**			
Dry matter category		**Biogas yields**						
Type	**Range (% FM)**	**Type**	**Absolute biogas yield (NL/kg FM)**	**Specific biogas yield (NL/kg DM)**	**Type**	**Absolute biogas yield (NL/kg FM)**	**Specific biogas yield (NL/kg DM)**	**Source**
Very low	>0.4 – 2	*Stream 5* *Stream 6* *Biosludge*	*ND* *ND* *ND*	*ND* *ND* *ND*	Blackwater from vacuum toilets	2	489	1
Low	>2 – 7	*Stream 1* *Stream 3*	*4.2* *ND*	*343* *ND*	Sewage sludge Greasy water Pig manure	15 30 28	525 1066 583	2 1 3
Medium	>7 – 20	*Stream 2*	10[a], 7.4[b], 11[c]	253[a], 275[b], 417[c]	Liquid cow manure	25	312	3
High	>20	*Stream 4*	ND	ND	Food waste Solid cow manure Chicken manure Green waste Lawn cuttings	411 80 140 50 78	1663 400 466 NA 393	4 3 3 5 1

ND: Not determined; NA: Not available by author; [a]W70; [b]W80; [c]*W90/100*

1 Hertel et al., 2015 2 ARCHEA, n.d. 3 Friehe et al., 2016a ; 4 Al-Wahaibi et al., 2020 5 Richter et al., 2017

5.2.2 Results of 100 L bioreactor semi-continuous tests

This section discusses the results obtained in the AD of DS by the application of a semi-continuously feeding mode. The three AD systems, 100 L bioreactor with recirculation pump (R1A), 100-L bioreactor with a recirculation pump and highly inclined bottom (R1B) and 100-L bioreactor with a stirrer (R2) were used for this purpose (section 4.5.3.2.(2)). All the AD test systems were operated under mesophilic conditions and the *Stream 2-W70* was used as substrate in all cases.

5.2.2.1 Bioreactor with recirculation pump

The bioreactor with recirculation pump (R1A) was operated first in a batch mode for 21 days before the semi-continuous feeding mode started. This was done to compare the output with that obtained from the 1-L batch test system. It further proved the airtightness of the reactor. The results of the batch phase, as well as the semi-continuously operated phase, are discussed.

1.) Initiation phase

The cumulative biogas yield of DS during the batch phase of bioreactor R1A is shown in Appendix J.1. The inoculum's contribution to the biogas production of the mixture was neglected because the inoculum was warmed up under mesophilic condition for about 2 weeks to reduce the amount of readily degradable organics before beginning the batch test. The biogas production began without a lag phase and continued in a rapid phase until the 4th day with a biogas yield of about 200 NL/kg oDM when a technical breakdown was encountered. The system was restarted after refilling some lost mass with consideration of the organic fraction of DS and inoculum.

The system continued production in a rapid phase and began to approach a stationary phase at about the 10th day. At the end of the 20th day, a cumulative biogas yield of 277 NL/kg oDM was observed for DS. This is in range with values obtained for the AD of *Stream 2-W70* in the 1-L batch test. Also, the average concentration of methane in biogas at 20 days was found to be 51.5% Vol. The maximum H_2S concentration observed in the batch phase was 127 ppm. This result confirms that the system is airtight (anaerobic) and the condition of the microbial consortium in the reactor was in good conditions.

2.) Semi-continuous phase

The semi-continuous phase of bioreactor R1A is divided into two phases, the feeding phase until process limitation and the reactivation phase.

a.) Feeding phase until process limitation

The operation of the bioreactor R1A (see the design in section 4.5.2.1) began with a daily feeding mode (semi-continuous) after the initiation phase. The feeding pattern is shown in Appendix C.8. The HRT of the semi-continuous phase was gradually reduced from 30 to 15 days before a process limitation was ascertained (Figure 5.13). The reduction of HRT denotes an increase in the amount of daily fed DS. The biogas production at HRT 30 days was between 166 and 386 NL/kg oDM_fed. This large variation within a constant HRT is due to variation in the oDM of input DS (Appendix L.2).

The biogas production during HRT 25 was initially similar to that of HRT 30 days until the latter period, where it declined to about 70 NL/kg oDM_fed. This occurred in the 33rd week of operation. A further declination in biogas production was observed for HRT 20 days. The biodegradation of DS at HRT 20 days computed using Eq B.13 of Appendix B.9 was 30% oDM.

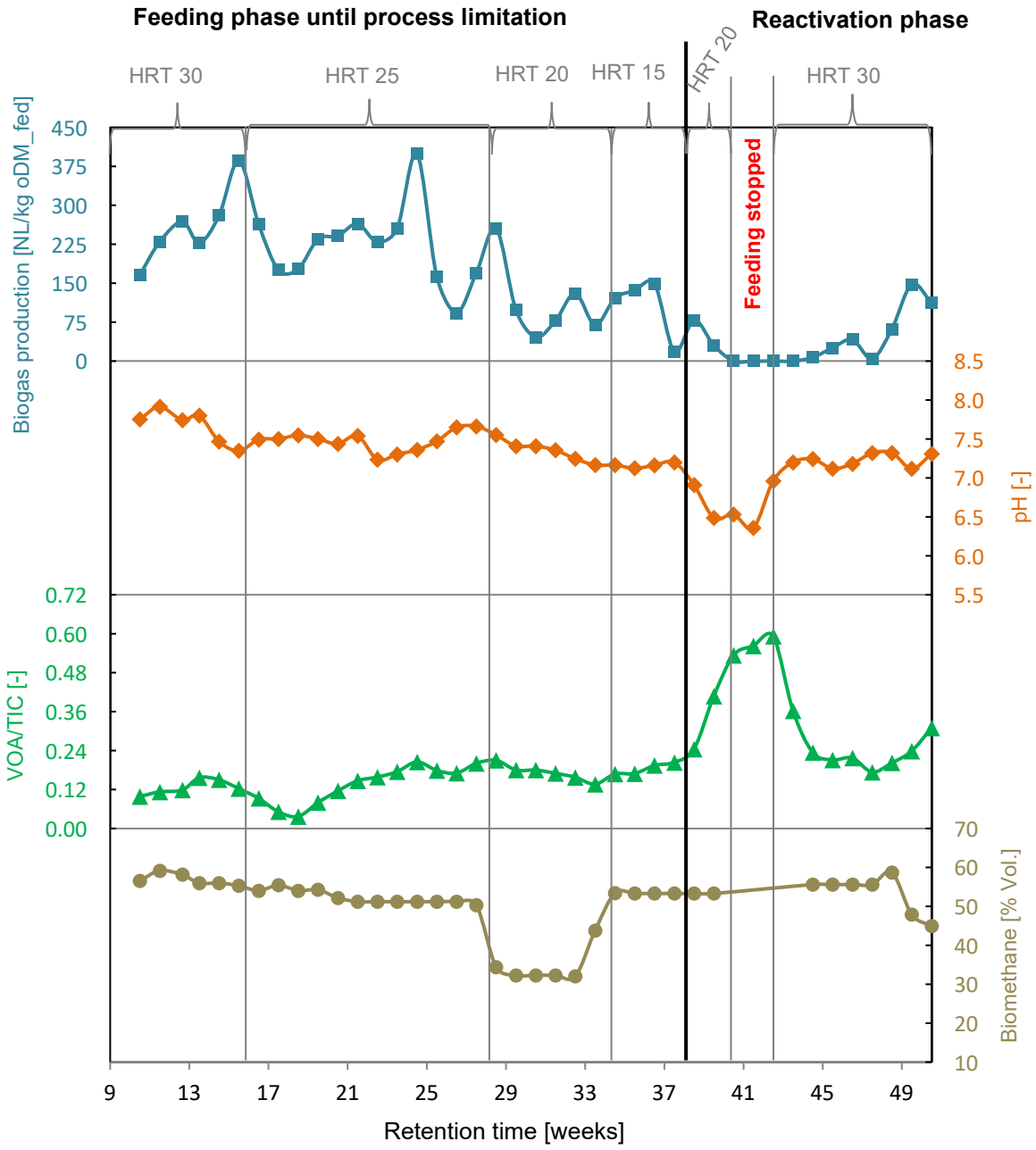

Figure 5.13 Biogas production and other operation parameters obtained from semi-continuous AD of DS using bioreactor R1A

The biogas production worsened with HRT 15 days, and in the week 39 of the operation time, the system was taken as being process limited due to observed continuous declination in biogas production. The pH value during HRT 30 and 25 days was between 7.4 and 7.9. The pH dropped continuously during HRT 20 and 15 days to a value of 7.2. The declination in biogas production during HRT 20 and 15 days can further be explained by the VOA/TIC values observed. Beginning with a value of 0.10 at HRT 30 days, VOA/TIC increased and then dropped to 0.04 during HRT 25 days at week 18. Thereafter it continued to increase until a final value of about 0.20, which remained fairly constant during the HRT 20 and 25 days. This VOA/TIC value of 0.20 denotes a condition of too low biomass input according to Lili et al. (2011) (Appendix L.3). The biomethane content of biogas during the HRT 30 and 25 days was between 50 and 59% Vol. Biomethane content dropped during the HRT 20 days and returned to an average of 53% Vol. during the HRT 15 days.

b.) Reactivation phase

Due to the continuous decrease in biogas production measures were taken to reactivate the process. Measures taken were first an increase in HRT and secondly, a stopping of feeding operations. From week 39, the system was operated at HRT 20 days which implies a reduction of daily DS feed in comparison to HRT 15 days. The biogas production however further declined to zero during the HRT 20 days. During this period pH dropped to 6.4. Also, the VOA/TIC increased to about 0.6 which indicates a highly acidic condition that is not buffered by the total alkalinity of the system. Lili et al. (2011) suggested stopping substrate feeding with VOA/TIC at about this value. The feeding was stopped from week 40 to 42 and biogas production remained at zero. An HRT of 30 days was initiated in week 42. Biogas production started again in week 44 and reached a maximum value of 148 NL/kg oDM_fed in week 49.

During the period of reactivation the pH value was at an average of 7.2 and VOA/TIC declined to an average of 0.2. The biomethane content observed during the reactivation phase was between 45% and 55%. When the bioreactor R1A was opened at the end of the AD process, a substantial mass accumulation was found within the bioreactor (Appendix. L.4). This was possible because of a mild mixing pattern that was adopted. The result obtained suggest that HRT 30 and 25 days may be suitable for AD of DS in a semi-continuous system. It also showed a poor biogas production during the HRT 20 and 15 days which suggests an excessive organic loading. This is however not conclusive due to the occurrence of substantial sedimentation during the process.

The main impact was ab H_2S concentration in biogas observed above 1000 ppm from week 7 of the AD process. It remained above this value all through the process limitation and the reactivation phase. The very high H_2S concentration observed in biogas may be connected to the ineffective mixing in the bioreactor R1A. A common source of sulphate in DS is magnesium sulphate (Singh et al.,2019; Sridhar et al.,1998), which is used as a stabiliser in the bleaching of recycled fibre with hydrogen peroxide. The sulphate content of DS in this study is not influenced by magnesium sulphate as it is not used by the partner company. The sulphate source is rather from the aluminium sulphate used as flocculant during the solid-liquid separation of DS streams in the plant. The low concentration of sulphur measured in DS (0.5 g/kg FM, Appendix I.2) does not suggest a substantially high H_2S production during biogas. The high concentration of H_2S in biogas is thought to be due to the sedimentation process in the reactor which might have led to an accumulation of sulphate in the reactor. The accumulated sulphate in the AD system can induce a competitive condition for methanogenic organisms. Their presence increases the growth of sulphate reducing bacteria (SRB) which compete for acetates with the methanogens and also produce toxic H_2S which eventually leads to reduced biogas production. The inhibitory effect of SRB can be removed as discussed in section 3.3.3.2.(6)(a).

The 100-L bioreactor experiment R1A was therefore tagged as a worst-case scenario. Upgraded and improved systems with more efficient mixing were further investigated in sections 5.2.2.2 and 5.2.2.3.

5.2.2.2 Bioreactor with recirculation pump and highly inclined bottom

The bioreactor with a recirculation pump and highly inclined bottom (R1B) as shown in section 4.5.2.1 is similar to the bioreactor R1A but differs in pump capacity and nature of the reactor bottom. As an upgraded system, the higher flow rate and the 45^o inclined bottom were designed to help improve mixing. The operation of the system began also with a batch phase and then a semi-continuous phase with a daily feeding pattern followed.

1.) Initiation phase

The batch phase was monitored for 12 days before the start of the semi-continuous phase. The inoculum used was monitored using a 1-L batch test system. This was necessary to estimate the biogas contribution of inoculum from the DS–inoculum mixture in the bioreactor R1B test system. Appendix J.2 shows the cumulative specific biogas yield observed during the period. The slightly lag phase of about 1 day is not typical of DS. It could be due to the inoculum used.

The biogas builds in a rapid phase until day 4 and continued with a stationary phase. At the end of day 12, a cumulative biogas yield of 250 NL/kg oDM was observed. This is however not the maximum as the curve shows that the biogas formation is yet to culminate. The values observed were consistent with the 1-L batch system (section 5.2.1). This test confirms that an anaerobic condition was attained in the 100-L bioreactor R1B system due to airtightness and that no inhibitory component in the system hinders the AD process.

2.) Semi-continuous phase

The system was operated in a semi-continuous feeding mode with an HRT of 19 days. The entire feeding of HRT 19 days was kept constant but input DS varied in oDM (Appendix L.5). The HRT 19 days is equivalent to an average of 1.4 kg oDM/ (m^3·d) The process was stopped for a period due to a technical problem. In this phase, the biogas production values were not used. Instead, biodegradability was used to describe the AD process. The biodegradations were computed as in Eq B.13 (Appendix B.9). Figure 5.14 shows a biodegradation in the range of 46 and 64% oDM in the first feeding phase. The high biodegradability can be explained due to the influence of the inoculum. After the no feeding mode, the AD system was restarted and in the second feeding phase, a lower biodegradation between 31% and 47% was observed. The pH of bioreactor R1B was in the range of 7.1 to 7.7, which is about the optimal range during the entire period of operation.

The NH_3/NH_4^+-N or ammoniacal N content reduced from 476 to 224 mg/L. A relationship can be observed between biodegradation and the ammoniacal N concentration. The biomethane contents of biogas for the entire period were between 54 and 60% Vol. In both feeding periods, H_2S was significantly lower compared to bioreactor R1A (maximum first phase, 36 ppm; in the second phase, 105 ppm).

The mass balance of bioreactor R1B shows that there is an appropriate mixing of the content of bioreactor R1B (Appendix D.1). The biodegradation in the first and second feeding phase was in the range of 46 - 64% oDM and 30 - 46% oDM respectively. The biomethane content obtained confirmed a well anaerobic process with the production of biogas. The result suggests that HRT 19 (1.38 ± 0.65 kg oDM/m^3 d) is suitable for the semi-continuous AD process of DS.

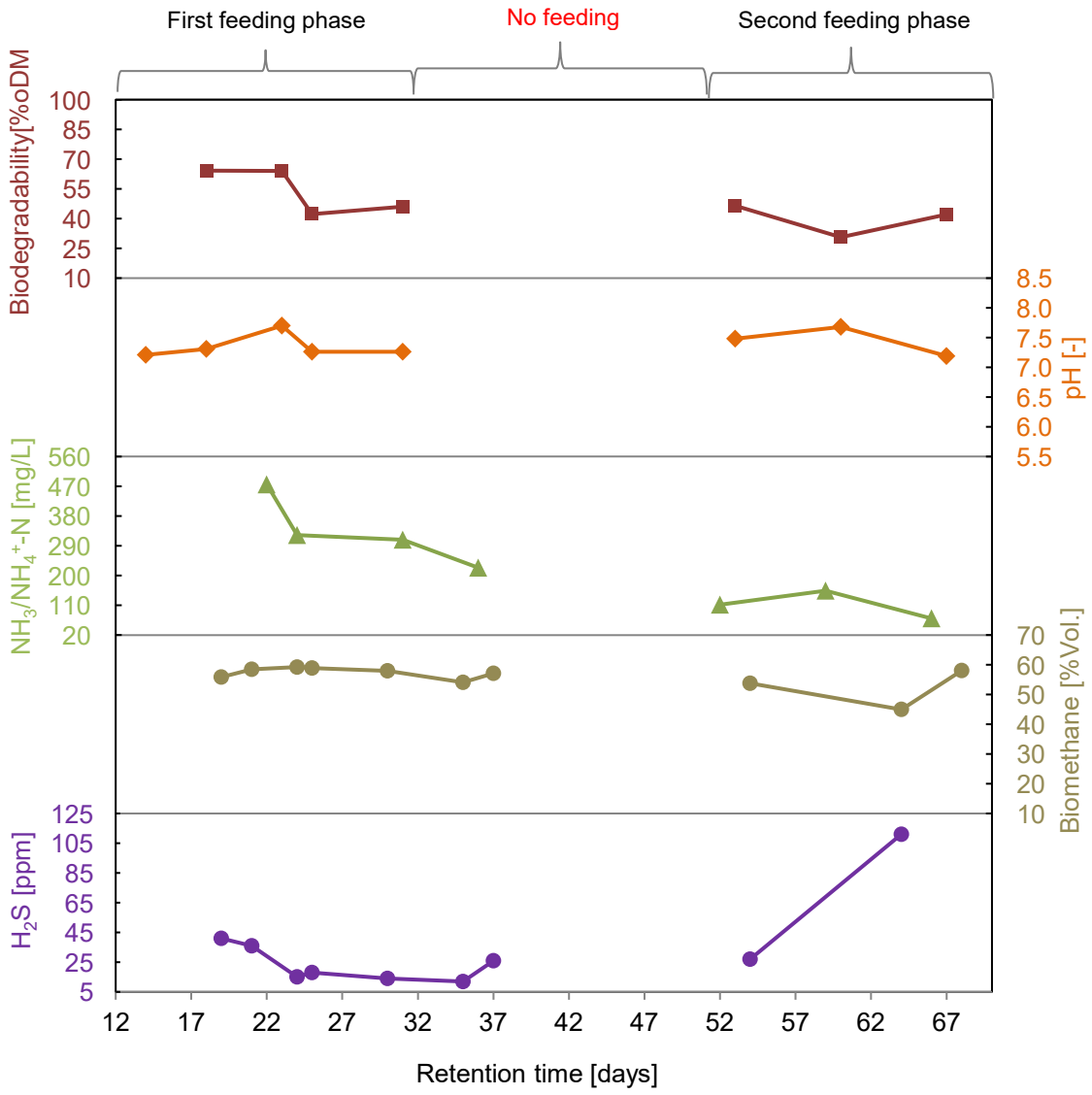

Figure 5.14 Biodegradation and other operation parameters obtained from semi-continuous AD of DS using bioreactor R1B

5.2.2.3 Bioreactor with stirrer

Bioreactor R2 differs from R1A and R1B in pump capacity and adopts the use of a stirrer for mixing the bioreactor's content (section 4.5.2.1). The operation of the system began with a batch phase followed by a semi-continuous phase with a daily feeding pattern.

1.) Initiation phase

The initiation phase of 12 days was monitored in a batch mode similar to bioreactor 1B. Appendix J.3 shows the cumulative specific biogas yield observed during the period with a result similar to R1B.

2.) Semi-continuous phase

Bioreactor R2 (section 4.5.2.1) was operated in a semi-continuous feeding mode with HRT 19 days for the whole period. The entire feeding of HRT 19 days was kept constant, however, input DS varied in oDM (Appendix L.5) leading to variation in biogas yield. The result is presented in Figure 5.15. Due to a similar technical problem, as in bioreactor R1B, feeding was interrupted for a few days.

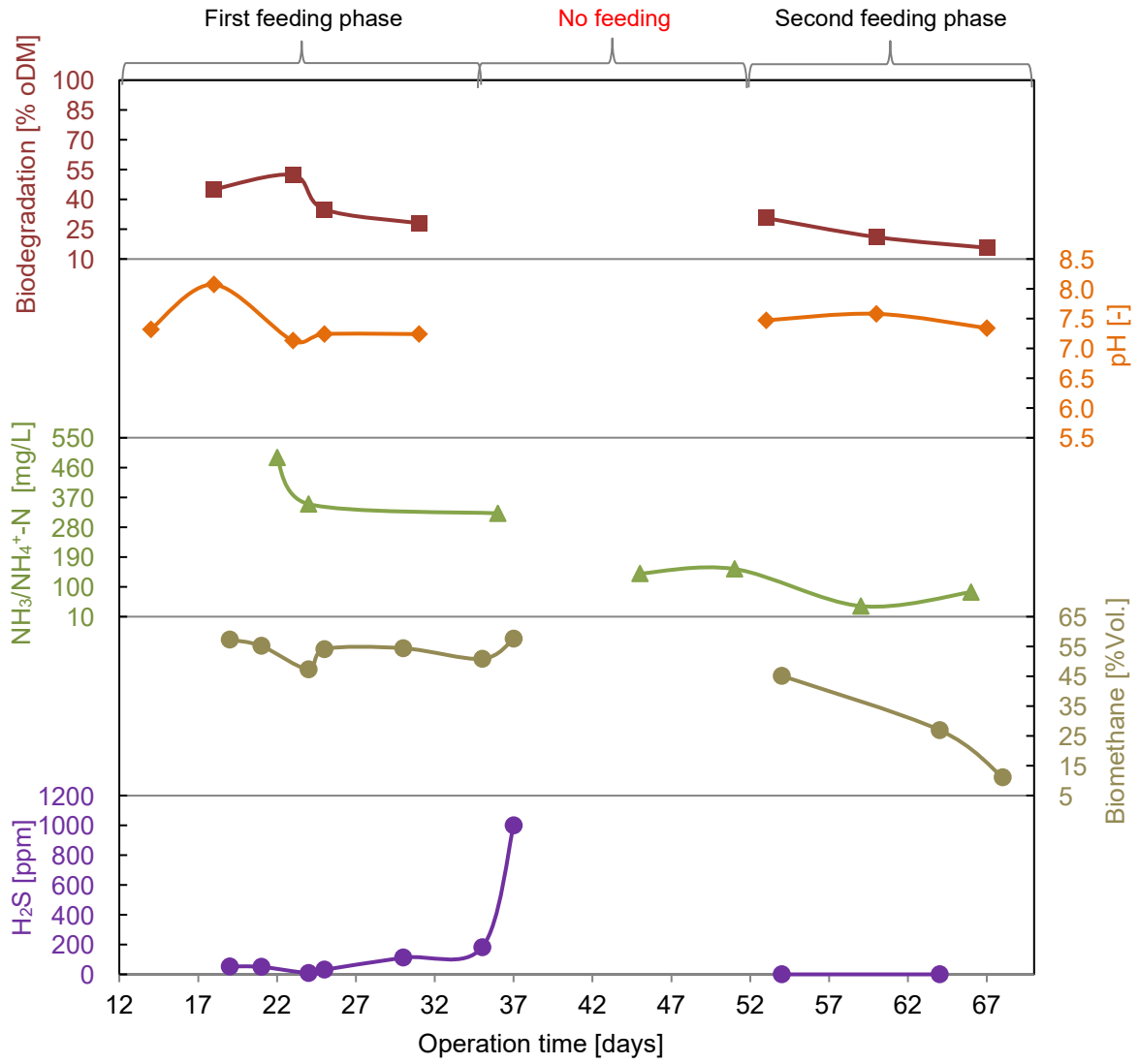

Figure 5.15 Biodegradation and other parameters obtained from semi-continuous AD of DS using R2

The biodegradation was computed the same wayas in bioreactor R1B (Eq B.13 - Appendix B.9). The biodegradation was between 28 and 52% oDM during the first feeding phase. In the second feeding phase, a continuous decline in biogas production was observed resulting in biodegradation of 11% oDM.

The pH values in the entire process were in a basic range with a maximum of 8.1. The ammoniacal N also showed a relationship with biodegradation. The biomethane contents of biogas were between 47 and 57% Vol. in the first feeding phase. A decline was observed during the second feeding phase which also shows a direct relationship to biodegradation. This sharp decline was thought to be due to a technical issue of leakage which might have disturbed the anaerobic process towards the end of the operation. H_2S values were all-time below 37 ppm except on day 37 when the value of 1000 ppm was measured. It returned to zero at the next reading.

5.2.2.4 Comparison of AD processes in the 100-L bioreactors

The section compares the AD processes of the three 100-L bioreactors beginning with mass balance followed by other process parameters. A summary of the comparison is shown in Table 5.5.

1.) Mass balance

Mass balances were computed for calcium carbonate flow in the bioreactors as it is assumed that it is not significantly used up in the AD process. It was computed using Eq B.16 and B.17 (Appendix B.9). The summary of the calcium carbonate mass balances are available in Appendix D.1 The results obtained showed 61.9%, 91.5% and 99.0% balances for bioreactor R1A, R1B and R2 respectively. The low balance of R1A explains the reason for the poor performance after the operation with HRT 25 days. Also, the sedimentation layers observed at the opening of the bioreactor revealed that its operating size gradually reduced with time during operation (Appendix L.4). On the other hand with the installation of efficient mixing devices such as the combination of a 45^o inclined bottom and a higher capacity pump the mixing efficiency of bioreactor R1B improved sufficiently. Also during the opening phase of bioreactor R1B, no substantial sedimentation was observed. The bioreactor R2 with a stirrer has the best mixing efficiency and also did not show any substantial sedimentation during the opening phase of the bioreactor.

2.) Biogas production and biodegradability

The biogas production as computed for R1A had median and maximum values of 136 and 399 NL/kg oDM_fed in the entire period of operation. During its operation with an HRT of 20 days which is similar to the HRT of R1B and R2, it showed lower values. The poor performance at HRT 20 days operation was caused by the poor mixing of R1A (section 5.2.2.4.(1)). The biodegradabilities of R1B and R2 which were operated at HRT 19 days further confirmed this.

Also, the median biodegradabilities of 46.0% oDM and 30.6% oDM for R1B and R2 respectively suggest a better biogas production in favour of R1B.

Table 5.5 Comparison of AD process between the 100-L bioreactors

Parameters (Units)	**Bioreactors** / **Range**	**R1A**	**R1A[a]**	**R1B**	**R2**
Mixing (-)	-	Recirculation pump	Recirculation pump	Recirculation pump and bottom inclined at 45°	Stirrer
HRT (days)	-	30, 25, 20, 15, 20[b] and 30	20	19	19
Duration of semi-continuous operation (weeks)	-	47	7	8	8
Biogas production (NL/kg oDM_fed)	minimum	5[c]	46	ND	ND
	median	136	121	ND	ND
	maximum	399	149	ND	ND
Biodegradation (% oDM)	minimum	ND	ND	30.6	15.7
	median	ND	ND	46.0	30.6
	maximum	ND	ND	64.2	52.3
pH (-)	minimum	6.4	7.1	7.2	7.1
	median	7.3	7.2	7.3	7.3
	maximum	7.9	7.4	7.7	8.1
NH_4^+/NH_3-N (mg/L)	minimum	ND	ND	70	28
	median	ND	ND	224	147
	maximum	ND	ND	476	490
Biomethane content (% Vol.)	minimum	32.0	32.0	44.9	11.1
	median	53.3	43.8	57.5	52.5
	maximum	59.2	53.4	59.2	57.6
H_2S content (ppm)	Minimum	> 1000	ND	7	0
	median	ND	ND	21	52
	maximum	ND	ND	106	1000
$CaCO_3$ mass balance (% $CaCO_3$)	-	61.9	ND	91.5	99.0

[a]HRT 20 days phase of R1A which began after operating at HRT 30 and 25 days for a period of 14 and 12 weeks respectively

[b] a second operating phase with HRT 20 days

[c] the non-zero minimum value

ND Not determined

3.) pH

The pH observed during operation with R1A declined from a basic pH until it was acidic with a minimum of 6.4. This was not the case with R1B and R2 which had pHs in the range of 7.1 to 8.1 all through the period of operation.

4.) Ammoniacal nitrogen

Ammoniacal N declined gradually for both R1B and R2 during operation. Both bioreactors, therefore, confirm the utilization of N in the biogas production process. The reduction of ammoniacal N in bioreactors during the entire period of operation was 85% for R1A and 94% for R2. This establishes that conditions of significant N depletion occur in the AD of DS when operated semi-continuously. A proper measure for N supplementation is therefore required as explained in section 5.2.1.(6).

5.) Biomethane content

The maximum biomethane content for all three bioreactors was in the range of 57 to 59% Vol. This establishes that all the three bioreactors did operate at the anaerobic condition with the availability of organics, in this case from DS that is converted to biogas. The R1B showed the highest median value of 57.5% Vol., while the lowest value of 11.1% Vol. was observed for R2.

5.) H_2S content

The H_2S content of above 1000 ppm was observed althrough the operation with R1A. The R1B and R2 on the other hand showed very low H_2S production during operation, except for R2 which had a value of 1000 ppm on day 37 of operation. The H_2S production is connected to their mixing efficiency. This explains that a semi-continuous AD process of DS requires proper mixing to prevent high H_2S production.

Special attention should be given to the mixing efficiency of a semi-continuously operated AD of DS due to the fast sedimentation of the solids present in DS. The result obtained suggests that bioreactors R1B and R2 were well mixed and could be taken as improved operation when compared to that of R1A. HRT of 19 days was suitable for the AD of DS due to a higher daily input of substrate and higher biodegradation observed. It informs that slurry circulation (R1B) and mechanical mixing (R2) are both efficient for the mixing in semi-continuously or continuously operated AD of DS. This is also consistent with the report of Wu, (2010).

5.2.3 Comparison of biogas production between 1 and 100-L bioreactors

The 1-L and 100-L bioreactors used for the AD of DS were compared based on biogas yields and biodegradation.

1.) Biogas yield

The specific biogas yields of DS (*Stream 2-W70*) using the 1-L bioreactors in a batch process were between 232 - 286 NL/kg oDM. During the semi-continuous AD process with the 100-L bioreactors, a median and maximum specific biogas production of 136 and 399 NL/kg oDM_fed were observed for the same DS type (R1A).

A semi-continuous process tends to a steady-state condition during operation while a batch process does not (Morin et al., 2021; Vásquez-Bahena et al., 2004). This may be the reason for the higher maximum biogas production observed for the semi-continuous AD of DS in comparison to the batch process. Also, at steady-state conditions, intermediate products resulting from AD phases which come after the slowest among the AD phases are sufficiently reduced (Sötemann et al., 2006), and results in an efficient biogas yields. It therefore suggests that a semi-continuous operated AD of DS may show a higher maximum biogas yields compared to the batch process.

2.) Biodegradation

The biodegradation of the batch AD process with the 1-L bioreactors were computed using Eq B.11 and B.12 (Appendix B.9). The outcomes of these equations are referred to as the biodegradability of the substrates, as the biodegradation results from a fixed amount of substrate until the end of the AD process. Those of the semi-continuous process (100-L bioreactors) were computed using a different equation (Eq B.13, Appendix B.9), since the biodegradations were estimated from the daily substrates fed into the bioreactor.

Biodegradability in the range of 16 - 26% oDM for DS (Stream 2-W70) from the 1-L bioreactors can be interpreted as the percentage of the organic fraction in the DS fed that is converted into biogas. The biodegradation in the range of 16 - 64% oDM for the 100-L bioreactors informs on the amount of organic in DS (Stream 2-W70) converted into biogas by a comparison between the inflow and outflow organics of the bioreactors. Both methods of biodegradation computation confirm that a significant amount of organic in DS is converted anaerobically into biogas.

The result showed that batch and semi-continuous processes are both suitable for the application of AD of DS. The batch process may show a lower biogas yield compared to the semi-continuous process due to steady-state conditions. Both systems also differ in other operating parameters such as of pumping and energy input requirements as explained in section 3.3.3.4.(1).

5.2.4 Key findings on biogas production from deinking sludges

The following are the key findings of the investigation of AD of DS.

1.) DS can be used as feedstock to produce biogas. Biogas yield in the range of 4.1 - 12 NL/kg oDM and 227 - 417 NL//kg FM with biomethane content in the range of 55 - 70% Vol. is possible with DS.

2.) AD of DS can be initiated by common inocula such as those from digesters utilizing maize silage or sewage sludge as feedstock. Also, the high calcium carbonate content of DS does not pose any inhibitory concern to the AD process.

3.) Due to the low lignin content in the organic fraction of DS that are generated from high wastepaper grades, they have a higher biogas yield than those from low grades of waste paper.

4.) A pre-dewatered DS has a lower specific biogas yield compared to the raw DS which suggests that some readily degradable organics in the raw DS are lost during the pre-dewatering process.

5.) Adjusting the C/N ratio to 29 - 34 during semi-continuous AD can overcome the low nitrogen content in DS and improve biogas efficiency in the rapid production phase.

6.) Using DS as biogas feedstock in a semi-continuous process requires optimal mixing due to the fast settling characteristics of DS. This can help prevent the building of H_2S.

7.) The HRT 19 days which amounts to OLR in the range of 1 - 4 kg oDM/(m^3 d) is suitable for DS.

5.3 Kinetic modelling of biogas yields of deinking sludges

This section discusses the fittings of five different kinetic models to experimental data of the AD of DS (batch test) and the selection of the most suitable model among them.

5.3.1 Fitting of different kinetic models to experimental data

The five different kinetic models as described in section 4.8.2.1 were given names of Models 1 to 5, for ease of identification. They were fitted separately to the experimental data of the AD of DS in the 1-L batch test.

- Model 1: One step first order kinetics
- Model 2: Two steps first order kinetics
- Model 3: Modified Gompertz
- Model 4: Transfer function
- Model 5: Logistic function

The fittings were carried out in two groups for the AD of raw DS and of pre-dewatered DS. The fittings for the two groups were further divided into three categories, corresponding to the wastepaper grades (*W70, W80 and W90/100*) of DS (section 4.3). This was done due to possible differences in organic types or concentrations that may exist in DS types considered.

5.3.1.1 Fittings for raw deinking sludges

Figure 5.16 shows the fittings of the five different models (section 4.8.2.1) to the experimental data of raw DS (*W70)*. Models 3 and 5 did not predict a similar start as suggested by experimental data. The other three models are very much consistent with the zero-lag phase as shown by experimental data. Models 1, 2 and 4 fit considerably with the rapid phase except models 3 and 5. During the stationary phase, a relatively poor fitting was observed for models 3 and 5. The three models that fit considerably for both the rapid and stationary phases of the AD of raw DS *(W70)*, were models 1, 2 and 4. Amongst these, model 2 shows the best fittings for the AD of DS *(W70)* by visual observation of Figure 5.16.

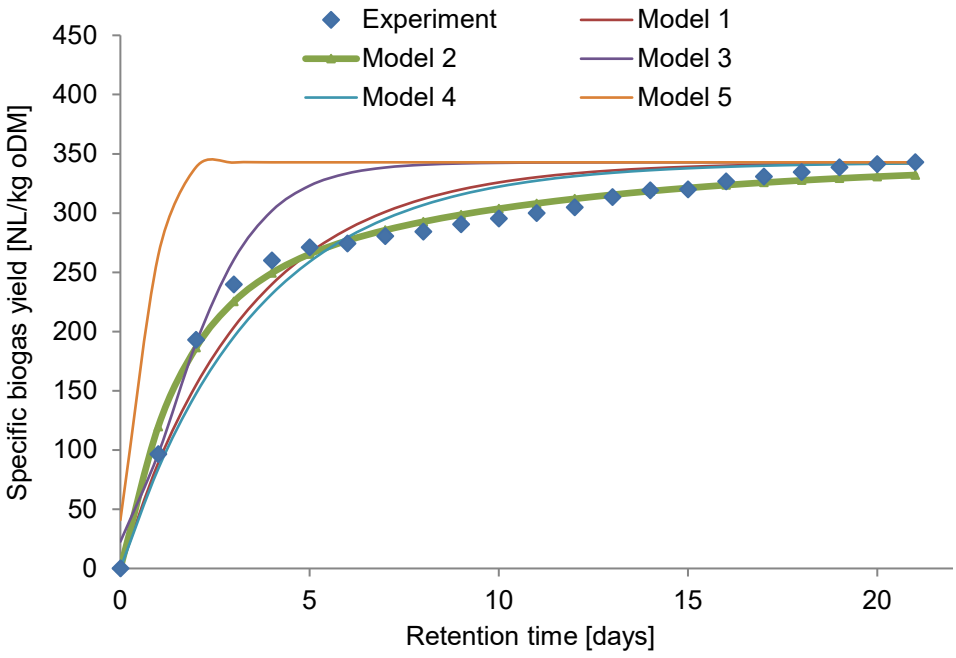

Figure 5.16 Fitting of five different models to the experiment data from AD of *Stream 1-W70* in a batch test

As shown in Table 5.6, model 1 predicted a single hydrolysis constant (k), while model 2 predicted two different hydrolysis constants for readily (k_1) and less readily (k_2) biodegradable organics respectively. The coefficient of determination (R^2) of model 2 is the highest among the models. Model 2 has the lowest RMSE[13] as well as the lowest AIC[14] and BIC[15]. Model 1 has the second-lowest AIC and BIC. The comparison of model 1 (candidate model) with the best model yielded a ΔAIC[16] and ΔBIC[17] of 38 respectively. According to Fabozzi et al. (2014), as a general rule of thumb, a ΔAIC greater than 10 indicates that there is essentially no support for the candidate model to be the best model. Also, a ΔBIC greater than 10 shows very strong evidence against the candidate model as the best model. This suggests that model 2 is the most suitable model for the AD of raw DS (*W70).*

[13] RMSE- Root Mean Square Error
[14] AIC - Akaike Information Criterion: a criterion for selecting model from a finite set of models
[15] BIC - Bayesian Information Criterion: a criterion for selecting model from a finite set of models
[16] ΔAIC - The difference in AIC value between the best model and the candidate model being compared
[17] ΔBIC - The difference in BIC value between the best model and the candidate model being compared

Table 5.6 AD model fitting parameters and indicators of raw DS of type *W70*

Model	Parameters		Indicators					
	hydrolysis constant	Biogas yield	R^2	RMSE	AIC	BIC	ΔAIC	ΔBIC
	[day^{-1}]	[NL/kgoDM]	[-]	[-]	[-]	[-]	[-]	[-]
Model 1	0.301[a]	-	0.934	21.0	136	137	38	38
Model 2	0.667[b], 0.117[c]	217.5[d], 125.3[e]	0.988	8.8	98	99	-	-
Model 3	-	-	0.821	34.4	158	159	60	60
Model 4	-	-	0.931	21.3	137	138	39	39
Model 5	-	-	0.338	66.2	187	188	89	89

a-single hydrolysis constant of one step first order kinetics (k)
b-hydrolysis constant associated to fast biodragadble organics (k1);
c-hydrolysis constant associated to slow biodragadble organics (k2)
d-biogas yield associated to fast biodragadble (Y2); e-biogas yield associated to fast biodragadble (Y2)

A similar result for model 2 has been reported by other authors using other substrates. model 1 was reported more suitable than model 2 for the modelling of corn stover (Li et al., 2016). Also, Yang et al. (2018) reported an improved fitting by model 2 for the AD of elephant grass. The structure of model 2 assumes a heterogeneous mixture of organic components with fast and slow hydrolysis fractions. The good fitting of model 2 with experimental data informs on a disparity in the characteristics of possible different organic types present in raw DS (*W70*). The organic types include fibres, fines, inks, soaps and fatty acids as discussed in section 5.2.1.1. The result of model 2 further establishes that the organics in raw DS *(W70)* can be grouped into two different types which resulted into two different hydrolysis constants. Model 1 on the other hand has computed these two organic types together. The observation is consistent with that explained in section 5.2.1.4, where it was shown that the raw DS contains more readily biodegradable organics than the pre-dewatered DS. It therefore further establishes that the fraction of organic matter that flows into the liquid phase during pre-dewatering operation is different in properties from the fraction that are collected in the solid phase (pre-dewatered DS).

5.3.1.2 Fittings for pre-dewatered deinking sludges

The fittings of the five different kinetic models to the experimental AD data from the batch test were done separately for the pre-dewatered DS from wastepaper grades *W70*, *W80* and *W90/100*.

1.) Model fitting for pre-dewatered DS of W70 wastepaper grade

The fitting was done with three sets [1], [2], [3] of experimental data for pre-dewatered DS (*W70*) varying in terms of sample dates, oDM concentration and S/I[18] ratios (Table 5.7). From the data used to draw Figure 5.17, the specific biogas yields of models 3 and 5 did not begin from zero which is similar to what was observed with the model fitting of the AD of pre-dewatered DS (*W70*).

Table 5.7 oDM of different pre-dewatered DS and the S/I ratio used for AD mixtures

Experiment data	Date of collection	oDM (g/L)	oDM of DS to inoculum in the mixture (S/I)
[1]	05.11.2013	37.8	0.52
[2]	02.12.2013	33.8	0.46
[3]	24.04.2014	41.9	1.70

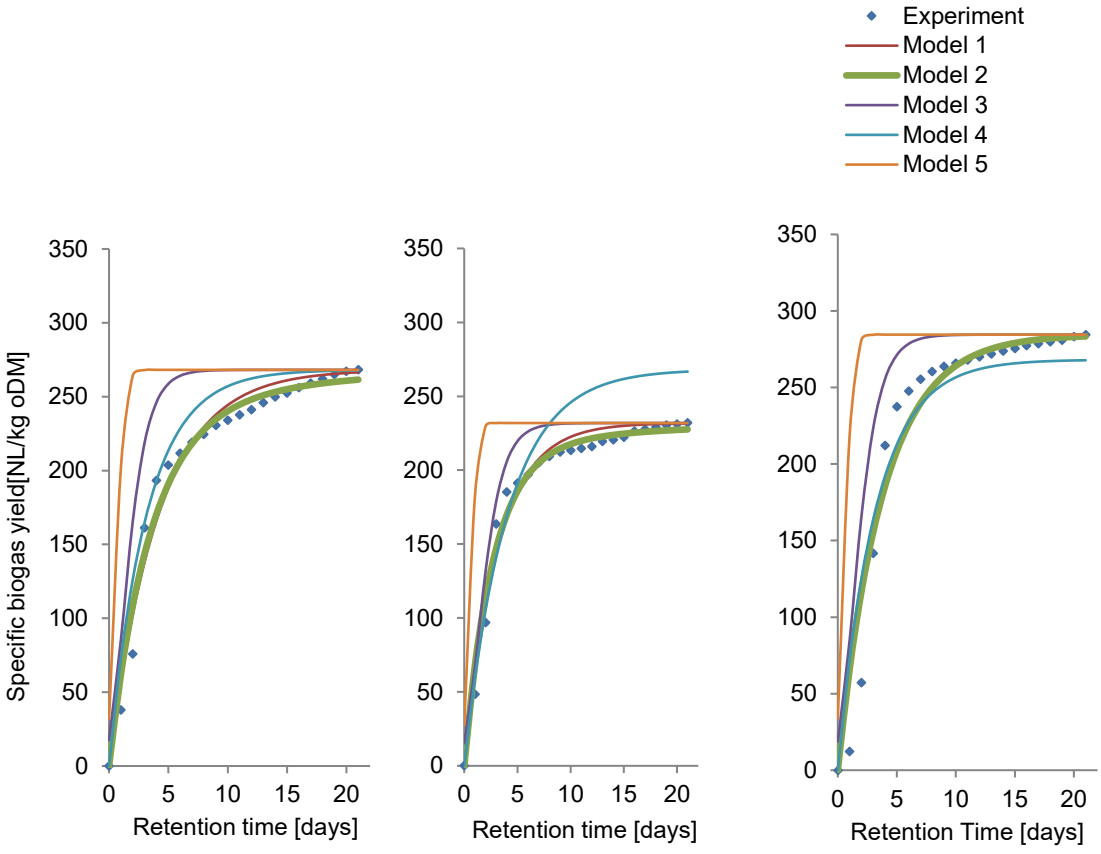

Figure 5.17 Fitting of five different models to three experimental data sets [1], [2], [3] from batch AD tests of pre-dewatered DS (*W70*). Samples differ in terms of date of collection, oDM and the S/I ratios used (left:[1]; middle: [2]; right: [3])

[18] S/I ratio- ratio of oDM of DS to inoculum

Among the five models only the models 1 and 2 show consistently good fittings during the rapid and stationary AD phases and have the highest R^2 (Appendix K.1). Considering the RMSE, BIC and AIC values obtained for sample [1], [2] and [3] in Table 5.8, model 2 can be taken as the best model. For sample [3], models 1 and 2 showed similar parameters and statistical indicators. It appears that samples [1] and [2] contain more readily biodegradable fractions of oDM as compared to sample [3].

Table 5.8 AD model fitting parameters and indicators of pre-dewatered DS of type *W70*

Model	Parameters		Indicators					
	hydrolysis constant	Biogas yield	R^2	RMSE	AIC	BIC	ΔAIC	ΔBIC
	[day^{-1}]	[NL/kgoDM]	[-]	[-]	[-]	[-]	[-]	[-]
Stream 2-W70_[1]								
Model 1	0.242[a]	-	0.971	12.6	115	114	4	4
Model 2	0.295[b], 0.086[c]	230.8[d], 37.4[e]	0.975	11.7	111	110	-	-
Model 3	-	-	0.728	38.3	164	163	53	53
Model 4	-	-	0.932	19.2	133	132	22	22
Model 5	-	-	0.178	66.7	188	187	77	77
Stream 2-W70_[2]								
Model 1	0.321[a]	-	0.978	9.0	100	99	6	6
Model 2	0.372[b], 0.070[c]	213.6[d], 18.3[e]	0.983	7.9	94	93	-	-
Model 3	-	-	0.916	17.6	129	128	35	35
Model 4	-	-	0.768	29.1	151	151	57	58
Model 5	-	-	0.395	47.1	173	172	79	79
Stream 2-W70_[3]								
Model 1	0.263[a]	-	0.946	20.3	136	135	-	-
Model 2	0.263[b], 0.263[c]	142.3[d], 142.3[e]	0.946	20.3	136	135	-	-
Model 3	-	-	0.815	37.5	163	162	27	27
Model 4	-	-	0.926	23.7	142	142	6	7
Model 5	-	-	0.244	75.7	193	193	57	58

a-single hydrolysis constant of one step first order kinetics (k)
b-hydrolysis constant associated to fast biodragadble organics (k1);
c-hydrolysis constant associated to slow biodragadble organics (k2)
d-biogas yield associated to fast biodragadble organics (Y2); e-biogas yield associated to slow biodragadble organics (Y2)

This can be inferred from the hydrolysis constants shown by model 2 for the three different samples (Table 5.8). Steffen et al. (2017) also reported model 1 to be suitable for pre-dewatered DS *(W70)* but did not compare to other kinetic models.

With the result obtained from the different pre-dewatered DS (*W70*), it can be concluded that models 1 and 2 are well suitable for the modelling of its AD. Considering only model 2, the hydrolysis constants (k_1, k_2) of ([1]: 0.295, 0.086 day^{-1}), ([2]: 0.372, 0.070 day^{-1}) and ([3]: 0.263, 0.263 day^{-1}) depends on oDM concentration of 3.8 g/L, 33.8 g/L and 41.9 g/L respectively (Table 5.8). A relationship between their oDM concentration and their respective experimental biogas yield is available in Appendix K.3.

2.) Model fitting for pre-dewatered DS of W80 and W90/100 wastepaper grades

The experimental data of the AD of pre-dewatered DS *(W80 and W90/100*) were also fitted with the five different models (section 4.8.2.1). Similar to the previous fittings, models 3 and 5 did not begin from zero specific biogas yield based on modelling data. Figure 5.18 shows a considerable deviation of model 5, especially in the rapid phase. The other four models show considerably good fittings for both the rapid and stationary phases. Model 2 has a single hydrolysis constant for the pre-dewatered DS (*W80* and *W90/100*) which is equal to that of model 1. This suggests that the organic types in these DS sample types are similarly distributed.

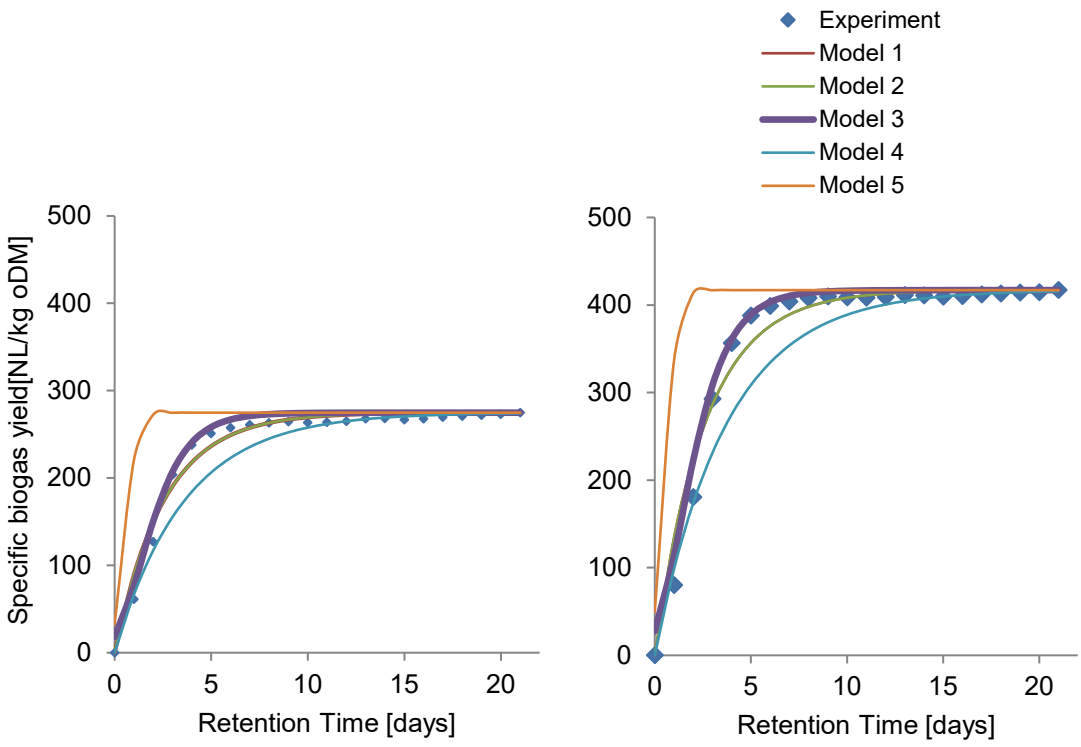

Figure 5.18 Fitting of five different models to the experimental data of the AD of pre-dewatered DS in a batch test (left: *W80 and right: W90/100)*

As shown in Table 5.9, the model with the lowest AIC and BIC for pre-dewatered DS *W80* and *W90/100* is model 3. Model 1 and 2 have the same AIC and BIC values for both DS samples. They have the second-lowest AIC and BIC among the models (Table 5.9). According to Fabozzi et al. (2014), a ∆AIC of 4 is a less support for the candidate models while a ∆AIC of 12 implies there is essentially no support for both candidate models. Also, a ∆BIC of implies positive evidence against both candidate models while a ∆BIC of 12 indicate a very strong evidence against them. This suggests model 3 as the best model for the AD of pre-dewatered DS of type *W80* and *W90/100*.

Table 5.9 AD model fitting parameters and indicators of pre-dewatered DS of type *W80 and W90/100*

Model	Parameters		Indicators					
	hydrolysis constant	Biogas yield	R^2	RMSE	AIC	BIC	ΔAIC	ΔBIC
	[day^{-1}]	[NL/kgoDM]	[-]	[-]	[-]	[-]	[-]	[-]
Stream 2-W80								
Model 1	0.394[a]	-	0.978	10.7	108	107	4	4
Model 2	0.394[b], 0.394[c]	137.4[d], 137.4[e]	0.978	10.7	108	107	4	4
Model 3	-	-	0.981	9.9	104	103	-	-
Model 4	-	-	0.916	21.0	137	136	33	33
Model 5	-	-	0.512	50.5	176	175	72	72
Stream 2-W90/100								
Model 1	0.386[a]	-	0.973	18.6	132	131	12	12
Model 2	0.386[b], 0.386[c]	208.5[d], 208.5[e]	0.973	18.6	132	131	12	12
Model 3	-	-	0.985	14.1	120	119	-	-
Model 4	-	-	0.906	34.9	159	159	39	40
Model 5	-	-	0.498	80.7	196	195	76	76

a-single hydrolysis constant of one step first order kinetics (k)
b-hydrolysis constant associated to fast biodragadble organics (k1);
c-hydrolysis constant associated to slow biodragadble organics (k2)
d-biogas yield associated to fast biodragadbel (Y2); e-biogas yield associated to fast biodragadbel (Y2)

The suitability of model 3 for kinetic modelling of AD substrates has also been reported for other AD substrates among which include, food waste (Pramanik et al., 2019) and food waste co-digested with poultry manure (Deepanraj et al., 2016). The result here, therefore, suggests that pre-dewatered DS of *W80* and *W90/100* types may behave similarly to food waste during the AD process.

It is however notable that the drawback in model 3 although it is statistically the best model has a poor prediction of the starting phase of the AD process.

5.3.2 Further discussions on kinetic models fitted

Five different kinetic models have been fitted to the experimental data of the AD of different DS types. The result obtained shows that model 1(one step first order kinetics), model 2 (two steps first order kinetics) and model 3 (modified the Gompertz) are the relevant models for the AD of DS. Model 2 has the best fit for raw DS (*Stream 1-W70*) while both models 1 and 2 are suitable for the pre-dewatered DS of type *W70*. Raw and pre-dewatered DS varied in the nature of organic matter. Several authors have reported that first order kinetics models are most suitable for AD when hydrolysis is the rate-limiting step (Pramanik et al., 2019; Sanders, 2001; Vavilin et al., 2008). Therefore the result obtained here for the AD of DS from *W70* establishes that the rate-limiting step is hydrolysis. The high lignin content of DS from *W70* may be the reason for its hydrolysis limitation. Bekiaris et al. (2015) have reported that the hydrolysis of celluloses and hemicelluloses are inhibited by lignin. Mussatto et al. (2008) also showed that cellulose hydrolysis was optimal when hemicelluloses and lignin were removed. This suggests that the bioavailability of the cellulose fraction of DS from *W70* wastepaper grades is probably limited leading to a slower degradation rate during the AD process.

The model 3 showed the best fit for the AD of the pre-dewatered DS of the *W80* and *W90/100*. These DS are generated from higher grade wastepapers and contains less lignin when compared to that of *W70* (section 5.2.1.3). The result obtained from model fitting suggests that the variation of the microbial cells over time in the AD process as described by the Gompertz model is the most appropriate for the pre-dewatered DS of *W80* and *W90/100* types.

5.3.3 Suitable models for anaerobic digestion of deinking sludges

In summary, the suitable models for the modelling of DS are model 2 (Two steps first order kinetics) and model 3 (Modified Gompertz). The application of the two previously selected models for DS is explained in this section.

1.) Two steps first order kinetics

The first order kinetics in two steps is the most suitable model for the AD of raw and pre-dewatered DS of type W70. The mathematical representation of the model as shown in Eq 4.2 of section 4.8.2.1 is again shown below,

$$Y_t = Y_1 \times [1 - \exp(-k_1 t)] + Y_2 \times [1 - \exp(-k_2 t)] \quad \text{Eq 4.2}$$

Where;

Y_t is biogas yield (NL/kg oDM) with respect to time (day)

Y_1 is biogas yield (L/kg oDM) associated with bioconversion of readily biodegradable organics

Y_2 is biogas yield (L/kg oDM) associated with bioconversion of less readily biodegradable organics

k_1 is the hydrolysis rate constant of Y_1 (1/day)

k_2 is the hydrolysis rate constant of Y_2 (1/day)

t is time (days)

This model does not require information on the maximum biogas yield of a substrate (Y_m). The required parameter for the application are shown in Table 5.10.

Table 5.10 Parameters for the kinetic modelling of the AD of pre-dewatered DS (*W70*) using the two steps first order kinetics model

DS type	Parameters			
	Biogas yield associated to organic type [NL/kg oDM]		Hydrolysis rate constant (1/day)	
	Readily degradable organics [Y_1]	Less readily degradable organics [Y_2]	Rate constant associated with Y_1 [k_1]	Rate constant associated with Y_2 [k_2]
Raw DS_*W70**	217.5	125.3	0.667	0.117
Pre-dewatered DS_*W70*	142.3 - 230.8	18.3 - 142.3	0.263 - 0.372	0.070 - 0.263

Parameters generated from oDM of pre-dewatered DS in the range 38 - 42 g/L
S/I (oDM of sludge to inoculum) ratios were in the range of 0.46 -1.70
* applicable for oDM of raw DS_W70 of about 12 g oDM /L

2.) Modified Gompertz

The modified Gompertz model is suitable for the modelling of the biogas yield of DS. It has its best performance with pre-dewatered DS of *W80* and *W90/100* types. Eq 4.3 as shown in section 4.8.2.1 is again presented below,

$$Y_t = Y_m \times \exp\left\{-\exp\left[\frac{R_m \times e}{Y_m}(\lambda - t) + 1\right]\right\} \qquad \text{Eq 4.3}$$

Where,

Y_t is biogas yield (NL/kg oDM) with respect to time (day)
Y_m is the maximum biogas yield of a substrate (NL/kg oDM)
R_m is the maximum biogas production rate (NL/kg oDM.day)
λ is the lag phase time (days)
e is Euler's number; 2.7183
T is time (days)

The three main parameters needed for modelling DS using the Eq. 4.3 are Y_m, R_m and λ. The lag phase (λ) can be set to zero as established by AD of DS experimentally. The parameters Y_m and R_m used for the application of the Gompertz model in section 5.3.1.1 were obtained from experimental data in this study. However, for the modelling of DS without any prior data, the parameters such as Y_m and R_m have to be mathematically computed using laboratory data and parameters available. The required laboratory data are organic dry mater of DS (mg/L) and the elemental anaylsis (carbon, hydrogen, nitogen and oxygen). A seven steps process of computing for Y_m and R_m of pre-dewatered DS of *W80* and *W90/100* is described in Appendix K.2.

5.3.4 Key findings on the application of kinetic models of deinking sludges

The following are the key findings on the modelling of the AD of DS

1.) Study on the modelling of AD of DS revealed that its biodegradation process can be grouped into two steps: The readily and less readily biodegrading steps.

2.) The two steps first order kinetics (Model 1) and the modified Gompertz (Model 3) were the most suitable model for the AD of DS. While the first fit best for the raw and pre-dewatered DS from ordinary wastepaper grades (*W70*), the second fits best for pre-dewatered DS from medium and high wastepaper grades (*W80* and *W90/100*).

3.) The model fitting results suggests that hydrolysis is rate-limiting for the AD of DS generated from ordinary wastepaper grades (W70) while the variation of the microbial cells over time describes best the AD process of DS from high wastepaper grades (*W80* and *W90/100*).

5.4 Solid-Liquid separation of deinking sludges and their digestates

In this section, comparisons between DS and DS-digestate characteristics were carried out. They were compared in terms of dry matter, organic dry matter and calcium carbonate content. The differences in their particle size distributions as well as their sedimentation and centrifugation charateristics were discussed.

5.4.1 Characteristics of deinking sludges and their digestates

The investigated effluents of AD termed “digestate” were received from the three 100-L bioreactors (R1A, R1B and R2) (section 4.5.2.1). The DS used as input was the pre-dewatered DS of the type *W70* and the outputs were denoted as DS-digestates. Their characteristics are shown in Figure 5.19 and 5.20.

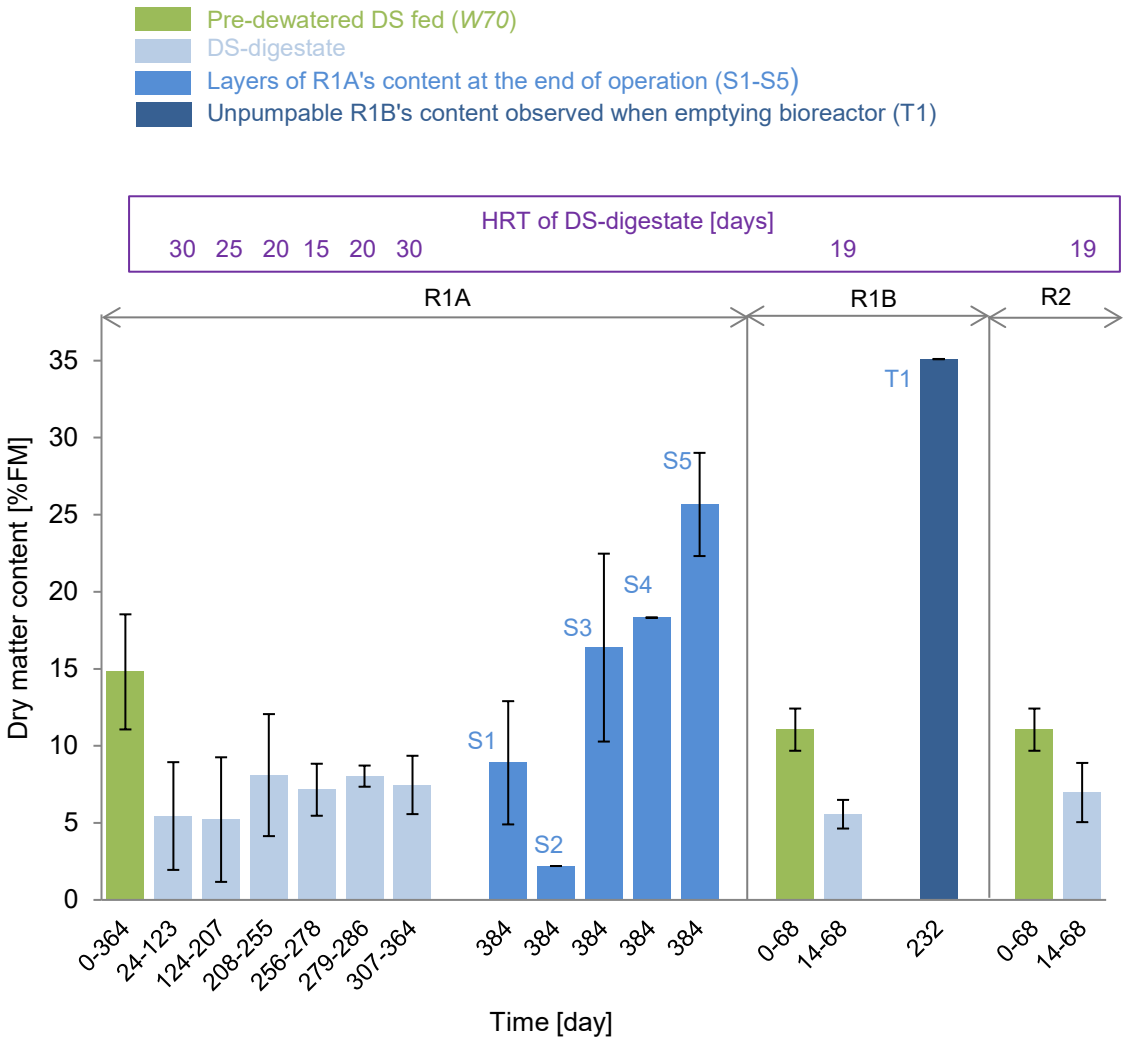

Figure 5.19 DM content of samples collected during the semi-continuous running of the three different 100-L bioreactors.

R1A : bioreactor with a recirculating pump of capacity 170 -1000 L/h
R1B : bioreactor with a recirculating pump of capacity 100 -3000 L/h with 45° inclined bottom
R2 : bioreactor with stirrer

The different DS-digestates of R1A correspond to the HRTs in the range 15 to 30 days used. The R1B and R2 samples have a single DS-digestate resulting from an HRT of 19 days. The layers S1-S5 observed in R1A (Appendix L.4) resulted due to poor mixing. Such layers were not observed in R1B and R2 due to improved mixing. At the end of the AD process all content of the R2 could be emptied by pumping. For the R1B, a thick mass of 3.5 kg which is about 6% of bioreactor's content was observed at the bottom which was not pumpable due to it high dry matter content. The emptying of R1B and R2 was done at 164 days after the end of AD process. The delay was due to the covid-19 pandemic.

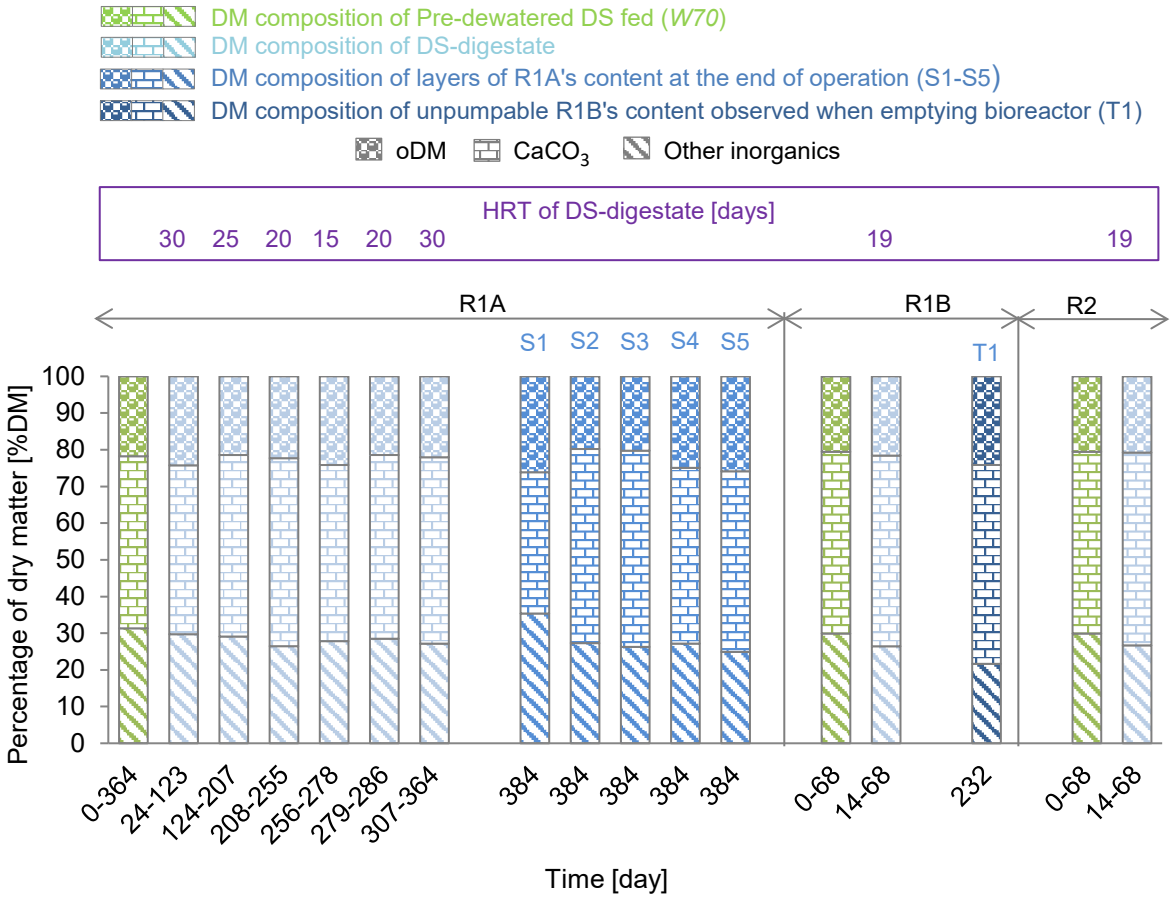

Figure 5.20 DM composition of the DS and DS-digitates samples collected during the running of the three different 100-L bioreactors.

R1A : bioreactor with a recirculating pump of capacity 170 - 1000 L/h
R1B : bioreactor with a recirculating pump of capacity 100 - 3000 L/h with 45° inclined bottom
R2 : bioreactor with stirrer

The characteristics of the different input DS, DS-digestates and layers of R1A's content are available in Appendix L.2. The Appendix L.5 contains the characteristics of the input DS and the DS-digestes of R1B and R2 as well as the unpumpable fraction of R1B's content during the emptying phase.

1.) Dry matter contents: 100-L bioreactor R1A

The DM of different DS fed, DS-digestates as well as of the samples S1- S5 at the end of the AD process are shown in Figure 5.19. The average DM of DS fed into bioreactor was 14.8 ± 3.7% FM. It results into DS-digestates having reduced DM in a similar range of 5% FM for the first two HRTs (30 and 25 days). The average DM during the subsequent HRT investigated before stopping the AD process was in the range of 7 - 8% FM.

The DM of DS-digestate for the first two HRTs (30 and 25 days) were significantly lower than the average DM of input DS. For the subsequent HRTs, the DS-digestate resulted in a less DM reduction of DM. It can be explained by settling of solids within the bioreactor due to insufficient mixing. This resulted in different digestates (S1 - S5) by sedimentation of solids in R1A collected after opening of the bioreactor at the end of the experiment. The five different settled layers (S1 - S5) had varying DM content between 2 - 29% FM. S4 was the main layer with the largest quantity. A sketch of the layers S1 to S5 can be seen in Appendix L.4.

2.) Dry matter contents: 100-L bioreactors R1B and R2

These bioreactors resulted in DS-digestates with an average DM of 6% FM and 7% FM respectively. The input DS had an average DM of 11.1 ± 1.4% FM in both cases (Figure 5.19). The substantial reduction of DM can be assigned to the dilution caused by inoculum (4.7 ± 2.8% FM) and the DM consumption for the production of biogas. Bioreactors were operated for a shorter period (68 days) when compared to experiment with R1A (384 days). However, their improved mixing condition resulted in DS-digestate with DM which is expected to be consistent even for a longer run of the bioreactors. While the R1A resulted in the settling of solids due to poor mixing, the R1B and R2 reactors produced consistently low DM with less variation when compared to that of R1A.

The DS T1 which was about 6% of R1B's content was not pumpable and had a DM of 35% FM. During the long period of waiting before emptying of bioreactors, mixing was done irregularly. It appears that during this period some solids could have settled and stick to the bottom of the bioreactors. One can infer that the mixing capacity of R1B was not sufficient for the mixing of the high DM solid sticked to the bottom of bioreactor. On the other hand the stirrer of R2 had efficient mixing capacity which resulted into an improved mixing in the aforementioned condition.

3.) Organic dry matter contents: 100-L bioreactors R1A, R1B and R2

The organic dry matter content (oDM) of input DS and DS-digestates of the three 100-L bioreactors as well as that of settled samples (S1 - S5: R1A only) and unpumpable sample (T1: R1B only) are shown in Figure 5.20. The oDM of the input DS for the three bioreactors were in the range of 29 - 37% DM (Appendix L.2 and L.5). The DS-digestates for the different HRT had average values below the range of 26 to 30% DM. The samples S1 - S5 are in the range of 25 to 35% DM. The floating sample (S1) has the higest oDM among them. This informs that a considerable amount of oDM was converted to biogas. The result further informs that input inoculum does not strongly impact the characteristics of DS-digestate.

4.) Ash and calcium carbonate content: 100-L bioreactors R1A, R1B and R2

The $CaCO_3$ content of DS used as input substrate during the period of investigation ranged from 44 to 52% DM. As seen in Figure 5.20, a substantial amount of ash and $CaCO_3$ content is present in the different digestates of DS. Considering all HRT phases of the three different 100-L bioreactors, the ash contents in the range of 70 to 74% DM were observed. The $CaCO_3$ contents were in the range of 46 - 53% DM. The ash and the $CaCO_3$ content are not affected by AD. This implies that the majority flowed into the digestate and probably just a few fractions settled at the bottom of the bioreactor.

5.) pH- values: 100-L bioreactors R1A, R1B and R2

The pH values of the DS-digestates from the three 100-L bioreactors were in the alkaline range between 7.0 and 7.7 except during the process limitation phase in R1A where a range of 6.2 - 6.8 was observed (Figure 5.13). The average pH values of the DS-digestates from R1B were 7.3 and for R2 7.4 (Figures 5.14 to 5.15).

The pH of a DS could influence its solid-liquid separation as it contains a high amount of calcium carbonate whose precipitation is pH-dependent (Hart et al., 2012; Koutsoukos & Kontoyannis, 1984). Hart et al. (2012) showed that calcium carbonate solubility increases substantially when the pH drops from 8.5 to 7.5 for cooling water used in pulp mills. Therefore adjustment of the pH of DS-digestate to a pH of about 8.5 may improve its settling characteristics.

The comparison of the characteristics of DS-digestates with their input DS showed that the DM in DS is be reduced by bioconversion into biogas. Both the input DS and the DS-digestate contain high amount of calcium carbonate. The characteristics of the input DS and DS-digestate obtained are key data that can be used for the planning of treatment systems for DS.

5.4.2 Particle size analysis of deinking sludges and digestate

This section discusses and compares the result obtained for the particle size distribution of raw and pre-dewatered DS as well as from the DS-digestate generated from pre-dewatered DS.

1.) Particle size of deinking sludges: W70 and W90/100 wastepaper grades

The particle size analysis of two different DS types (wastepaper grades, *W70* and *W90/100)* and their respective raw and pre-dewatered streams have been investigated according to the method described in section 4.6.2. The different samples used are shown in Appendix E.1. Figure 5.21 shows the particle size distribution using selected mesh sizes for the sieve analysis.

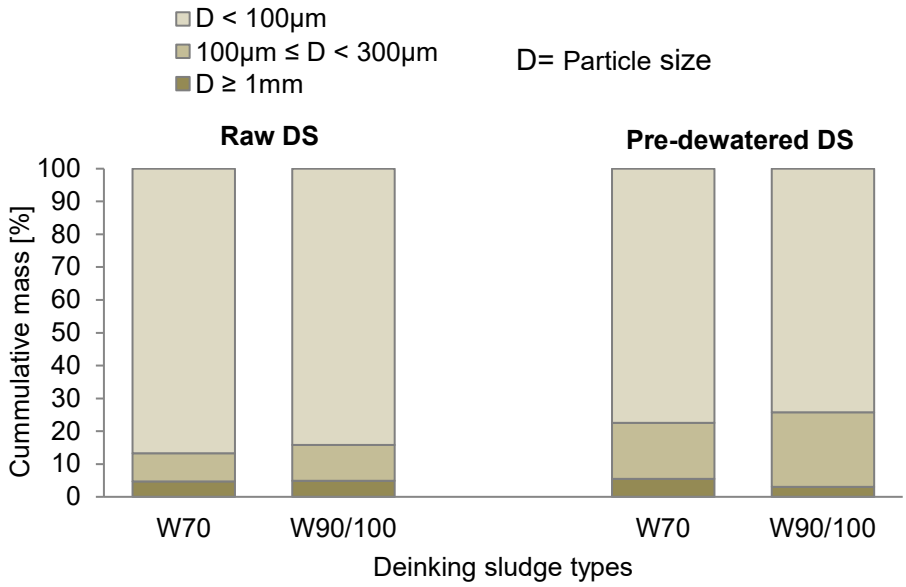

Figure 5.21 Particle size analysis of different DS samples differentiated by wastepaper grade and by dewatering stage

For both the raw and pre-dewatered DS, the cumulative mass of particles below 100 µm were the highest, but varied between the DS types. The raw DS had more particles <100 µm in comparison with the pre-dewatered DS for both the *W70* and the *W90/100* wastepaper grades. The pre-dewatering step reduced smaller particles in raw DS probably due to their flow into the liquid phase.

The particle sizes of the two different raw DS types had differences. The pre-dewatered DS, *W90/100* showed fewer particles ≥ 1mm and more particles in the range of 100 and 300 µm when compared with *W70*.

This could result either from smaller fibre fines or the higher calcium carbonate content of *W90/100* when compared to *W70* (section 5.1.2). By optical observation (eye) the particles ≥ 1mm appeared fibrous. These fibrous materials especially the light and larger ones are reported to have low settling velocities (Feist et al., 2007) and may impact the sedimentation characteristics of DS. Smaller organic particles are easily biodegradable compared to bigger ones due to their larger surface area to volume ratio. This informs that, provided that the smaller particles contained in the pre-watered DS of *W90/100* type are organic, it has the tendency of a faster bioconversion into biogas when compared to the pre-dewatered DS of *W70* type. This is consistent with the result of the biogas production as reported in section 5.2.1.3. Also, the higher fibrous particles present in the pre-dewatered DS *W70* type imply a poor settling for the sludge during sedimentation.

2.) Comparison of particle sizes between a deinking sludge and its digestate

The AD of DS involves the breaking down of organic particles, hence a comparison of the particle size distribution between pre-dewatered DS and the resulting digestate was carried out. The digestate was collected from a 10-L bioreactor which was operated semi-continously with pre-dewatered DS from the *W70* type as input (Appendix C.6).

Figure 5.22 shows the particle sie distribution for a wider range of mesh sizes. According to the Figure 5.22, the majority (93%) of the particles in pre-dewatered DS < 63 µm. The four groups of larger particles in pre-dewatered DS reduced differently in the range of 52 - 96% due to AD treatment. The particle sizes between 63 and 100 µm showed the highest reduction of 96%. The particles size > 100 µm had a lower degradation. This informs that during the AD process, the breakdown of smaller organic particles is faster when compared to the bigger ones.

The majority of the particles in DS-digestate were smaller than those in pre-dewatered DS and this may impact the settling property positively. It is because fibrous particles which belong to the category of larger particles and are known to impair settling have been reduced significantly. The calcium carbonate may possiblly belong to the categories of particle size < 63 µm.

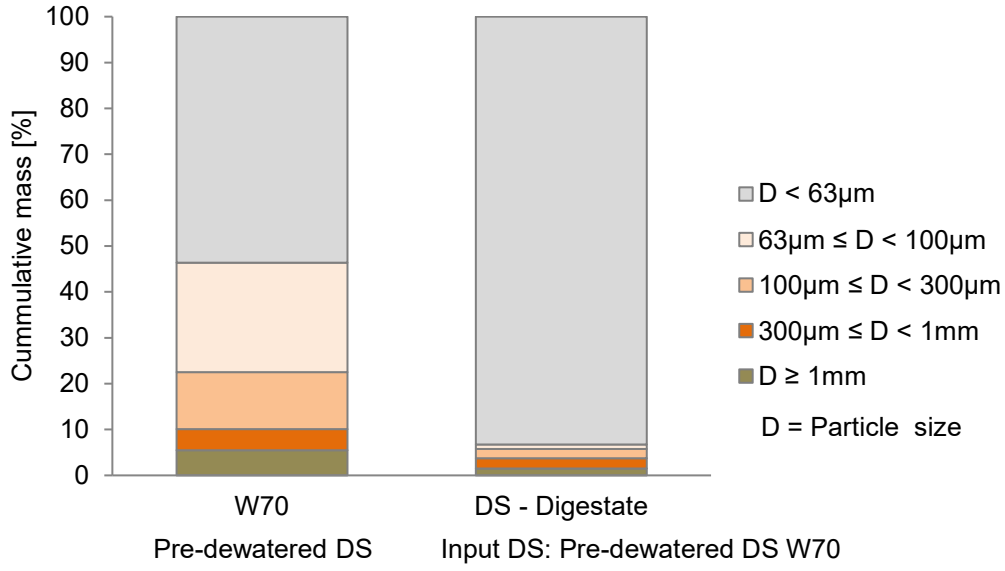

Figure 5.22 Comparison of the particle size distribution of pre-dewatered DS (*Stream 2-W70*) and digestate (see samples in Appendix E.1)

5.4.3 Sedimentation of deinking sludges and its digestates

The sedimentation characteristics of different DS types were investigated as described in section 4.6.3 using imhoff cones. The DS samples investigated are characterised in Appendix E.1. Figure 5.23 shows the distinct layers observed during the settling status of untreated pre-dewatered DS and DS-digestate upto 48 h. The three distinct layers observed for the pre-dewatered DS from top to bottom were a layer stained with dark foam and floating solids, a clear layer without foam and a settled sludge layer. For the DS-digestate only a clear layer and settled sludge layer was observed.

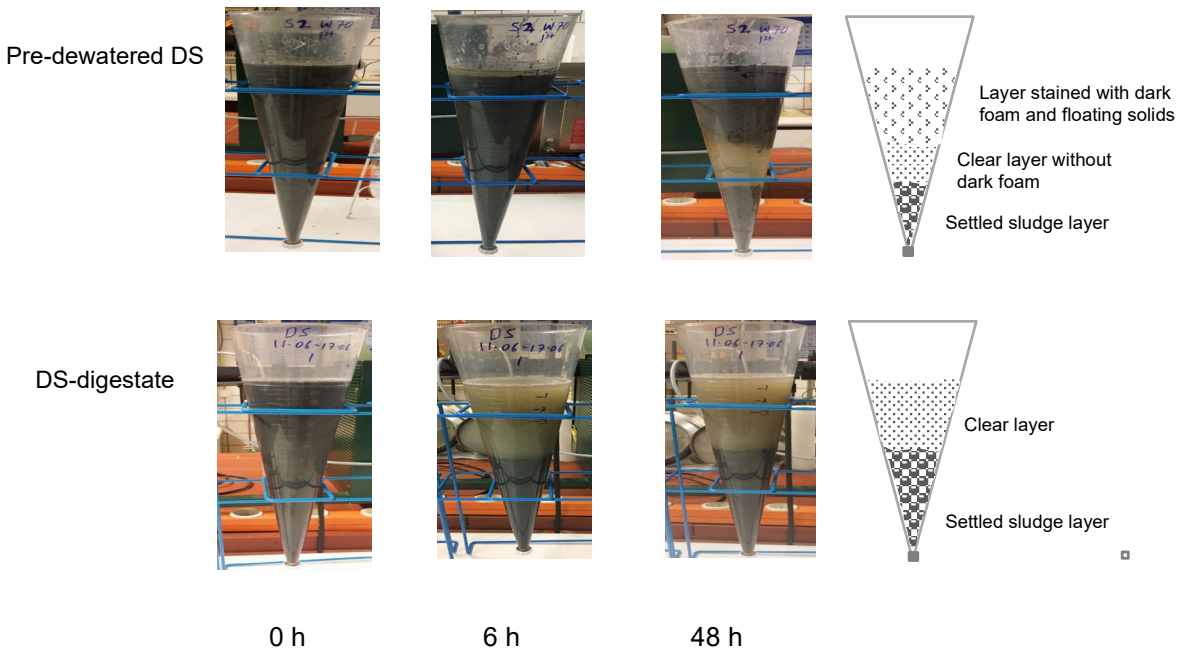

Figure 5.23 Settling of untreated pre-dewatered deinking sludge and digestate of deinking sludge by sedimentation (*W70*)

1.) Raw DS

The raw DS types of *W70*, *W80* and *W90/100* are characterized in Figure 5.24. It can be observed that all DS types showed a considerable amount of the settled fraction after a period of 24 h. The *W70* and *W80* samples had settled sludge in the range of 250 - 310 mL, which was lower than that of W90*/100.* This might be caused by different particle sizes in the DS types (Figure 5.23). Sludges with denser particles or non-fibrous materials may tend to settle better than less dense and fibrous ones. However, the particle size distribution of raw DS (section 5.4.2) does not suggest a huge difference between the types.

2.) Pre-dewatered DS

In Figure 5.24 it can be observed that pre-dewatered DS settled poorer than the raw DS. This can be explained to be due to the higher amount of small and denser denser particles probably in the raw DS which were probably removed during pre-dewatering compared to the larger and less dense particles in the pre-dewatered DS. Pre-dewatered DS from *W70* and *W80* showed a poor settling property compared to the *W90/100* DS.

The better settling of pre-dewatered *W90/100* may be due to the type of chemicals used during deinking or its higher calcium carbonate as compared to the *Stream 2-W70 and Stream 2-W80* (section 5.1.4). Calcium carbonate has low solubility in water (Caciagli & Manning, 2003; Coto et al., 2012) and may result in good settling characteristics. The volume of raw DS can be substantially reduced by sedimentation. It is however still important to further reduce sludge volume by the use of a mechanical treatment option.

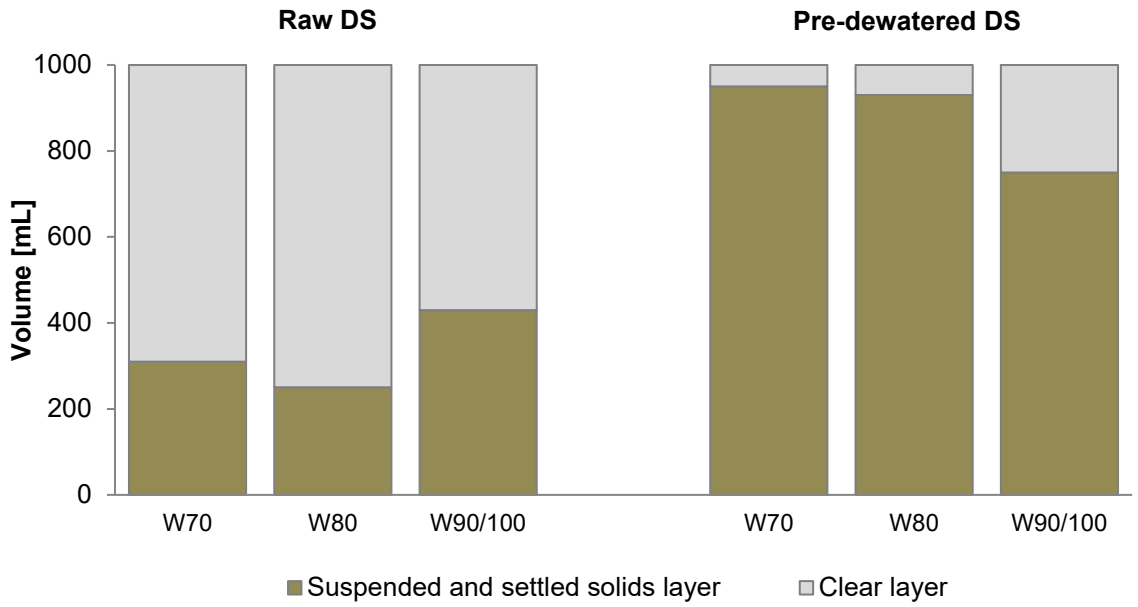

Figure 5.24 Sedimentation behaviour after 24 h in Imhoff cones of different DS samples differentiated by wastepaper grade and by dewatering stage (see samples in Appendix E.1)

3.) Deinking sludge and its digestate

The determination of settling characteristics with time were investigated for a pre-dewatered DS (*W70*) and DS-digestate as described in section 4.6.3. The results are shown in Figure 5.25. To exclude differences in the settling behaviour of DS resulting from varying DM, the DM of pre-dewatered DS (*Stream 2-W70*) was adjusted by the addition of water (Appendix E.2). The settling characteristics is shown in Figure 5.25. A faster settling rate can be observed for the digestates within the first 6 h. The widest difference in settling between pre-dewatered DS and DS-digestate occurred at 2 h. This difference in settling may be due to the reduction of poor settling fibrous materials during the AD process by biodegradation.

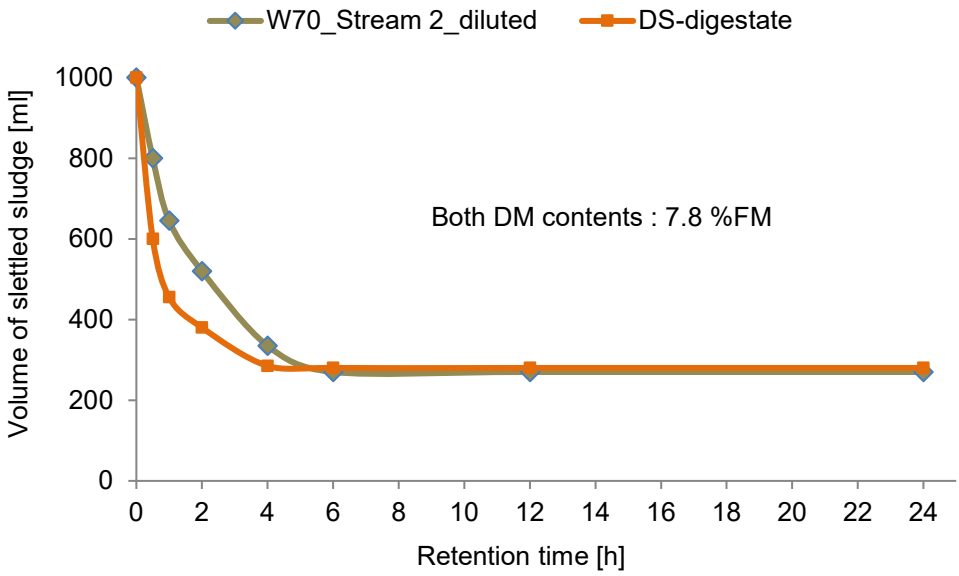

Figure 5.25 Comparison of the settling of pre-dewatered DS and DS-digestate by sedimentation. The DM content of DS was adjusted to attain the same DM content as the DS-digestate

4.) Properties of phases of digestate after sedimentation

The characteristics of pre-dewaterd DS poured into the Imhoff cone and the suspended and settled phases after sedimentation were analysed and the result is presented in Table 5.11. The characteristics presented are pH, DM, oDM, total organic carbon (TOC) and total nitrogen (TN).

The two phases had the same pH value in the basic range unlike the pre-dewatered DS having an average value of 7.8. The DM is concentrated in the settled phase, thereby having a 30-fold higher DM content than the suspended phase.The difference in oDM is not huge and informs that the suspended phase contains a substantial amount of poor settling. Interesting are the TOC and the TN contents of the suspended phase. According to the German ordinance on requirements for the discharge of wastewater into water bodies, a certain condition must be met. For institutions generating wastewater, where the TOC in raw samples is not up to 16000 mg/L, an annual average discharge of up to 100 mg/L of TOC is allowed provided the average elimination rate of TOC is at least 90% (AbwV, 2020).

The pre-dewatered DS has a total carbon (TC) between 4668 and 13321 mg/L, resulting in a TOC below 16000 mg/L. However, the suspended phase after centrifugation has a TOC of over 100 mg/L, indicating non-compliance with discharge standards. Further TOC reduction is therefore required by treatments such as centrifugation or aerobic treatment.

Also, the annual average discharge of TN of up to 40 mg/L is allowed provided the annual average elimination rate is at least 70% (AbwV, 2020). The TN of the suspended phase is above this value informing that it also does not meet the discharge requirement.

Table 5.11 The characteristics of the suspended and settled phases of the digestate after sedimentation test in the Imhoff cone

Parameter	Unit	Input DS	DS-digestate	
			Suspended phase (after Sedimentation)	Settled phase (after Sedimentation)
pH	-	7.8	8 ± 0.1	8 ± 0.1
DM	% FM	14	0.5 ± 0.08	15 ± 1.3
oDM	% DM	28.9	20 ± 1.2	25 ± 1.4
TOC	mg/L	ND	277 ± 82.7	ND
TN	mg/L	ND	65 ± 22.0	ND

Results from 3 samples of DS-digestate taken from a 10-L semi-continuously operated bioreactor with pre-dewatered DS of type *W70 as feed* (sampling date: 11.03.2015)

ND: Not determined

It can be concluded that after AD of DS followed by sedimentation of the digestate, the resulting suspended phase does not meet the discharge requirement into water bodies. It requires further treatment steps for TOC and TN removal before discharge.

5.4.4 Centrifugation of deinking sludge and its digestate

The centrifugation characteristics of pre-dewatered DS of type *W70 (Stream2-W70)* and DS-digestates from one of the 100-L bioreactors (R1A) were investigated as described in section 4.6.4. Figure 5.26 shows the fresh masses as well as the DM contents of three different samples before and after centrifugation. The DM of the DS sample *(Stream2-W70)* was 13.0% FM which is similar in DM to the DS-digestate 1 that was sampled from the first period of the second feeding phase of the bioreactor R1A (Appendix L.2). The DS-digestate 2 is a settled phase of DS-digestate with an original DM of 18.2% FM which was diluted to a DM of 13.1% FM with water. To ensure centrifugation results were unaffected by differences in DM, all three samples were diluted to achieve similar DM. Figure 5.26 illustrates that the resulting cakes from centrifugation of DS digestates 1 and 2 exhibited slightly higher DM than Stream 2-W70.

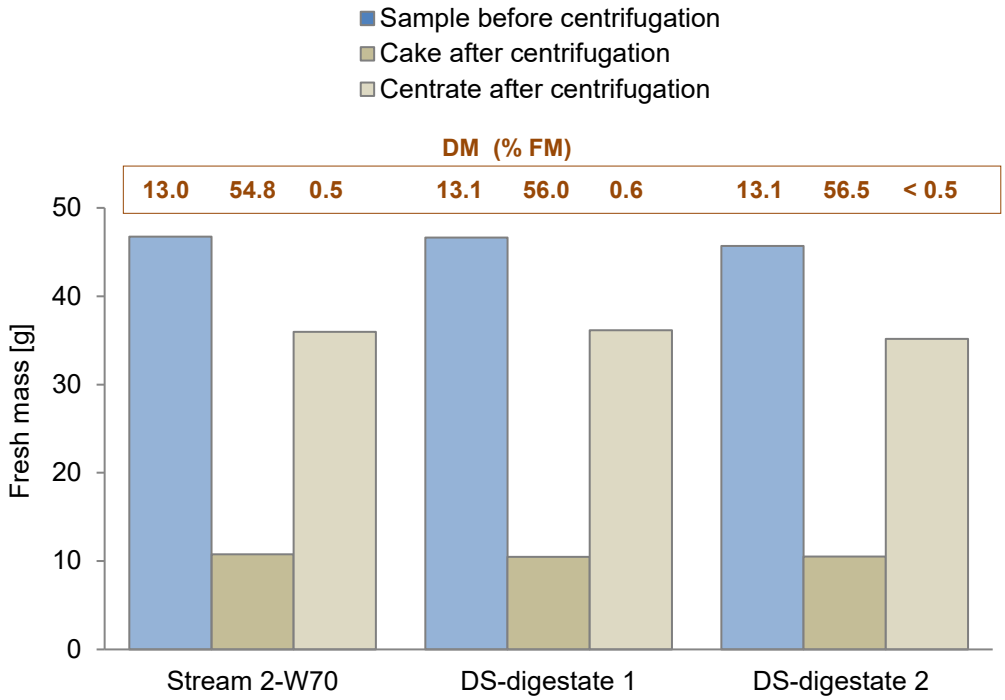

Figure 5.26 Mass separation and DM of centrifuge cake obtained by subjecting a pre-dewatered DS (Stream 2-W70) and three different digestate samples from 100-L to centrifugation

The result informs that AD of DS such as the *Stream 2-W70* can result in a mild improvement in the dewatering characteristics during centrifugation. When the DM of the cake from DS-digestate 2 is compared with that of DS (*Stream 2-W70*), an improvement of up to 3% increase in DM is observable due to treatment by AD.

Table 5.12 shows relevant parameters of the centrate from three different DS-digestates after centrifugation. A low DM of the different centrates between 0.4 - 0.5% FM was obtained. A considerable amount of oDM is still present in the centrate. The oDM is in the digestate range of 22.8 - 31.6% DM. The oDM content in the centrate was still high and may pose a disposal challenge. The $CaCO_3$ contents between 52.2 - 66.4% DM were large and have a potential for further utilization. Since the centrate is free from fibrous material, the $CaCO_3$ can be precipitated to produce calcium carbonate (Krigstin & Sain, 2006).

Table 5.12 The characteristics of the centrate of the digestate after centrifugation W70

Parameter	Unit	Centrate after centrifugation		
		Digestate 1	Digestate 2	Digestate 3
DM	% FM	0.5	0.4	0.5
oDM	% DM	22.8	36.7	31.6
$CaCO_3$	% DM	66.4	67.0	52.2

5.4.5 Key findings on importance of solid-liquid separation on valorization

The following are the key findings in the investigation of the solid-liquid separation of DS and DS-digestate as it influences their valorization.

1.) DS-digestates from DS *Stream 2-W70* has an average DM in the range of 5.2 - 7.5% FM and contains average residual organics in the range of 25 - 30% DM. The largest fraction is calcium carbonate in averages in the range of 46 - 51% DM.

2.) Particle sizes in DS *Stream 2-W70* were reduced significantly due to AD treatment. 93% of particles in DS-digestate are less than 63 µm. The poor settling fibrous particles in DS are thought to be reduced in the AD process thereby improving the dewaterability of DS-digestate.

3.) Due to reduced fibrous particles in DS-digestate from DS *Stream 2-W70* it settled about 30% faster than pre-dewatered DS for a 2 h settling time.

4.) Particles in the DS-digestate from DS *Stream 2-W70* can be separated by sedimentation and centrifugation. The suspended phase after sedimentation and the centrate after centrifugation still contain pollutants. They therefore require further treatment before discharge into the water bodies.

5.5 Deinking sludges and digestate ashes as supplementary building material

The suitability of ashes from DS and DS-digestate as supplementary building material was investigated by analysing their characteristics and their influence on wet mortar and motar prisms. The ashes from a pre-dewatered DS of type W70 and a DS-digestate from 100-L bioreactor (R1A) were prepared as described in section 4.7.1.

5.5.1 Characteristics of ashes from deinking sludges and its digestates

The particle size distribution, chemical composition and phases were the characteristics of DS and DS-digestate ash determined and discussed.

5.5.1.1 Particle size distribution

The particle size distributions of DS and DS-digestate ashes were determined using a laser diffraction technique (section 4.7.4). Table 5.13 shows their particle size distributions and the curve can be found in Appendix M.1. The D10, D50 and D90 are the sizes for which the percentage by mass of ash particles in ash with sizes less than them are equal to 10, 50 and 90% respectively. Differences in particle size distribution can be observed for the two ashes. The D10, D50 and D90 of DS-digestate ash were less than that of DS ash. It suggests that the DS-digestate ash has smaller particles when compared to DS ash. A large standard deviation can be observed for the D90 of the DS ash which might be due to sampling.

Table 5.13 Particle size distribution of DS ash and DS-digestate ash[19]

Ash	Number of Samples	Particle size distribution [µm]		
		D10	D50	D90
DS ash	5	1.33 ± 0.07	25.10 ± 3.12	295 ± 68.30
DS-digestate ash	3	0.92 ± 0.01	10.43 ± 0.21	222 ± 4.60

Conversely, since anaerobic bioactivity is not likely to affect the particle size of calcium carbonate, the main component of both ashes, variations in particle size distribution might come from distinct characteristics of the DS input substrate. The result however shows that both the DS and DS-digestate ashes have significant amount of fine particles. In comparison with the particle size distribution of portland cement is as follows: D10: 2.00 µm; D50: 7.90 µm; D90: 19.90 µm (section 3.4.3). D10 of DS and DS-digestate ash are finer but their D50 and D90 are not. Compared to fly ash from coal combustion (D10: 4.62 µm; D50: 27.96 µm; D90: 75.39 µm), already used in cement clinker (section 3.4.3), the D10 and D50 of DS and DS-digestate ash consist of finer particles.

[19] Analysis by Institute of Advanced Ceramics at TUHH

The result suggests that the particle sizes of DS and DS-digestate ash can be grouped as fine with reference to portand cement and fly ash. Bizley (2022) reported that a large portion of a cement plant's electrical demand is accounted for by the grinding process. Genç (2016) also reported that the typical specific energy consumed for grinding cement is 30 kWh/Mg. Since the DS and DS-digestate ashes are relatively fine based on cement and fly ash particles, they may not require the energy intensive grinding steps if proven to be suitable as a supplementary building material. However, their particle size can further be milled to achieve more finer particle size thereby improving their property for application.

5.5.1.2 Chemical composition

The chemical composition of DS and DS-digestate ashes which comprises calcium and other elements were investigated according to Schmidt-Döhl (2013) as shown in section 4.7.4. X-ray fluorescence analyses were carried out. On Table 5.14, the results were presented alongside with that of portland cement and fly ash. The first was taken as reference since it is a common cement type globally applied (Helmuth et al., 2000; Hotza & Maia, 2015). Due to the high CO_2 release during the production of portland cement clinker (Prakasan et al., 2020), it is notable that the proportion of portland cement has been declining for a long time. Also presented on Table 5.14 for discussion is the chemical composition of coal fly ash. Fly ashes from coal combustion plants are pozzolanic[20] materials containing siliceous or calcareous components and are already being used as supplementary building materials (Favier et al., 2018; Thomas, 2007). The images of the spectra which denote the elements present in the DS and DS-digestate ashes are available in Appendix M.2 and M.3.

In DS and DS-digestate ashes, Ca can be identified as the main element. Si and Al are also present. The difference between the DS ash and DS-digestate may be due to different sampling days in the treatment facility. An important non-heavy metal present is inorganic carbon since calcium is available in the form of $CaCO_3$ in DS and DS- digestate ash samples. They also showed high Na content which may result from the sodium hydroxide and other Na related chemicals used as deinking chemicals during deinking operation (section 2.3.3.1).

However, the Na content of 8.1% DM in DS-digestate ash appears too high and questionable. Other non-heavy metals such as Mg, P, S, K and Sr can be identified in DS and DS-digestate ashes in smaller proportions.

[20] Pozzolanic material are materials without cementitious property but they react with calcium hydroxide and water at room temperature

Heavy metals such as Ti, Cr, Mn, Fe, Ni, Cu and Zn can also be identified. Cr, Ni and Cu are heavy metals of health concern. Cr can cause contact allergies and occupational disease in construction (Hansen et al., 2003; Hedberg et al., 2014). Ni is reported carcinogenic and high copper exposure has been connected to Wilson disease in human causing cellular damage (Tchounwou et al., 2012). The elements in own DS and DS-digestate ash samples can be compared with that of other authors who investigated DS ash samples (Frias et al.; Pera & Amrouz, 1998). Their results are available in Appendix M.4. Ca in own sample is about 2-folds of the highest reported. The Si and Al content can be regarded to be in a similar range. Inorganic carbon content was not reported by the authors. Na content in own sample is sufficiently higher than theirs. In converse to own sample Cr, Mn, Ni, Cu and Zn were not reported to be present in their samples.

Table 5.14 Composition of elements (% mass) present in DS ash, DS-digestate ash, portland cement and coal fly ash

Element	DS ash [% DM]	DS-digestate ash [% DM]	Portland cement[a] [% DM]	Coal fly ash[b] [% DM]
Main elements				
Ca	33.14	30.10	45.46 – 47.34	1.87 – 3.43
O	47.14	45.58	35.55 – 37.01	49.70 – 53.56
Si	3.19	3.69	8.34 – 10.00	23.51 – 25.24
Al	2.20	1.07	2.00 – 2.84	12.28 – 13.81
Other elements (non- heavy metals)				
C	9.92	9.01	0.00	0.00
Na	2.89	8.12*	0.08 – 0.55	0.02 – 0.40
Mg	0.69	1.18	0.55 – 1.10	0.38 – 1.09
P	0.00	0.01	0.05 – 0.07	0,08 - 0,37
S	0.09	0.21	0.80 – 1.54	0.20 – 1.91
K	0.14	0.21	0.12 – 0,37	0.00 – 0.66
Sr	0.07	0.06	0.00 – 0.13	0.00
Other elements (heavy metals)				
Ti	0.13	0.14	0.14 – 0.34	0.53 – 0.78
Cr	0.01	0.04	0.00 – 0.01	0.00 – 0.02
Mn	0.02	0.02	0.03 – 0.10	0.00 – 0.03
Fe	0.31	0.49	2.10 – 3.08	3.15 – 7.41
Ni	0.02	0.01	0.00 – 0.01	0.00
Cu	0.04	0.04	0.00 – 0.01	0.00
Zn	0.02	0.02	0.00 – 0.04	0.00
Total	**100**	**100**		

a- Computed from Ahmed et al., 2018; Serpell & Zunino, 2017 and Elakneswaran et al., 2019
b- Computed from Song et al., 2015; Nordin et al., 2016 and Gilbert et al., 2019
*too high content that is unexplainable

In comparism with portland cement and coal fly ash as shown in Table 5.14, the Ca content of DS and DS-digestate ashes are less than that in portland cement but higher than that in coal fly ash. The Ca content in coal fly ash is not the main element when compared with DS and DS-digestate ashes and portland cement. Si and Al in coal fly ash are significantly higher than that in portland cement and in DS and DS-digestate ashes. Inorganic carbon was not reported for portland cement and coal fly ash as obtainable in own DS and DS-digestate samples. A higher sodium content in comparism to portland cement and coal fly ash is observable for DS and DS-digestate samples. It is notable that the heavy metal concentrations in DS and DS-digestate ash are not in concentration of concern when compared to those in portland cement and coal fly ash.

The chemical composition in DS and DS-digestate ash showed substantial similarities in element content with portland cement. Also, they do not contain heavy metals in the health-concerning concentration. It therefore concludes that based on their chemical composition, they may be used as a component for the raw material of a cement work.

5.5.1.3 Phases

Analysis were carried out to determine the phases present in DS ash and DS-digestate ash as described in section 4.7.4.2. The two tests methods applied on phases determination are Fourier Transform Infrared (FT-IR) spectroscopy and X-ray diffraction (XRD) analysis. The FT-IR spectra are shown in Appendix M.5 and M.6 while the XRD results are shown in Appendix M.7 and M.8. The different peaks identified in the FT-IR spectra show that carbonate is present in DS and DS-digestate ashes, which is most likely $CaCO_3$. The analysis results of the spectra based on peaks at different wavenumbers are shown in Table 5.15. Six peaks in the ashes correspond to calcite while four correspond to silicate.

The XRD results further confirm the identifiable components in the main phase of the ashes. The diffractogram establishes that calcite can be identified as the main phase of both ashes. A certain amount of quartz can be identified with uncertainites. Also included is a phase responsible for the peak at about 9.2 degrees (Appendix M.7 and M.8), which could be ettringite, thaumasite or a calcium silicate hydrate phase (riversideite). The result showing calcite as the main phase in the ashes suggests that the ashes can play a supplementary role to improve cement hydration as explained in section 3.4.3.

Table 5.15 FT-IR analysis results of DS and DS-digestate ash

Peaks (cm^{-1})		Assigned stretching/ bond	Mineral type	Reference
DS-ash	DS-digestate ash			
2515	2514	$v_1 + v_3$	Calcite	[1]
1796	1796	$v_1 + v_4$	Calcite	[1]
1416	1412	v_3	Calcite	[1]
1011	1015	Si-O	Silicate	[2]
874	873	v_2	Calcite	[1]
848	848	v_2	Calcite	[1]
700	700	-	Calcite & Silicate	-
669	669	Si-O-Si	Silicate	[2]
465	465	O-Si-O	Silicate	[2]

v_1, v_2, v_3, and v_4 are the four intramolecular vibration peaks of CO_3^{2-}. v_1 = symmetrical stretching, v_2= bending beyond the plane, v_3 = symmetrical stretching and v_4= bending in the plane (Stanienda-Pilecki, 2019; Zhuravlev & Atuchin, 2021)

Si-O, Si-O-Si & O-Si-O are typical bonds found in silicates minerals such as Talc, Lizardite, Sarponite and Montmorillonite (Hofmeister & Bowey, 2006)

[1] - Stanienda-Pilecki, 2019, [2] - Hofmeister & Bowey, 2006

Conclusively, the DS and DS-digestate ashes contain chemicals and minerals which can make them suitable as a supplementary building material, especially their high calcite concent.

5.5.2 Influences of ashes on mortar

The influence of ashes from DS and DS-digestate on mortar was investigated through mechanical properties such as flow value, density, flexural and compressive strength. Flow values were tested using fresh mortars while densities, flexural and compressive strengths were tested using cured mortar prism. The steps as recommended by DIN EN 196-1 for determining cement strength were adhered to for the flexural and compressive strength test.

5.5.2.1 Flow value

The flow values of prepared mortars (cement, sand and water mixure without and with ash) were determined. Information on the preparation of mortars is available in section 4.7.2 and Appendix F.2. The flow value gives information on the fluidity of a building material regarding its consistency and the cohesiveness of particles.

The method of flow value determination can be seen in 4.7.4.3. The different mortars prepared were put into three groups. They are mortars with no addition of ash (reference mortars), mortars with different fractions of cement substituted by DS ash (mortars with DS ash) and mortars with different fractions of cement substituted by DS-digestate ash (mortars with DS-digestate ash). The reference mortars of 0, 5, 15, 25 and 35% reduction of cement in mortar as shown in Figure 5.27 correspond to water to cement ratio (w/c ratio) of 0.6, 0.63, 0.70, 0.80 and 0.92 respectively. The w/c ratios in the reference mortars were made to correspond to that of their respective mortars in which cement fractions were substituted by either DS or DS-digestate ash (Appendix F.2). The mass of sand was kept constant.

As shown in Figure 5.27(a), the flow values of the reference mortars have only slight changes for mortars in the range of 0 to 35% reduction of cement fraction. On the other hand, the flow values of mortars with the substitution of cement by DS or DS-digestate ash in the range of 0 to 35% showed a distinct continuous reduction trend Figure 5.27(b).

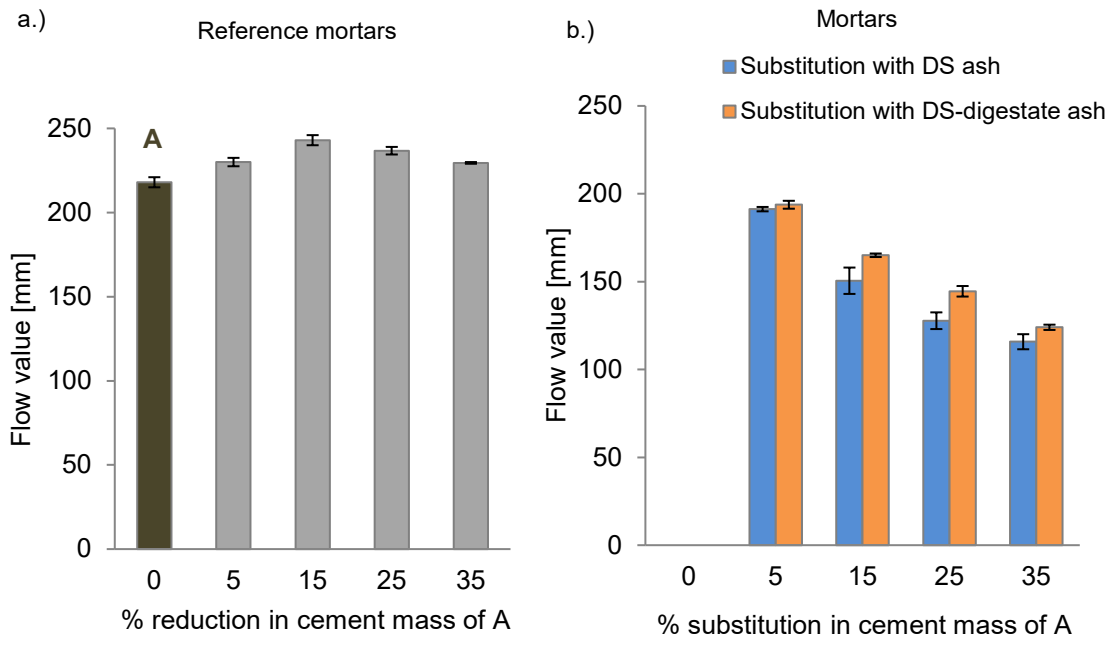

Figure 5.27 Flow value of different mortar mixtures at different cement reduction and substitution. The reference mortar did not contain ash

This informed that DS and DS-digestate ash have properties that could impair flow value when applied for building construction such as masonry. According to the SEM observation carried out by García et al. (2008) and Segui et al. (2012), they reported a distinct high porosity of wastepaper sludge ash caused by the fibre content of the sludge. The wastepaper sludge though is different in property than DS.

They share a similarity in the sense that they both contain paper fibres and similar $CaCO_3$ types used as fillers for paper making. The reported porosity observed for wastepaper sludge ash may also be the case for DS and DS-digestate ashes which led to the observed reduction of flow value when used in mortar. The ability of a mortar to spread or flow during construction work is often essential for construction work. For this reason, when applying DS and DS-digestate ash as a building material, it should be expected that they impair flow. If proven that they contribute to strength in construction then a compromise must be reached between the negative influence on the flow value of their mortar and possible increase with respect to the contribution of mechanical strength.

5.5.2.2 Density

The densities of mortar prisms after a curing period of 28 days were determined as described in section 4.7.4.4. The mortar prisms were also grouped in similar categories as described for mortars in section 5.5.2.1. The results of the densities obtained for the different mortar prisms are shown in Figure 5.28. The average density of reference mortar prisms ranged from 2256 to 2295 kg/m^3. With a 5% substitution of cement by DS and DS-digestate ash, the density of mortar prisms reduced by 0.4 and 1.0% respectively.

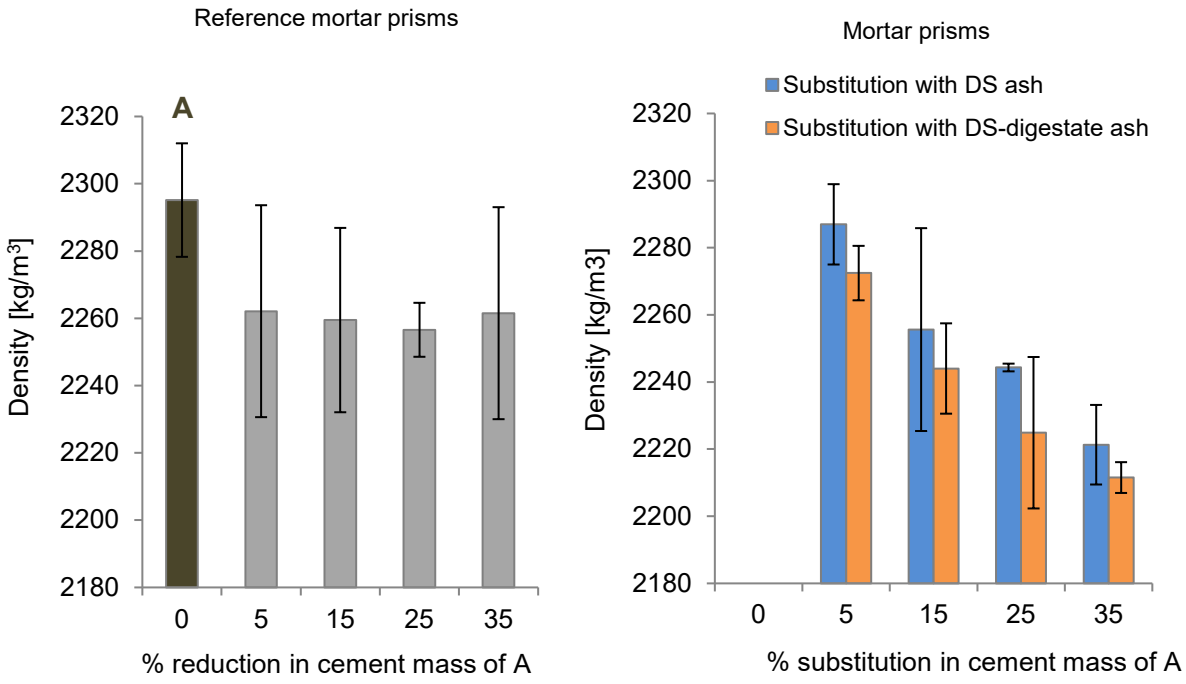

Figure 5.28 Densities of different mortar prisms at different cement substitutions. The reference mortar prism did not contain ash and the cement substitution fraction was removed.

A continuous decreasing trend in the density of mortar prisms can be observed until the 35% cement substitution, which showed 1.8 and 2.2% density reduction due to DS ash and DS-digestate ash respectively. The result obtained shows that DS ash or DS-digestate ash are less dense than portland cement.

5.5.2.3 Flexural strength

The flexural strengths of the different mortar prisms were analysed as described in section 4.7.4.5. The mortar prisms are in the same three groups as in section 5.5.2.1. Figure 5.29 show the results obtained for the reference mortar prism and the other prisms with the addition of either DS or DS-digestate ash. The flexural strength of reference samples dropped continuously from an average value of 7.0 to 3.8 N/mm^2 due to cement reduction (Figure 5.29a).

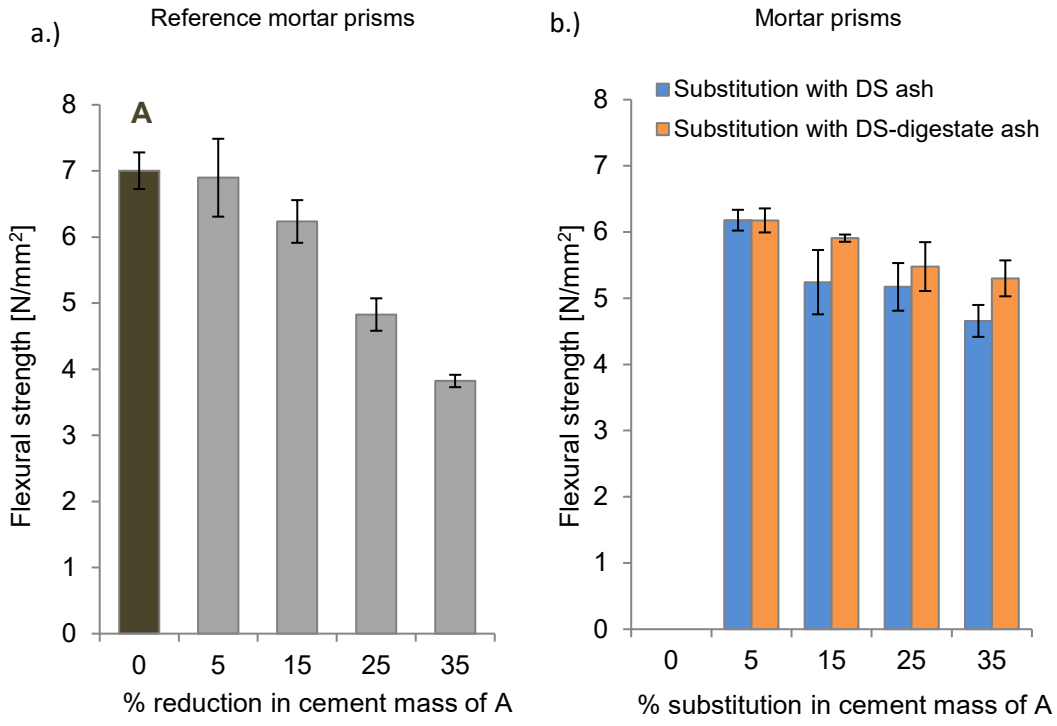

Figure 5.29 Flexural strength of different mortar prisms at different cement substitution. The reference mortar prism did not contain ash but the cement substitution fraction was removed.

With a 5% substitution of cement mass fraction, the flexural strength of the mortar prism was reduced by 10% for both DS and DS-digestate ash respectively. The flexural strength of the mortar prism was further reduced by a 15% substitution of cement mass fraction (Figure 5.29b).

This amounts to a flexural strength reduction of 15.3% for DS ash and 5.3% for DS-digestate ash. The trend of flexural strength changed when 25 and 35% of ash were used to substitute cement. . An increase in regard to mortar without ash in flexural strength of 7.1 and 21.9% for DS ash and 13.5 and 38.7% for DS-digestate were observed respectively.

This result obtained suggests that DS and DS-digestate ash must exceed a minimum fraction in mortar mixture before their effect regarding flexural strength can be seen in mortar prism. It establishes that DS and DS-digestate ash can contribute to flexural strength. The positve effect increases with an increase in the quantity used in the mixture.

5.5.2.4 Compressive strength

The compressive strengths of the different mortar prisms were analysed as described in section 4.7.4.5. The mortar prisms are in the same three groups as in section 5.5.2.1. Figure 5.30 shows the result obtained for the reference mortar prism and the other prisms with the addition of either DS or DS-digestate ash. All the mortar prisms analysed fall in the mortar class of M15 (minimum compressive strength of 15 N/mm^2) according to the DIN EN 998-2. The initial compressive strength of the reference mortar prism with 0% cement reduction (w/c ratio of 0.6) is 40.9 N/mm^2.

The reduction of cement fraction from 5 to 35% resulted in a compressive strength drop in the reference mortar prisms (Figure 5.30a). They reduced sharply in the order 4.8, 26.8, 47.3 and 61.8% respectively when compared to the prism with no reduction. A reduction in compressive strength can also be observed for the mortar prisms with cement fraction substituted either with DS ash or DS-digestate ash at a moderate rate (Figure 5.30b). With cement substituted by DS ash the reduction in compressive strength are 4.4, 17.9, 27.7 and 38.3% for cement substitution of 5, 15, 25 and 35% respectively. Also with DS-digestate ash mortar prisms resulted in a compressive strength reduction of 3.0, 14.7, 22.0 and 27.8% respectively. A reduction in compressive strength in reference mortar prism due to cement reduction can be observed. This reduction due to cement fraction reduction (increase in w/c ratio) is consistent with other authors (Chan et al., 2018; Salem & Pandey, 2017).

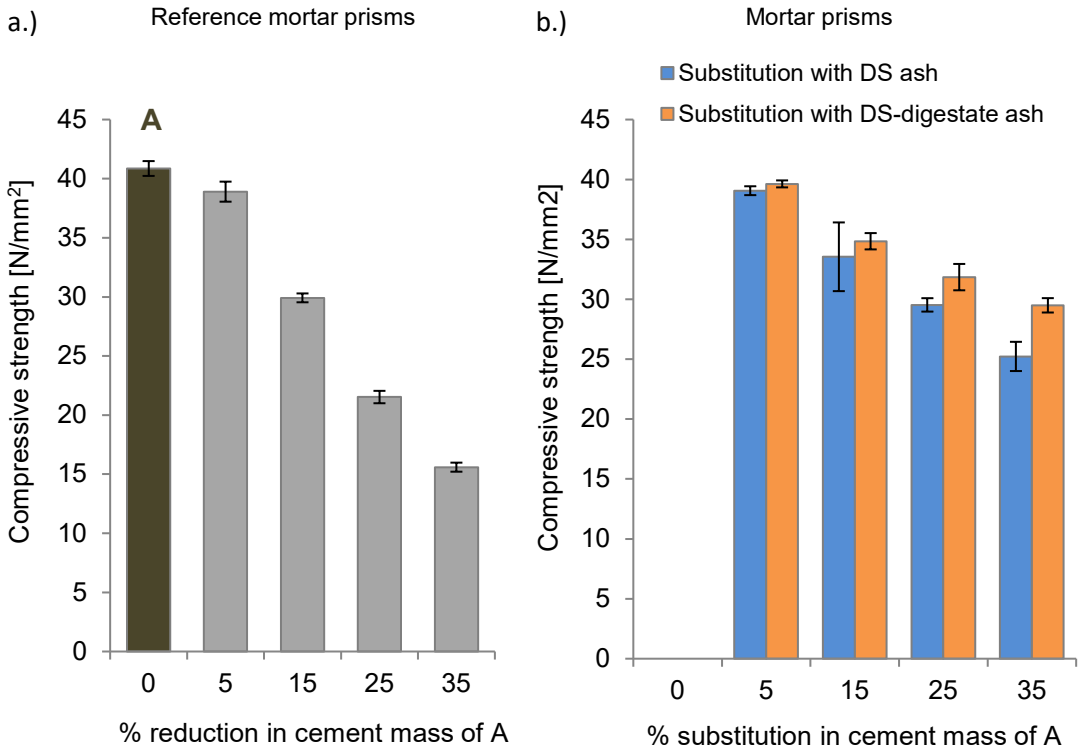

Figure 5.30 Compressive strength of different mortar prisms at different cement substitution. The reference mortar prism did not contain ash but the cement substitution fraction was removed

Samples with DS and DS-digestate ashes also lost some amount of compressive strength when compared with the sample A. It is observable that they contributed to compressive strength when compared to their respective samples of cement reduction. Figure 5.31 shows the different contribution of DS and DS-digestate ashes to compressive strength when used to substitute cement fraction in mortars. The computation is available in Appendix M.9 and M.10.

Figure 5.31 shows that as cement mass fraction substitution with ashes increases, the contribution to compressive strength of mortar prisms also increases. At 35% of cement mass fraction substitution, a decline in contribution can be observed. It indicates that the optimal substitution by DS and DS-digestate ashes are at about 25% cement mass fraction which yielded 38 and 55% contribution respectively to the compressive strength lost due to substitution. For real application, the amount of DS and DS-digestate ash to be added must not impair the required compressive strength of the construction or building product.

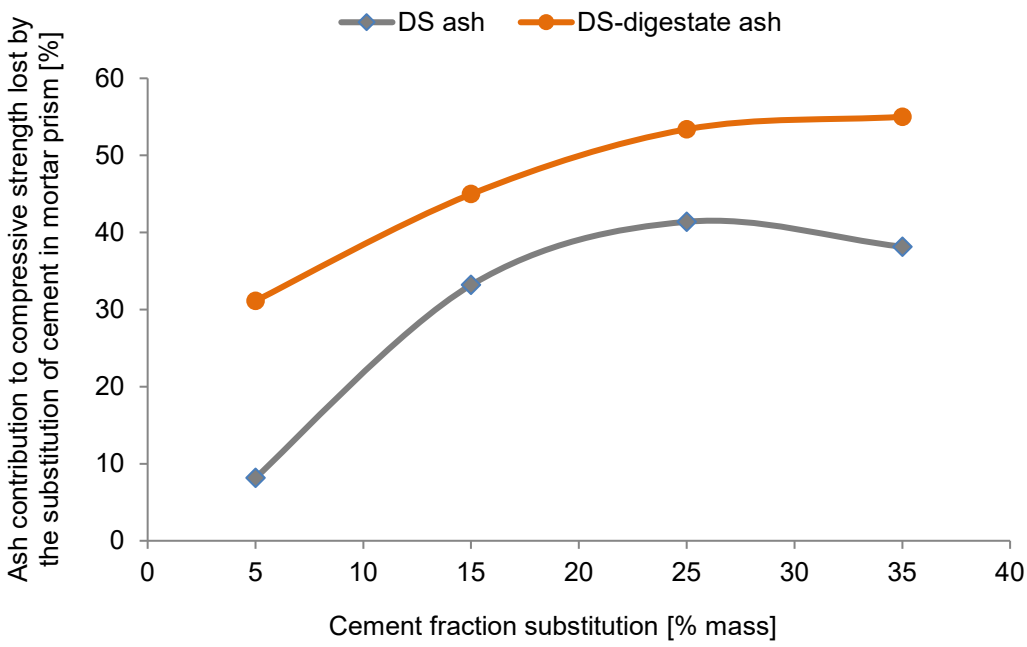

Figure 5.31 Contribution of DS ash and DS-digestate ash to compressive strength lost when used to substitute cement in mortar

The result obtained shows that DS ash and DS-digestate ash can add strength to mortar in building construction work. Their synergistic interaction with portland cement in the presence of water and fine aggregate (sand) to contribute to flexural and compressive strength is notable.

5.5.3 Key findings of ash supplementation on mortar

The following are the key findings of the investigation of ashes from DS and DS-digestate as supplementary building material in mortar and mortar prism.

1.) The particles in DS and DS-digestate ash are sufficiently small with D10 (0.92 - 1.33 µm), D50 (19.40 - 25.10 µm) and D90 (222 - 295 µm). They can be considered also as small particles when compared to portland cement and coal fly ash. However, milling can further improve their application as a supplementary building material.

2.) The main elements in portland cement such as calcium, oxygen, silicon and aluminium are also present in DS and DS-digestate ash in substantial quantities. They do not contain heavy metals in a concentration of toxicity concern.

3.) The ashes are rich in calcite and also contain some amount of silicate.

4.) They show a negative impact on the flow property of mortar.

5.) They can contribute to the flexural and compressive strength of mortar.

6.) The optimal contribution of DS and DS-digestate ashes to compressive strength lost due to cement substitution were 38 and 55% respectively. This occured at substitution of about 25% mass fraction of cement in mortar. For real application, an appropriate mortar mixture with proportion of the ash which do not impair with the required compressive strength must be determined.

5.6 Concept for energy and material valorization of deinking sludge

This section brings together the findings from the previous chapters. The mass flow of dry matter, organic dry matter and $CaCO_3$ of the partner's DS treatment plant is discussed. This is followed by a discussion on three different treatment scenarios for the application of combined energy valorization by anaerobic digestion and material valorization by $CaCO_3$ recovery. Finally, the biogas energy and $CaCO_3$ potential of DS in Germany is discussed.

5.6.1 Mass flows in a conventional deinking sludge treatment

The flow of material in the partner's treatment plant for DS (Figure 4.1) which is a conventional method for the treatment of DS was used as basis for anaylsis of mass flows. Analysed parameters are DM, oDM and $CaCO_3$ flows. Computation of mass flow was done using the experimental data obtained in the study. Assumptions and simplifications for the models are as follows;

1.) No mass was lost during flow in the entire system and all material flow is homogenous.

2.) Mass flows that do not contain a substantial amount of DS were regarded as negligible.

3.) The DS stream which enters as input into the wastewater treatment plant recycles 50% of its dry matter, 40% of its organic matter (corresponding to 40% aerobic biodegradability) and 50% of calcium carbonate into the into the sludge buffer.

The visualization of the mass flow models was done using the STAN software (Cencic & Rechberger, 2008). The models are explained in the following:

5.6.1.1 Dry matter flow

Figure 5.32 is the mass flow of dry matter of DS in a conventional treatment plant for DS. The computation is shown in Appendix N.1. The analyses began with the discharge of DS from the deinking operation. The dry matter content of raw DS as discharged was taken as 100%. This represents the basis for the analysis of further streams and flows. The raw DS was fed into the pre-dewatering unit and was distributed into 20% for *stream 5* and 80% for *stream 2* flows. The *Stream 2* continues into the sludge buffer, while the *Stream 5* is treated in the microflotation plant belonging to the water recycling scheme of the plant. The output (Stream 5i) is reused as process water in the plant.

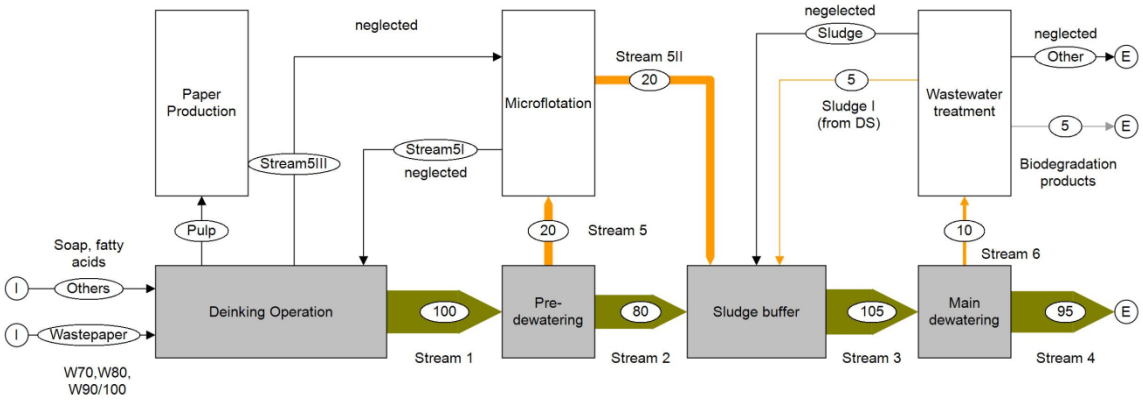

Input (I)	Output (E)	Unit of mass flow (%DM of Stream 1)
(main dry matter flow)	(other dry matter flow)	

Figure 5.32 Flow of dry matter content in the conventional treatment of DS

The *Stream 5* has different characteristics compared to the raw DS, due to treatment chemicals used for the microflotation unit. The flow of mass from the sludge buffer (*Stream 3*) is 105% which is higher than the mass of flow of the raw DS discharge due to biosludge. The outflow of DM from the main-dewatering unit results in a dry matter flow of 95% for *Stream 4* and 10% for *Stream 6.* The increase in the flow of *Stream 3* was due to the recycling of extra DM in the wastewater treatment plant. The flow of the DM in the treatment of DS informs that the DS treatment aims at solid-liquid separation. The raw DS passes through different treatment steps to concentrate the DM fraction. It is observable from the mass flow that that the *Streams 1, 2, 3 & 4* and combined a substantial amount of initial dry matter and are therefore options to locate an anaerobic digester.

5.6.1.2 Organic dry matter flow

The organic dry matter flows of DS in a conventional treatment plant is shown in Figure 5.33. The computation of the mass flow of the organic matter is available in Appendix N.2. Beginning with 100% as the oDM in raw DS. The pre-dewatering unit results in the distribution of organic matter of 26% for *Stream 5* and 74% for *Stream 2*. *Stream 3* entering with an organic dry matter flow of 105% into the main-dewatering unit is distributed into 9% and 96% for *Stream 6* and *Stream 4* respectively. The increase in the output of organic dry matter flow of the sludge buffer above 100% can be ascribed to the recycling of organics from the installed wastewater treatment plant as shown in Figure 5.33.

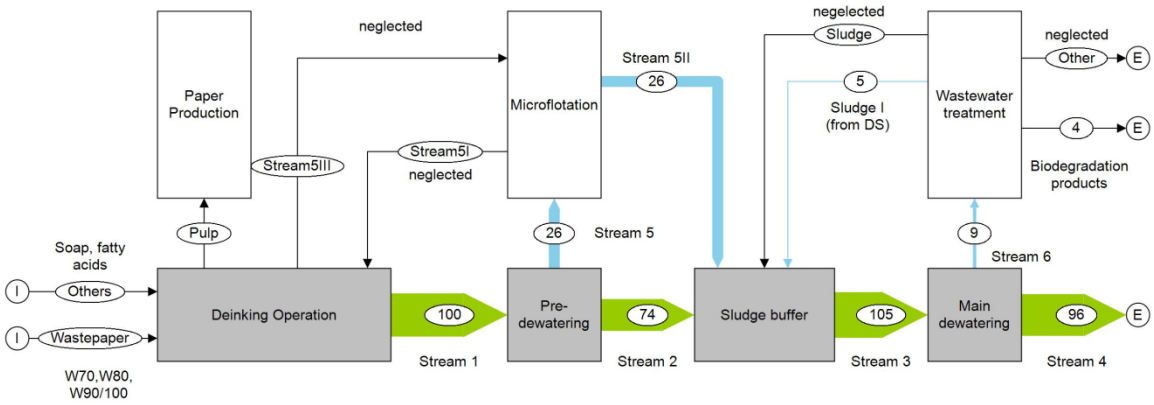

Input (I)	Output (E)	Unit of mass flow (% oDM of Stream 1)
(main organic flow)	(other organic flow)	

Figure 5.33 Flow of organic matter content in the conventional treatment of DS

The organic mass flow of *Stream 1* and *Stream 3* are similar in magnitude and implies a higher biogas yield compared to the other streams. It followed by *Stream 4* and lastly by *Stream 2*. Although the organic mass flow play a very important role in the suitability of a stream for its utilization as a biogas feedstock other factors also affects the selection. In section 5.6.2 some factors that may influence the selection of a DS stream for the application for combine biogas production and calcium carbonate recovery is discussed.

5.6.1.3 Calcium carbonate flow

Calcium carbonate is the DM fraction of DS which can be used as a supplementary building material (section 5.6). The computation of the mass flow of $CaCO_3$ in the conventional DS treatment plant is available in Appendix N.3. Since it is a major constituent of the DS, it also flows along the treatment line. As seen in Figure 5.34, a 100% mass flow of calcium carbonate from raw DS leaves the deinking plant into the pre-dewatering unit. They are distributed along the DS treatment streams until *Stream 4* as output. The order of $CaCO_3$ potential based on the flow of $CaCO_3$ is similar to that of organic dry matter mass flow with *Stream 1* and *Stream 3* in a similar group followed by *Stream 4* and then *Stream 2*. It is observable that all the four streams considered have substantial amount of $CaCO_3$ that can be recovered. The magnitude of $CaCO_3$ may not not have so much advantage in selection as the novel treatment approach require that biogas is first generated from DS before reciovering the $CaCO_3$.

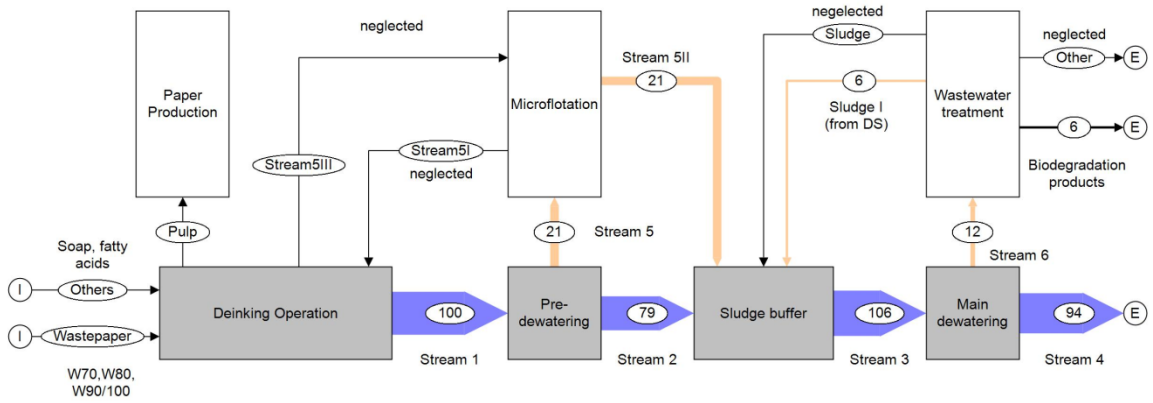

Input (I)	Output (E)	Unit of mass flow (% oDM of Stream 1)
(main $CaCO_3$ flow)	(other $CaCO_3$ flow)	

Figure 5.34 Flow of $CaCO_3$ content in the conventional treatment of DS

5.6.2 Novel treatment scenarios for deinking sludges

AD treatment coupled with $CaCO_3$ recovery of DS is a novel treatment approach for the wastepaper recycling plant. Due to the possible occurrence of different DS streams in a conventional plant, it is important to find the most promising candidate for application. In this section, factors for consideration and three scenarios for the application of the novel treatment approach for DS are discussed.

5.6.2.1 Scenario with raw deinking sludge for biogas

The scenario is discussed with considertion of the factors in Table 5.16. This scenario utilizes the raw DS as input for the combined AD and calcium carbonate recovery. Figure 5.35 shows the integration of an AD step combined with a $CaCO_3$ recovery step in the treatment of DS. The pre-dewatering step from the original DS treatment plant which is combined with a water recycling scheme via a microflotation is removed compared to Figure 4.1. Also, a centrifugation unit is used instead of the main-dewatering unit of the original DS treatment plant, because the efficiency of centrifugation for DS-Digestion was observed in this study to be high (section 5.4.6).

Based on the DM of *Stream 1* (1.1 - 4.7% FM), a wet type AD process can be used for treatment. The biogas energy generated can be utilized to dry the cake of the centrifuged DS-digestate at 100 °C in other to remove water and then burnt at about 550 °C to remove residual fibres. The resulting ash has a substantial economic value as it is can be used as a supplementary building material.

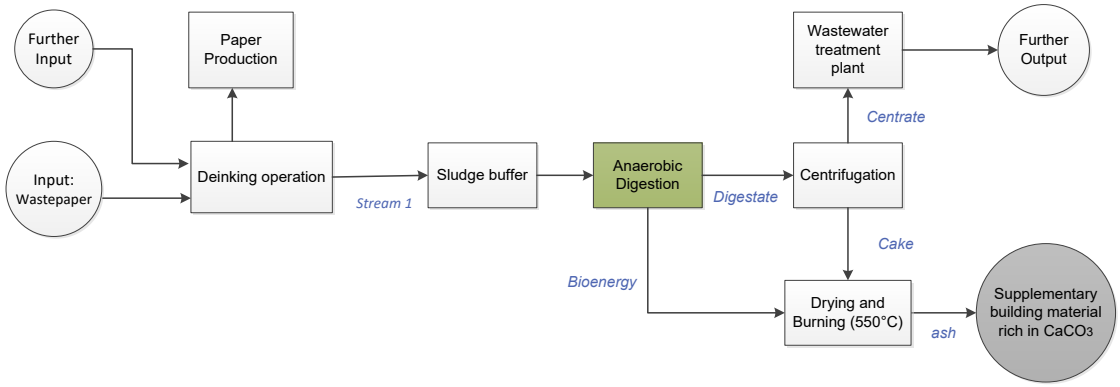

Figure 5.35 Combined anaerobic digestion and calcium recovery with raw deinking sludge as biogas substrate

Though this scenario utilizes a DS *Stream 1* with a high mass of organic (Figure 5.35), it however introduces a water consumption problem when compared with the original DS treatment plant. This is due to the elimination of the installed water recycling process. It is practicable to install another water recycling step at the discharge of the biogas plant, but the contamination from biomass from the AD step might make it more capital intensive. The need for a high redesign of an existing DS treatment plant to achieve this scenario is another technical challenge to be dealt with.

It also requires a bigger digester size for targeted biogas energy when compared to *Stream 2* and *4* in consideration of the organic content present in their respective fresh mass. It can be applied either in a batch or semi-continuously feeding mode since it is pumpable. It is possible to apply this scenario to treat DS by utilizing the high organic and $CaCO_3$ content of *Stream 1*, but its competition with the initial water recycling step is a big challenge. This is because the wastepaper recycling process is a huge water consuming process for which compromising a cost-effective water recycling step can lead to sustainability problem.

5.6.2.2 Scenario with pre-dewatered deinking sludge for biogas

Figure 5.36 is drawn with stream 2 as AD feedstock. An attempt was made to retain the water recycling scheme of the original plant (Figure 4.1). *Stream 5II* from the water recycling scheme and biosludge flow into a sludge buffer and mixed with DS-digestate.

Based on the DM of *Stream 2* (5.1 - 16.4% FM), a wet type AD process can as well be used for treatment. Similar to the scenario in section 5.6.2.2, the biogas energy produced from *Stream 2* can be used to dry and burn residual fibres from the cake of the centrifuged mixed sludge. The ash obtained can then be applied as a supplementary building material.

.

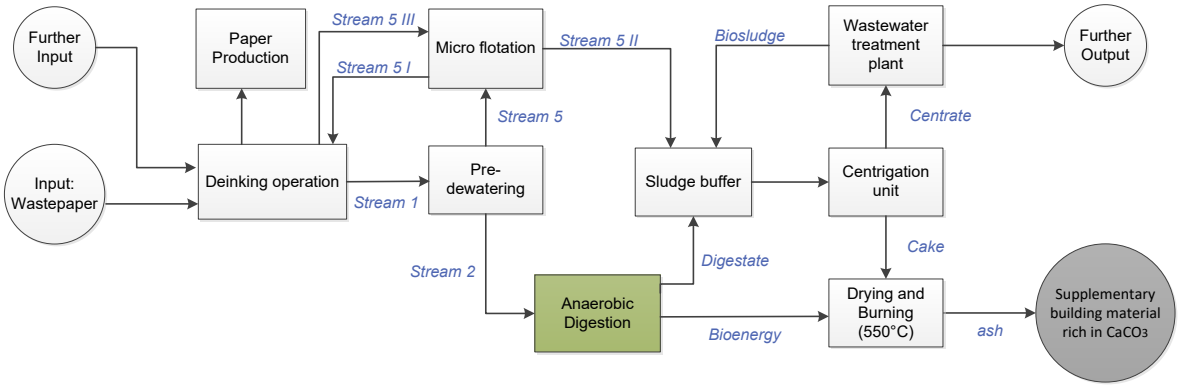

Figure 5.36 Combined anaerobic digestion and calcium recovery with pre-dewatered deinking sludge as biogas substrate

This scenario requires a moderate redesign of the original DS treatment plant in comparison to the scenario in section 5.6.3.1 since it does not alter the water recycling scheme. One drawback of this scenario is the mixing of DS-digestate with other fibre and organic containing streams. Though the added Streams are low in organic, they still increase the energy required for removing residual organics in the dried cake of the centrifuged mixture. The digester size required for targeted biogas energy will be less than that of *Stream 1* but bigger than that for *Stream 4*. It can as well be fed by batch or semi-continuous mode.

This scenario is a good approach to applying AD in the original treatment of DS as it does not compete with the water recycling goal of the wastepaper recycling industry and also requires only a moderate redesign of the original DS treatment plant.

5.6.2.3 Scenario with main-dewatered deinking sludge for biogas

This scenario retains the water recycling scheme too (Figure 5.37). The scenario does not require any redesign as it does not alter any part of the existing DS treatment plant (Figure 4.1) but adds an AD treatment to the original output (*Stream 4*). *Stream 4* is used as the feedstock for AD. Since most wastepaper recycling plant dewaters their DS to a dry matter content similar to *Stream 4*, it makes this scenario relatively easy to apply. Based on the DM of *Stream 4* (49.5 - 62.5% FM), a dry type AD process is suitable for treatment.

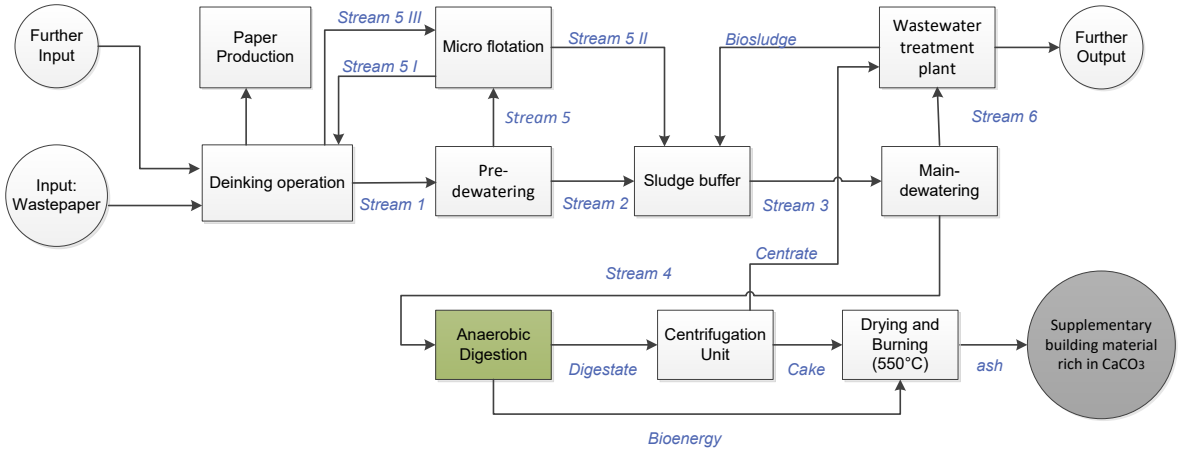

Figure 5.37 Combined anaerobic digestion and calcium recovery with main-dewatered deinking sludge as biogas substrate

This scenario is a good approach to applying AD in the original treatment of DS. Aside from the fact that it does not compete with the water recycling scheme, it is advantageous in the sense that no redesign or reconstruction cost is involved. The digester size required for targeted biogas energy is lower when compared to *Stream 1* and *2*. It can be easily operated in a batch feeding mode as pumping is not possible. One drawback of the scenario is the dry fermentation process which can impair efficient biogas production due to the poor flow of gas or liquid in the AD system. To improve sustainability in the wastepaper recycling process it is necessary to consider all options in a holistic view. The recycling of water is already established in the industry as a huge step to reduce water consumption. This makes the use of raw DS not a very suitable option as it impairs an efficient water recycling scheme. Either *Stream 2* or *Stream 4* are preferable for consideration as AD feed stock. Based on the analysis of the influence of water content on AD of DS as discussed in section 5.2.1.5, a 65% water content was optimal in terms of biodegradability and digester size required for targeted bioenergy. This implies that generating an optimal DS based on water content for AD, it may require that *Stream 2* be further dewatered until about 65% water content.

5.6.2.4 Comparison of the novel treatment scenarios

Different factors are identified to influence the choice of DS stream proposed to be used as input for the novel treatment approach. Five possible factors are discussed in the following:

1.) Alteration of water recycling scheme: This refers to the need to modify or remove the existing water recycling scheme of the conventional DS treatment process such as microflotation before the integration of an AD system.

2.) Degree of redesign of existing plant: It considers the extent to which general modification of the current process have to be carried out in order to integrate an AD system. It also include the alteration of the water recycling scheme.

3.) Suitable AD type: The choice of whether a wet or dry fermentation is applied depends on the dry matter content of the potential AD feedstock selected which varies across DS streams.

4.) Digester size: The size of digester to be installed is dependent on the targeted biogas energy for a given period of time. This will vary across DS streams due to their different biogas yields.

5.) Feeding mode: The choice of whether a batch or semi-continuous feeding is applied is determined by the ease of pumpability which in turn depends of the dry matter content of the different DS streams.

A comparative analysis of different scenarios for application of AD is presented in Table 5.16, which takes into account the aforementioned factors.

Table 5.16 Three different scenarios for the application of novel treatment of DS

Factors	Scenario A *(Stream 1)*	Scenario B *(Stream 2)*	Scenario C *(Stream 4)*
Biogas potential	highest	lowest	medium
Calcium carbonate potential	medium	lowest	highest
Alteration of water recycling scheme	yes	no	no
Degree of redesign of existing plant	high	medium	none
Suitable AD type	wet fermentation	wet fermentation	dry fermentation
Digester size for an equal targeted biogas energy	bigger	big	smaller
Feeding mode	semi-continuous	semi-continuous	batch

Table 5.16 outlines three distinct scenarios proposed for the application of novel treatment methods to DS with a focus on AD as in section 5.6.2.1 to 5.6.2.3. Each scenario, represented by Stream (raw DS) in Scenario A, Stream 2 (pre-dewatered DS) in Scenario B and Stream 4 (main-dewatered DS) in Scenario C, is evaluated across various aforementioned critical factors essential for understanding their potential impact and feasibility within the context of DS treatment and resource recovery.

- In terms of biogas potential, Scenario A demonstrates the highest capability for biogas production among the evaluated Scenarios. Conversely, Scenario B exhibits the lowest biogas potential, while Scenario C falls in between, with a medium rating for biogas potential, positioning it between the extremes observed in Scenarios A and B.
- Moving to calcium carbonate potential, Scenario A is rated as having a medium potential for calcium carbonate recovery. In contrast, Scenario B shows the lowest potential for calcium carbonate recovery among the scenarios. Conversely, Scenario C presents the highest potential for calcium carbonate recovery.
- Regarding alterations to the water recycling scheme, Scenario A necessitates alterations to the scheme, while Scenarios B and C require no such modifications, ensuring a smoother integration into existing DS treatment facility.
- In terms of plant redesign, Scenario A requires the most extensive redesign, while Scenario B necessitates a moderate level of redesign compared to Scenario A. Conversely, Scenario C requires no redesign of the existing plant.
- Considering suitable AD types, both Scenario A and Scenario B utilize wet fermentation, while Scenario C opts for dry fermentation.
- For digester size requirements, Scenario A requires a bigger digester size compared to the other scenarios. Scenario B requires a big digester size, and Scenario C necessitates a smaller digester size.
- Finally, in terms of feeding mode, both Scenarios A and B employ a semi-continuous feeding mode, whereas Scenario C utilizes a batch feeding mode.

This comparative analysis of Table 5.16 offers valuable insights into the potential implications and considerations associated with each scenario, aiding decision-making processes in the development and implementation of the novel treatment approaches for DS with focus on AD.

Overall, the combination of moderate requirements for plant redesign, compatibility with existing operational practices and the utilization of wet AD technology makes Scenario B a promising option for the novel treatment of DS. Its ability to offer substantial biogas production while minimizing disruptions to current processes positions it as a favourable choice for further consideration and implementation.

5.6.3 Benefits of energy and material valorization of deinking sludges

Figure 5.38 shows an estimate of the potential biogas yield of the raw DS and pre-dewatered DS for Germany based on data from literature and own data (Appendix A.3, Appendix N.4). It can be seen that biogas energy potential in the range of 247 to 328 million MJ per year for raw DS, 146 to 204 million per year for pre-dewatered DS and 167 to 261 million per year for main-dewatered DS can be utilized.

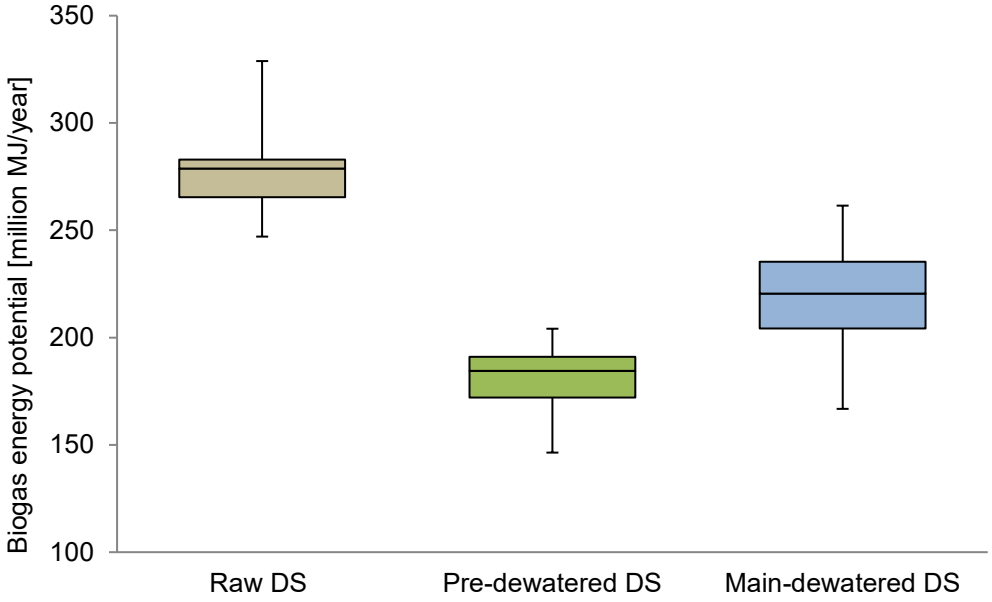

Figure 5.38 Estimates of the biogas energy potential of deinking sludges generated in Germany

Owing to the sustainability structure of pulp and paper mills whereby water recycling is carried out to reduce water consumption significantly, it might be meaningful to consider both water recycling and biogas energy recovery by valorizing the pre-dewatered DS instead of the raw DS. Biogas energy is regarded as CO_2 neutral since it is generated from non-fossil fuel. Therefore the biogas energy possibly generated from DS is a huge contribution to the CO_2 saving goal of the pulp and paper industry in Germany and Europe.

According to the European Biogas Association, renewable energy sources, such as biogas, are anticipated to play a pivotal role in attaining carbon neutrality by 2050, thereby assisting the EU in reducing its reliance on external energy sources (EBA, 2023). Specifically for the wastepaper recycling company, the bioenergy generated can find application in energy demanding process or for the drying and burning of DS-digestate to produce DS-digestate ash which are rich in $CaCO_3$.

The $CaCO_3$ recovery potential from DS was also estimated in a similar way in Figure 5.39. Additionally, the monetary value of $CaCO_3$ as a supplementary buidling material was estimated. The computation was based on the fact that the optimal contribution of DS and DS-ash to compressive strength of test prisms was estimated at 25% of partial substitution of portland cement in test prisms (section 5.5.2.4).

Figure 5.39 shows that all DS types, have a huge amount of $CaCO_3$ present in them. The potentials are skewed due to varying amount $CaCO_3$ in the DS sample collected from wastepaper recycling plant. Since the $CaCO_3$ is not used in the biogas process it is available in the digestate. This implies that after biogas generation from DS the resulting digestate can be dried and used or sold out to be applied as a supplementary building material.

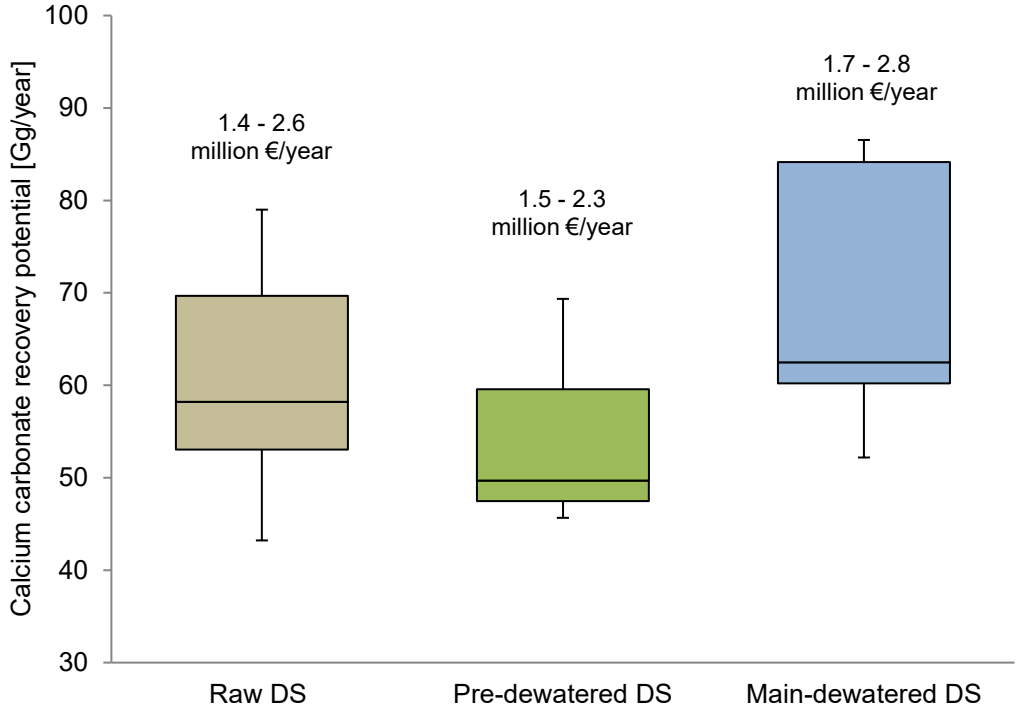

Figure 5.39 Calcium carbonate recovery potentials from deinking sludges generated in Germany

Applying DS generated in the wastepaper recycling process for biogas production is in tandem with the improvement opportunities such as resource efficiency and bioeconomy as identified in the report of EC, 2021 for the EU pulp and paper industry. Also, biogas energy is regarded as CO_2 neutral since it is generated from non-fossil fuel (Audrey, 2018; EBA, 2020).

The EU reported a roadmap with a CO_2 emission goal of up to 80% reduction between the years 1990 and 2050 (EC, 2011). The biogas production from DS treatment is a bold step towards achieving this goal. The utilization of the $CaCO_3$ present in the ash of DS-digestate is also a resource efficiency approach which can further improve the sustainability of the EU wastepaper recycling industry.

5.6.4 Key findings on energy and material valorization of deinking sludges

The following are the key findings for combined energy and material valorization of DS in general and regarding the estimation of the valorization potentials of DS in Germany.

1.) Raw DS has a high biogas energy generation potential related to oDM, but are impaired handling is rather economical to recycle water from it by pre-dewatering.

2.) Pre- dewatered and main-dewatered DS are suitable streams that can be valorized by biogas production without impairing the water recycling scheme in wastepaper recycling facilities similar to that studied. The biogas energy potential can further be impoved by the adjustment of the dewatering unit.

3.) An annual biogas energy generation potential in the range of 146 to 329 million MJ is possible by the application of DS as a biogas feedstock in Germany. This can contributes to the CO_2 saving goals of the German pulp and paper industry or used for the drying and burning process for $CaCO_3$ recovery.

4.) The $CaCO_3$ potential in the range of 43 to 86 Gg/year is possible for DS generated in the wastepaper recycling industry with the amount of 1.4 to 2.8 million euros per year in Germany. They can be utilized as supplemetany building material.

5.) A combined biogas production and recovery of the $CaCO_3$ for DS-digestate is an innovative approach to treating DS under consideration of sustainability. It can further improve resource management in waste paper recycling companies.

CHAPTER 6 CONCLUSIONS AND RECOMMENDATIONS

The results presented in this study showed that DS generated from wastepaper recycling processes can be valorized by the application of combined anaerobic digestion and calcium carbonate recovery. It was established that DS in a conventional DS treatment plant can be grouped based on wastepaper grades and degree of dewatering (streams). The different DS types contain organic matter, but the calcium carbonate fraction has the highest share of their dry matter content. The AD process of DS can be initiated by simply using common inocula such as those from sewage sludge or maize silage.

It was shown that biogas yield in the range of 227 and 417 NL/kg oDM is possible for DS. The different DS types show different biogas yields either due to wastepaper grade or degree of dewatering. High wastepaper grade DS such as those generated for example from wood free, coated, lightly painted and free from wet-strength papers will show the highest biogas yield. The raw DS generated from ordinary wastepaper grades has a higher biogas yield (*W70*: 343 NL /kg oDM) compared to pre-dewatered DS from the same wastepaper (*W70:* 250 NL /kg oDM) due to loss in biodegradable fraction during pre-dewatering. The main-dewatered DS due to its high dry matter content may be considered for dry fermentation. In terms of fresh mass biogas yield, DS falls into the range of 4.1 and 12 NL/kg FM. The average biomethane content determined for DS was of 53% Vol. The water content of about 65% was identified as optimal for the AD of DS. The biodegradability of DS and size of the plant were key factors taken into consideration. When DS has too high water content, dewatering can be applied to DS to attain a suitable WC.

In a semi-continuous AD process, an HRT of 19 days is recommended and corresponds to an average OLR of 1.6 ± 0.42 kg oDM/(m^3·d). It must be ensured that proper mixing of the plant is achieved to avoid settling of inorganics. Also, in a semi-continuous process, a nitrogen limitation may occur in a long run. This can be controlled by adjusting the C/N ratio of the system to a range of 29 and 34 by nitrogen supplementation. A proactive measure to the aforementioned nitrogen limitation condition can be the use of co-substrates that are rich in nitrogen such as urine, grass silage, chicken manure or cattle manure in liquid form. Using the first order kinetics in two steps and the Gompertz model one can effectively model the biogas production of DS.

The models in converse to the time-consuming biomethane potential test (BMP) can help to quickly predict the biogas and biomethane production of different DS types and apply it for AD design purposes.

While the first-order kinetics is most suitable for pre-dewatered DS from ordinary wastepaper grades, the Gompertz model is most suitable for DS generated from medium and high wastepaper grades.

The ash of DS or DS-digestate which is primarily calcium carbonate can be recovered and used as a supplementary building material. It was evident that the calcium carbonate present in DS and DS-digestate has properties that interact with sand, cement and water to contribute to strength. The application can be achieved by partially substituting a fraction of cement in a water-cement-sand mixture with either ash of DS or DS-digestate and use for building purposes. Partial substitution of cement in water-cement-sand mixture by the ash of DS and DS- digestate in the range of 5 to 35% by mass can contribute to strength. 25% cement mass substitution with ash is optimal in terms of contribution to compressive strength. Due to DS and DS-digestate ash showing a significant reduction in flow property of mortar mixture, the choice of percentage partial substitution of cement would depend on the requirement for flow during application. A lower substitution is recommended if a high flow is required while a higher value for applications where flow is not critical.

DS can be valorized by combined energy and material recovery approach. It involves first executing an AD treatment of DS which leads to biogas production and the generation of DS-digestate. This is followed by the recovery of calcium carbonate from DS-digestate by converting it to ash. The energy required for the drying and burning of DS-digestate to produce DS-digestate ash can be used from the biogas energy generated. Although the implementation of this novel concept is feasible, it may be challenging for existing wastepaper recycling plants. This is due to the need to redesign and integrate the new processes into the existing ones. With investment into the AD treatment of DS, substantial energy can be generated that contributes to meeting the high energy demand of the industry. Also, the calcium carbonate recovered from the DS-digestate can be sold as a supplementary building material. The adoption of combined energy and material recovery approaches in the treatment of DS makes a significant contribution to UN sustainability goal 7 (Affordable and clean energy) and goal 12 (Responsible consumption and production) and as well as toward the realization of a circular and bioeconomy.

For further research on optimising the AD of DS, important aspects to consider include pre-treatment and co-digestion with other common substrates. Investigating the co-digestion of DS with organic waste, which is common in the pulp and paper industry, may significant increase biomethane yields. In addition, investigating the feasibility of semi-continuous AD of DS with HRT below 19 days is imperative to determine comparative biogas yields of DS.

Furthermore, it is essential to investigate alternative methods for calcium carbonate recovery from DS or DS-digestate other than incineration. Chemical precipitation of calcium carbonate within wet DS and DS-digestate is a promising option for further investigation. In addition, determining the optimum percentage of cement substitution by DS or DS-digestate ash in mortar for different construction applications requires further investigation.

Practically, the combination of biogas production from DS and subsequent utilisation of the DS-digestate produced as a supplementary building material is a promising treatment method. This may lead to avoidance of high temperature incineration of DS, potentially contributing to cost savings and company revenues. In this regard, it is crucial to perform a cost-benefit analysis to understand the extent of combined biogas production and calcium carbonate utilisation from DS for a wastepaper recycling company.

Regarding the bioreactor used in this study, it is recommended to improve the air-tightness to prevent biogas leakage, which may occur due to agitation caused by recirculation pumps and stirrers during mixing. Modification of the groove on which the O-ring seal sits could be a viable solution. In addition, it is important to address issues such as rapid sedimentation of DS, which leads to rapid settling of the bioreactor contents during the AD process. Optimising the design of bioreactors with recirculation pumps, as illustrated in Appendices O.1 and O.2, warrants consideration for improved efficiency.

CHAPTER 7 SUMMARY

Chapter 1 is the introductory section. The global increase in the consumption of paper and board consumption was discussed. The contribution of wastepaper recycling to the UN sustainable development goal 12 (responsible consumption and production) was noted. The energetic valorization of deinking sludge (DS) was described as possible option to promoting UN sustainability goal 7 (*Affordable and Clean energy*) while the calcium carbonate recovery as means to further advances the UN sustainability goal 12 (*responsible consumption and production)*. The research question of the dissertation was stated as „*Can deinking sludges from wastepaper recycling be valorized energetically and materially ? ".*

Chapter 2 introduces paper as a material used for writing, decoration, sanitary purposes and packaging. The timeline of paper from the usage of papyrus to the discovery of the printing press was highlighted. The paper chain from utilizing of wood and wood related bioresources as input materials for production was discussed. Emphasis was laid on wastepaper recycling as a sustainable paper production approach compared to the usage of virgin paper due to wood, water and energy savings as well as carbondioxide reduction. The wastepaper recycling process was shown to consume a high amount of energy. The recycling steps involved in deinking were explained in detail. Importantly was the generation of DS from deinking operation identified. DS as a type of sludge has been reported as an important waste generated in the European pulp and paper industry.

In chapter 3 the characteristics of DS as obtainable in literature were discussed. It was identified that DS contains a high amount of organic solids and calcium carbonate. The common treatments of DS which are land spreading, landfilling and incineration were noted. Further discussion was made on the current treatment options for pulp and paper residues in Germany which include DS. They include incineration, bricks making and cement industry application. Amongst these options, incineration had a share of about 55%. The concept of anaerobic digestion leading to the production of renewable energy in the form of biogas was introduced. It was noted that anaerobic treatment does not have any application for DS generated in European pulp and paper mills.

However, few recent studies exist that test the suitability of DS as a substrate for biogas production. This was followed by an introduction to the fundamentals of anaerobic digestion which include milieu conditions and operation parameters. Also, a brief overview of kinetic models for anaerobic digestion such as one step-first order kinetics, two step-first order kinetics, modified Gompertz, transfer function and logistic function were given.

Calcium carbonate was introduced as a filler which increases the whiteness of paper. It was noted that reducing the cost of paper production is a major factor influencing the increased usage of calcium carbonate for paper making. Different options for material valorization of DS due to its high calcium carbonate content were identified. Based on the findings in **chapter 3**, the strategy of the dissertation to answer the research question was presented. It considers the flow and transformation of DS starting from the deinking operation. The integration of the anaerobic treatment to produce biogas and the usage of the calcium carbonate was included as well.

In **chapter 4**, the experimental methods of study were introduced. DS investigated were grouped based on wastepaper grades and dewatering stages. Ashes of DS and DS-digestate were also investigated. Basic characterisation methods were carried out and included dry matter, organic dry matter, calcium carbonate, carbon, nitrogen, pH, elemental composition and phases determination. The anaerobic digestion experiments using a 1-L batch test systems and three different automatically fed 100-L system were explained. Experiments with the 1-L batch system were described. They focused on the influences of different inocula, the ash, the wastepaper grades, water content and nitrogen supplementation on the biogas yields. Influence of nitrogen supplementation. The investigations on optimal organic loading rate and hydraulic retention time were carried out with the 100-L test systems.

The methods for sieve analysis, sedimentation and centrifugation of DS and DS-digestate were described. The methods for flow value, density, flexural and compressive strength determination of mortars produced with portland cement and partial substitution of DS or DS-digestate ashes were explained. The statistical methods used for the analysis of results obtained and the method for material flow design was also described.

Chapter 5 is the results and discussion section. It began with the characteristics of DS and derivatives. It was shown that the dry matter content of DS varied largely based on the dewatering stage as obtainable in the wastepaper recycling company. Based on dry matter contents, four DS types were differentiated: very low (>0.4 - 2% FM), low (>2 - 7% FM), medium (>7 - 20% FM) and high (>20% FM). The organic dry matter content of the various DS types varied narrowly between 29 and 33% DM. The different DS groups were compared with other biogas feedstock such as blackwater from vacuum toilets, sewage sludge, greasy water, pig manure, liquid manure and food waste.

The result showed that the various DS types based on dry matter content correspond to the different aforementioned biogas feedstocks. Also, the organic dry matter contents of the various DS types are lower when compared to the biogas feedstocks considered in the same dry matter content category. The organic dry matter contents of the various DS types are however substantial, therefore DS can be considered a potential AD feedstock. Calcium carbonate and ash contents are in the ranges of 47 - 52% DM and 67 - 71% DM respectively for DS and its derivatives. Calcium carbonate which is the main component of DS's dry matter can also be utilized as a supplementary building material.

The results from the 1-L batch tests showed that common inocula such as those from the AD of sewage sludge and maize silage were suitable with DS. Its biogas yield was about half of that of cellulose under similar anaerobic conditions. This was due to the high inorganic fraction of DS. The high calcium carbonate content of DS did not have a negative influence. Regarding wastepaper grades, pre-dewatered DS generated from the mixture of high and medium wastepaper grades showed the highest specific biogas yield (*W90/100*: 417 NL/kg oDM), followed by DS from medium wastepaper grades (*W80*: 275 NL /kg oDM) and those from ordinary wastepaper grades (*W70:* 250 NL /kg oDM) belonging to a similar biogas yield group. Pre-dewatering of DS led to a loss of organic dry matter and thereby to the reduction of biogas yield of DS (fresh *W70*: 343 NL /kg oDM). The average biomethane content of DS was 53 Vol.%. The water content of about 65%, was optimal for biogas production in terms of absolute and specific yields. An optimal C/N ratio of between 29 and 34 was also identified for the AD of DS. Supplementation with nitrogen sources is only necessary when biogas yield reduces as a result of the condition of significant nitrogen depletion, possibly in a long-term period of a semi-continuously operated AD of DS and not in a batch process. The comparison of the biogas yields of different DS types with some common biogas feedstocks showed that their biogas yields are substantial and can be beneficial for the wastepaper recycling company.

The results from the automatically fed 100-L systems, comprising the R1A (bioreactor with a low-capacity recirculation pump and 5° inclined bottom), R1B (bioreactor with a higher recirculation pump and 45° inclined bottom) and R2 (bioreactor with stirrer and 5° inclined bottom) were presented. It was shown that DS settles quickly in bioreactors and requires an efficient mixing mechanism during the AD process. DS biodegradability at HRT of 20 days in R1A was 30% oDM, while R1B and R2 which were operated only at HRT of 19 days were in the range of 16 and 46% oDM in their second feeding phase. The maximum biomethane content observed in the 100-L systems was 59 % Vol. The computation of the calcium carbonate mass balance across bioreactors showed a balance of 72.4, 91.5 and 99.0% respectively for the three bioreactors.

An HRT of 19 days which corresponds to an organic loading rate of 1.4 kg oDM/ (m^3·d) was observed as optimal.

The results from the fitting of five different kinetic models with experimental data of the AD of DS obtained in the 1-L AD test system were presented. The two-step first-order kinetics was the best model for the AD of raw and pre-dewatered DS of type *W70* based on comparison. The modified Gompertz model was the best for the pre-dewatered DS of *W80* and *W90/100* types. Since oDM in the pre-dewatered DS are similar to the main dewatered DS.

The results from the particle sizes determination and settling behaviour of DS and DS-digestate were discussed. It was shown that raw DS had finer particles than the pre-dewatered DS. This is due to the flow of finer particles into the liquid phase during the pre-dewatering step. Furthermore, the DS-digestate from pre-dewatered DS showed finer particles compared to untreated pre-dewatered DS due to the biodegradation of bigger particles. The raw DS settled better than the pre-dewatered DS because of its denser particles. Also, the settling of DS-digestate was improved due to the breakdown of the large fibrous material by AD treatment. The AD process results in a higher share of calcium carbonate in DS-digestate when compared to untreated DS.

The results from the characterisation of DS and DS-digestate ash and the investigation of their suitability as supplementary building materials were presented. The particle size distribution of DS ash was reported as D10 (1.3 µm), D50 (25.1 µm) and D90 (295.0 µm) while that of DS-digestate as D10 (0.92 µm), D50 (10.4 µm) and D90 (222.0 µm). Their particle sizes were identified to be bigger than the D50 and D90 of portland cement. DS-digestate ash had smaller D10 and D50 than fly ash, which is already been used as a supplementary building material. Some elements which are present in portland cement were also found in DS and DS-digestate ashes. The result of phase determination of the ashes showed that calcium carbonate is present in a substantial concentration in the ashes. The flow value test showed that ash of DS and DS-digestate negatively impacts the flow of mortar. However, they contribute to flexural and compressive strength when a fraction of cement in the range of 5 to 35% is substituted.

The results from the investigation of the concept for combined energy and material valorization of DS were presented. The dry matter of flow in a conventional treatment plant of DS was analysed using characteristics data of DS and their derivatives. The visualisation of the mass flow was done using the STAN software. The mass flow of organic and calcium carbonate decreased as it flows through the pre-dewatering unit.

At the output of the main-dewatering unit, the flows increased again due to the collection of other intermediate streams carrying some amount of organics and calcium carbonate. Three scenarios for the application of combined biogas production and calcium carbonate recovery of DS were discussed. The AD feedstocks for the scenarios are raw DS, pre-dewatered DS and main-dewatered DS. The comparison showed that the pre-dewatered DS is the most suitable due to moderate need for redesign to integrate a digester and does not alter the process of the existing water recycling scheme of the conventional DS treament plant considered. The biogas and calcium carbonate potential of DS in the German wastepaper recycling were computed and discussed. The computation of the potentials showed that the combined production of biogas from DS and the utilization of the calcium carbonate in the DS-digestate as a supplementary building material can further improve the sustainability of the wastepaper recycling industry in Europe.

Chapter 6 is the conclusion which summarizes the main results of this thesis and **Chapter 7** contain recommendations and outlook which states further aspects of the investigation of this thesis.

REFERENCES

Abdelgadir, A., Chen, X., Liu, J., Xie, X., Zhang, J., Zhang, K., Wang, H., & Liu, N. (2014). Characteristics, process parameters, and inner components of anaerobic bioreactors. BioMed Research International, 841573. https://doi.org/10.1155/2014/841573

Abubaker, J., Risberg, K., & Pell, M. (2012). Biogas residues as fertilisers – Effects on wheat growth and soil microbial activities. Applied Energy, 99, pp. 126–134. https://doi.org/10.1016/j.apenergy.2012.04.050

Abubakr, S., Smith A., & Scott, G. (1995). Sludge characteristics and disposal alternatives for the pulp and paper industry. In: Proceedings of the 1995 International Environmental Conference, Madison; May 7-10. Pappi Press, pp. 269–279.

AbwV (2022). Abwasserverordnung in der Fassung der Bekanntmachung vom 17. Juni 2004 (BGBl. I S. 1108, 2625), die zuletzt durch Artikel 1 der Verordnung vom 20. Januar 2022 (BGBl. I S. 87) geändert worden ist" (*English translation: Wastewater ordinance in the version published on June 17, 2004 (BGBl. I p. 1108, 2625), which was last amended by Article 1 of the ordinance of January 20, 2022 (BGBl. I p. 87)*). https://www.gesetze-im-internet.de/abwv/BJNR056610997.html[last accessed 25/08/2022].

Ahmed, N. M., Mohamed, M. G., Tammam, R. H., & Mabrouk, M. R. (2018). Performance of coatings containing treated silica fume in the corrosion protection of reinforced concrete. Pigment & Resin Technology, 47(4), pp. 350–359. https://doi.org/10.1108/PRT-08-2017-0076

Ahn, J.-H., Do, T. H., Kim, S. D., & Hwang, S. (2006). The effect of calcium on the anaerobic digestion treating swine wastewater. Biochemical Engineering Journal, 30(1), pp. 33–38. https://doi.org/10.1016/j.bej.2006.01.014

Ait Bouh, H. (2020). X-ray fluorescence technique analysis (Principles and instrumentations). LAP LAMBERT Academic Publishing. ISBN: 978-620-2-78771-0.

Akunna, J. C. (2018). Anaerobic waste-wastewater treatment and biogas plants: A practical handbook. CRC Press. https://doi.org/10.1201/9781351170529

Al Omari, M. M. H., Rashid, I. S., Qinna, N. A., Jaber, A. M., & Badwan, A. A. (2016). Calcium carbonate. Profiles of drug substances, excipients, and related methodology, 41, pp. 31–132. https://doi.org/10.1016/bs.podrm.2015.11.003

Alepu, E. O., Zifu, L., Ikhumhen, H. O., Kalakodio, L., Wang, K., & Segun, G. A. (2016). Effect of hydraulic retention time on anaerobic digestion of Xiao Jiahe municipal sludge. International Journal of Waste Resources, 6(3). https://doi.org/10.4172/2252-5211.1000231

Al-Wahaibi, A., Osman, A. I., Al-Muhtaseb, A. H., Alqaisi, O., Baawain, M., Fawzy, S., & Rooney, D. W. (2020). Techno-economic evaluation of biogas production from food waste via anaerobic digestion. Scientific Reports, 10(1), 15719. https://doi.org/10.1038/s41598-020-72897-5

Amare, D. E., Ogun, M. K., & Körner, I. (2019a). Anaerobic treatment of deinking sludge: Methane production and organic matter degradation. Waste Management, 85, pp. 417–424. https://doi.org/10.1016/j.wasman.2018.12.046

Amare, D. E., Ogun, M. K., & Körner, I. (2019b). Improving methane yields of semi-continuous anaerobic digestion of deinking sludge from wastepaper recycling. Waste and Biomass Valorization, 11(9), pp. 4667-4676. https://doi.org/10.1007/s12649-019-00778-8

Andersen, N. (2007). Enzymatic hydrolysis of cellulose: Experimental and modeling studies [Doctoral dissertation,Technical University of Denmark]. https://backend.orbit.dtu.dk/ws/portalfiles/portal/5466093/Afhandling+A4+format.pdf[last accessed 25/07/2022].

Angelidaki, I., Alves, M., Bolzonella, D., Borzacconi, L., Campos, J. L., Guwy, A. J., Kalyuzhnyi, S., Jenicek, P., & van Lier, J. B. (2009). Defining the biomethane potential (BMP) of solid organic wastes and energy crops: A proposed protocol for batch assays. Water Science and Technology, 59(5), pp. 927–934. https://doi.org/10.2166/wst.2009.040

Anukam, A., Mohammadi, A., Naqvi, M., & Granström, K. (2019). A review of the chemistry of anaerobic digestion: Methods of accelerating and optimizing process efficiency. Processes, 7(8), 504. https://doi.org/10.3390/pr7080504

ARCHEA (n.d.). Gaserträge und Nährstoffgehalte - Abfall (*English translation: Gas yields and nutrient levels - Waste*). https://www.archea-biogas.de/_mediafiles/9-substrate.pdf[last accessed 15/07/2022].

Archer, C. (2004). Cyperus papyrus. National Herbarium, Pretoria. http://pza.sanbi.org/cyperus-papyrus*[last accessed 25/07/2022].

Argiz, C., Reyes, E., & Moragues, A. (2018). Ultrafine portland cement performance. Materiales De Construcción, 68(330), 157. https://doi.org/10.3989/mc.2018.03317

Audrey. (2018). Biogas, an unparalleled ally against climate change. Biogas world (Ed.). https://www.biogasworld.com/news/biogas-climate-change/[last accessed 25/07/2022].

Babaei, A., & Shayegan, J. (2011). Effect of organic loading rates (OLR) on production of methane from anaerobic digestion of vegetables waste: In: Proceedings of the World Renewable Energy Congress - Sweden, May 8-13, Linköping, Sweden, pp. 411–417. https://ep.liu.se/ecp/057/vol1/055/ecp57vol1_055.pdf[last accessed 25/07/2022].

Bajpai, P. (2014a). Black liquor gasification. https://www.sciencedirect.com/book/9780081000090/black-liquor-gasification#book-info*[last accessed 25/07/2022].

Bajpai, P. (2014b). Recycling and deinking of recovered paper. https://www.sciencedirect.com/book/9780124169982/recycling-and-deinking-of-recovered-paper[last accessed 25/07/2022].

Bajpai, P. (2015). Paper machine loops and papermaking. Pulp and paper industry, pp. 13–20. https://doi.org/10.1016/B978-0-12-803409-5.00002-1

Balwaik, A., & Raut, S. P. (2011). Utilization of waste paper pulp by partial replacement of cement in concrete. Engineering Research and Applications, 1(2), pp. 300-309, ISSN: 2248-9622.

Baucke, F. G. K. (2002). New IUPAC (International union of pure and applied chemistry) recommendations on the measurement of pH - background and essentials. Analytical and Bioanalytical Chemistry, 374(5), 772–777. https://doi.org/10.1007/s00216-002-1523-4

Bayr, S., & Rintala, J. (2012). Thermophilic anaerobic digestion of pulp and paper mill primary sludge and co-digestion of primary and secondary sludge. Water Research, 46(15), pp. 4713–4720. https://doi.org/10.1016/j.watres.2012.06.033

Bekiaris, G., Lindedam, J., Peltre, C., Decker, S. R., Turner, G. B., Magid, J., & Bruun, S. (2015). Rapid estimation of sugar release from winter wheat straw during bioethanol production using FTIR-photoacoustic spectroscopy. Biotechnology for Biofuels, 8, 85. https://doi.org/10.1186/s13068-015-0267-2

Berger, H., Shahri, N., & Farghadan, M. (2021). Energy efficiency in the pulp and paper industry : Technical guidelines on energy efficiency in major energy-consuming sectors. Sino-German demonstration project on energy efficiency in Industry, ALLPLAN GmbH. https://www.energypartnership.cn/fileadmin/user_upload/china/media_elements/publications/2021/Technical_Guideline_Energy_Efficiency_Pulp_and_Paper_EN.pdf[last accessed 25/07/2022].

Bergland, W. H., Saldias, Dinamarca, C. A., & Bakke, R. (2015). Temperature effects in anaerobic digestion modeling. In: Proceedings of the 56th conference on simulation and modelling (SIMS 56), Linköping University, Sweden, October 7-9, pp. 261-269, doi:10.3384/ecp15119261.

Bgiraudi. (2016). The printing press during the scientific enlightenment. https://scientificenlightenment4726.wordpress.com/2016/12/09/the-printing-press-during-the-scientific-enlightenment/*[last accessed 28/07/2022].

Bhardwaj, N. K., & Nguyen, K. L. (2005). Charge aspects of hydrogen peroxide bleached de-inked pulps. Colloids and Surfaces a: Physicochemical and Engineering Aspects, 262(1-3), pp. 232–237. https://doi.org/10.1016/j.colsurfa.2005.05.008

Bienert, C., Walz, M., & Hentschke, C. (2015). Co-Vergärung von Papierschlämmen in mechanisch biologischen Anlagen, Phase 1 (Co-Vergärung Papierschlämme): (*English translation: Co-fermentation of paper sludges in mechanically biological plants, phase 1 (co-fermentation of paper sludges)*). PTS FIBER based solutions (Ed.). https://www.dbu.de/OPAC/ab/DBU-Abschlussbericht-AZ-30964.pdf[last accessed 15/07/2022].

Bizley, D. (2022). World cement grinding & milling Q&A. World Cement (Ed.). https://www.worldcement.com/special-reports/18022022/world-cement-grinding-milling-qa/*[last accessed 15/07/2022].

Blanco, A., Negro, C., Fuente, E., & Sánchez, L. M. (2008). Alternative use of deinking sludge as a source of fibers in fiber-cement manufacture. Cellulose Chemistry Technology. 42, pp. 89–95.

Bloom, J. M. (2017). Papermaking: The historical diffusion of an ancient technique. In: H. Jöns, P. Meusburger & M. Heffernan (Eds.), Mobilities of Knowledge. Knowledge and Space, 10. https://doi.org/10.1007/978-3-319-44654-7_3.

Blum, J., Epstein, R., Watts, S., & Thalacker-Mercer, A. (2021). Importance of nutrient availability and metabolism for skeletal muscle regeneration. Frontiers in Physiology, 12, 696018. https://doi.org/10.3389/fphys.2021.696018

Boe, K., & Angelidaki, I. (2009). Serial CSTR digester configuration for improving biogas production from manure. Water Research, 43(1), pp. 166–172. https://doi.org/10.1016/j.watres.2008.09.041

Bousios, S. (2016). Novel biobased products from side streams of paper and board production. European Community's 7th Framework Programme (Grant n° 604187). https://reffibre-valorisation-tool.cepi.org/downloads/novel-biobased-products-from-side-streams-of-paper-and-board-production.pdf[last accessed 26/07/2022].

Bousios, S., & Worrell, E. (2017). Towards a multiple input-multiple output paper mill: Opportunities for alternative raw materials and sidestream valorisation in the paper and board industry. Resources Conservation and Recycling, 125, pp. 218-232.

Briffa, J., Sinagra, E., & Blundell, R. (2020). Heavy metal pollution in the environment and their toxicological effects on humans. Heliyon, 6(9), e04691. https://doi.org/10.1016/j.heliyon.2020.e04691

Bunaciu, A. A., Udriştioiu, E. G., & Aboul-Enein, H. Y. (2015). X-ray diffraction: Instrumentation and applications. Critical Reviews in Analytical Chemistry, 45(4), pp. 289–299. https://doi.org/10.1080/10408347.2014.949616

Caciagli, N. C., & Manning, C. E. (2003). The solubility of calcite in water at 6-16kbar and 500-800C. Contributions to Mineralogy and Petrology, 146(3), pp. 275–285. https://doi.org/10.1007/s00410-003-0501-y

Cantavalle, S. (2019). The history of paper: from its origins to the present day. https://www.pixartprinting.co.uk/blog/history-paper/*[last accessed 03/10/2021].

CEMEX. (n.d.). Preisliste CEMEX Zement: Gültig ab 1.Januar 2020 *(English translation: Price list of CEMEX cement: valid from January 1.2020)*. Retrieved June 28, 2022, from https://www.cemex.de/documents/46167902/0/191125+CEMEX+Zement+Preisliste+%281%29.pdf/12bd4121-d15f-296e-b4bf-ed14b65ef43f[last accessed 28/06/2022].

CEN (2002). European list of standard grades of recovered paper and board. http://www.ciparo.nl/wp-content/uploads/2014/06/European-List-of-Standard-Grade-of-Recovered-Paper-and-Board.pdf[last accessed 15/07/2022].

Cencic, O., & Rechberger, H. (2008). Material flow analysis with software STAN. Journal of Environmental Enginering and Management.18., pp. 3-7.

CEPI (2011). Key statistics 2009: Confederation of European Paper Industries. (Ed.). http://www.cobelpa.be/pdf/Key%20Statistics%202011%20FINAL.pdf[last accessed 27/07/2022].

CEPI (2017). Key statistics 2016: Confederation of European Paper Industries (Ed.). https://www.cepi.org/wp-content/uploads/2021/01/Final-Key-Statistics-2017.pdf[last accessed 27/07/2022].

CEPI (2021a). 19th century emergence of wood based paper and increased mechanisation. Confederation of European Paper Industries (Ed.). https://www.cepi.org/19th-century-emergence-of-wood-based-paper-and-increased-mechanisation/*[last accessed 23/07/2022].

CEPI (2021b). Key statistics 2020: Confederation of European Paper Industries (Ed.). https://www.cepi.org/wp-content/uploads/2021/07/Key-Stats-2020-FINAL.pdf[last accessed 24/07/2022].

Ceron-Vivas, A., Cáceres-Cáceres, K. T., Rincón-Pérez, A., & Cajigas, A. A. (2019). Influence of pH and the C/N ratio on the biogas production of wastewater. Revista Facultad De Ingeniería Universidad De Antioquia(92), 70–79. https://doi.org/10.17533/udea.redin.20190627

Chaffey, D. (2021). Forecast e-commerce growth in percentage of online retail / e-commerce sales 2017 to 2023. Smart Insights. https://www.smartinsights.com/digital-marketing-strategy/online-retail-sales-growth/[last accessed 27/07/2022].

Chan, N., Young-Rojanschi, C., & Li, S. (2018). Effect of water-to-cement ratio and curing method on the strength, shrinkage and slump of the biosand filter concrete body. Water Science and Technology, 77(5-6), pp. 1744–1750. https://doi.org/10.2166/wst.2018.063

Chen, H. (2014). Biotechnology of lignocellulose: Theory and practice. https://doi.org/10.1007/978-94-007-6898-7

Chen, W. L., Chow, C.-J., & Ochiai, Y. (1999). Effects of some food additives on the gel-forming ability and color of milkfish meat paste. Fisheries Science, 65(5), pp. 777–783. https://doi.org/10.2331/fishsci.65.777

Chen, X., Qian, X., & An, X. (2011). Using calcium carbonate whiskers as papermaking filler. BioResources. 6(3), pp. 2435-2447.

Chen, Y., Cheng, J. J., & Creamer, K. S. (2008). Inhibition of anaerobic digestion process: A review. Bioresource Technology, 99(10), pp. 4044–4064. https://doi.org/10.1016/j.biortech.2007.01.057

Cheremisinoff, N. P., & Rosenfeld, P. (2010). Best practices in the wood and paper industries. Oxford, UK: William Andrew. ISBN: 9780080964461.

Chong, S., Sen, T. K., Kayaalp, A., & Ang, H. M. (2012). The performance enhancements of upflow anaerobic sludge blanket (UASB) reactors for domestic sludge treatment--a state-of-the-art review, 46(11), pp. 3434–3470. https://doi.org/10.1016/J.WATRES.2012.03.066

Cioabla, A. E., Ionel, I., Dumitrel, G.-A., & Popescu, F. (2012). Comparative study on factors affecting anaerobic digestion of agricultural vegetal residues. Biotechnology for Biofuels, 5, 39. https://doi.org/10.1186/1754-6834-5-39

Connaughton, S., Collins, G., & O'Flaherty, V. (2006). Psychrophilic and mesophilic anaerobic digestion of brewery effluent: A comparative study. Water Research, 40(13), pp. 2503–2510. https://doi.org/10.1016/j.watres.2006.04.044

Conrad, R., Klose, M., & Noll, M. (2009). Functional and structural response of the methanogenic microbial community in rice field soil to temperature change. Environmental Microbiology, 11(7), pp. 1844–1853. https://doi.org/10.1111/j.1462-2920.2009.01909.x

Coto, B., Martos, C., Peña, J. L., Rodríguez, R., & Pastor, G. (2012). Effects in the solubility of $CaCO_3$: Experimental study and model description. Fluid Phase Equilibria, 324, pp. 1–7. https://doi.org/10.1016/j.fluid.2012.03.020

Cyr, M., & Tagnit-Hamou, A. (2001). Particle size distribution of fine powders by LASER diffraction spectrometry. Case of cementitious materials. Materials and Structures, 34. pp. 342-350.

Damayanti, S. I., Sarto, Astiti, D. F., & Budhijanto, W. (2019). The effectiveness of pH adjustment and controlled oxygen injection to enhance acidogenic performance in two stage anaerobic digestion. In: AIP conference proceedings 20085, 020016. https://doi.org/10.1063/1.5094994.

Deepanraj, B., Sivasubramanian, V., & Jayaraj, S. (2015). Experimental and kinetic study on anaerobic digestion of food waste: The effect of total solids and pH. Journal of Renewable and Sustainable Energy, 7(6), 63104. https://doi.org/10.1063/1.4935559

Deepanraj, B., Sivasubramanian, V., & Jayaraj, S. (2016). Experimental and kinetic study on anaerobic co-digestion of poultry manure and food waste. Desalination and Water Treatment, 59, pp. 72–76. https://doi.org/10.5004/dwt.2016.0162

Deepenraj B., Sivasubramanian, V., & Jayaraj, S. (2014). Biogas generation through anaerobic digestion process - An overview. Research Journal of Chemistry and Environment. 18(5), pp. 80-94.

Demirel, B., & Yenigün, O. (2002). Two-phase anaerobic digestion processes: a review. Journal of Chemical Technology & Biotechnology, 77(7), pp. 743–755. https://doi.org/10.1002/jctb.630

Deviatkin, I., Kujala, A., & Horttanainen, M. (2015). Deinking sludge utilization possibilities: technical, economic and environmental assessments: Report on responsibilities of LUT energy. In: EMIR Project 2012- 2014. Lappeenranta University of Technology; School of energy systems. https://lutpub.lut.fi/bitstream/handle/10024/104853/EMIR%20Final%20report.pdf?sequence=2*[last accessed 27/07/2022].

Diamantis, V. I., Vaiopoulou, E., & Aivasidis, A. (2007). Fundamentals and applications of anaerobic digestion for sustainable treatment of food industry wastewater. In: V. Oreopoulo & W. Russ (Eds), Utilization of by-products and treatment of waste in the food industry, 3, pp. 73–97. https://doi.org/10.1007/978-0-387-35766-9_5

Dickson, N., Richard, T., & Kozlowski, R. (1991). Composting to reduce the waste stream - A guide to small scale food and yard waste composting. https://ecommons.cornell.edu/handle/1813/44736*[last accessed 28/07/2022].

DIN EN 1015-3: 2007-05 (2007). Methods of testing for mortar for masonry-part 3: Determination of consistence of fresh mortar by flow table (DIN). Beuth-Verlag, Berlin.

DIN EN 12879:2001-02 (2001). Characterization of sludges-Determination of the loss on ignition of dry mass (DIN). Beuth-Verlag, Berlin.

DIN EN 12880: 2001-02 (2001). Characterization of sludges-Determination of dry residue and water content. Beuth-Verlag, Berlin.

DIN EN 196-1: 2016-11 (2016). Methods of testing cement: Determination of strength. Beuth-Verlag, Berlin.

Doelle, K., & Amaya, J. J. (2012). Application of calcium carbonate for uncoated digital printing paper from 100% eucalyptus pulp. TAPPI Journal, 11(1), pp. 51–59. https://doi.org/10.32964/TJ11.1.51

Dong, C., Song, D., Patterson, T., Ragauskas, A., & Deng, Y. (2008). Energy saving in papermaking through filler addition. Industrial & Engineering Chemistry Research, 47(21), pp. 8430–8435. https://doi.org/10.1021/ie8011159

Dong, J., Jeswani, H. K., Nzihou, A., & Azapagic, A. (2020). The environmental cost of recovering energy from municipal solid waste. Applied Energy, 267, 114792. https://doi.org/10.1016/j.apenergy.2020.114792

Donoso-Bravo, A., Pérez-Elvira, S. I., & Fdz-Polanco, F. (2010). Application of simplified models for anaerobic biodegradability tests. Evaluation of pre-treatment processes. Chemical Engineering Journal, 160(2), pp. 607–614. https://doi.org/10.1016/j.cej.2010.03.082

Duangmanee, T., Kumar, S., & Sung, S. (2007). Micro-aeration for sulfide removal in aerobic treatment of high solid wastewater: A pilot-scale study. Proceedings of the Water Environment Federation, 2007(16), pp. 2748–2760. https://doi.org/10.2175/193864707787960152

Durand, B., & Pesaresi, E. (2007). Empirical estimation of a discrete choice model for filler calcium carbonates in the paper industry. Competition Policy Newsletter. https://ec.europa.eu/competition/publications/cpn/2007_1_92.pdf[last accessed 13/11/2021].

Durmaz, S., Erisir, E., Yildiz, U. C., & Kurtulus, O. C. (2015). Using kraft black liquor as a wood preservative. Procedia - Social and Behavioral Sciences, 195, pp. 2177–2180. https://doi.org/10.1016/j.sbspro.2015.06.291

Dyckerhoff. (n.d.). *Preisliste: Siloware-Grauzement/Bindemittel (English Translation: Price list: siloware gray cements/binders)*. Retrieved June 28, 2022, from https://www.dyckerhoff.com/documents/209745/0/Preisliste+Siloware+-+Grauzement++Bindemittel.pdf/8e549700-26aa-abe3-3ff6-51fefa9e074c[last accessed 28/08/2022].

EBA (2020). The contribution of the biogas and biomethane industries to medium-term greenhouse gas reduction targets and climate-neutrality by 2050. European Biogas Association. https://www.europeanbiogas.eu/wp-content/uploads/2020/04/20200419-Background-paper_final.pdf[last accessed 26/07/2022].

EBA (2023). About biogas and biomethane. European Biogas Association. https://www.europeanbiogas.eu/about-biogas-and-biomethane/*[last accessed 31/12/2023].

EC (2011). A Roadmap for moving to a competitive low carbon economy in 2050 [European Parliament the council the european economic and social committe and the committee on the regions]. https://eur-lex.europa.eu/LexUriServ/LexUriServ.do?uri=COM:2011:0112:FIN:en:PDF[last accessed 19/10/2021].

EC (2021). Pulp and paper industry: Internal Market, Industry Entrepreneurship and SMEs. https://ec.europa.eu/growth/sectors/raw-materials/related-industries/forest-based-industries/pulp-and-paper-industry_en*[last accessed 14/06/2021].

Ekstrand, E. (2019). Anaerobic digestion in the kraft pulp and paper industry: Challenges and possibilities for implementation. In: Linköping Studies in Arts and Sciences No. 769. http://liu.diva-portal.org/smash/get/diva2:1313936/FULLTEXT01.pdf[last accessed 24/09/2021].

Elakneswaran, Y., Noguchi, N., Matumoto, K., Morinaga, Y., Chabayashi, T., Kato, H., & Nawa, T. (2019). Characteristics of ferrite-rich portland cement: Comparison with ordinary portland cement. Frontiers in Materials, 6, Article 97. https://doi.org/10.3389/fmats.2019.00097

Elamin, A. E. M., & Gasmelseed, G. A. (2018). Biogas production from tannery liquid waste. European Journal of Engineering Research and Science, 3(10), pp. 117–119. https://doi.org/10.24018/ejers.2018.3.10.912

Elliott, A., & Mahmood, T. (2005). Survey benchmarks generation, management of solids residues. Pulp Pap. 79 (12), pp. 49–55.

Elliott, A., & Mahmood, T. (2006). Beneficial uses of pulp and paper power boiler ash residues. TAPPI J. 5(10), pp. 9–16.

Engwa, G. A., Ferdinand, P. U., Nwalo, F. N., & Unachukwu, M. (2019). Mechanism and health effects of heavy metal toxicity in humans. In Karcioglu, O.; Arslan, B.(Eds.), Poisoning in the Modern World-New tricks for an old dog? Medical Toxicology,5, https://doi.org/10.5772/intechopen.82511.

EPRC (2017). European declaration on paper recycling 2016-2020. European Paper Recycling Council. https://www.paperforrecycling.eu/publications/*[last accessed 23/07/2022].

Erdogan, N., & Eken, H. A. (2017). Precipitated calcium carbonate production, synthesis and properties. Physicochemical Problems of Mineral Processing, 53. pp 57-68. https://doi.org/10.5277/ppmp170105.

EuPIA (2020). EuPIA guideline on printing inks applied to food contact materials. https://www.eupia.org/fileadmin/Documents/Food_contact_material/2020-12-22_EuPIA_Guideline_on_Printing_Inks_applied_to_Food_Contact_Materials.pdf[last accessed 15/07/2022].

Ezebuiro, N. C. (2014). Optimization of anaerobic digestion: Influence of trace elements on methanization processes [Doctoral dissertation, Hamburg University of Technology]. https://doi.org/10.15480/882.3926

Fabozzi, F. J., Focardi, S. M., Rachev, S. T., & Arshanapalli, B. G. (2014). The basics of financial econometrics. https://doi.org/10.1002/9781118856406

Favier, A., DeWolf, C., Scrivener, K., & Habert, G. (2018). A sustainable future for the European cement and concrete industry: Technology assessment for full decarbonisation of the industry by 2050. Swiss Federal Institute of Technology (ETHZ), Zürich, Switzerland. https://europeanclimate.org/wp-content/uploads/2018/10/AB_SP_Decarbonisation_report.pdf[last accessed 25/07/2022].

Feist, M., Nirschl, H., Wagner, J., Hirsch, G., & Schabel, S. (2007). Experimental results for the settling behaviour of particle-fiber mixtures. Physical Separation in Science and Engineering, pp. 1–6. https://doi.org/10.1155/2007/91740

Felchner-Zwirello, M. (2014). Propionic acid degradation by syntrophic bacteria during anaerobic biowaste digestion. Karlsruhe Institute of Technology. https://doi.org/10.5445/KSP/1000037825

Feng, L., Gao, Y., Kou, W., Lang, X., Liu, Y., Li, R., Yu, M., Shao, L., & Wang, X. (2017). Application of the initial rate method in anaerobic digestion of kitchen waste. BioMed Research International, 3808521. https://doi.org/10.1155/2017/3808521

Fierro, A., Norrie, J., Gosselin, A., & Beauchamp, C. J. (1997). Deinking sludge influences biomass, nitrogen and phosphorus status of several grass and legume species. Canadian Journal of Soil Science, 77(4), pp. 693–702. https://doi.org/10.4141/S96-114

Fišerová, M., Opálená, E., Gigac, J., & Stankovská, M. (2018). Oxidative and reduction bleaching of deinked pulp. Wood Research, 63(4), pp. 639-954 http://www.woodresearch.sk/wr/201804/10.pdf[last accessed 15/08/2022].

Fisgativa, H., Tremier, A., & Dabert, P. (2016). Characterizing the variability of food waste quality: A need for efficient valorisation through anaerobic digestion. Waste Management, 50, pp. 264–274. https://doi.org/10.1016/j.wasman.2016.01.041

Frias, M., Vegas, I., La Villa, R. V. de, & Garcia, R. Recycling of waste paper sludge in cements: Characterization and behavior of new eco-efficient matrices. In: S. Kumar (Ed.), Integrated Waste Management, Volume II. IntechOpen https://doi.org/10.5772/20850.

Fricker, A., Thompson, R., & Manning, A. (2007). Novel solutions to new problems in paper deinking. Pigment & Resin Technology, 36(3), pp. 141–152. https://doi.org/10.1108/03699420710749009

Friehe, J., Schattauer, A., & Weiland, P. (2016a). Beschreibung ausgewählter Substrate (*English translation: Description of selected substrates*). In: FNR (Ed.), Leitfaden Biogas von der Gewinnung zur Nutzung. pp. 68-76. Fachagentur Nachwachsende Rohstoffe. ISBN: 3-00-014333-5.

Friehe, J., Schattauer, A., & Weiland, P. (2016b). Grundlagen der anaeroben Fermentation (*English translation: Basics of anaerobic fermentation*). In: FNR (Ed.), Leitfaden biogas von der Gewinnung zur Nutzung. pp. 11-20. Fachagentur Nachwachsende Rohstoffe. ISBN: 3-00-014333-5.

Gaber, M. W. (2018). Characterizations of El Minia limestone for manufacturing paper filler and coating. Egyptian Journal of Petroleum, 27(4), pp. 437–443. https://doi.org/10.1016/j.ejpe.2017.07.007

García, R., La Vigil de Villa, R., Vegas, I., Frías, M., & Sánchez de Rojas, M. I. (2008). The pozzolanic properties of paper sludge waste. Construction and Building Materials, 22(7), pp. 1484–1490. https://doi.org/10.1016/j.conbuildmat.2007.03.033

Gaur, R., Mishra, L., & Sen Gupta, S. K. (2014). Diffusion and transport of molecules in living cells. In: S. K. Basu & N. Kumar (Eds.), Modelling and simulation of diffusive processes, pp. 27–49. https://doi.org/10.1007/978-3-319-05657-9_2

Gavala, H. N., Angelidaki, I. & Ahring, B. K. (2003). Kinetics and modeling of anaerobic digestion process. Advances in Biochemical Engineering/biotechnology, 81, pp. 57–93. https://doi.org/10.1007/3-540-45839-5_3

Genç, Ö. (2016). Energy-efficient technologies in cement grinding. In: S. Yilmaz & H.B. Ozmen (Eds.), High performance concrete technology and applications. IntechOpen https://doi.org/10.5772/64427.

Gerardi, M. H. (2003). The microbiology of anaerobic digesters. Wastewater Microbiology Series., https://doi.org/10.1002/0471468967.

Gilbert, C., Ayanda, O. S., Fatoba, O. O., Madzivire, G., & Petrik, L. F. (2019). A novel method of using iron nanoparticles from coal fly ash or ferric chloride for acid mine drainage remediation. Mine Water and the Environment, 38(3), pp. 617–631. https://doi.org/10.1007/s10230-019-00605-5

Gonzalez, J. M., & Stres, B. (2019). Trace element enzymes in reactions essential for anaerobic digestion. In: F.G. Fermoso, E. Van Hullebusch, G. Collins, J. Roussel, A.P. Mucha & G. Esposito (Eds.), Trace Elements in Anaerobic Biotechnologies: pp. 51–72. https://doi.org/10.2166/9781789060225_0051.

González, C., Alvarez, R., & Coca, J. (1992). Use of kraft black liquors from a pulp mill for the production of soil conditioners. Waste Management & Research: The journal for a sustainable circular economy, 10(2), pp. 195–201. https://doi.org/10.1177/0734242X9201000207

Göttsching, L., Pakarinen, H., Gullichsen, J., & Paulapuro, H. (2000). Recycled fiber and deinking. In: O Fapet (Ed.), Papermaking science and technology. ISBN: 9525216071.

Guyot, J. P., & Brauman, A. (1986). Methane production from formate by syntrophic association of methanobacterium bryantii and desulfovibrio vulgaris JJ. Applied and Environmental Microbiology, 52(6), pp. 1436–1437. https://doi.org/10.1128/aem.52.6.1436-1437.1986

Habert, G. (2013). Environmental impact of portland cement production. In: F. Pacehco-Torgal, S. Jalali, J. Labrincha & V.M. John (Eds.), Eco-Efficient Concrete. https://doi.org/10.1533/9780857098993.1.3. https://sr.b-ok.cc/book/2075949/5bf35a?dsource=recommend. [last accessed 15/08/2022].

Hamelin, M., Jokerinne, E., & Gooding, R. (2014). Fundamental advances in pulp screening technology. In: 41st International meeting of Slovene paper industry, November 19-20, https://www.gzs.si/Portals/183/vsebine/dokumenti/2014/17_Fundamental_Advances_In_Pulp_Screening_Technology-R.Gooding_Aikawa_Ft.pdf[last accessed 29/07/2022].

Han, J. S., Jung, S. Y., Kang, D. S., & Seo, Y. B. (2020). Development of flexible calcium carbonate for papermaking filler. ACS Sustainable Chemistry & Engineering, 8(24), pp. 8994–9001. https://doi.org/10.1021/acssuschemeng.0c01593

Hansen, M. B., Johansen, J. D., & Menné, T. (2003). Chromium allergy: Significance of both Cr(III) and Cr(VI). Contact Dermatitis, 49(4), pp. 206–212. https://doi.org/10.1111/j.0105-1873.2003.0230.x

Harju, L., Lill, J.-O., Saarela, K.-E., Heselius, S.-J., Hernberg, F. J., & Lindroos, A. (1997). Analysis of trace elements in trunk wood by thick-target PIXE using dry ashing for preconcentration. Fresenius' Journal of Analytical Chemistry, 358(4), pp. 523–528. https://doi.org/10.1007/s002160050459

Hart, P. W., Colson, G., & Burris, J. (2012). Application of carbon dioxide to reduce water side lime scale in heat exchanges. Pulp and Paper Canada 1(2), pp. 67-70.

He, F., Yang, F., Zhu, J., Peng, Y., Tian, X., & Chen, X. (2015). Fabrication of a novel calcium carbonate composite ceramic as bone substitute. Journal of the American Ceramic Society, 98(1), pp. 223–228. https://doi.org/10.1111/jace.13285

Hedberg, Y. S., Gumulka, M., Lind, M.-L., Matura, M., & Lidén, C. (2014). Severe occupational chromium allergy despite cement legislation. Contact Dermatitis, 70(5), pp. 321–323. https://doi.org/10.1111/cod.12203

Helmuth, R. A., Miller, F. M., Greening, N. R., Hognestad, E., Kosmatka, S. H., & Lang, D. (2000). Cement. In Kirk-Othmer Encyclopedia of Chemical Technology. John Wiley & Sons, Inc. https://doi.org/10.1002/0471238961.0305130508051213.a01

Hemmerich, W. (2018). StatistikGuru: Normalverteilung online prüfen. (*English translation: StatistikGuru: Check for normal distribution online*). https://statistikguru.de/rechner/normalverteilung-rechner.html[last accessed 27/07/2022].

Hertel, S., Navarro, P., Deegener, S., & Körner, I. (2015). Biogas and nutrients from blackwater, lawn cuttings and grease trap residues-experiments for Hamburg's Jenfelder Au district. Energy, Sustainability and Society, 5(1). https://doi.org/10.1186/s13705-015-0057-5

History. (2019). Printing press. https://www.history.com/topics/inventions/printing-press*[last accessed 05/08/2021].

History of Paper. (2021). Timeline of paper and papermaking. http://www.historyofpaper.net/paper-history/timeline-of-paper/*[last accessed 03/02/2021].

Hofmeister, A. M., & Bowey, J. E. (2006). Quantitative infrared spectra of hydrosilicates and related minerals. Monthly notices of the Royal Astronomical Society, 367(2), pp. 577–591. https://doi.org/10.1111/j.1365-2966.2006.09894.x

Holik, H. (2006). Handbook of paper and board., Wiley-VCH, 978-3-527-30997-9, https://doi.org/10.1002/3527608257.

Holmes, D. E., & Smith, J. A. (2016). Biologically produced methane as a renewable energy source. Advances in Applied Microbiology, 97, pp. 1–61. https://doi.org/10.1016/bs.aambs.2016.09.001

Hotza, D., & Maia, B. (2015). Environmental performance and energy assessment of fired-clay brick masonry. In: F. Pacheco-Torgal, P.B. Lourenço, J. Labrincha, P. Chindaprasirt & S. Kumar (Eds.), Eco-efficient masonry bricks and blocks, pp. 447–459. https://doi.org/10.1016/B978-1-78242-305-8.00020-6

Hubbe, M. A., & Gill, R. A. (2016). Fillers for papermaking: A review of their properties, usage practices, and their mechanistic role. BioResources, 11(1), pp. 2886-2963. https://doi.org/10.15376/biores.11.1.2886-2963

Hubbe, M. A., Metts, J. R., Hermosilla, D., Blanco, M. A., Yerushalmi, L., Haghighat, F., Lindholm-Lehto, P., Khodaparast, Z., Kamali, M., & Elliott, A. (2016). Wastewater treatment and reclamation: A review of pulp and paper industry practices and opportunities. BioResources, 11(3), pp. 7953–8091. https://doi.org/10.15376/biores.11.3.Hubbe

IRENA (2018). Biogas for road vehicles: Technology brief. https://www.irena.org/publications/2017/Mar/Biogas-for-road-vehicles-Technology-brief[last accessed 28/07/2022].

IWS (2021). Internet growth statistics: Today's road to e-commerce and global trade Internet technology reports. Internet Word Stats. https://www.internetworldstats.com/emarketing.htm*[last accessed 28/07/2022].

Jackson-Moss, C. A., Duncan, J. R., & Cooper, D. R. (1989). The effect of calcium on anaerobic digestion. Biotechnology Letters, 11(3), pp. 219–224. https://doi.org/10.1007/BF01026064

Jagadabhi, P. S., Kaparaju, P., & Rintala, J. (2010). Effect of micro-aeration and leachate replacement on COD solubilization and VFA production during mono-digestion of grass-silage in one-stage leach-bed reactors. Bioresource Technology, 101(8), pp. 2818–2824. https://doi.org/10.1016/j.biortech.2009.10.083

Jiang, C., & Ma, J. (2000). Deinking of wastepaper: Flotation. Enzymatic Deinking Technologies, 1-2, pp. 2537-2544.

Johansen, J.-E., & Bakke, R. (2006). Enhancing hydrolysis with microaeration. Water Science and Technology, 53(8), pp. 43–50. https://doi.org/10.2166/wst.2006.234

John, S., Murugesan, M., & Sudheer, K. S. (2007). Alkaline and neutral sizing: Latest trends and selection of specialty chemicals to make fine quality paper cost effectively. https://ippta.co/wp-content/uploads/2021/01/2007_Issue_4_IPPTA_Articel_09.pdf[last accessed 28/07/2022].

Jung, H., Kappen, J., Hesse, A., & Götz, B. (2014). Rückstandsumfrage 2013 – Aufkommen und Verbleib der Rückstände aus der Zellstoff- und Papierindustrie. (*English translation: Residue survey 2013 - Generation and fate of residues from the pulp and paper industry*). Wochenblatt Für Papierfabrikation, pp. 628-630.

Jung, H., & Pauly, D. (2011). Water in the pulp and paper industry. In: P. Wilderer (Ed.),Treatise on Water Science, pp. 667–683. https://doi.org/10.1016/B978-0-444-53199-5.00100-7

Kakali, G., Tsivilis, S., Aggeli, E., & Bati, M. (2000). Hydration products of C_3A, C_3S and portland cement in the presence of $CaCO_3$. Cement and Concrete Research, 30(7), pp. 1073–1077. https://doi.org/10.1016/S0008-8846(00)00292-1

Kamusoko, R., Jingura, R. M., Chikwambi, Z., & Parawira, W. (2022). Biogas: microbiological research to enhance efficiency and regulation. In: S. Sahay (Ed.), Handbook of biofuels, pp. 485–497. https://doi.org/10.1016/B978-0-12-822810-4.00025-7

Kariyama, I. D., Zhai, X., & Wu, B. (2018). Influence of mixing on anaerobic digestion efficiency in stirred tank digesters: A review. Water Research, 143, pp. 503–517. https://doi.org/10.1016/j.watres.2018.06.065

Karlsson, A., Truong, X.-B., Gustavsson, J., Svensson, B. H., Nilsson, F., & Ejlertsson, J. (2011). Anaerobic treatment of activated sludge from swedish pulp and paper mills--biogas production potential and limitations. Environmental Technology, 32(13-14), pp. 1559–1571. https://doi.org/10.1080/09593330.2010.543932

Kashyap, D., Dadhich, K., & Sharma, S. (2003). Biomethanation under psychrophilic conditions: a review. Bioresource Technology, 87(2), pp. 147–153. https://doi.org/10.1016/S0960-8524(02)00205-5

Khanal, S. K. (2008). Anaerobic biotechnology for bioenergy production: Principles and applications. https://doi.org/10.1002/9780813804545

Khanna, Y. P., & Xanthos, M. (2010). Calcium carbonate. In: M. Xanthos (Ed.), Functional fillers for plastics. pp. 291–306. https://doi.org/10.1002/9783527629848.ch16.

Kim, S., Chen, J., Cheng, T., Gindulyte, A., He, J., He, S., Li, Q., Shoemaker, B. A., Thiessen, P. A., Yu, B., Zaslavsky, L., Zhang, J., & Bolton, E. E. (2019). Pubchem 2019 update: Improved access to chemical data. Nucleic Acids Research, 47(D1), pp. D1102-D1109. https://doi.org/10.1093/nar/gky1033

Kobayashi, H., Kaiki, H., Shrotri, A., Techikawara, K., & Fukuoka, A. (2016). Hydrolysis of woody biomass by a biomass-derived reusable heterogeneous catalyst. Chemical Science, 7(1), pp. 692–696. https://doi.org/10.1039/C5SC03377B

Körner, I. (2015). Civilization biorefineries: Efficient utilization of residue based bioresources. In: A. Pandey, R. Höfer, M. Taherzadeh, K.M. Nampoothiri & C. Larrcohe (Eds.), Industrial biorefineries and white biotechnology, pp. 295-340. https://doi.org/10.1016/B978-0-444-63453-5.00009-4.

Koutsoukos, P. G., & Kontoyannis, C. G. (1984). Precipitation of calcium carbonate in aqueous solutions. Journal of the Chemical Society, Faraday Transactions 1: Physical Chemistry in Condensed Phases, 80(5), 1181. https://doi.org/10.1039/F19848001181

Krigstin, S., & Sain, M. (2006). Characterization and potential utilization of recycled paper mill sludge. Pulp and Paper Canada, 107(5), pp 29-32.

Kujala, A. (2012). Papermaking sludges and possibilities of utilization as material. Lappeenranta University of Technology (BH10A0300). https://lutpub.lut.fi/handle/10024/73980?show=full[last accessed 28/07/2022].

Kusch-Brandt, S., & Oechsner, H. (2005). Dry fermentation - An overview. In: VDI Wissensforum (Ed.), Biogas - Energieträger der Zukunft. VDI-Berichte 1872. pp. 165-180.

Kythreotou, N., Florides, G., & Tassou, S. A. (2014). A review of simple to scientific models for anaerobic digestion. Renewable Energy, 71, pp. 701–714. https://doi.org/10.1016/j.renene.2014.05.055

Laurijssen, J. (2013). Energy use in the paper industry: An assessment of improvement potentials at different levels [Doctoral dissertation, Utrecht University, Netherland]. ISBN: 978-90-8672-055-2.

Lehtinen, E. (2000). Papermaking science and technology: Book 11, Pigment coating and surface sizing of paper. (Ed.), Fapet, ISBN 10: 952521611X.

Leschine, S. B. (1995). Cellulose degradation in anaerobic environments. Annual Review of Microbiology, 49(1), pp. 399–426. https://doi.org/10.1146/annurev.mi.49.100195.002151

Levlin, J.-E., Read, B., Grossmann, H., Hooimeijer, A., Ervasti, I., Lozo, B., Julien Saint Amand, F., Cochaux, A., Faul, A., Ringman, J., Stawicki, B., Bobu, E., Miranda, R., Blanco, A., & Stanic, M. (2010). The future of paper recycling in europe: Opportunities and limitations: Action: E48. The Paper Industry Technical Association (PITA). https://www.cost.eu/uploads/2018/07/53628.pdf[last accessed 28/07/2022].

Li, D., Huang, X., Wang, Q., Yuan, Y., Yan, Z., Li, Z., Huang, Y., & Liu, X. (2016). Kinetics of methane production and hydrolysis in anaerobic digestion of corn stover. Energy, 102, pp. 1–9. https://doi.org/10.1016/j.energy.2016.02.074

Li, H.-M., Zhang, N., Guo, X., Dou, M.-Y., Feng, Q., Zou, S., & Huang, F.-C. (2020). Summary of flue gas purification and treatment technology for domestic waste incineration. IOP Conference Series: Earth Environmental Science, 508(1), 12016. https://doi.org/10.1088/1755-1315/508/1/012016

Lili, M., Biró G., Sulyok, E., Petis, M., Borbély J., & Tamás, J. (2011). Novel approach on the basis of FOS/TAC method. In: International symposium ”Risk factors for environment and food safety” & ”natural resources and sustainable development” & ”50 years of agriculture research in Oradea”, November 4-5, XVII, pp. 802-807,. http://protmed.uoradea.ro/facultate/anale/protectia_mediului/2011B/im/15.%20Mezes%20Lili.pdf[last accessed 28/07/2022].

Lin, Y., Lü, F., Shao, L., & He, P. (2013). Influence of bicarbonate buffer on the methanogenetic pathway during thermophilic anaerobic digestion. Bioresource Technology, 137, pp. 245–253. https://doi.org/10.1016/j.biortech.2013.03.093

Lindmark, J., Thorin, E., Bel Fdhila, R., & Dahlquist, E. (2014). Effects of mixing on the result of anaerobic digestion: Review. Renewable and Sustainable Energy Reviews, 40, pp. 1030–1047. https://doi.org/10.1016/j.rser.2014.07.182

Liu, Z., Yin, H., Lin, Z., & Dang, Z. (2018). Sulfate-reducing bacteria in anaerobic bioprocesses: basic properties of pure isolates, molecular quantification, and controlling strategies. Environmental Technology Reviews, 7(1), pp. 46–72. https://doi.org/10.1080/21622515.2018.1437783

Loferer-Krössbacher, M., Klima, J., & Psenner, R. (1998). Determination of bacterial cell dry mass by transmission electron microscopy and densitometric image analysis. Applied and Environmental Microbiology, 64(2), pp. 688–694. https://doi.org/10.1128/AEM.64.2.688-694.1998

Luna-delRisco, M., Normak, A., & Orupõld, K. (2011). Biochemical methane potential of different organic wastes and energy crops from Estonia. Agronomy Research, 9, pp. 331-342.

Lynd, L. R., Weimer, P. J., van Zyl, W. H., & Pretorius, I. S. (2002). Microbial cellulose utilization: Fundamentals and biotechnology. Microbiology and Molecular Biology Reviews, 66(3), pp. 506–577. https://doi.org/10.1128/MMBR.66.3.506-577.2002

Malina, J. F., & Pohland, F. G. (1992). Design of anaerobic processes for treatment of industrial and municipal waste. Water Quality Management Library, Volume VII, ISBN: 978-0877629429.

Malvern. (2013). Mastersizer 3000: User manual, MANO474 Issue 2.1, Malvern Instruments Ltd. https://www.montana.edu/eal-lres/documents/Mastersizer-3000-user-manual-English-MAN0474-2-1.pdf[last accessed 26/07/2022].

Marjolaine. (2021). State-of -the -art dry and wet anaerobic digestion systems for solid waste. biogas World. https://www.biogasworld.com/news/dry-wet-anaerobic-digestion-systems/*[last accessed 28/07/2022].

Mark, J. J. (2016). Egyptian papyrus. https://www.worldhistory.org/Egyptian_Papyrus/*[last accessed 29/07/2022].

Martin, A. R., Erickson, D. L., Kress, W. J., & Thomas, S. C. (2014). Wood nitrogen concentrations in tropical trees: Phylogenetic patterns and ecological correlates. The New Phytologist, 204(3), pp. 484–495. https://doi.org/10.1111/nph.12943

Martius, C. (1992). Density, humidity, and nitrogen content of dominant wood species of floodplain forests (várzea) in Amazonia. Holz Als Roh- und Werkstoff, 50(7-8), pp. 300–303. https://doi.org/10.1007/BF02615357

Mayeli, N., & Talaeipour, M. (2015). Influence of hydrophile–lipophile balance and sodium tripolyphosphate on the properties of biological deinked pulps. International Journal of Environmental Science and Technology, 12(11), pp. 3587–3596. https://doi.org/10.1007/s13762-015-0794-1

McCabe, B. K., Hamawand, I., Harris, P., Baillie, C., & Yusaf, T. (2014). A case study for biogas generation from covered anaerobic ponds treating abattoir wastewater: Investigation of pond performance and potential biogas production. Applied Energy, 114, pp. 798–808. https://doi.org/10.1016/j.apenergy.2013.10.020

McCue, T. J. (2018). E learning climbing to $325 billion by 2025 UF canvas absorb schoology moodle. https://www.forbes.com/sites/tjmccue/2018/07/31/e-learning-climbing-to-325-billion-by-2025-uf-canvas-absorb-schoology-moodle/?sh=7a7929353b39*[last accessed 28/07/2022].

Mckinney R. (1995). Technology of paper recycling. Chapman and Hall, (Ed.), Springer. London ISBN: 978-94-010-4578-0.

Merlino, G., Rizzi, A., Schievano, A., Tenca, A., Scaglia, B., Oberti, R., Adani, F., & Daffonchio, D. (2013). Microbial community structure and dynamics in two-stage vs single-stage thermophilic anaerobic digestion of mixed swine slurry and market bio-waste. Water Research, 47(6), pp. 1983–1995. https://doi.org/10.1016/j.watres.2013.01.007

Meyer, T., & Edwards, E. A. (2014). Anaerobic digestion of pulp and paper mill wastewater and sludge. Water Research, 65, pp. 321–349. https://doi.org/10.1016/j.watres.2014.07.022

Michael, J. D., & Downs, T. A. (1996). Alkaline sizing applications surge ahead. https://cool.culturalheritage.org/byorg/abbey/ap/ap09/ap09-3/ap09-306.html[last accessed 29/07/2022].

Michas, A., Harir, M., Lucio, M., Vestergaard, G., Himmelberg, A., Schmitt-Kopplin, P., Lueders, T., Hatzinikolaou, D. G., Schöler, A., Rabus, R., & Schloter, M. (2020). Sulfate alters the competition among microbiome members of sediments chronically exposed to asphalt. Frontiers in Microbiology, 11, 556793. https://doi.org/10.3389/fmicb.2020.556793

Monchau, F., Hivart, P., Genestie, B., Chai, F., Descamps, M., & Hildebrand, H. F. (2013). Calcite as a bone substitute. Comparison with hydroxyapatite and tricalcium phosphate with regard to the osteoblastic activity. Materials Science & Engineering, 33(1), pp. 490–498. https://doi.org/10.1016/j.msec.2012.09.019

Mongkhonsiri, G., Gani, R., Malakul, P., & Assabumrungrat, S. (2018). Integration of the biorefinery concept for development of sustainable processes for the pulp and paper industry. Computers & Chemical Engineering, 119, pp. 70-84, https://doi.org/10.1016/j.compchemeng.2018.07.019.

Monte, M. C., Fuente, E., Blanco, A., & Negro, C. (2009). Waste management from pulp and paper production in the European Union. Waste Management, 29(1), pp. 293–308. https://doi.org/10.1016/j.wasman.2008.02.002

Morin, M. A., Mallik, D., Zhang, W., Pietro, W., Manthorpe, J. M., & Organ, M. G. (2021). Obtaining kinetics from continuous processes: Sampling multiple time points concurrently with a single valve rotation. Chemistry–Methods, 1(2), pp. 131–134. https://doi.org/10.1002/cmtd.202100003

Morita, E., Imai, M., Okawa, M., Miyaura, T., & Miyazaki, S. (2011). A before and after comparison of the effects of forest walking on the sleep of a community-based sample of people with sleep complaints. BioPsychoSocial Medicine, 5(1), 13. https://doi.org/10.1186/1751-0759-5-13

Mussatto, S. I., Fernandes, M., Milagres, A. M., & Roberto, I. C. (2008). Effect of hemicellulose and lignin on enzymatic hydrolysis of cellulose from brewer's spent grain. Enzyme and Microbial Technology, 43(2), pp. 124–129. https://doi.org/10.1016/j.enzmictec.2007.11.006

Nathan, V. K., & Rani, M. E. (2019). Microbial enzymes in paper and pulp industries for bleaching application MedDocs eBooks. In: Research Trends of Microbiology. pp. 1-11. https://meddocsonline.org/ebook-microbiology.html[last accessed 28/07/2022].

Ni, M., & Ratner, B. D. (2008). Differentiation of calcium carbonate polymorphs by surface analysis techniques - An XPS and TOF-SIMS study. Surface and Interface Analysis : SIA, 40(10), pp. 1356–1361. https://doi.org/10.1002/sia.2904

Nicodimos, E., & Haynes, D. (2011). Introduction of sodium sulfite free neutral deinking. In: Tappi peers conference, October 2-5, pp. 466-479.

Nielfa A., Cano R., Fdz-Polanco M. (2014). Theoretical methane production generated by the co-digestion of organic fraction municipal solid waste and biological sludge. Biotechnol Rep (Amst). 5. pp. 14-21. doi: 10.1016/j.btre.2014.10.005. PMID: 28435805; PMCID: PMC5374264.

Nielsen, M., Holst-Fischer, C., Malmgren-Hansen, B., Bjerg-Nielsen, M., Kragelund, C., Møller, H. B., & Ottosen, L. D. M. (2017). Small temperature differences can improve the performance of mesophilic sludge-based digesters. Biotechnology Letters, 39(11), pp. 1689–1698. https://doi.org/10.1007/s10529-017-2418-y

Niessen, W. R. (2002). Combustion and incineration processes. CRC press, Boca Raton, ISBN: 0-8247-0629-3.

Nordin, N., Abdullah, M., Tahir, M., Sandu, V., & Kamarudin, H. (2016). Utilization of fly ash waste as construction material. International Jounal of Conversation Science. 7, pp. 161–166.

Ochoa de Alda, J. A. (2008). Feasibility of recycling pulp and paper mill sludge in the paper and board industries. Resources, Conservation and Recycling, 52(7), pp. 965–972. https://doi.org/10.1016/j.resconrec.2008.02.005

O'Flaherty, V., Lens, P., Leahy, B., & Colleran, E. (1998). Long-term competition between sulphate-reducing and methane producing bacteria during full-scale anaerobic treatment of citric acid production wastewater. Water Research, 32(3), pp. 815–825. https://doi.org/10.1016/S0043-1354(97)00270-4

Olivia, J., Bernhardt, A., Reisinger, H., Domennig, M., & Krammer, H. (2009). Klärschlamm: Materiallen zur Abfallwirtschaft (*English translation: Sewage sludge: Waste management materials*). Umweltbundesamt GmbH, Austria, REP-0221. https://www.umweltbundesamt.at/fileadmin/site/publikationen/rep0221.pdf[last accessed 28/07/2022].

Osbaeck, B., & Johansen, V. (1989). Particle size distribution and rate of strength development of portland cement. Journal of the American Ceramic Society, 72(2), pp. 197–201. https://doi.org/10.1111/j.1151-2916.1989.tb06101.x

Özcan, A., & Zelzele, Ö. B. (2017). The effect of binder type on the physical properties of coated paper. Muş Alparslan Üniversitesi Fen Bilimleri Dergisi, 5(1), 399. https://doi.org/10.18586/msufbd.322353

Panichnumsin, P., Nopharatana, A., Ahring, B., & Chaiprasert, P. (2012). Enhanced biomethanation in co-digestion of cassava pulp and pig manure using a two-phase anaerobic system. Journal of Sustainable Energy & Environment. 3, pp. 73-79.

Paolini, V., Petracchini, F., Segreto, M., Tomassetti, L., Naja, N., & Cecinato, A. (2018). Environmental impact of biogas: A short review of current knowledge. Journal of Environmental Science and Health. Part A, Toxic/hazardous Substances & Environmental Engineering, 53(10), pp. 899–906. https://doi.org/10.1080/10934529.2018.1459076

Pásztory, Z., Mohácsiné, I. R., Gorbacheva, G., & Börcsök, Z. (2016). The utilization of tree bark. BioResources, 11(3), pp. 7859-7888. https://doi.org/10.15376/biores.11.3.

Patumsawad, S., & Cliffe, K. R. (2002). Experimental study on fluidised bed combustion of high moisture municipal solid waste. Energy Conversion and Management, 43(17), pp. 2329–2340. https://doi.org/10.1016/S0196-8904(01)00179-0

Pera, J., & Amrouz, A. (1998). Development of highly reactive metakaolin from paper sludge. Advanced Cement Based Materials, 7(2), pp. 49–56. https://doi.org/10.1016/S1065-7355(97)00016-3

Péra, J., Husson, S., & Guilhot, B. (1999). Influence of finely ground limestone on cement hydration. Cement and Concrete Composites, 21(2), 99–105. https://doi.org/10.1016/S0958-9465(98)00020-1

Petersson, A., & Wellinger, A. (2007). Biogas upgrading technologies developments and innovations: Task 37-Energy from biogas and landfill. https://www.ieabioenergy.com/wp-content/uploads/2009/10/upgrading_rz_low_final.pdf[last accessed 28/07/2022].

Petit, P. (1992). Post bleaching of deinked pulp for newsprint production. Appita Journal, 45(6), pp. 385-388.

Pilarski, M. (2020). Some uses of woody biomass in gardening and regenerative agriculture. Friends of the Trees Society, and Global Earth Repair Foundation. https://globalearthrepairfoundation.org/some-uses-of-woody-biomass-in-gardening-and-regenerative-agriculture/*[last accessed 26/07/2022].

Pokhrel, D., & Viraraghavan, T. (2004). Treatment of pulp and paper mill wastewater - a review. The Science of the Total Environment, 333(1-3), pp. 37–58. https://doi.org/10.1016/j.scitotenv.2004.05.017

Porteous, A. (2001). Energy from waste incinerationn - a state of the art emissions review with an emphasis on public acceptability. Applied Energy, 70(2), pp. 157–167. https://doi.org/10.1016/S0306-2619(01)00021-6

Prakasan, S., Palaniappan, S., & Gettu, R. (2020). Study of energy Use and CO_2 emissions in the manufacturing of clinker and cement. Journal of the Institution of Engineers (India): Series a, 101(1), pp. 221–232. https://doi.org/10.1007/s40030-019-00409-4

Pramanik, S. K., Suja, F. B., Porhemmat, M., & Pramanik, B. K. (2019). Performance and kinetic model of a single-stage anaerobic digestion system operated at different successive operating stages for the treatment of food waste. Processes, 7(9), 600. https://doi.org/10.3390/pr7090600

Prats, D., Rodrguez, M., Varo, P., Moreno, A., Ferrer, J., & Berna, J. L. (1999). Biodegradation of soap in anaerobic digesters and on sludge amended soils. Water Research, 33(1), pp. 105–108. https://doi.org/10.1016/S0043-1354(98)00199-7

Prentice, A. M. (2005). Macronutrients as sources of food energy. Public Health Nutrition, 8(7A), pp. 932–939. https://doi.org/10.1079/PHN2005779

Puhakka, J. A., Alavakeri, M., & Shieh, W. K. (1992). Anaerobic treatment of kraft pulp-mill waste activated-sludge: Gas production and solids reduction. Bioresource Technology, 39(1), pp. 61–68. https://doi.org/10.1016/0960-8524(92)90057-5

Qasem, N. A. A., Mohammed, R. H., & Lawal, D. U. (2021). Removal of heavy metal ions from wastewater: a comprehensive and critical review. Npj Clean Water, 4(36). https://doi.org/10.1038/s41545-021-00127-0

Ramanathan, A., Begum, K. M. S., Pereira, A. O., & Cohen, C. (2022). Energy recovery from biomass through gasification technology. In: A thermo-economic approach to energy from waste, pp. 107–132. https://doi.org/10.1016/B978-0-12-824357-2.00007-3

Rende, S. D. (2015). Global neutral/alkaline papermaking overview. NALCO, An Ecolab company, Reprint R-835. https://kipdf.com/alkaline-papermaking-overview_5b3050ba097c47a3308b46ca.html[last accessed 27/07/2022].

Reungsang, A., Pattra, S., & Sittijunda, S. (2012). Optimization of key factors affecting methane production from acidic effluent coming from the sugarcane juice hydrogen fermentation process. Energies, 5(11), pp. 4746–4757. https://doi.org/10.3390/en5114746

Reuss, L. (2008). Water transport across cell membranes. In: eLS (Encyclopaedia of Life Science)., https://doi.org/10.1002/9780470015902.a0020621.

Richter, F., Raussen, T., Siepenkothen, H. J., Wagner, J., & Kern, M. (2017). Nahrungs- und Küchenabfälle – Potenziale, Nutzung und Auswirkung auf die Prozesskette Biogutverwertung. In: K. Wiemer, M. Kem & T. Raussen (Eds), Bio- und Sekundärrohstoffverwertung XII, stofflich-energetisch. Witzenhausen 2017, April 25-27 2016, pp. 237-256.

Ritter (2017). Gas meters. https://mdvonline.com/files//2017-10/ritter-catalog-full.pdf[last accessed 29/07/2022].

Romanova, N. D., & Sazhin, A. F. (2010). Relationships between the cell volume and the carbon content of bacteria. Oceanology, 50(4), pp. 522–530. https://doi.org/10.1134/S0001437010040089

Safley, L. M., & Westerman, P. W. (1988). Biogas production from anaerobic lagoons. Biological Wastes, 23(3), 181–193. https://doi.org/10.1016/0269-7483(88)90033-X

Salem, H.J., Gooding, R. W., Martinez, D.M., & Olson, J. A. (2013). Some fundamental aspects of pulp screen capacity. In: I'Anson, S.J.(Ed.), Advances in pulp and paper research, https://doi.org/10.15376/frc.2013.1.261.

Salem, M. A. A., & Pandey, R. K. (2017). Effect of cement-water ratio on compressive strength and density of concrete. International Journal of Advances in Mechanical and Civil Engineering. http://www.iraj.in/journal/journal_file/journal_pdf/13-425-152179543475-77.pdf[last accessed 29/07/2022].

Salmons, J. (2012). A history of German: What the past reveals about today's language. Oxford University Press. ISBN: 9780199697939.

Samir, K. K., Tjokorda, G. T. N., & Saoharit, N. (2019). Biogas from wastes processes and applications. In: M. Taherzadeh, K. Bolton, J. Wong, A. Pandey (Eds.), Sustainable resource recovery and zero waste approaches. pp. 165-174. https://doi.org/10.1016/B978-0-444-64200-4.00011-6.

Sánchez, E., Borja, R., & López, M. (1996). Determination of the kinetic constants of anaerobic digestion of sugar-mill-mud waste (SMMW). Bioresource Technology, 56(2-3), pp. 245–249. https://doi.org/10.1016/0960-8524(96)00037-5

Sanders, W. (2001). Anaerobic hydrolysis during digestion of complex substrates [Doctoral dissertation, Wageningen University, Netherlands]. ISBN: 90-5808-375-6. https://edepot.wur.nl/198997[last accessed 28/07/2022].

Sannigrahi, A. K. (2018). Management of hazardous paper mill wastes for sustainable agriculture. In: Hussain, C.M. (Ed.), Handbook of environmental materials management, pp. 1–23. https://doi.org/10.1007/978-3-319-58538-3_17-1

Santos, R. B., & Hart, P. W. (2014). Brown stock washing – A review of the literature. MWV Corp. Covington, VA 24426 and Atlanta GA 30327. https://www.eucalyptus.com.br/artigos/outros/2014_Brown_stock_washing_review.pdf[last accessed 28/07/2022].

Saxena, A., & Singh Chauhan, P. (2017). Role of various enzymes for deinking paper: A review. Critical Reviews in Biotechnology, 37(5), pp. 598–612. https://doi.org/10.1080/07388551.2016.1207594

Schmidt-Döhl, F. (2013). Materialprüfung im Bauwesen (*English translation: Material testing in civil engineering*). ISBN: 9783816787471.

Schmitt, J., & Flemming, H.-C. (1996). FTIR spectroscopy. In: E. Heitz, H.C. Flemming, & W. Sand (Eds.), Microbially influenced corrosion of materials. pp. 143–157. https://doi.org/10.1007/978-3-642-80017-7_11.

Schuck, A., Päivinen, R., Hytönen Tuomo, & Pajari, B. (2002). Compilation of forestry terms and definitions. European forest institute internal report, No. 6. https://efi.int/sites/default/files/files/publication-bank/2018/ir_06.pdf[last accessed 27/07/2022].

Segui, P., Aubert, J. E., Husson, B., & Measson, M. (2012). Characterization of wastepaper sludge ash for its valorization as a component of hydraulic binders. Applied Clay Science, 57, pp. 79–85. https://doi.org/10.1016/j.clay.2012.01.007

Serpell, R., & Zunino, F. (2017). Recycling of hydrated cement pastes by synthesis of α′H-C_2S. Cement and Concrete Research, 100, pp. 398–412. https://doi.org/10.1016/j.cemconres.2017.08.001

Seyyedalipour, S. F., Kebreia, D.,Y., & Ranjbar, N. (2014). Study of utilization of pulp and paper industry wastes in production of concrete. International Journal of Engineering Research and Applications, 4, 1(3), pp. 115-122. https://www.ijera.com/papers/Vol4_issue1/Version%203/S4103115122.pdf[last accessed 28/07/2022].

Siddiqui, Z., Horan, N. J., & Anaman, K. (2011). Optimisation of C:N Ratio for co-digested processed industrial food waste and sewage sludge using the BMP test. International Journal of Chemical Reactor Engineering, 9(1). https://doi.org/10.1515/1542-6580.2327

Siggins, A., Enright, A.-M., & O'Flaherty, V. (2011). Temperature dependent (37–15°C) anaerobic digestion of a trichloroethylene-contaminated wastewater. Bioresource Technology, 102(17), pp. 7645–7656. https://doi.org/10.1016/j.biortech.2011.05.055

Singh, A., Kaur, A., Yadav, R. D., & Mahajan, R. (2019). An efficient eco-friendly approach for recycling of newspaper waste. 3 Biotech, 9(2), 51. https://doi.org/10.1007/s13205-019-1590-2

Singh, S. K., Kulkarni, S., Kumar, V., & Vashistha, P. (2018). Sustainable utilization of deinking paper mill sludge for the manufacture of building bricks. Journal of Cleaner Production, 204, pp. 321–333. https://doi.org/10.1016/j.jclepro.2018.09.028

Sivakumar, P., Bhagiyalakshmi, M., & Anbarasu, K. (2012). Anaerobic treatment of spoiled milk from milk processing industry for energy recovery – A laboratory to pilot scale study. Fuel, 96, pp. 482–486. https://doi.org/10.1016/j.fuel.2012.01.046

Slimane, K., Mohammed, D., Kamel, K., Mostafa, K., Ahmed, T., Fethya, S., & Abdelkader, T. (2016). Study of start-up of a continuous digester for biogas production. In: IEEE International conference on smart energy grid engineering (SEGE), August 21-24, pp. 313-316, https://doi.org/10.1109/SEGE.2016.7589543.

Sokolinski, F. (2014). Prozesssteuerung für 1 Bioreaktor: LabView Steuer- und Messprogramm. Dokumentation V2.0. TUHH- Forschungswerkstatt-Elektrotechnik. FWE 12D030. (*English translation: Process control for 1 bioreactor: LabView control and measurement program*): unpublished.

Sokolinski, F. (2019). Bioreaktor II: LabView Steuer- und Messprogramm. Dokumentation TUHH-Forschungswerkstatt- Elektrotechnik. FWE 18-016E. (*English translation: Bioreactor II: LabView control and measurement program*): unpublished.

Song, Y., Li, B., Yang, E.-H., Liu, Y., & Ding, T. (2015). Feasibility study on utilization of municipal solid waste incineration bottom ash as aerating agent for the production of autoclaved aerated concrete. Cement and Concrete Composites, 56, pp. 51–58. https://doi.org/10.1016/j.cemconcomp.2014.11.006

Sötemann, S. W., Ristow, N. E., Wentzel, M. C., & Ekama, G. A. (2006). A steady state model for anaerobic digestion of sewage sludges. Water SA, 31(4). https://doi.org/10.4314/wsa.v31i4.5143

Sridhar P., Reddy J.V.R., Venugopal C.S., & Karmakar G.R. (1998). Recycled fibre bleaching with hydrogen peroxide. https://ippta.co/wp-content/uploads/2021/01/IPPTA-CI-1998-55-60-Recycled-Fibre-Bleaching.pdf[last accessed 28/07/2022].

Stadtreinigung Hamburg. (2021). Papier: Umweltschutz vom Allerfeinsten (*English translation: Paper: Environmental protection at its finest*). Stadtreinigung Hamburg. https://www.stadtreinigung.hamburg/privatkunden/wertstoffe/papier/index.html[last accessed 28/07/2022].

Stanienda-Pilecki, K. J. (2019). The importance of fourier-transform infrared spectroscopy in the identification of carbonate phases differentiated in magnesium content. Spectroscopy, 34(6), pp. 32–42. https://www.spectroscopyonline.com/view/spec0619-pilecki*[last accessed 28/07/2022].

Steffen, F., Janzon, R., & Saake, B. (2018). Enzymatic treatment of deinking sludge - effect on fibre and drainage properties. Environmental Technology, 39(21), 2810–2821. https://doi.org/10.1080/09593330.2017.1365948

Steffen, F., Janzon, R., Wenig, F., & Saake, B. (2017). Valorization of waste streams from deinked pulp mills through anaerobic digestion of deinking sludge. BioResources, 12(3), pp. 4547-4566. https://doi.org/10.15376/biores.12.3.4547-4566

Steinberg, L. M., Kronyak, R. E., & House, C. H. (2017). Coupling of anaerobic waste treatment to produce protein- and lipid-rich bacterial biomass. Life Sciences in Space Research, 15, 32–42. https://doi.org/10.1016/j.lssr.2017.07.006

STP. (2021). Printing and photocopying papers. Steinbeis Paier GmBH. https://www.stp.de/en/products/steinbeis-printing-and-photocopying-papers/steinbeis-no4*[last accessed 29/07/2022].

Sudarshan, K., Maruthaiya, K., Kotteeswaran, P., & Murugan, A. (2017). Reuse the pulp and paper industry wastewater by using fashionable technology. Applied Water Science, 7(6), pp. 3317–3322. https://doi.org/10.1007/s13201-016-0477-1

Suhr, M., Klein, G., Kourti, I., Gonzalo, M. R., Santonja, G. G., Roudier, S., & Delgado Sancho, L. (2015). Best available techniques (BAT) reference document for the production of pulp, paper and board. Industrial emissions directive 2010/75/EU (Integrated pollution prevention and control)., JRC science and policy reports, ISBN: 9789279481673, https://doi.org/10.2791/370629.

Suksankraisorn, K., Patumsawad, S., & Fungtammasan, B. (2003). Combustion studies of high moisture content waste in a fluidised bed. Waste Management, 23(5), pp. 433–439. https://doi.org/10.1016/S0956-053X(03)00060-6

Sulbarán-Rangel, B., Alzate, H., Delgado, E., Saucedo, A. R., & Turrado, J. (2016). Deinking by flotation under neutral condition using fatty alcohol ethoxylates. Nordic Pulp & Paper Research Journal, 31(1), pp. 170–174. https://doi.org/10.3183/NPPRJ-2016-31-01-p170-174

Tabata, T. (2018). Environmental impacts of utilizing woody biomass for energy: A case study in Japan. Waste Biorefinery, pp. 751–778. https://doi.org/10.1016/B978-0-444-63992-9.00026-4

Takashima, M., Speece, R. E., & Parkin, G. F. (1990). Mineral requirements for methane fermentation. Critical Reviews in Environmental Control, 19(5), pp. 465–479. https://doi.org/10.1080/10643389009388378

Tchounwou, P. B., Yedjou, C. G., Patlolla, A. K., & Sutton, D. J. (2012). Heavy metal toxicity and the environment. Experientia Supplementum, 101, pp. 133–164. https://doi.org/10.1007/978-3-7643-8340-4_6

Tejada, J., Wiedenmann, J., Gall, B., Kaiser, B., Greißl, O., Unterberger, S., Kappler, A., & Thorwarth, H. (2020). Trace element behavior in wood-fueled heat and power stations in terms of an urban mining perspective. Fuel, 267(2), 116887. https://doi.org/10.1016/j.fuel.2019.116887

Teng, Z., Hua, J., Wang, C., & Lu, X. (2014). Design and optimization principles of biogas reactors in large scale applications. Reactor and Process Design in Sustainable Energy Technology, pp. 99–134. https://doi.org/10.1016/B978-0-444-59566-9.00004-1

Thauer, R. K., Jungermann, K., & Decker, K. (1977). Energy conservation in chemotrophic anaerobic bacteria. Bacteriological Reviews, 41(1), pp. 100–180. https://doi.org/10.1128/br.41.1.100-180.1977

Thomas, M. (2007). Optimizing the use of fly ash in concrete. PCA- Portland Cement Association Illinous USA. https://www.cement.org/docs/default-source/fc_concrete_technology/is548-optimizing-the-use-of-fly-ash-concrete.pdf[last accessed 28/07/2022].

Thompson, G., Swain, J., Kay, M., & Forster, C. (2001). The treatment of pulp and paper mill effluent: a review. Bioresource Technology, 77(3), pp. 275–286. https://doi.org/10.1016/s0960-8524(00)00060-2

Trad, Z., Fontaine, J.-P., Larroche, C., & Vial, C. (2016). Multiscale mixing analysis and modeling of biohydrogen production by dark fermentation. Renewable Energy, 98, pp. 264–282. https://doi.org/10.1016/j.renene.2016.03.094

Ueki, A., Ono k., Tsuchiya, A., & Ueki, k. (1997). Survival of methanogens in air-dried paddy field soil and their heat tolerance. Water Science and Technology, 36(6-7), pp. 517-522. https://doi.org/10.1016/S0273-1223(97)00563-5

UN. (2019). The sustainable development goals report 2019. United Nations (UN). (Ed.) https://doi.org/10.18356/55eb9109-en

van Haandel, A. C., & van der Lubbe, J. G. (2007). Handbook biological waste water treatment: Design and optimisation of activated sludge systems. Uitgeverij Quist, ISBN: 9789077983225.

van Langerak, E., Gonzalez-Gil, G., van Aelst, A., van Lier, J. B., Hamelers, H., & Lettinga, G. (1998). Effects of high calcium concentrations on the development of methanogenic sludge in upflow anaerobic sludge bed (UASB) reactors. Water Research, 32(4), pp. 1255–1263. https://doi.org/10.1016/S0043-1354(97)00335-7

van Pagel Zee, J., Geraci, N. S., Guerrero, F. D., Wikel, S. K., Stuart, J. J., Nene, V. M., & Hill, C. A. (2007). Tick genomics: The Ixodes genome project and beyond. International Journal for Parasitology, 37(12), pp. 1297–1305. https://doi.org/10.1016/j.ijpara.2007.05.011

Vásquez-Bahena, J., Montes-Horcasitas, M. C., Ortega-López, J., Magaña-Plaza, I., & Flores-Cotera, L. B. (2004). Multiple steady states in a continuous stirred tank reactor: An experimental case study for hydrolysis of sucrose by invertase. Process Biochemistry, 39(12), pp. 2179–2182. https://doi.org/10.1016/j.procbio.2003.11.007

Vavilin, V. A., Fernandez, B., Palatsi, J., & Flotats, X. (2008). Hydrolysis kinetics in anaerobic degradation of particulate organic material: An overview. Waste Management, 28(6), pp. 939–951. https://doi.org/10.1016/j.wasman.2007.03.028

VDP (2021). Papier 2021- Statistken zum Leistungsbericht. (*English translation: Paper 2021 – Performance Report Statistics*), Verband Deutscher Papierfabriken e.V. (Ed.) https://www.papierindustrie.de/papierindustrie/statistik/papier-2021-download#c4450*[last accessed 29/07/2022].

Velázquez-Martí, B., W. Meneses-Quelal, O., Gaibor-Chavez, J., & Niño-Ruiz, Z. (2019). Review of mathematical models for the anaerobic digestion process. In Rajesh, B.J & Yukesh, K.R.(Eds.), Anaerobic digestion, IntechOpen. https://doi.org/10.5772/intechopen.80815.

Venditti, R., Lucas, B., & Jameel, H. (2007). The effects of adhesive properties on the removal of pressure sensitive adhesive contaminants by pressure screens. Progress in Paper Recycling. 16(3).

Walker, R., & Pavía, S. (2011). Physical properties and reactivity of pozzolans, and their influence on the properties of lime–pozzolan pastes. Materials and Structures, 44(6), pp. 1139–1150. https://doi.org/10.1617/s11527-010-9689-2

Wang, F., Zhang, X., Zhang, G., Chen, J., Sang, M., Long, Z., & Wang, B. (2018). Studies on the environmentally friendly deinking process employing biological enzymes and composite surfactant. Cellulose, 25, pp. 3079–3089. https://doi.org/10.1007/s10570-018-1778-3

Wang, S.-J., & Zhong, J.-J. (2007). Bioreactor engineering. In: Yang, S. (Ed.), Bioprocessing for value-added products from renewable resources, Elsevier, pp. 131–161. https://doi.org/10.1016/B978-044452114-9/50007-4

Wang, X., Yang, G., Feng, Y., Ren, G., & Han, X. (2012). Optimizing feeding composition and carbon-nitrogen ratios for improved methane yield during anaerobic co-digestion of dairy, chicken manure and wheat straw. Bioresource Technology, 120, pp. 78–83. https://doi.org/10.1016/j.biortech.2012.06.058

Wang, Y., Yang, X., Sun, M., Ma, L., Li, X., & Shi, L. (2016). Estimating carbon emissions from the pulp and paper industry: A case study. Applied Energy, 184, pp. 779–789. https://doi.org/10.1016/j.apenergy.2016.05.026

Watterson, J. G. (1988). The role of water in cell architecture. Molecular and Cellular Biochemistry, 79(2), pp. 101–105. https://doi.org/10.1007/BF02424550

Wei, J., Raynor, J., Nguyen, T.-L. M., & Chi, H. (2017). Nutrient and metabolic sensing in T cell responses. Frontiers in Immunology, 8, 247. https://doi.org/10.3389/fimmu.2017.00247

Whitman, W. B., Bowen, T. L., & Boone, D. R. (2006). The methanogenic bacteria. In: M. Dworkin, S. Falkow, E. Rosenberg, K.H. Schleifer & E. Stackebrandt (Eds.), The prokaryotes, 25, pp. 165–207. https://doi.org/10.1007/0-387-30743-5_9

William, K. T. (2000). Mohrs hardness test. https://www.oakton.edu/user/4/billtong/eas100lab/hardness.htm*[last accessed 28/07/2022].

WNA (2021). Heating values of various fuels. World Nuclear Association. https://world-nuclear.org/information-library/facts-and-figures/heat-values-of-various-fuels.aspx*[last accessed 28/07/2022].

Wu, B. (2010). CFD simulation of gas and non-newtonian fluid two-phase flow in anaerobic digesters. Water Research, 44(13), pp. 3861–3874. https://doi.org/10.1016/j.watres.2010.04.043

Wu, M., Sun, K., & Zhang, Y. (2006). Influence of temperature fluctuation on thermophilic anaerobic digestion of municipal organic solid waste. Journal of Zhejiang University Science B, 7(3), pp. 180–185. https://doi.org/10.1631/jzus.2006.B0180

Xie, T., Reddy, K. R., Wang, C., & Xu, K. (2014). Effects of amendment of biochar produced from woody biomass on soil quality and crop yield. In: Geoshanghai 2014 International Conference, Shanghai, China, May 26-28, pp. 170–180. https://doi.org/10.1061/9780784413432.018

Yang, G., Sun, Y., Li, L., Lv, P., Kong, X., & Huang, D. (2018). Hydrolysis dynamics for batch anaerobic digestion of elephant grass. RSC Advances, 8(40), pp. 22670–22675. https://doi.org/10.1039/C8RA01115J

Zhang, C., Su, H., & Tan, T. (2013). Batch and semi-continuous anaerobic digestion of food waste in a dual solid-liquid system. Bioresource Technology, 145, pp. 10-16. https://doi.org/10.1016/j.biortech.2013.03.030

Zhang, Y. M., & Napier-Munn, T. J. (1995). Effects of particle size distribution, surface area and chemical composition on Portland cement strength. Powder Technology, 83(3), pp. 245–252. https://doi.org/10.1016/0032-5910(94)02964-P

Zhang, Y.-H. P., & Lynd, L. R. (2004). Toward an aggregated understanding of enzymatic hydrolysis of cellulose: Noncomplexed cellulase systems. Biotechnology and Bioengineering, 88(7), pp. 797–824. https://doi.org/10.1002/bit.20282

Zhou, W., Imai, T., Ukita, M., Li, F., & Yuasa, A. (2007). Effect of limited aeration on the anaerobic treatment of evaporator condensate from a sulfite pulp mill. Chemosphere, 66(5), pp. 924–929. https://doi.org/10.1016/j.chemosphere.2006.06.004

Zhuravlev, Y. N., & Atuchin, V. V. (2021). First-principle studies of the vibrational properties of carbonates under pressure. Sensors Basel-Switzerland, 21(11). https://doi.org/10.3390/s21113644

PHOTOGRAPHS AND GRAPHICS

Leopold Siegrist (n.d). Biogas 5000.
https://siegrist.de/wp-content/uploads/2021/12/Si_DB_Biogas5000.pdf
[last accessed 25/07/2022]

Ogun M. K. (2022). Valorization of deinking sludges from wastepaper recycling: Biogas production and calcium carbonate recovery. [Doctoral dissertation, Hamburg University of Technology]

Pronova (n.d) Equipment für die extraktive Beurteilung des Gärprozesses- FOS/TAC 2000 *(english: Equipment for the extractive assessment of the fermentation process- FOS/TAC 2000)*
https://pronova.de/produkte/biogasanalysentechnik/fermenteranalyse/291/fos/tac-2000 [last accessed 29/07/2022]

Ritter. (2017). *Gas meters*. https://mdvonline.com/files//2017-10/ritter-catalog-full.pdf*[last accessed 29/07/2022].

Sokolinski, F. (2014). *Prozesssteuerung für 1 Bioreaktor: LabView Steuer- und Messprogramm. Dokumentation V2.0. TUHH- Forschungswerkstatt-Elektrotechnik. FWE 12D030. (English translation: Process control for 1 bioreactor: LabView control and measurement program): unpublished*.

Sokolinski, F. (2019). *Bioreaktor II: LabView Steuer- und Messprogramm. Dokumentation TUHH-Forschungswerkstatt- Elektrotechnik. FWE 18-016E. (English translation: Bioreactor II: LabView control and measurement program): unpublished*.

WERT (2016). Altpapier (*English translation:* Wastepapers).
https://www.wert.de/geschaeftskunden/altpapier/ [last accessed 28/07/2022]

APPENDICES

Appendix A Characteristics of wastepaper recycling residues, equations and samples

Appendix A.1 Residues related to input mass of raw material during wastepaper recycling (based on Suhr et al., 2015)

Product	Paper types	Total loses	Rejects		Sludge		
			Coarse	Fine	Deinking	Process water clarification	Fine
		[% FM]	[% FM]	[% FM]	[% FM]	[% FM]	[% FM]
Graphic papers	Newspaper, magazines of higher qualities	15 - 20 20 - 35	1 - 2 < 2	3 - 5 < 3	8 - 13 10 - 13	2 - 5 1 - 5	~ 1
Tissues	Office paper for recycling, files, ordinary and medium qualities	28 - 40	1 - 2	3 - 5	8 - 13	15 - 25	~ 1
Market deinked pulp	Office paper for recycling	32 - 40	< 1	4 - 5	12 - 15	15 - 25	~ 1

Appendix A.2 Amount of solid residues generated by wastepaper recycling during the production of different paper grades (based on Sannigrahi, 2018)

Paper types	Amount of solid residues [kg / Mg air dried pulp]
Packaging paper	50 - 100
Newsprint	170 - 190
Lightweight coated paper/ supercalendar paper	450 - 550
Tissue and market pulp	500 - 600

Appendix A.3 Estimation of the amount of deinking sludge generated in Germany in 2015, 2019 and 2020

Year	Paper for recycling[a]		Estimated recycled paper[b]		Estimated Deinking Sludge[c] [dried]		Estimated DS[d] [moist]	
	Total	For deinking	Min.	Max.	Min.	Max.	Min.	Max.
	Mio. Mg	Mio. Mg	Mio. Mg	Mio. Mg	Mio. Mg	Mio. Mg	Mio. Mg	Mio. Mg
2015	16.8	5.9	2.9	4.9	0.29	0.73	2.28	5.75
2019	17.2	6.6	3.3	5.5	0.33	0.83	2.60	6.54
2020	16.9	6.0	3.0	5.0	0.30	0.75	2.36	5.91

[a] VDP 2021

[b] 1200 - 2000 kg PFR /Mg recycled paper is required for deinking process (Suhr et al., 2015)

[c] Deinking process generates 100 - 150 kg dried DS /Mg recycled paper (Berger et al., 2021)

[d] assumed that moist DS is similar to pre-dewatered DS in own study (median dry matter – 12.7% FM)

Appendix A.4 Equations to compute the physico-chemical properties of DS and derivatives

1.) Dry Matter Content [DM]

$$DM\ [\%\ FM] = \frac{m_{105°C}}{m_{FM}} * 100\ \% \qquad \text{Eq A.1}$$

Where,

m_{FM} is the fresh mass of the sample [g]

$m_{105°C}$ is the dry mass of the sample dried at 105°C [g]

2.) Water Content [WC]

$$\text{Water Content}\ [\%\ FM] = \frac{m_{FM} - m_{105°C}}{m_{FM}} * 100\ \% \qquad \text{Eq A.2}$$

$$\text{Water Content}\ [\%\ FM] = 100\ \% - DM\ [\%] \qquad \text{Eq A.3}$$

3.) Organic Dry Matter content [oDM]

$$\text{oDM [\% DM]} = \frac{m_{105°C} - m_{550°C}}{m_{105°C}} * 100\ \% \qquad \text{Eq A.4}$$

4.) Ash content [ash]

$$\text{Ash content [\% DM]} = \frac{m_{550°C}}{m_{105°C}} * 100\ \% \qquad \text{Eq A.5}$$

$$\text{Ash content [\% DM]} = 100\ \% - \text{oDM[\%]} \qquad \text{Eq A.6}$$

5.) Calcium Carbonate content [$CaCO_3$]

$$CaCO_3 \rightarrow CaO + CO_2 \qquad \text{Eq A.7}$$

$$\text{Calcium carbonate [\% DM]} = \frac{m_{550°C} - m_{900°C}}{m_{105°C}} * f * 100\ \% \qquad \text{Eq A.8}$$

$$f = \frac{M_{CaCO_3}}{M_{CO_2}} = 2.273 \qquad \text{Eq A.9}$$

Where,

$m_{550°C}$	is mass of sample after burning at 550°C [g]
$m_{990°C}$	is mass of sample after burning at 990°C [g]
M_{CaCO_3}	is the molar mass of $CaCO_3$ [100 g/mol]
M_{CaO}	is the molar mass of CO_2 [44 g/mol]
f	is the molar ratio of $CaCO_3$ to CO_2

Appendix A.5 Pictures of main samples used in this study

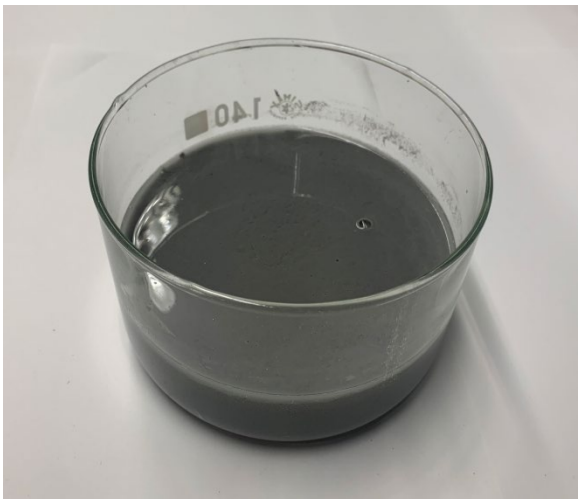

Pre-dewatered deinking sludge of type *W70*
(Sludge collected on 27.12.2019)

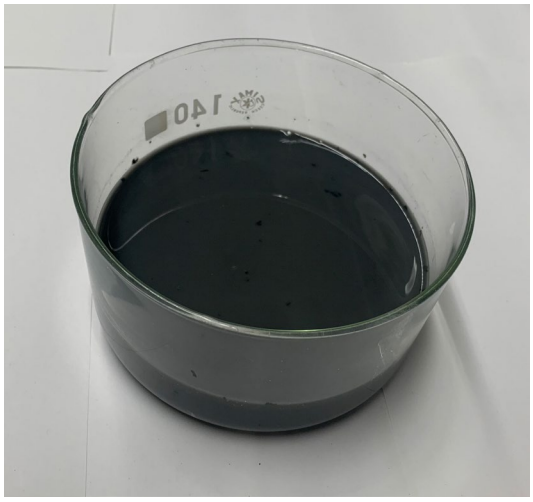

Digestate of deinking sludge of type *W70*
from 100-L AD system (R1B)
(Mixed digestate from 18.12.2019 - 09.02.2020)

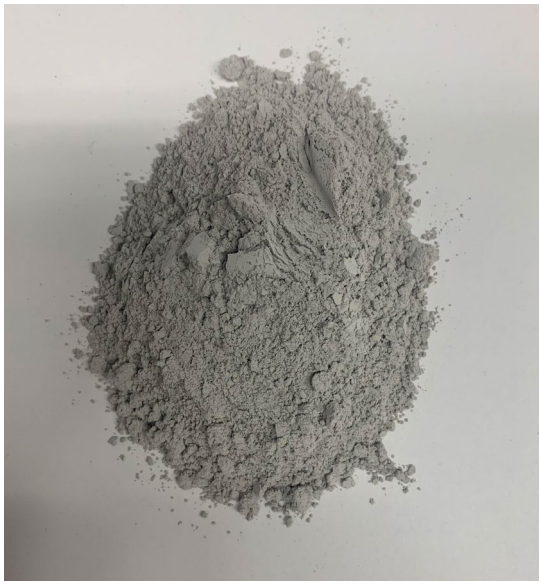

Ash of pre-dewatered deinking sludge of
type *W70* (burnt at 550°C)
(DS collected on 07.02.2017)

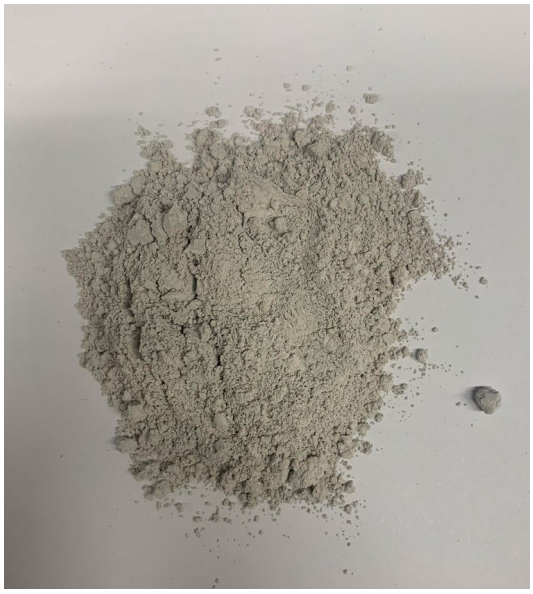

Ash of digestate of deinking sludge
of type *W70* (burnt at 550°C)
(Digestate collected from sedimented
phases of R1A on 01.06.2017)

Appendix A.6 List of samples analysed with periods and number of collections

Sample name	Period of collection	Number of collections
Stream 1-W70	01.10.2010 – 12.10.2016	8
Stream 2-W70	05.11.2013 – 27.12.2019	13
Stream 3-W70	18.12.2014 – 12.10.2016	2
Stream 4-W70	18.12.2014 – 12.10.2016	6
Stream 5-W70	18.12.2014 – 12.10.2016	5
Stream 6-W70	18.12.2014 – 12.10.2016	6
Stream 1-W80	25.06.2015 – 15.02.2016	2
Stream 2-W80	20.05.2015 – 26.01.2016	2
Stream 3-W80	25.06.2015	1
Stream 1-W90/100	25.06.2015 – 30.11.2016	3
Stream 2- W90/100	21.05.2015 – 20.11.2016	3
Stream 3-W90/100	25.06.2015 – 30.11.2016	2
Stream 4-W90/100	30.11.2016	1
Stream 5-W90/100	30.11.2016	1
Stream 5 I-W90/100	30.11.2016	1
Stream 5 II-W90/100	30.11.2016	1
Stream 5 III-W90/100	30.11.2016	1
Stream 6-W90/100	30.11.2016	1
Biosludge	01.04.2015 – 12.10.2016	3

Appendix B Description of AD systems and equations for calculations of biogas from DS

Appendix B.1 Description of components of the 1-L AD test system

Item	Component	Unit	Composition/functions	Supplier
1	Rectangular Vessel	1	Water bath	TUHH
2	Metal Frame	1	Stand to carry the water bath and the eudiometers made from steel	TUHH
3	Water	1	Heat exchange medium	TUHH
4	Heater with thermostat	1	For heat exchange temperature range [0-120°C] .	LAUDA DR.R.WOBSER GMBH & CO.KG
5	Reactor	1	1-L Duran glass bottle	DWK Life Sciences
6	Gas tubing	3	To transport biogas and barrier solution	TUHH
7	Eudiometer	1	Borosilicateglass 3.3 with volume of 1000 mL	H-W-S Labortechnik
8	Eudiometer Liquid	2	Water saturated with salt and coloured with methyl orange	TUHH
9	Coupler	1	The coupler blocks biogas from the passage. During sampling, a nipple is connected to the coupler to release the biogas. The coupler and the nipple are made from plastic.	SERTO AG
10	Barrier solution glass cylinder	1	Container	TUHH

Appendix B.2 Pictorial view of the 1-L AD test system

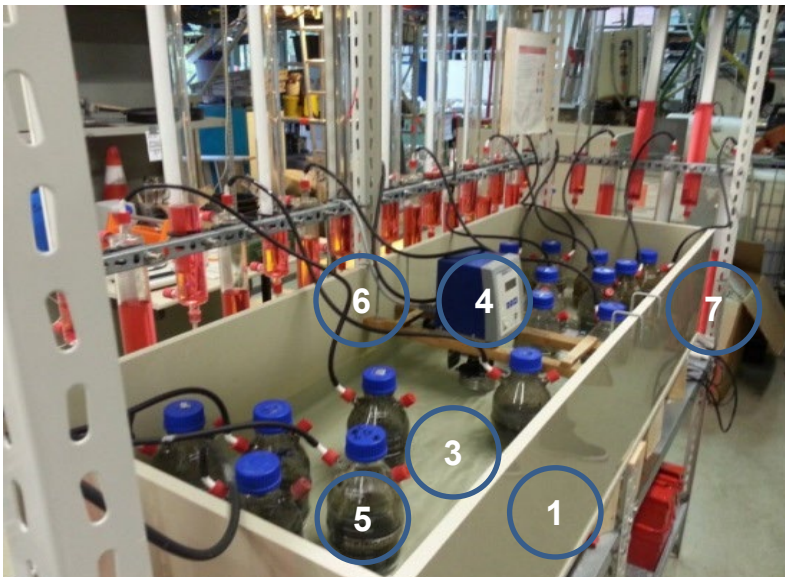

Labelling corresponds to Appendix B.1

Appendix B.3 Pictorial view of the 100-L automatically fed bioreactors

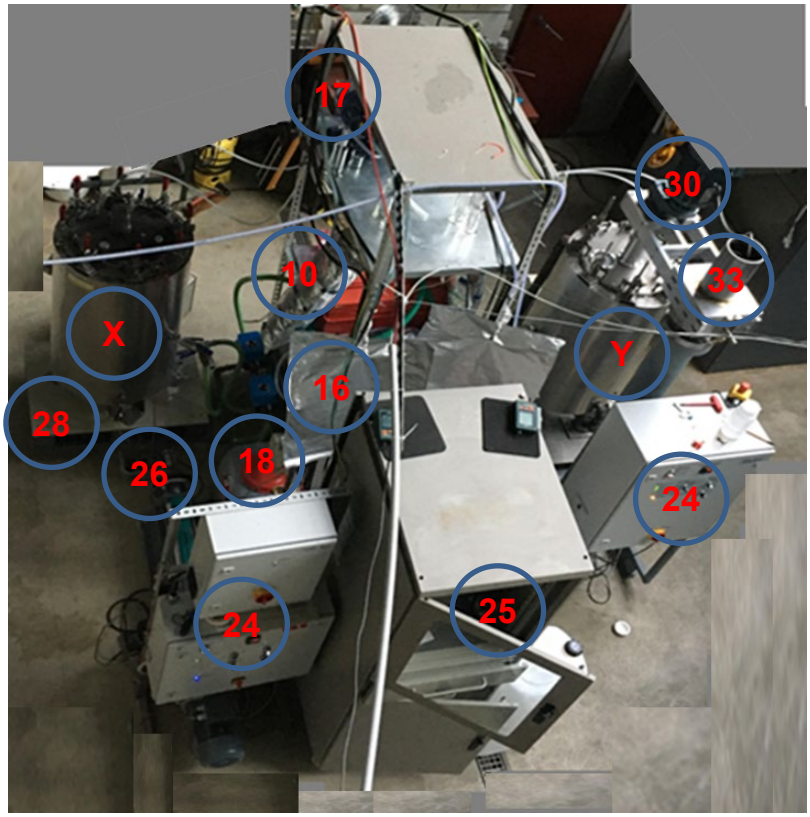

The description of the labels is available in Appendix B.6. The letters X and Y represent the bioreactors R1B and R2 respectively.

Appendix B.4 Schematics of the 1-L AD test system with eudiometer

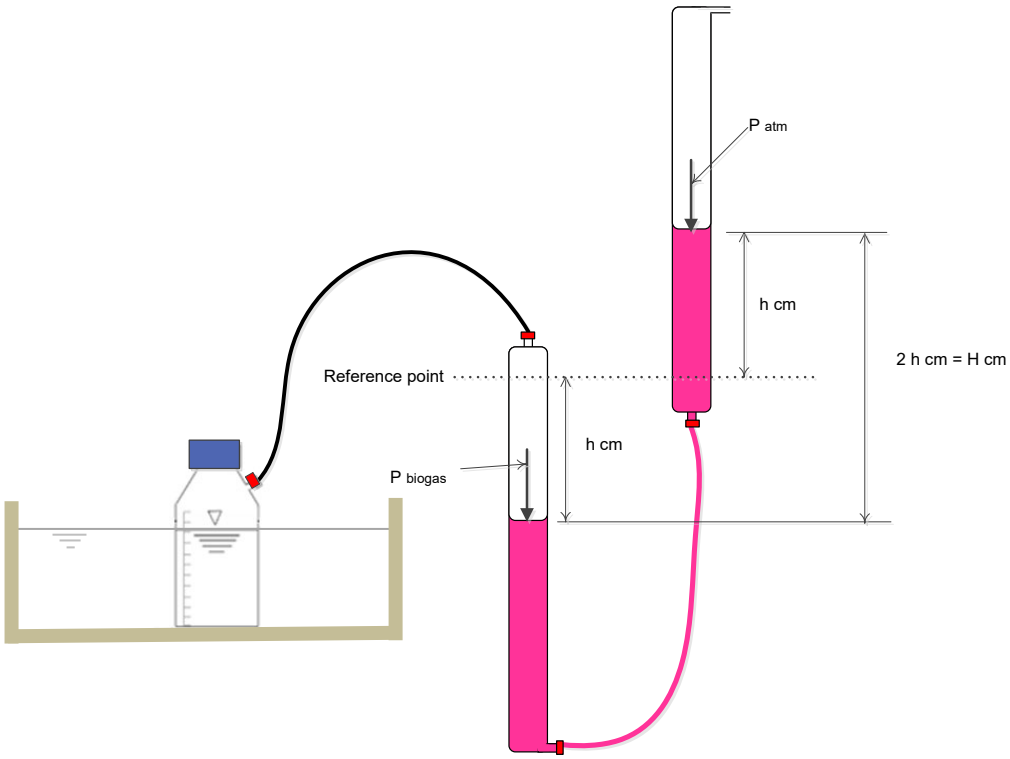

Appendix B.5 Equation to determine the pressure of biogas from eudiometer

$$P_{biogas} = P_{atm} + P_H \qquad \text{Eq B.1}$$

$$P_H = \rho * g * H \qquad \text{Eq B.2}$$

$$H = \frac{2 * V * 0.075}{10000} \qquad \text{Eq B.3}$$

Where,

h	is the distance between the reference point and meniscus of eudiometer liquid [cm]
H	is the total height of eudiometer liquid displaced by biogas pressure [cm]
P_{biogas}	is the pressure of biogas [mbar]
P_{atm}	is the pressure of the atmosphere [mbar]
P_H	is the guage pressure of biogas [mbar]
ρ	is the density of eudiometer liquid [kg/m^3]
g	is the acceleration due to gravity [9.81 m/s^2]
V	is the volume of biogas trapped by the eudiometer [mL]
0.075 and 10000	are conversion factors

Appendix B.6 Description of components of the 100-L automatically fed bioreactors (part 1)

Item	Component	Composition/functions	Supplier
1	Cross section – double jacketed reactor	A double jacket Reactor. The outer jacket contains water and the inner jacket contains a reactors mixture for anaerobic digestion	TUHH
2	Isolation	This is to reduce heat loss due to conduction	TUHH
3	Heater thermostat	Heat exchanger for the water jacket	TUHH
4	Temperature sensor 1	Pt100 with temperature range of 0- 50°C	Sensorshop24
5	Temperature sensor 2	Pt100 with temperature range of 0- 50°C	Sensorshop24
6	Recirculating water pump	To ensure uniform distribution of heat in the water jacket	TUHH
7	Inclined bottom	To support a smooth flow to the discharge outlet at the bottom	TUHH
8	Paddle stirrer	For mixing reactor's content	TUHH
9	Electric motor	Parallel shaft geared motor	SEW-EURODRIVE GmbH & Co KG
10	Clutch	To transmit torque from electric motor to stirrer	TUHH
11	Metal platform	To hold bioreactor and weighing balance firm to the ground	TUHH
12	Stand for electric motor & bioreactor	To hold the electric motor firmly	TUHH
13	Weighing balance	To weigh the bioreactor and its content (maximum sensitivity - 400 kg)	Hense wägetechnick GmbH
14	Pallet	A platform for Reactor three-foot to sear firmly on the weighing balance	KAISER + KRAFT GmbH
15	Cover	The cover sits on a ring seal to allow for airtightness of the reactor	Dichtelemente arcus GmbH
16	Bourdon gauge	To measure the gas pressure in a bioreactor	WIKA Alexander Wiegand SE & Co. KG
17	Solenoid valve 1	Regulation of biogas flow in and out of the nitrogen gasbag	Conrad Electronic
18	Nitrogen gasbag	For equalization of pressure during discharge of effluent and feeding of substrate	Linde AG
19	Solenoid valve 2	Regulation of biogas flow into the biogas storage bag	Conrad Electronic
20	Biogas scrubber 1	500 mL glass bottle	DWK Life Sciences

Appendix B.7 Description of components of the 100-L automatically fed bioreactors (part 2)

Item	Component	Composition/functions	Supplier
21	Biogas flow meter	For measurement of volume of biogas	Dr.Ing. Ritter Apparatebau GmbH & Co. KG
22	Biogas scrubber 2 and 3	500 mL glass bottle	DWK Life Sciences
23	Biogas storage bag	For temporal storage of biogas before analysis	Linde AG
24	Biogas quality analyser (Biogas 5000)	For analysing the quantity of CO_2, CH_4, O_2, H_2S	Leopold Siegrist GmbH
25	Progressive cavity pump -1 R1A (170-1000 L/h) ; R1B (1000-3000 L/h)	For mixing, feeding and discharge of effluent	NETZSCH Pumpen & Systeme GmbH
26	Feed tank	60 L container for storage of feed storage	BAUHAUS
27	Feed tank stirrer	To mix feedstock before feeding into the bioreactor	Heidolph Instruments
28	Digestate tank	60 L container for storage of feed storage of effluent (Digestate)	BAUHAUS
29	Control ball valve 1	3 way valve	bar pneumatische Steuerungssysteme GmbH
30	Control ball valve 2	3 way valve	bar pneumatische Steuerungssysteme GmbH
31	Progressive cavity pump 2 : R2 (5 - 25 L/h)	For feeding and discharge of digestate	NETZSCH Pumpen & Systeme GmbH
32	Data logger	Measures atmospheric pressure. humidity and room temperature	EXTECH
33	Control box	Serves as a central point that receives all digital and analog signals and convert them to data	TUHH
34	Computer	For visualization of process control and the input of control and storage of data	Fujitsu Esprimo

Appendix B.8 Complementary AD parameters analysed and equipment used

Parameter	Unit	Equipment	Supplier
VOA/TIC	-	 *Photo: Pronova n.d*	Pronova Analysentechnik GmbH & Co. KG
Kjeldahl nitrogen	mg/L	 *Photo: Ogun, 2022*	BÜCHI Labortechnik GmbH
Biogas volume	L	 *Photo: Ritter, 2017*	Dr.-Ing. RITTER Apparatebau GmbH & Co. KG
Biogas Characterization (CH_4, CO_2, O_2, H_2S)	% vol. of biogas	 *Source: Leopold Siegrist n.d.*	Leopold Siegrist GmbH

Appendix B.9 Equations used for the AD investigations

Different equations (Eq B.4 to Eq B.17) were used for deriving appropriate substrate mixtures, biogas related computations as well as feeding DS into a semi-continuously, operated AD process.

1.) Mixing formula for targeted dry matter content of the mixture

$$m_{s4}+m_{s6} = m \qquad \text{Eq B.4}$$

$$m_{s4} = \frac{[DM_{targ}- DM_{s6}]*m}{DM_{s4}-DM_{s6}} \qquad \text{Eq B.5}$$

Where,

m_{s4}	is the mass of *Stream* 4 required for mixture [kg]
m_{s6}	is the mass of *Stream* 6 required for mixture [kg]
m	is the mass of mixture [g]
DM_{s4}	is the dry matter content of *Stream 4* [% FM]
DM_{s6}	is the dry matter content of *Stream 6* [% FM]
DM_{targ}	is targeted dry matter of mixture [% FM]

The DM_{s4} and DM_{s6} can be determined experimentally. Provided the targeted dry matter content [DM_{targ}] of the mixture and the mass of mixture [m] are known. Eq B.4 and B.5 can be used to solve for m_{s4} and m_{s6}

2.) Biogas volume normalization

$$V_{NL}\ [NL]= \frac{V * [P_{atm}- P_{water}]* T_o}{p_o * T} \qquad \text{Eq B.6}$$

Where,

V_{NL}	is the volume of biogas produced under normalized conditions [NL]
V	is the volume of biogas produced at room temperature [NL]
P_{atm}	is atmospheric pressure [mbar]
P_{water}	is the vapour pressure of water as a function of room temperature [mbar]
T_o	is normal temperature [273.15 K]
p_o	is normal pressure [1013 mbar]
T	is room Temperature [K]

3.) Pressure of water

$$P_{water} = 10^{A - \frac{B}{C+T}} \quad \text{Eq B.7}$$

Where,

P_{water}	is the vapour pressure of water as a function of room temperature [mbar]
A	is Antoine parameter A [8.07131]
B	is Antoine Parameter B [1730.63]
C	is Antoine Parameter C [233.426]
T	is room temperature [^{o}C]

The parameters A, B and C of Eq B.5 (Antoine equation) are valid only for the temperature range 1 to 100^{o}C.

4.) Absolute and Specific Biogas yield

$$\text{Absolute biogas yield [NL/kg FM]} = \frac{Biogas_{cumm}}{m_{Feedstock}} \quad \text{Eq B.8}$$

Where,

$Biogas_{cumm}$	is the cumulative normalised biogas produced [NL]
$m_{feedstock}$	is the fresh mass of feedstock [kg]
$m_{oDM\text{-}feedstock}$	is the mass of organic dry matter in feedstock [kg]

$$\text{Specific biogas yield [NL/kg oDM]} = \frac{Biogas_{cumm}}{m_{oDM\text{-}Feedstock}} \quad \text{Eq B.9}$$

5.) Biogas quality correction

Biogas quality correction

$$\text{Dry biomethane concentration [\%]} = C_f * \frac{P_{atm}}{P_{atm} - P_w} \quad \text{Eq B.10}$$

Where,

C_f	is wet biomethane concentration [%]
P_{atm}	is the atmospheric pressure [mbar]
P_w	is the pressure of water vapour [mbar]

6.) Biodegradability

a.) Biodegradability [% oDM] = $\frac{m_{Biogas}}{m_{oDM}}$ *100% Eq B.11

Where,

m_{Biogas} is the mass of biogas produced from oDM fed into reactor [kg]

m_{oDM} is the mass of oDM fed into the reactor [kg]

$$m_{Biogas}\ [g] = \frac{P_{atm} * [M_{CH_4} * V_{CH_4} + M_{CO_2} * V_{CO_2}]}{R*T} \quad \text{Eq B.12}$$

Where,

m_{Biogas} is mass of biogas produced [g]

P_{atm} is atmospheric pressure [kpa]

M_{CH4} is the molar mass of methane [16.04 g/mol]

M_{CO2} is the molar mass of carbon dioxide [44.01 g/mol]

V_{CH4} is the normalised volume of methane [L]

V_{CO2} is the normalised volume of carbon dioxide [L]

R is molar gas constant [$L \cdot kPa \cdot K^{-1} \cdot mol^{-1}$]

T is the room temperature [K]

$$\text{b.) Biodegradation [\% oDM]} = \frac{[oDM_{fed} - oDM_{digestate}]}{oDM_{fed}} * 100\% \quad \text{Eq B.13}$$

Where,

oDM_{fed} is the organic matter fed [kg]

$oDM_{digestate}$ is the organic matter in digestate [kg]

7.) Hydraulic retention time (HRT)

$$HRT = \frac{V_R}{Q} \quad \text{Eq B.14}$$

Where,

V_R is the active volume of the reactor [L]

Q is feeding rate [L/day]

8.) Organic loading rate (OLR)

$$\text{OLR [kg oDM /(m}^3\text{day)]} = \frac{m_{oDM\text{-}daily}}{V_R} \qquad \text{Eq B.15}$$

Where,

$m_{oDM\text{-}daily}$	is the mass of oDM fed per day [kg oDM / day]
V_R	is Volume of Reactor [m^3]

9.) $CaCO_3$ mass balance across automatically fed 100-L automatically fed AD test system

$$CaCO_3\text{balance}(\%) = \frac{CaCO_{3\text{-}Dig\text{-}period} + CaCO_{3\text{-}Reactor\text{-}ld}}{CaCO_{3\text{-}Reactor\text{-}bf} + CaCO_{3\text{-}Fed\text{-}period}} \qquad \text{Eq B.16}$$

Where,

$CaCO_{3\text{-}Reactor\text{-}bf}$	is the estimated mass of $CaCO_3$ in the bioreactor before feeding in period considered [kg]
$CaCO_{3\text{-}Fed\text{-}period}$	is the total mass of $CaCO_3$ fed in the period considered [kg]
$CaCO_{3\text{-}Dig\text{-}period}$	is the total mass of $CaCO_3$ in digestate in the period considered [kg]
$CaCO_{3\text{-}Reactor\text{-}ld}$	is the estimated mass of $CaCO_3$ in a bioreactor after the last digestate in period considered [kg]

$$CaCO_{3\text{-}Reactor}\ (kg) = \frac{V * \rho * FM_{CaCO3}}{100} \qquad \text{Eq B.17}$$

Where,

$CaCO_{3\text{-}Reactor}$	is the mass of $CaCO_3$ in the bioreactor [kg]
V	is the volume of the bioreactor's content [L]
ρ	is the density of the bioreactor's content [kg/L]
FM_{CaCO3}	is the $CaCO_3$ content in the fresh mass of bioreactor's substrate [% FM]

Appendix C Properties of samples and AD mixtures for different AD batch test

Appendix C.1 Mixtures for experiment to study the AD of *Stream 1-W70* and *Stream 2-W70*

	Sample Name	Sample date	Nr. of samples [-]	Average mass of DS [gFM]	Average mass of inoculum [gFM]	Average mass of cellulose [gFM]
1	*Stream 1- W70*	02.12.2013	3	115.6	676.0	0.0
2	*Stream 2 - W70*	05.11.2013	2	116.0	676.0	0.0
3	*Stream 2 - W70*	02.12.2013	3	115.8	676.0	0.0
4	Cellulose	23.01.2014	3	0.0	676.0	4.4
5	Inoculum	23.01.2014	3	0.0	676.0	0.0

Appendix C.2 Mixtures for experiment to study the influence of different inocula on AD of DS

Nr.	Sample Name	Sample date	Inoculum used	Average mass of DS [gFM]	Average mass of inoculum [gFM]	Mass of cellulose [gFM]
1	*Stream 2 - W70*	24.04.2014	Inoculum1	306.0	516.0	0.0
2	*Stream 2 - W70*	24.04.2014	Inoculum2	99.0	495.0	0.0
3	*Stream 2 - W70*	24.04.2014	Inoculum3	130.6	490.0	0.0
4	Cellulose	15.05.2014	Inoculum1	0.0	516.0	3.5
5	Cellulose	15.05.2014	Inoculum2	0.0	495.0	3.5
6	Cellulose	15.05.2014	Inoculum3	0.0	490.0	3.5
7	Inoculum1	24.04.2014	Inoculum1	0.0	516.0	0.0
8	Inoculum2	24.04.2014	Inoculum2	0.0	495.0	0.0
9	Inoculum3	24.04.2014	Inoculum3	0.0	490.0	0.0
The numbers 1, 2, and 3 differentiate the inocula used. 1 is from an AD treatment plant with maize silage as input substrate, 2 is from an AD treatment plant with sewage sludge as input substrate while 3 is from another AD treatment plant also with sewage sludge as input substrate.						

Appendix C.3 Mixtures for experiment to study the influence of dewatering degree on AD of DS

Nr.	Average mass of DS		Number of samples	DM of DS mixture	Inoculum used	Mass of inoculum
	Stream 4- W70 [gFM]	Stream 6-W70 [gFM]		[%]	[gFM]	[gFM]
1	62.45	404.25	2	8.99	Inoculum 1	233.3
2	159.30	374.30	2	18.9	Inoculum 2	266.5
3	252.43	281.17	2	29.4	Inoculum 2	266.3
4	274.70	192.00	2	36.4	Inoculum 1	233.3
5	389.02	144.58	2	44.8	Inoculum 2	266.4
7	0.00	0.00	2	-	Inoculum 1	700.0
8	0.00	0.00	2	-	Inoculum 2	266.5
Stream 4-W70 and *Stream 6-W70* were sampled on 11.03.2015. Inoculum 1 and inoculum 2 were taken on 11.03.2015 and 26.01.2016 respectively.						

Appendix C.4 Mixtures for experiment to study the AD of *Stream 2-W80* and *Stream 2-W90/100*

Nr.	Sample	Sample date	Nr. of samples	Mass of DS [gFM]	Mass of inoculum [gFM]	Mass of inoculum [gFM]
1	*Stream 2- W80*	26.01.2016	2	266.85	533.15	0.00
2	*Stream 2- W90/100*	26.01.2016	1	266.40	533.20	0.00
3	Cellulose	01.02.2016	1	0.00	533.40	5.48
4	Inoculum	11.03.2015	3	0.00	266.50	0.00

Appendix C.5 Mixtures for experiment to study the influence of $CaCO_3$ on the AD of DS

Nr.	Cellulose [gFM]	$CaCO_3$ [gFM]	Inoculum [gFM]	$CaCO_3$ in feedstock [% DM]
1	4.65	0.00	533.89	0
2	4.65	2.09	528.69	12
3	4.65	4.15	533.03	22
4	4.63	10.0	533.42	40
5	0.00	0.00	534.16	0
The sample date of inoculum is 11.03.2016				

Appendix C.6 Semi-continuous AD of DS in a 10_L bioreactor to prepare DS-digestate with limited concentration of nitrogen

Period	Average HRT [days]	Number of days in Operation [days]
1	24 ± 3.3	17
2	29 ± 9.4	30
3	23 ± 8.9	21

Input DS: *Stream 2-W70* of sample dates 26.09.2019 and 27.12.2019

Inoculum used: DS-digestate from R1B (Initiation phase)

The NH_3/NH_4^+-N concentration declined in the bioreactor all through the period of operation leading to a corresponding reduction in the biogas production rate.

The minimum value of NH_3/NH_4^+-N observed was 18.4 mg/L.

The final DS-digestate was used as inoculum to investigate the influence of the C/N ratio on the AD of DS as in Appendix C.7.

Appendix C.7 Mixtures for experiment to study the influence of C/N ratio on the AD of DS

Nr.	DS [gFM]	Inoculum [gFM]	N supplementation [gFM]	C/N ratio
1	0	522.0	0	34
2	148	521.4	0	37
3	148	520.0	0.065	34
4	148	521.5	0.189	30
5	148	522.5	0.313	24

N is ammoniacal nitrogen (NH_3/NH_4^+-N)

N supplementation by ammonium chloride (NH_4Cl)

C/N ratio of inoculum = 34

C/N ratio of pre-dewatered DS = 49

Appendix C.8 Feeding pattern of semi-continuously operated AD of DS using automatically fed 100- AD systems

100-L bioreactor	Feeding phase	HRT (d^{-1})	Duration of operation (weeks)
R1A	1	30	14
	2	25	12
	3	20	7
	4	15	2
	5	20	2
	stop	stop	2
	6	30	9
R1B	1	19	6
R2	1	19	6

Appendix D.1 Computation for $CaCO_3$ mass balance across 100-L bioreactors

The computations were made using Eq B.16 and Eq B.17 in Appendix B.9

100-L bioreactor	Period considered	Number of days in period [days]	Estimated mass of $CaCO_3$ in bioreactor before feeding in period [kg]	Total mass of $CaCO_3$ fed in period [kg]	Total mass of $CaCO_3$ in digestate in period [kg]	Estimated mass of $CaCO_3$ in bioreactor after last digestate in period [kg]	$CaCO_3$ balance [%]
R1A	15.08.2016 - 31.10.2016	78	1.08	4.55	2.88	0.60	61.9
R1B	18.12.2019 - 09.02.2020	54	1.07	4.71	3.34	1.95	91.5
R2	18.12.2019 - 09.02.2020	54	1.40	5.39	4.18	2.54	99.0
Period considered was chosen to allow for a similar input mass in bioreactors. The HRT of R1A in the period considered are 30 and 25 days. The poor balances of R1 A indicate poor mixing and sampling. The rest $CaCO_3$ content not captured in the balance of all bioreactors are possibly in the bioreactors, pipes and pumps.							

Appendix E Characteristics of samples and preparation for solid-liquid separation tests

Appendix E.1 Samples for the different solid-liquid tests carried out

Solid-liquid separation	Sample	Number of samples
Sieve analysis (sieve sizes used: 63 µm, 100 µm, 200 µm, 300 µm, 500 µm and 1 mm)	*Stream 1-W70_04.06.2015*	2
	Stream 2-W70_04.06.2015	2
	Stream 1- W90/100_25.02.2016	2
	Stream 2- W90/100_26.01.2016	2
	DS-digestate_10L_Bioreactor (HRT: 50 days)	2
Sedimentation (Imhoff cone-size; 1000 mL)	*Stream 1-W70_25.02.2016*	2
	Stream 2-W70_02.06.2016	2
	Stream 1-W80_25.02.2016	2
	Stream 2-W80_26.01.2016	2
	Stream 1- W90/100_ 25.02.2016	2
	Stream 2- W90/100_ 26.01.2016	2
	Stream 2-W70_07.02.2017 (diluted)	1
	*DS Digestate_R1A_final sampling**	1
Centrifugation	*Stream 2-W70_07.02.2017*	2
	*DS Digestate _R1A_final sampling**	2
	*DS-digestate_ R1A_ final sampling** (diluted)*	2
	DS-digestate_ R1A _ (HRT: 15 days)	2
*final sampling occured on the 01.06.2017 when the reactor was opened, ** see dilution in Appendix E.2		

Appendix E.2 Characteristics of samples used for sedimentation tests

Sample	Dry matter content [% FM]	Water added to 1-L of sample [g]	Dry matter content_adjusted [% FM]	pH [-]
Stream 2-W70_07.02.2017 (diluted)	11.7	666.7	7.8	7.0
DS Digestate_Bioreactor 1A_final sampling	7.8	0.0	7.8	7.0

Appendix E.3 Preparation of samples to test for dewaterability by centrifugation tests

Sample	Sample description	Beginning DM [% FM]	Water added to 1-L of sample [g]	Final DM [% FM]
Stream 2-W70	*Stream 2- W70_07.02.2017*	13.0	0	13.0
DS-digestate 1	*DS-digestate_ R1A _ (HRT: 15 days)*	13.1	0	13.1
DS-digestate 2	*DS-digestate_ R1A_ final sampling (diluted with tap water)*	18.2	400	13.0

Appendix F Standard sand and mortar mixtures for formation of mortar

Appendix F.1 Grain size distribution of standard sand used (DIN EN 196-1) with standard deviation

Square mesh size [mm]	2.00	1.60	1.00	0.50	0.16	0.08
Cumulative sieve residue [%]	0	7 ± 5	33 ± 5	67 ± 5	87 ± 5	99 ± 1

Appendix F.2 The masses of water, sand, cement and ash for different mortars made

Sample Nr.	**Mortar type**	**Water [g]**	**Sand [g]**	**Cement [g]**	**Cement Reduction [% cement in reference]**	**Ash of DS [g]**	**Ash of DS-digestate [g]**	**Cement substitution [% cement in reference]**
1	Portland Cement (Reference)	260	1305	435	0	0	0	0
2								
3	Portland cement (Other Reference)	260	1305	413	5	0	0	0
4								
5				370	15			
4								
6				326	25			
7								
8				283	35			
9								
10	Partial substitution by ash of DS	260	1305	413	5	22	0	5
11								
12				370	15	65		15
13								
14				326	25	109		25
15								
16				283	35	152		35
17								
18	Partial substitution by ash of DS-digestate	260	1305	413	5	0	22	5
19								
20				370	15		65	15
21								
22				326	25		109	25
23								
24				283	35		152	35
25								

Appendix F.3 Pictorial view of mortar mixture components, form device and formed mortar prisms

Sand Cement Ash of DS-digestate

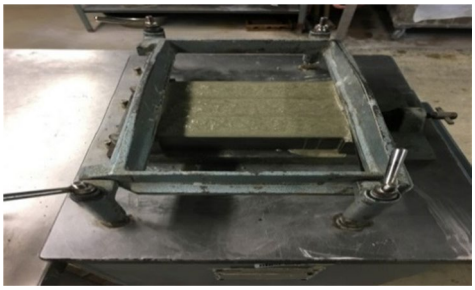

Form device for mortar prisms

Mortar prisms

Appendix G Computation of the characteristics of mortar prisms

Appendix G.1 Equations to compute characteristics of mortar prisms produced

To compute the density, flexural and compressive strength of the mortar prisms made from DS and digestate ashes the below equations were used.

1.) Density

$$\rho = \frac{m}{V} \qquad \text{Eq G.1}$$

where,

ρ is the density of mortar prism after curing [kg/mm^3]

m is the mass of mortar prism after curing [kg]

V is the volume of mortar prism after curing [m^3]

2.) Flexural strength

For a rectangular sample under a load in a three-point bending setup

$$R_f = \frac{1.5 * F_f * l}{b^3} \qquad \text{Eq G.2}$$

Where,

R_f is the flexural strength of mortar prism [N/mm^2]

b is the width of mortar prism [mm]

F_f Is the load (force) at the point of fracture on mortar prism [N]

l is the length of the support span of the test device [mm]

3.) Compressive strength

$$R_c = \frac{F_c}{A} \qquad \text{Eq G.3}$$

Where,

R_c is the compressive strength of mortar prism [N/mm^2]

F_c is the load applied on mortar prism [N]

1600 is the cross sectional area of mortar prism [40mm x 40mm] [mm^2]

Appendix H Statistical evaluation of physico-chemical properties of DS and derivatives

Appendix H.1 Statistical evaluation of dry matter (DM) contents of the DS and DS derivatives

Processing stage	***Stream 1***	***Stream 2***	***Stream 3***	***Stream 4***	***Stream 5***	***Stream 6***	***Bio-sludge***
Mean value (% FM)	3.37	11.69	5.12	56.18	0.96	0.59	1.52
Median value (% FM)	3.48	12.68	5.00	56.70	0.88	0.52	1.45
Standard deviation (% FM)	0.84	3.39	0.85	4.24	0.34	0.16	0.23
0.25 - Quantile (% FM)	3.10	8.98	4.91	53.38	0.70	0.50	1.36
0.75 - Quantile (% FM)	3.96	14.27	5.04	58.93	1.05	0.61	1.64
Minimum (% FM)	1.07	5.08	4.01	49.48	0.61	0.46	1.28
Maximum (% FM)	4.69	16.40	6.64	62.46	1.63	0.94	1.83
Number of samples (samples from various dates)	13	16	5	7	6	7	3
Number of samples (including multiple detections)	30	34	12	15	12	18	5
Normal distribution ^{KS}	yes	yes	yes	yes	yes	no	-
Normal distribution ^{SW}	yes	yes	yes	no	yes	no	-

KS - Kolmogorow-Smirnow-Test with Lilliefors-Correction; SW - Shapiro-Wilk-Test

Appendix H.2 Statistical evaluation of oDM, ash and $CaCO_3$ contents of DS and DS derivatives

Processing stage	*Stream 1*	*Stream 2*	*Stream 3*	*Stream 4*	*Stream 5*	*Stream 6*	*Bio-sludge*
oDM content							
Mean value (% DM)	33.4	30.5	32.8	30.9	39.0	31.3	51.3
Median value (% DM)	33.4	31.0	29.5	31.2	39.1	29.2	53.4
Standard deviation (% DM)	2.6	2.4	5.8	4.2	8.5	6.7	5.2
0.25 - Quantile (% DM)	31.8	28.9	28.7	28.9	31.7	25.8	48.8
0.75 - Quantile (% DM)	33.9	32.1	33.3	33.3	42.8	36.1	54.9
Minimum (% DM)	29.6	24.6	28.4	23.6	28.6	23.3	44.2
Maximum (% DM)	39.4	34.3	43.9	37.0	53.7	42.6	56.5
Number of samples (samples from various dates)	13	16	5	7	6	7	3
Number of samples (including multiple detections)	25	34	12	14	14	16	5
Normal distribution ^{KS}	no	yes	yes	yes	yes	yes	-
Normal distribution ^{SW}	yes	Yes	no	yes	yes	yes	-
Ash content							
Mean value (% DM)	66.6	70.3	67.2	69.1	61.0	68.7	48.7
Median value (% DM)	66.6	71.4	70.5	68.8	60.9	70.8	46.6
Standard deviation (% DM)	2.6	7.6	5.8	4.2	8.5	6.7	5.2
0.25 - Quantile (% DM)	66.1	70.3	66.7	66.7	57.2	63.9	45.1
0.75 - Quantile (% DM)	68.2	72.1	71.3	71.1	68.3	74.2	51.2
Minimum (% DM)	60.6	43.0	56.1	63.0	46.3	57.4	43.5
Maximum (% DM)	70.4	80.7	71.6	76.4	71.4	76.7	55.8
Number of samples (samples from various dates)	13	16	5	7	6	7	3
Number of samples (including multiple detections)	26	34	12	14	14	16	5
Normal distribution ^{KS}	no	yes	yes	yes	yes	yes	-
Normal distribution ^{SW}	yes	yes	no	yes	yes	yes	-
$CaCO_3$ content							
Mean value (% DM)	48.2	53.7	47.6	57.7	46.6	62.8	42.5
Median value (% DM)	46.2	49.3	50.8	52.2	46.3	73.1	42.5
Standard deviation (% DM)	9.0	8.1	11.0	11.5	15.4	18.1	17.5
0.25 - Quantile (% DM)	42.1	47.1	41.8	50.3	40.5	53.2	33.7
0.75 - Quantile (% DM)	55.3	59.1	56.5	70.3	61.0	77.7	51.2
Minimum (% DM)	34.3	45.3	30.4	43.6	21.4	31.6	25.0
Maximum (% DM)	62.7	68.8	58.5	72.3	63.9	78.3	60.0
Number of samples (samples from various dates)	10	7	4	5	5	5	2
Number of samples (including multiple detections)	20	22	8	10	10	9	4
Normal distribution ^{KS}	yes	yes	-	yes	yes	yes	-
Normal distribution ^{SW}	yes	yes	yes	yes	yes	yes	-

KS - Kolmogorow-Smirnow-Test with Lilliefors-Correction; SW - Shapiro-Wilk-Test

Appendix H.3 Results of two-sided t-test for the comparison of the mean values of different DS and DS derivative types (*Streams 1-6*)

DS	Degree of freedom	t-statistic	Critical t-value	Result
Organic dry matter (oDM)				
Stream 1 & 2	27	2.992	2.052	*Stream 1 > Stream 2*
Stream 1 & 5	17	-2.039	2.110	Not different
Stream 2 & 3	19	-1.198	2.093	Not different
Stream 3 & 4	10	0.600	2.228	Not different
Stream 4 & 6	10	-0.126	2.228	Not different
Calcium carbonate ($CaCO_3$)				
Stream 1 & 2	15	-1.215	2.131	Not different
Stream 1 & 5	5	0.192	2.571	Not different
Stream 2 & 3	5	0.853	2.571	Not different
Stream 3 & 4	7	-1.183	2.364	Not different
Stream 4 & 6	7	-0.474	2.364	Not different

Appendix H.4 Statistical evaluation of DS main streams based on influence of wastepaper grades

Processing stage	***Stream 1***			***Stream 2***			***Stream 4***	
Wastepaper grade	***W70***	***W80***	***W90/100***	***W70***	***W80***	***W90/100***	***W70***	***W90/100***
DM content								
Mean value (% FM)	3.3	3.1	3.9	11.5	14.5	9.9	54.6	56.8
Median value (% FM)	3.5	3.1	4.1	12.2	14.6	9.0	54.3	58.0
Standard deviation (% FM)	0.9	0.4	0.8	3.0	0.2	3.4	4.0	5.1
0.25 - Quantile (% FM)	3.2	2.7	3.3	9.5	14.4	7.4	52.0	55.5
0.75 - Quantile (% FM)	3.8	3.5	4.6	13.7	14.7	9.3	55.9	59.3
Minimum (% FM)	1.1	2.7	2.7	5.0	14.2	7.3	49.3	48.5
Maximum (% FM)	4.0	3.5	4.7	14.9	14.8	16.4	62.5	62.4
Number of samples (samples from various dates)	8	2	3	11	2	3	6	1
Number of samples (including multiple detections)	17	4	6	26	3	5	11	4
Normal distribution ^{KS}	no	yes	yes	no	-	no	yes	yes
Normal distribution ^{SW}	no	no	yes	no	-	no	yes	-
oDM content								
Mean value (% DM)	33.7	33.7	31.3	30.4	25.6	25.4	33.6	23.6
Median value (% DM)	33.3	33.8	31.1	29.8	24.7	25.7	31.3	23.4
Standard deviation (% DM)	2.7	0.5	1.4	1.6	1.4	3.4	5.1	0.4
0.25 - Quantile (% DM)	32.8	33.6	30.3	28.9	24.6	25.1	30.6	23.3
0.75 - Quantile (% DM)	34.5	34.0	32.5	31.7	26.1	28.1	37.1	23.7
Minimum (% DM)	28.3	33.0	29.2	28.0	24.5	19.3	27.7	23.3
Maximum (% DM)	39.4	34.2	33.3	33.7	27.5	28.8	42.6	24.1
Number of samples (samples from various dates)	8	2	3	11	2	3	6	1
Number of samples (including multiple detections)	15	4	6	25	3	5	11	3
Normal distribution ^{KS}	yes	yes	yes	no	-	yes	yes	-
Normal distribution ^{SW}	yes	no	yes	no	-	yes	no	-
$CaCO_3$ content								
Mean value (% DM)	44.2	43.1	57.4	46.5	58.6	64.2	53.5	70.3
Median value (% DM)	41.7	43.7	56.1	46.9	58.6	64.4	51.1	65.9
Standard deviation (% DM)	9.2	2.6	4.2	2.5	0.2	4.6	8.9	8.3
0.25 - Quantile (% DM)	37.9	41.6	53.7	44.6	58.5	59.9	50.2	65.1
0.75 - Quantile (% DM)	48.5	45.2	60.9	47.1	58.7	68.7	52.3	71.1
Minimum (% DM)	33.7	39.1	52.8	42.4	58.4	59.2	43.6	64.8
Maximum (% DM)	63.4	45.8	63.6	54.1	58.7	69.0	72.3	84.6
Number of samples (samples from various dates)	5	2	3	4	1	2	4	1
Number of samples (including multiple detections)	10	4	6	16	2	4	6	4
Normal distribution ^{KS}	yes	yes	yes	no	-	yes	no	no
Normal distribution ^{SW}	yes	-	yes	no	-	-	no	-

KS - Kolmogorow-Smirnow-Test with Lilliefors-Correction; SW - Shapiro-Wilk-Test

Appendix H.5 Results of two-sided t-test for the comparison of the mean values of DM, oDM and $CaCO_3$ from *Stream 1, 2* and *4* regarding wastepaper grade (W70, W80, W90/100)

DS Stream	Wastepaper grades	Degree of freedom	t-statistic value	Critical t-value	Result
DM content					
Stream 1	W70 & W80	19	0.420	2.093	Not different
	W70 & W90/100	21	-1.460	2.080	Not different
	W80 & W90/100	8	-1.938	2.306	Not different
Stream 2	W70 & W80	27	-4.821	2.052	W80 > W70
	W70 & W90/100	5	0.889	2.571	Not different
	W80 & W90/100	6	2.061	2.447	Not different
Stream 4	W70 & W90/100	4	-0.663	2.776	Not different
oDM content					
Stream 1	W70 & W80	17	-0.009	2.110	Not different
	W70 & W90/100	19	1.963	2.093	Not different
	W80 & W90/100	8	2.906	2.306	W80 > W90/100
Stream 2	W70 & W80	2	4.652	4.303	W70 > W80
	W70 & W90/100	28	4.798	2.048	W70 > W90/100
	W80 & W90/100	6	0.075	2.447	Not different
$CaCO_3$ content					
Stream 1	W70 & W80	12	0.331	2.179	Not different
	W70 & W90/100	14	-3.066	2.145	W90/100 > W70
	W80 & W90/100	8	-5.926	2.306	W90/100 > W80
Stream 2	W70 & W80	16	-6.589	2.120	W80 > W70
	W70 & W90/100	18	-10.064	2.101	W90/100 > W70
	W80 & W90/100	4	-1.429	2.776	Not different

Appendix H.6 Statistical evaluation of C/N ratios of DS and DS derivative samples of W70 type

Processing stage	*Stream 1*	*Stream 2*	*Stream 4*	*Stream 5*	*Stream 6*
Mean value (-)	93	82	178	138	96
Median value (-)	88	96	178	138	96
Standard deviation (-)	24	51	7	4	2
0.25 - Quantile (-)	75	62	175	136	95
0.75 - Quantile (-)	106	119	182	140	97
Minimum (-)	52	36	171	134	94
Maximum (-)	115	185	185	142	98
Number of samples (samples from various dates)	4	8	2	2	2

Appendix H.7 Statistical evaluation of pH of DS and DS derivative samples

Processing stage	*Stream 1*	*Stream 2*	*Stream 5*	*Stream 6*	*Biosludge*
Mean value (-)	7.2	7.1	6.5	6.6	6.9
Median value (-)	7.4	6.9	6.4	6.8	6.9
Standard deviation (-)	0.5	0.6	0.2	0.3	0.0
0.25 - Quantile (-)	7.0	6.6	6.3	6.6	6.9
0.75 - Quantile (-)	7.6	7.7	6.5	6.8	6.9
Minimum (-)	6.3	6.3	6.3	6.0	6.9
Maximum (-)	7.7	8.0	6.8	6.9	6.9
Number of samples (samples from various dates)	12	14	4	5	1

Appendix I Some properties of AD mixtures for biogas test and sulphur content of DS

Appendix I.1 TN, C/N ratio, VOA/TIC of different mixtures prepared for AD batch test

Substrate	Inoculum	TN_{liq} [mg/L]	C/N_{liq} [-]	VOA/TIC [-]	Biogas yield [NL/kg oDM]	Biodegradability [% oDM]
Stream 2-W70	*Inoculum 1*	1437	52.2	0.2	235	16
Stream 2-W70	*Inoculum 2*	202	26.7	0.1	286	26
Stream 2-W70	*Inoculum 3*	1333	229.0	0.2	243	20
Cellulose	*Inoculum 1*	2263	-	0.1	585	56.2
Cellulose	*Inoculum 2*	237	-	0.1	586	52.3
Cellulose	*Inoculum 3*	1672	-	0.1	588	53.6
Inoculum 1	*Inoculum 1*	2278	-	0.1	29	-
Inoculum 2	*Inoculum 2*	239	-	0.0	126	-
Inoculum 3	*Inoculum 3*	1684	-	0.1	74	-

Appendix I.2 Sulphur content of deinking sludge

DS sample	Sulphur content	Source
	g/kg DM	
Stream 2-W70	0.50	Own study
Laboratory DS Sample	3 - 5	Steffen et al. 2017

Appendix J Biogas yield at initiation phases with automatically fed 100-L AD bioreactors

Appendix J.1 Specific biogas yield of DS at the initiation phase (batch) from the automatically fed 100-L AD bioreactor (R1A)

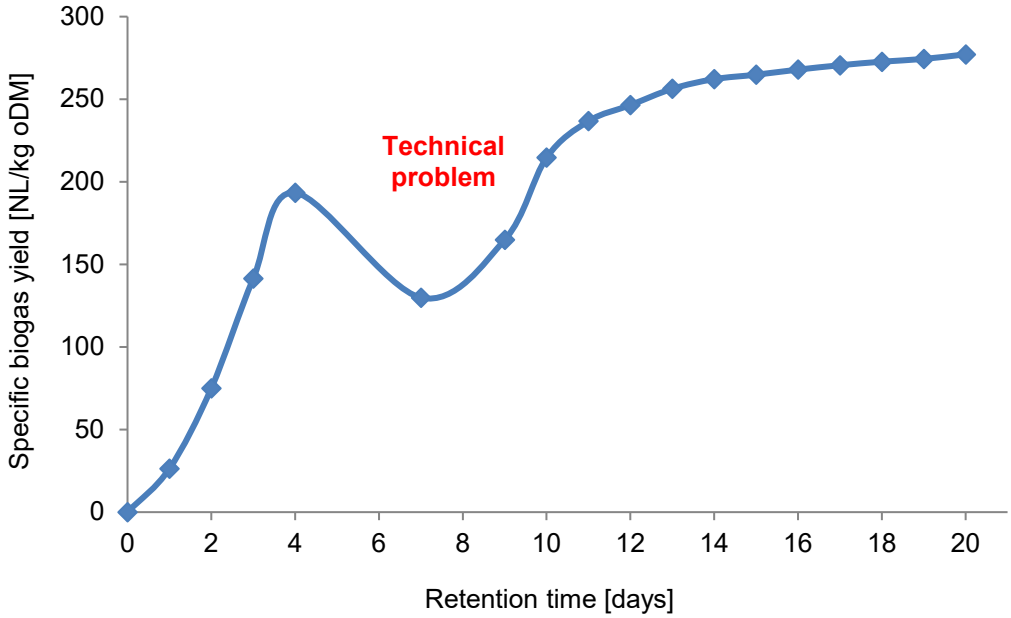

Appendix J.2 Specific biogas yield of DS at the initiation phase (batch) from the autamatically fed 100-L AD bioreactor (R1B)

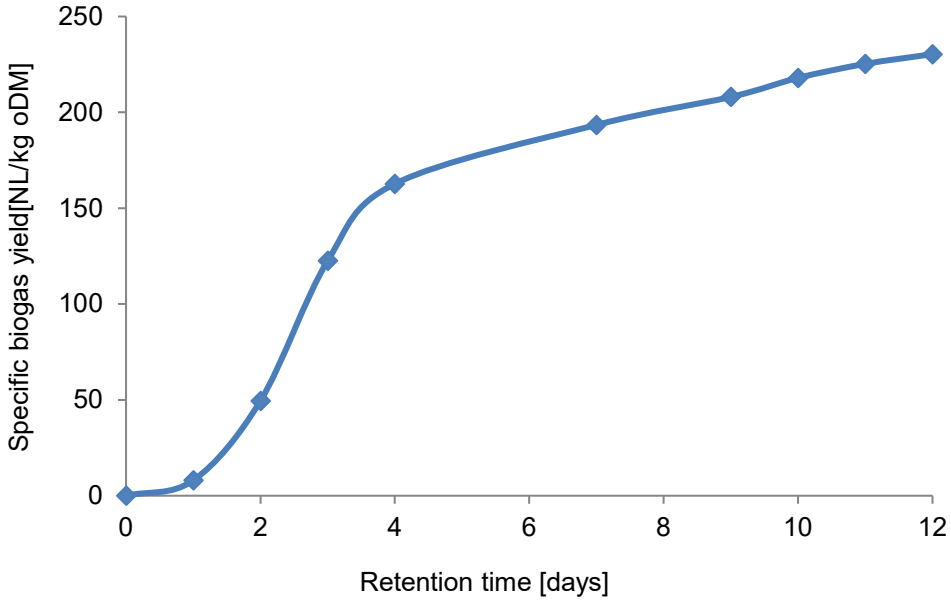

Appendix J.3 Specific biogas yield of DS at the initiation phase (batch) from the automatically fed 100-L AD bioreactor (R2)

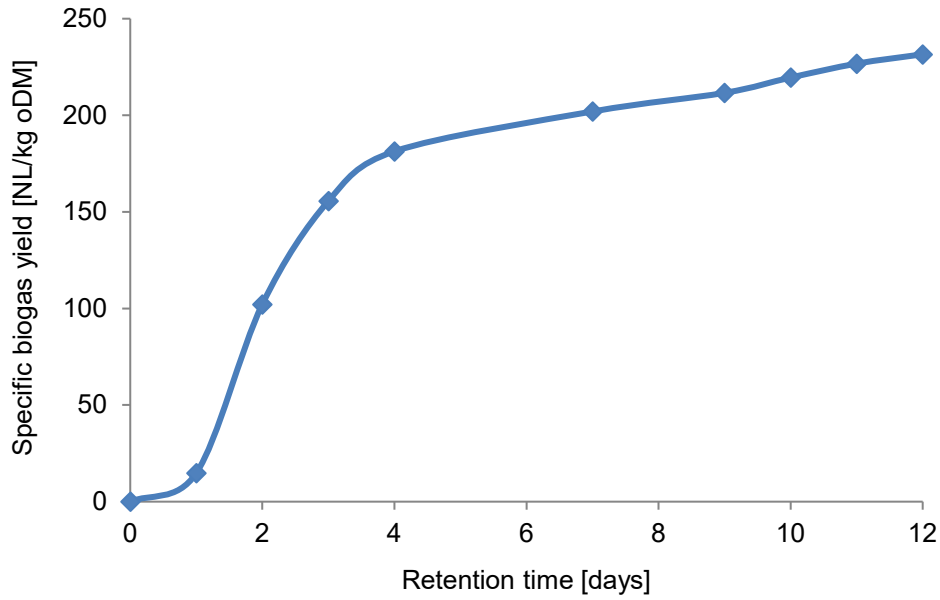

Appendix K Parameters obtained from model fitting and steps to apply Gompertz model

Appendix K.1 Data of model fitting to experimental data of the AD of different DS types

Models	Parameters					Indicators			
	k	k1	k2	Y_1	Y_2	R^2	RMSE	BIC	AIC
	[-]	[-]	[-]	[NL/kgoDM]	[NL/kgoDM]	[-]	[-]	[-]	[-]
Stream 1-W70									
Model 1	0.301	-	-	-	-	0.9336	21.0	137	136
Model 2	-	0.667	0.117	217.5	125.3	0.9883	8.8	99	98
Model 3	-	-	-	-	-	0.8211	34.4	159	158
Model 4	-	-	-	-	-	0.9314	21.3	138	137
Model 5	-	-	-	-	-	0.3382	66.2	188	187
Stream 2-W70_1									
Model 1	0.242	-	-	-	-	0.9706	12,6	115	114
Model 2	-	0.295	0.086	230.8	37.4	0.9749	11,7	111	110
Model 3	-	-	-	-	-	0.7284	38,3	164	163
Model 4	-	-	-	-	-	0.9321	19,2	133	132
Model 5	-	-	-	-	-	0.1776	66,7	188	187
Stream 2-W70_2									
Model 1	0.321	-	-	-	-	0.9777	9.0	100	99
Model 2	-	0.372	0,070	213.6	18.3	0.9828	7.9	94	93
Model 3	-	-	-	-	-	0.9157	17.6	129	128
Model 4	-	-	-	-	-	0.7684	29.1	151	151
Model 5	-	-	-	-	-	0.3947	47.1	173	172
Stream 2-W70_3									
Model 1	0,263	-	-	-	-	0.9455	20.3	136	135
Model 2	-	0.263	0.263	142.3	142.3	0.9455	20.3	136	135
Model 3	-	-	-	-	-	0.8150	37.5	163	162
Model 4	-	-	-	-	-	0.9258	23.7	142	142
Model 5	-	-	-	-	-	0.2443	75.7	193	193
Stream 2-W80									
Model 1	0.394	-	-	-	-	0.9779	10.7	108	107
Model 2	-	0.394	0.394	137.4	137.4	0.9779	10.7	108	107
Model 3	-	-	-	-	-	0.9811	9.9	104	103
Model 4	-	-	-	-	-	0.9156	21.0	137	136
Model 5	-	-	-	-	-	0.5121	50.5	176	175
Stream 2-W90/100									
Model 1	0.386	-	-	-	-	0.9732	18.6	132	131
Model 2	-	0.386	0.386	208.5	208.5	0.9732	18.6	132	131
Model 3	-	-	-	-	-	0.9846	14.1	120	119
Model 4	-	-	-	-	-	0.9059	34.9	159	159
Model 5	-	-	-	-	-	0.4977	80.7	196	195

Model1: One step first order kinetics; Model 2: Two steps first order kinetics ; Model 3:Modified Gompertz;
Model 4: Transfer function; Model 5: Logistic function

Appendix K.2 Application of the Gompertz model for the AD of DS

Step 1:

Obtain the elemental chemical composition (M) of the substrate (C, H, N, S) each in g/kg DM. Also, determine the oDM of the substrate in g/kg DM. You obtain M_c, M_H, M_N, M_s and $oDM_{substrate.}$

Step 2:

Compute the elemental chemical composition of the substrate (E) in weight percent of oDM. You obtain E_C, E_H, E_N and E_S.

Step 3:

To compute the weight percent of oxygen with respect to oDM. Subtract the sum of weight percent of chemical components in step 2 (E_c, E_H, E_N, E_S) from 100. You obtain E_O.

Step 4:

Determine the coefficient of C, H, O, N and S in the Bushwell equation (Eq K.1)

$$C_aH_bO_cN_dS_e + \left(a - \frac{b}{4} - \frac{c}{2} + \frac{3.d}{4} + \frac{e}{2}\right) H_2O \rightarrow$$

$$\left(\frac{a}{2} + \frac{b}{8} - \frac{c}{4} + \frac{3.d}{8} + \frac{e}{4}\right) CH_4 + \left(\frac{a}{2} - \frac{b}{8} + \frac{c}{4} + \frac{3.d}{8} + \frac{e}{4}\right) CO_2 + dNH_3 + e\ H_2S \qquad \text{Eq K.1}$$

Where,

$$a = \frac{E_C}{MM_C},\ b = \frac{E_H}{MM_H},\quad c = \frac{E_O}{MM_O},\quad d = \frac{E_N}{MM_N},\quad e = \frac{E_S}{MM_c}$$

MM is the molar mass of chemical component.

Step 5:

Compute the theoretical biogas yield of the DS sample using Eq K.2

$$Y_{TH}\ (NL/kg\ oDM) = \frac{Z * 22400 * \frac{a}{2} + \frac{b}{8} - \frac{c}{4} - \frac{3d}{8} - \frac{e}{4}}{12a + b + 16c + 14d + 32e} \qquad \text{Eq K.2}$$

Where Z is the factor related to methane fraction in biogas of DS (1.5 - 1.6 as obtained in this study)

Step 6:

Estimate the experimental biogas yield of the DS sample using Eq K.3. The equation is consistent with that reported by Nielfa et al. (2014) and Steffen et al. (2017). Take Y_{EXP} as the Y_m in the application of the Gompertz equation.

$$Y_{EXP} = \beta * Y_{TH} \qquad \text{Eq K.3}$$

Where β is biodegradability (oDM%). The pre-dewatered DS of *W80* and *W90/10* types from experimental observation are (25 - 28) and (39) respectively. Take Y_{EXP} as the Y_m in step 7.

Step 7:

Use the Eq K.4 to compute the maximum biogas production rate R_m. The Eq K. 4 was derived by running a linear regression for the experimental maximum yield (Y_m) and the maximum biogas production rate (R_m), which result in a coefficient of determination of 0.9971 as shown in Appendix K.3

$$R_m = 0.2555*Y_m + 6.0788 \qquad \text{Eq K.4}$$

Appendix K.3 Linear regression of maximum biogas production rate and biogas yield of pre-dewatered DS of type *W80* and *W90*

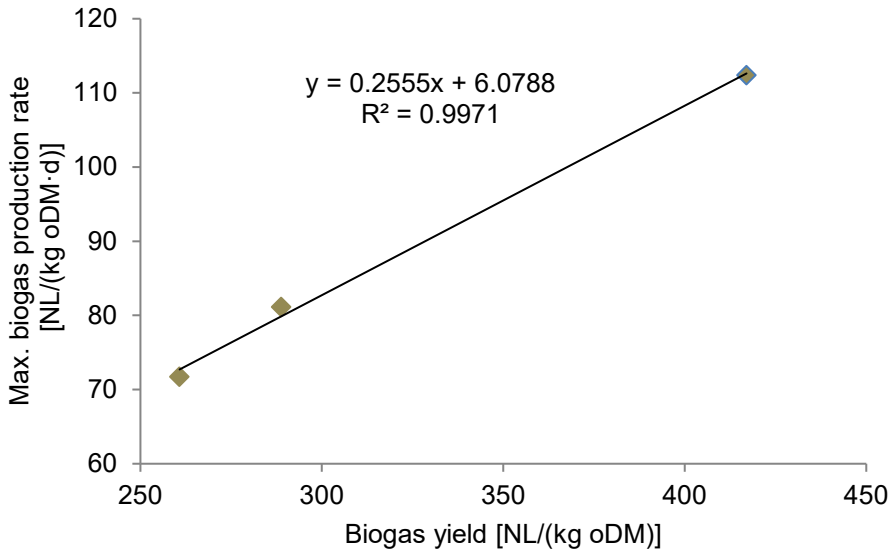

Data :

Pre-dewatered DS type	*W80*	*W80*	*W90/100*
Biogas yield [NL/(kg oDM)]	260.8	288.8	417.0
Max. biogas production rate [NL/(kg oDM·d)]	71.7	81.1	112.4

Appendix L Characteristics of inputs used and DS-digestate generated in biogas tests

Appendix L.1 Characteristics of input DS, inocula and DS-digestate from 1-L batch tests

Sample date	Number samples	DM [% FM]	oDM [% DM]	oDM [% DM]
Stream 2-W70 input for 1-L batch test				
05.11.2013	2	12.1	31.4	68.6
02.12.2013	3	12.0	28.2	71.8
24.04.2014	3	14.3	29.3	70.7
Inoculum used				
23.01.2014	5	2.0	62.7	37.3
24.04.2014**	1	7.9	68.7	31.3
24.04.2014**	1	0.8	61.5	38.5
24.04.2014**	1	1.9	61.6	38.4
DS-digestate				
23.01.2014-05.06.2014	8	5.0 ± 2.3	43.3 ± 4.5	56.7 ± 4.5
Each sample was analysed twice; **used only for DS sample *Stream 2-W70*_24.04.2014				

Appendix L.2 Characteristics of input DS and DS-digestate from semi-continuous AD using R1A

Sample Date	Number* of sample	Phases	DM [% FM]	oDM [% DM]	Ash [% DM]	$CaCO_3$ [% DM]
Stream 2-W70 input for bioreactor R1A						
26.01.2016	1	Phase 1 (Batch)	11.4	32.1	67.9	ND
25.05.2016 & 18.07.2016	1	Phase 2	13.3	31.2	68.8	ND
20.07.2016 & 04.10.2016	1	Phase 2	5.5	37.4	62.6	ND
12.10.2016	1	Phase 2	5.1	28.7	71.3	46.3
14.12.2016	1	Phase 2	8.5	28.9	71.1	46.5
07.02.2017	1	Phase 3	14.8	29.7	70.3	47.9
DS-digestate of bioreactor R1A						
06.06.2016 – 13.09.2016	14	30	5.4 ± 3.5	29.7 ± 2.8	70.3 ± 2.8	46.0 ± 5.0
13.09.2016 – 06.12.2016	12	25	5.2 ± 4.0	29.1 ± 2.3	70.9 ± 2.3	49.5 ± 8.8
06.12.2016 – 23.01.2017	7	20	8.1 ± 4.0	26.5 ± 1.8	73.5 ± 1.8	51.2 ± 3.1
23.01.2017 – 15.02.2017	3	15	7.2 ± 1.7	27.8 ± 1.0	72.2 ± 1.0	48.0 ± 3.0
15.02.2017 – 24.02.2017	2	20	8.0 ± 0.7	28.5 ± 1.4	71.5 ± 1.4	50.1 ± 4.5
15.03.2017 – 12.05.2017	8	30	7.5 ± 1.9	27.2 ± 2.6	72.8 ± 2.6	50.8 ± 4.2
Layers of bioreactor R1A (end of AD process)						
01.06.2017	2	S1	8.9 ± 4.0	35.4 ± 0.0	8.9 ± 4.0	38.5 ± 1.0
01.06.2017	1	S2	2.2 ± 0.0	27.3 ± 0.0	72.7 ± 0.0	52.9 ± 0.0
01.06.2017	4	S3	16.4 ± 6.1	26.3 ± 1.3	73.7 ± 1.3	53.5 ± 5.5
01.06.2017	1	S4	18.3 ± 0.0	27.2 ± 0.0	72.8 ± 0.0	47.9 ± 0.0
01.06.2017	3	S5	25.7 ± 3.3	24.9 ± 1.3	75.1 ± 1.3	49.2 ± 3.2
Each sample is analysed twice; ND: not determined, S1(floating layer), S2 (well mixed low solid substrate), the S3 (well mixed thickened substrate), and the S4 (boundary of sedimented layer) and S5 (thickened sedimented layer).						

Appendix L.3 Monitoring of AD system using VOA/TIC values (Lili et al., 2011)

VOA/TIC	Background	Measure
> 0.6	Highly excessive biomass input	Stop adding biomass
0.5 - 0.6	Excessive biomass input	Add less biomass
0.4 - 0.5	Plant is heavily loaded	Monitor the plant more closely
0.3 - 0.4	Biogas production at a maximum	Keep biomass input constant
0.2 - 0.3	Biomass input is too low	Slowly increase the biomass input
< 0.2	Biomass input is far too low	Rapidly increase the biomass input

Appendix L.4 Approximate sketch of sedimentation layers when the 100-L bioreactor was opened (R1A)

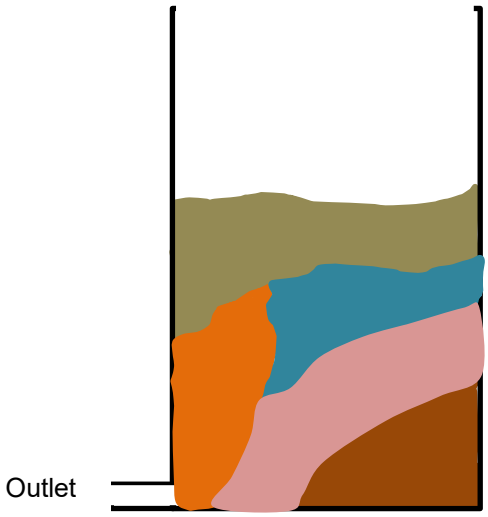

Layers of sedimented sludge	Description
S1	floating layer
S2	well mixed low solid substrate
S3	well mixed thickened substrate
S4	boundary of sedimented layer
S5	thickened sedimented layer

Appendix L.5 Characteristics of input DS and DS-digestate from semicontinuous AD using R1B and R2

Sample date	Number of analysis	DM [% FM]	oDM [% DM]	$CaCO_3$ [% DM]	pH [-]	NH_3/NH_4^+-N [mg/L]
***Stream 2-W70* input for bioreactor R1B**						
26.09.2019	2	12.4 ± 1.3	31.0 ± 0.3	49.9 ±1.6	6.3 ± 0.3	24.5 ± 2.7
27.12.2019	2	9.7 ±1.02	28.9 ±1.11	49.2 ± 1.3	7.0 ± 0.4	21.8 ±10.1
Bioreactor R1B content's before feeding						
18.12.2019	2	4.4 ± 0.0	30.2 ± 0.0	44.7 ± 0.2	7.20	476.00
DS-digestate of bioreactor R1B						
19.12.2019 - 24.02.2020	20	5.6 ± 0.9	26.4 ± 2.1	52.0 ± 3.5	7.3 ± 0.2	ND
Bioreactor R2 content's before feeding						
18.12.2019	2	5.6 ± 0.0	30.1 ± 0.0	45.2 ±1.8	7.30	490.0
DS-digestate of bioreactor R2						
19.12.2019 - 24.02.2020	20	7.0 ± 1.9	26.7 ± 2.8	52.5 ± 5.6	7.4 ± 0.2	ND
Unpumpable bioreactor R1B's when emptying bioreactor (end of AD process)*						
23.07.2022	2	35.1 ± 0.0	21.7 ± 0.08	54.2 ± 0.3	ND	ND
*Labelled sample T1						

Appendix M Particle size, elements, phases and compressibility of ashes

Appendix M.1 Particle size of ashes of DS and DS-digestate

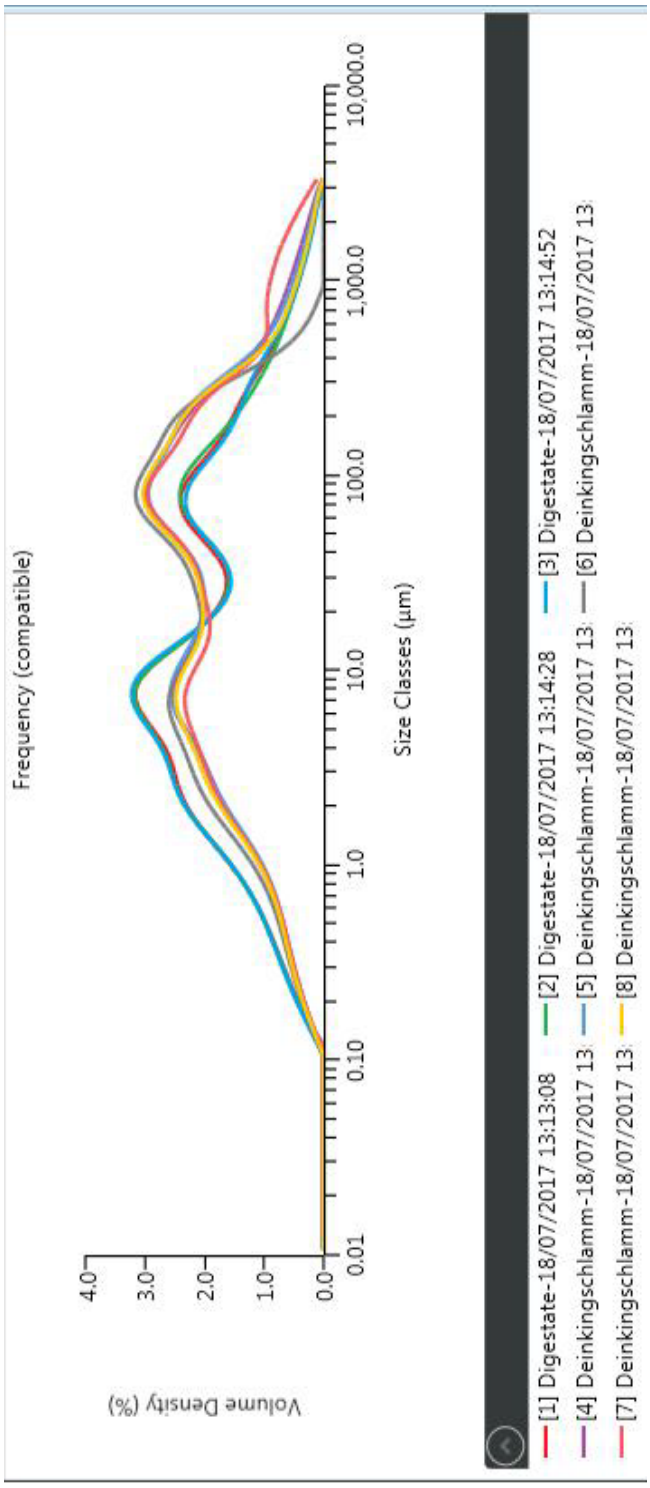

Appendix M.2 X-ray fluorescence analysis of ash of DS

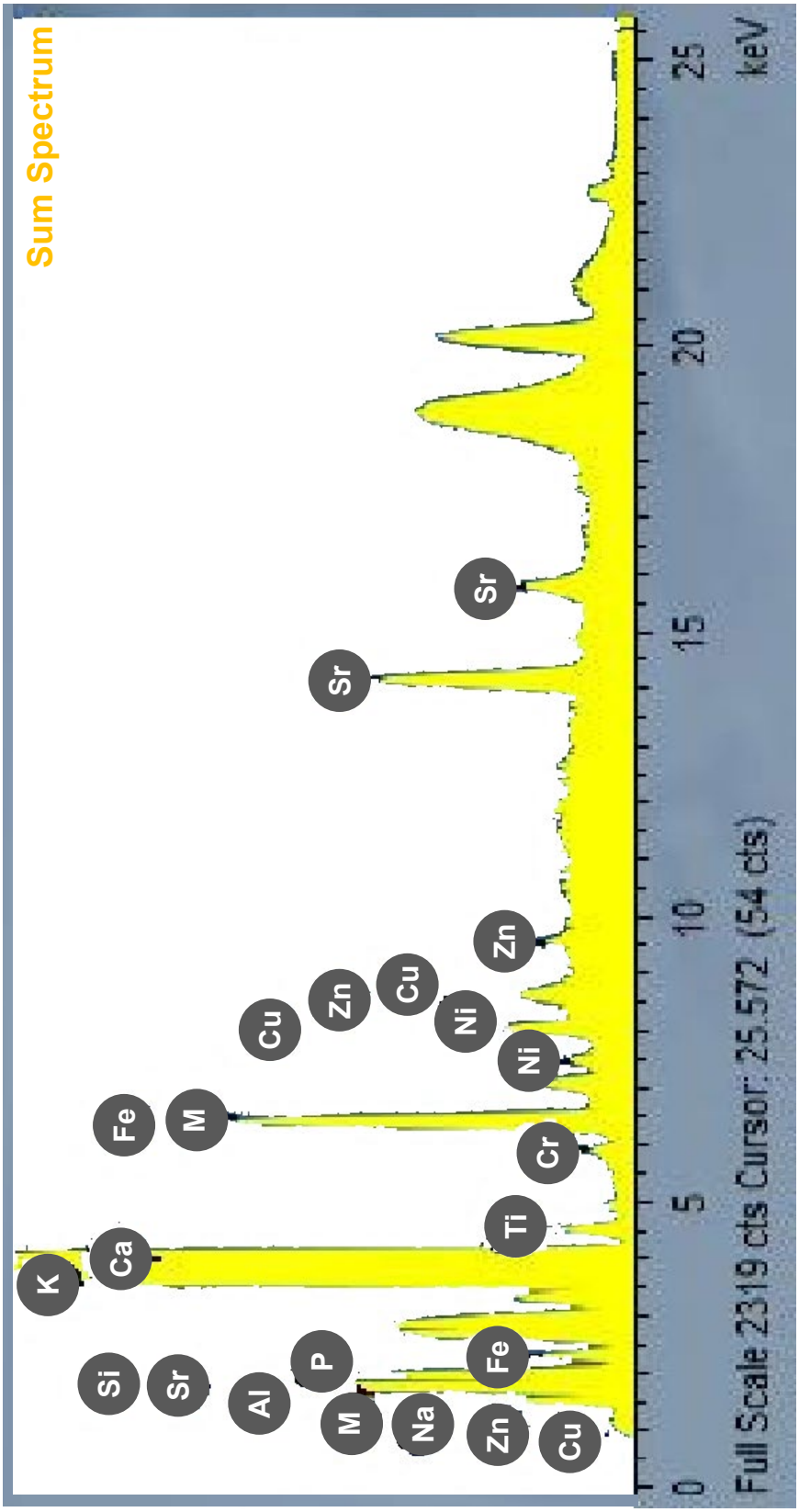

Appendix M.3 X-ray fluorescence analysis of ash of DS-digestate

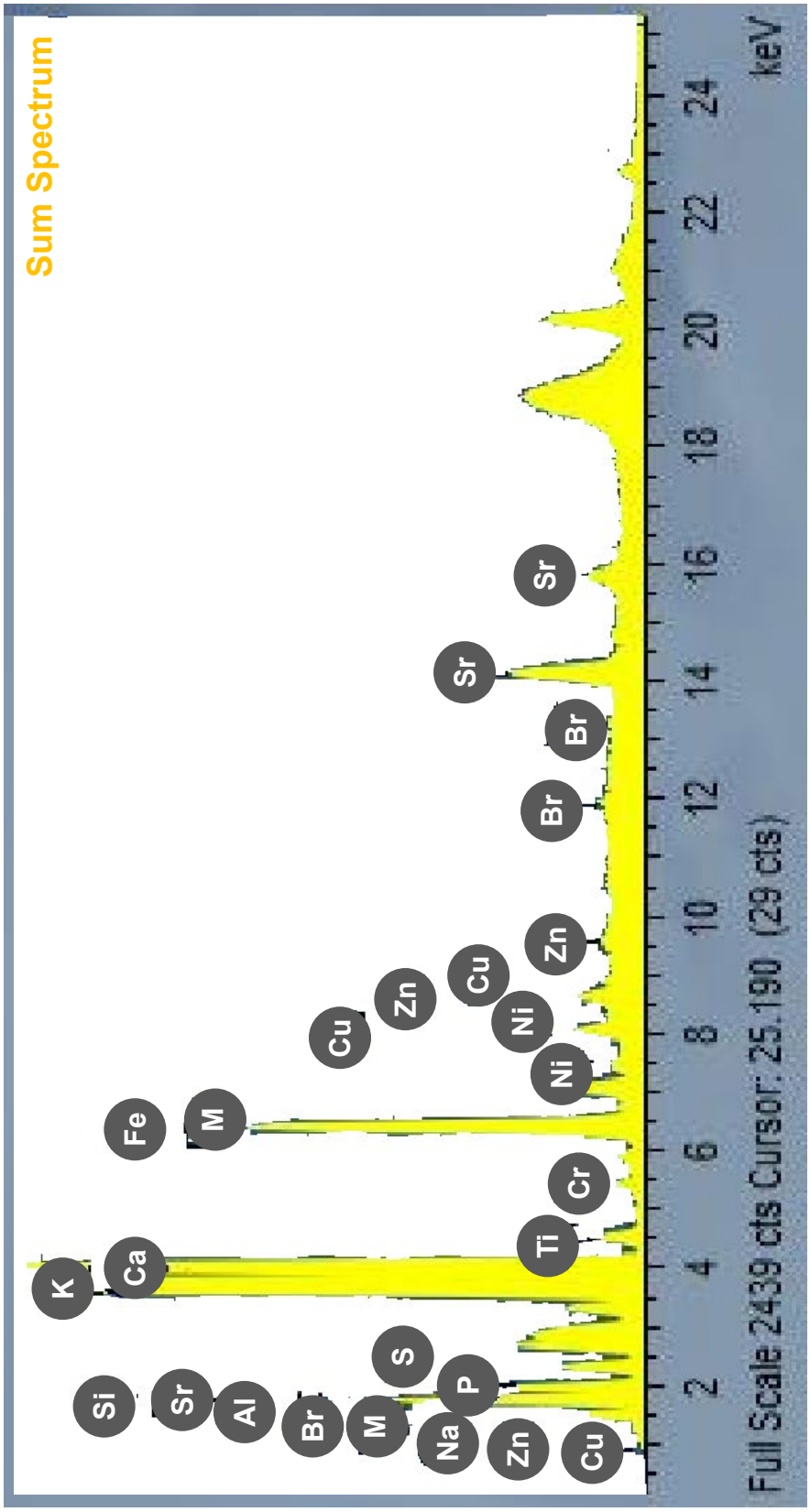

Appendix M.4 Elements present in deinking sludge ash as reported by different authors

Elements	Frias et al.* (DS ash Sample) [% DM]	Pera & Amrouz, 1998* (DS ash Sample 1) [% DM]	Pera & Amrouz, 1998* (DS ash Sample 2) [% DM]
Main elements			
Ca	18.17	10.22	4.68
Si	5.04	10.24	10.19
Al	3.61	5.93	8.68
O	71.70	70.00	73.87
Other elements (non- heavy metals)			
Na	0.10	0.15	0.07
Mg	0.52	2.47	0.72
P	0.04	0.03	0.34
S	0.13	0.00	0.00
K	0.20	0.17	0.58
Other elements (heavy metals)			
Ti	0.17	0.24	0.12
Cr	0.00	0.00	0.00
Mn	0.00	0.00	0.00
Fe	0.32	0.56	0.56
Total	100.0	100.0	99.8
*All values were computed from the oxides reported by authors			

Appendix M.5 Fourier Transform – Infra Red (FT- IR) spectra of ash of DS

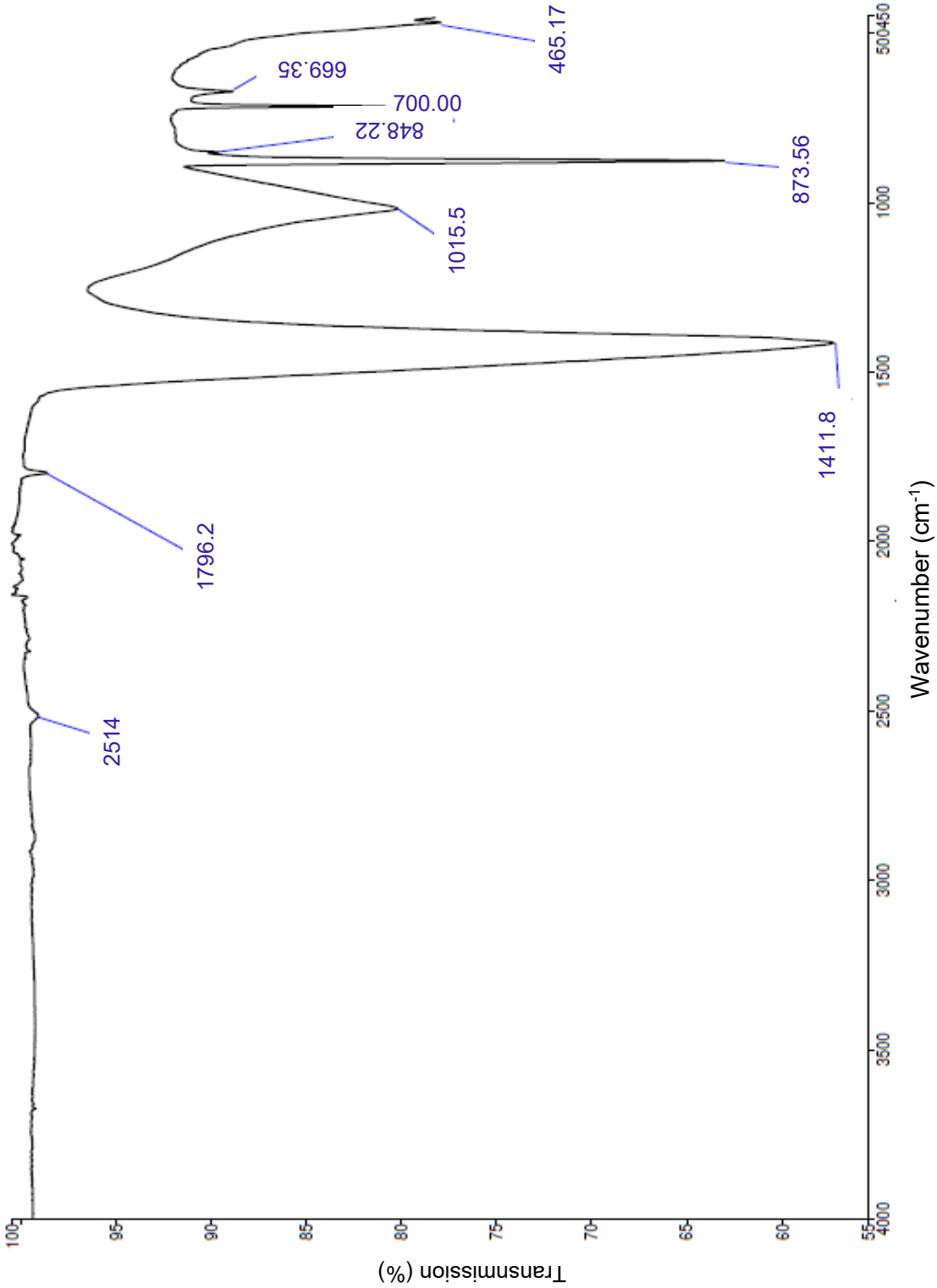

Appendix M.6 Fourier Transform – Infra Red (FT-IR) spectra of ash of DS-digestate

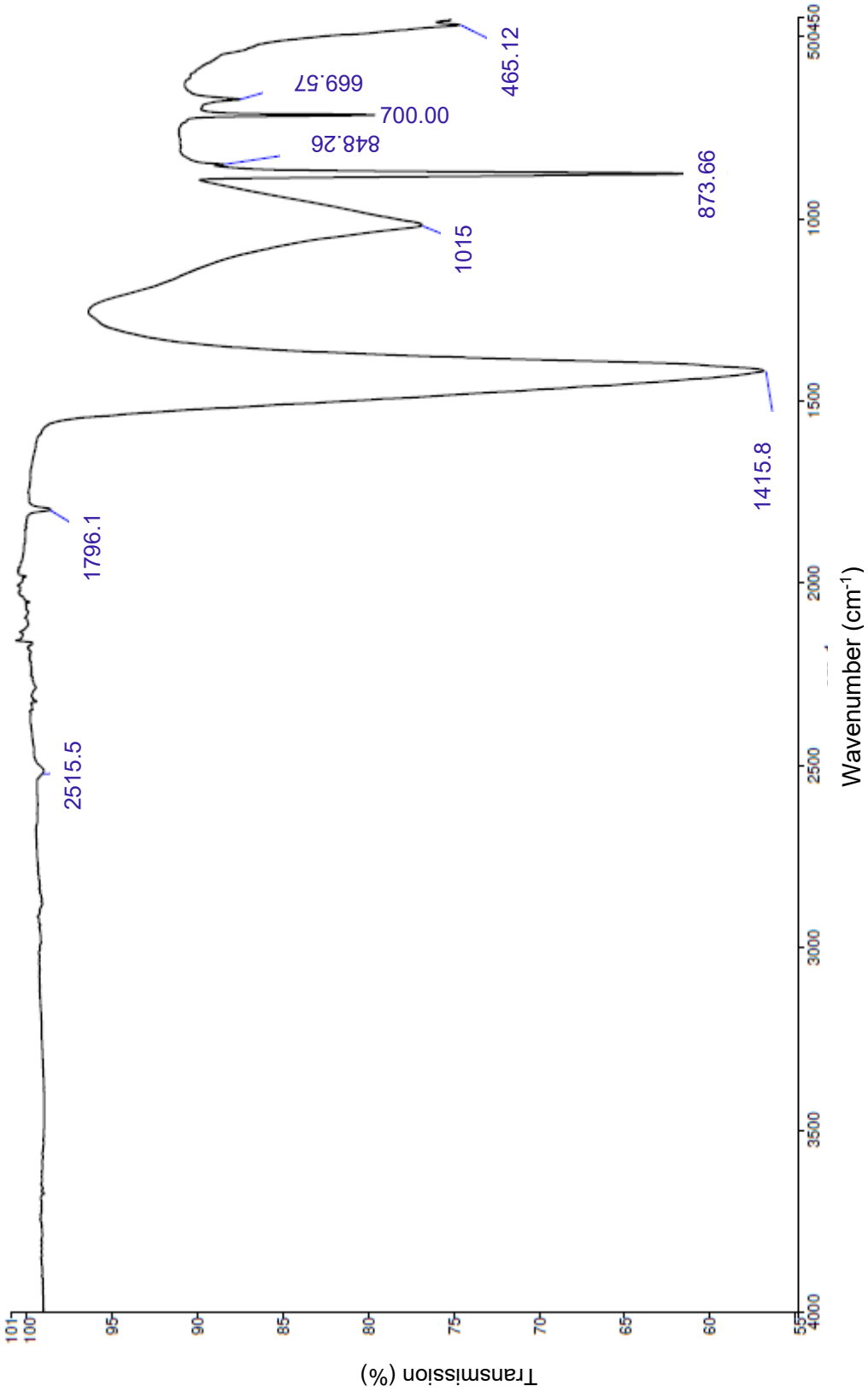

Appendix M.7 X-ray diffraction of ash of DS

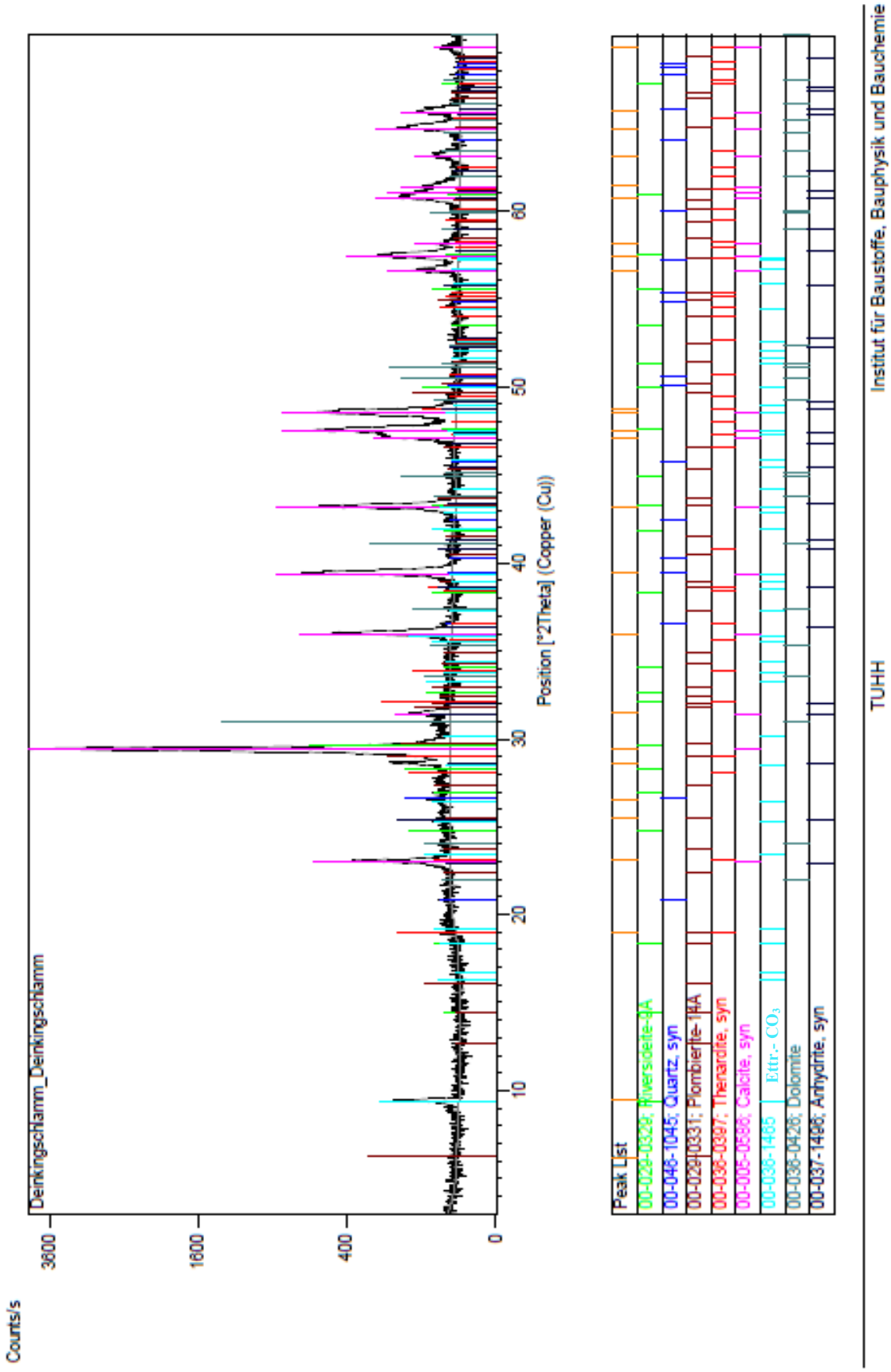

Appendix M.8 X-ray diffraction of ash of DS-digestate

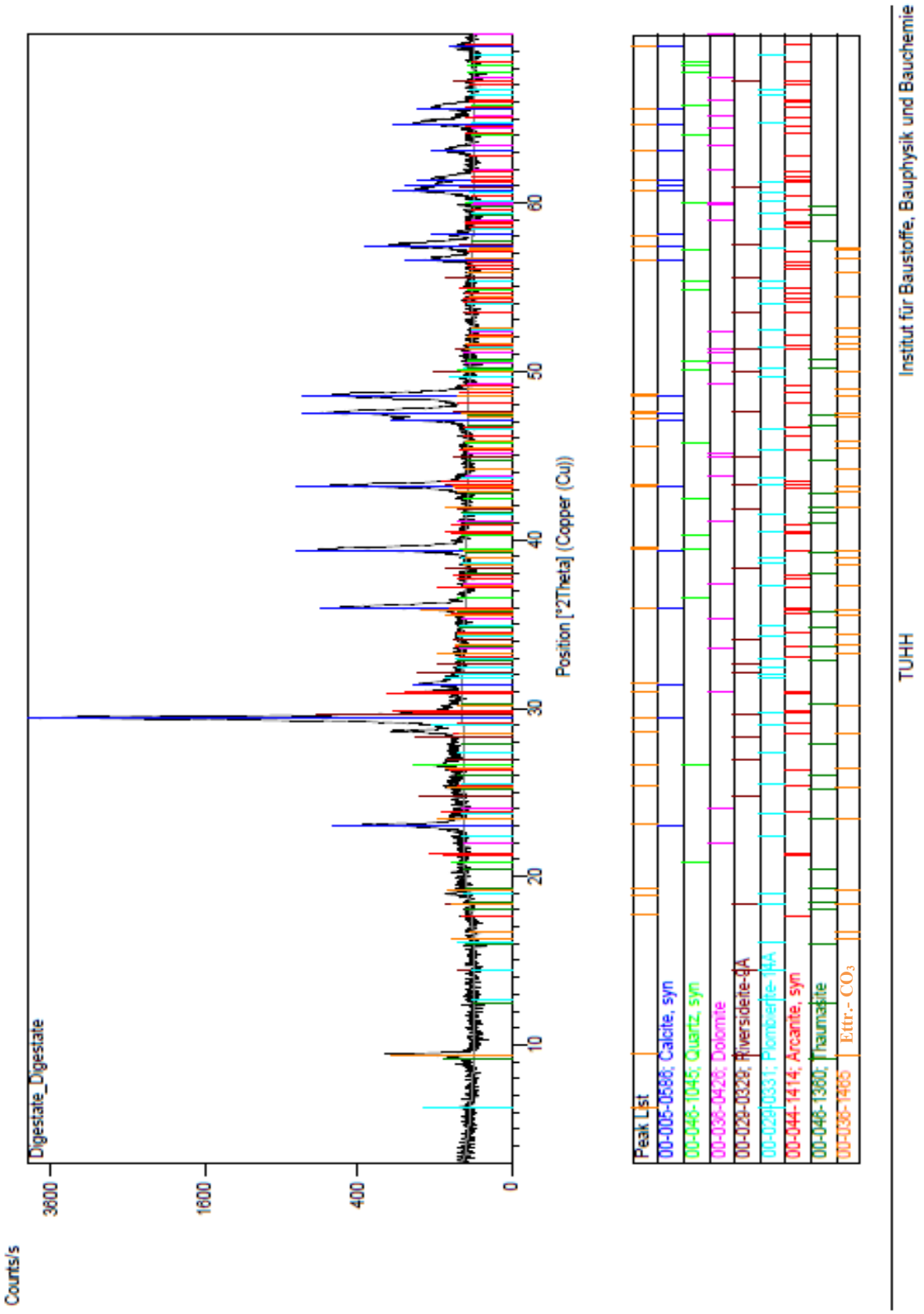

Appendix M.9 Computation of ash contribution to compressive strength lost by partial substitution of cement in mortar prism

Cement mass reduced/ substituted [%]	Compressive strength of reference mortar prism with cement mass reduction [N/mm^2]	Compressive strength of mortar prism with cement mass substituted by ash [N/mm^2]	Compressive strength lost by reference mortar prism due to cement reduction [N/mm^2]	Compressive strength added to mortar prism due to substitution with ash [N/mm^2]	Contribution of ash to compressive strength lost by substitution of cement in mortar prism [%]
DS ash					
0	40.9	-	-	-	-
5	38.9	39.1	2.0	0.16	8.2
15	29.9	33.6	10.9	3.63	33.2
25	21.5	29.5	19.3	8.00	41.4
35	15.6	25.2	25.3	9.64	38.2
DS-digestate ash					
0	40.9	-	-	-	-
5	38.9	39.5	2.0.	0.6	31.1
15	29.9	34.8	10.9	4.9	45.0
25	21.5	31.9	19.3	10.3	53.4
35	15.6	29.5	25.3	13.9	55.0

Appendix M.10 Equations to estimate ash contribution to compressive strength lost by substitution of cement in mortar prism

Compressive strength (N/mm^2) lost by reference mortar prism due to cement reduction ($\sigma_{lost-ref,\ x\,\%}$) = $\sigma_{ref,\ 0\%} - \sigma_{ref,\ x\%}$ Eq M.1

Compressive strength (N/mm^2) added to mortar prism due to substitution with ash ($\sigma_{added-test,\ x\,\%}$) = $\sigma_{test,\ x\%} - \sigma_{ref,\ x\%}$ Eq M.2

Contribution (%) of ash to compressive strength lost by substitution of cement in mortar prism = $\frac{\sigma_{added\text{-}test,\ x\%}}{\sigma_{lost\text{-}ref,\ x\%}} \times 100$ Eq M.3

Where,

$\sigma_{ref,\ 0\%}$ [%] is the compressive strength of reference mortar prism with no cement reduction

$\sigma_{ref,\ x\%}$ [%] is the compressive strength of reference mortar prism with x % cement reduction

$\sigma_{test,\ x\%}$ [%] is the compressive strength of mortar prism with x % cement substitution by ash

Appendix N Combined anaerobic treatment and calcium carbonate recovery of DS

Appendix N.1 Computation of the mass balance of the dry matter content of DS across dewatering units

DS	DM-median [% FM]	Mass of dry matter [kg DM]	Mass of dry matter (addition of recycled stream) [kg DM]
Mass balance across pre-dewatering unit			
Stream 1	3.5	100.0*	100.0
Stream 2	12.7	80.0	80.0
Stream 5	0.9	20.0	20.0
Mass balance across main-dewatering unit			
Stream 3	5.0	100.0	105.0
Stream 4	56.7	90.0	95.0
Stream 6	0.5	10.0	10.0
* taken as the basis for computation Computed using equations Eq N.1 and N.2 as well as the assumptions in section 5.6.1			

$$m_{DM\text{-}input} = m_{DM\text{-}S\text{-}output} + m_{DM\text{-}L\text{-}output} \quad \text{Eq N.1}$$

$$\frac{m_{DM\text{-}input}}{DM_{input}} = \frac{m_{DM\text{-}S\text{-}output}}{DM_{S\text{-}output}} + \frac{m_{DM\text{-}L\text{-}output}}{DM_{L\text{-}output}} \quad \text{Eq N.2}$$

Where,

$m_{DM\text{-}input}$ is mass of dry matter in input stream [kg DM]

$m_{DM\text{-}S\text{-}output}$ is mass of dry matter in solid phase (*Stream 2*) of the output stream [kg DM]

$m_{DM\text{-}S\text{-}output}$ is mass of dry matter in liquid phase (*Stream 5*) of the output stream [kg DM]

DM_{input} is mass of dry matter content of the input stream [% FM]

$DM_{S\text{-}output}$ is mass of dry matter content of the solid phase (*Stream 2*) of the input stream [% FM]

$DM_{L\text{-}output}$ is mass of dry matter content of the liquid phase (*Stream 5*) of the input stream [% FM]

Appendix N.2 Computation of the mass balance of the organic dry matter of DS across dewatering units

DS	Mass of DM of stream[a] [kg DM]	oDM-median [% DM]	oDM [kg oDM]	oDM_rounded [kg oDM]	oDM recalculation to 100% [kg oDM]	oDM (addition of recycled stream) [kg oDM]
Mass balance across pre-dewatering unit						
Stream 1	100	33.3	33.3	32.0[b]	100[c]	100
Stream 2	80	29.5	23.6	24.0	74	74
Stream 5	20	41.0	8.2	8.0	26	26
Mass balance across main-dewatering unit						
Stream 3	100	29.5	29.5	31.0[d]	100[e]	105
Stream 4	90	31.2	28.1	28.0	91	96
Stream 6	10	29.2	2.9	3.0	9	9

a- Taken from Appendix N.1

b & d- Adjusted to get a 100% mass balance

c & e -100 kg DM was taken as the basis for final computation of mass balance

Appendix N.3 Computation of the mass balance of the calcium carbonate content of DS across dewatering units

DS	Mass of DM of stream[a] [kg DM]	$CaCO_3$-median [% DM]	$CaCO_3$ [kg oDM]	$CaCO_3$_rounded [kg oDM]	$CaCO_3$ recalculation to 100% [kg oDM]	$CaCO_3$ (addition of recycled stream) [kg oDM]
Mass balance across pre-dewatering unit						
Stream 1	100	46.2	46.2	49.0[b]	100[c]	100
Stream 2	80	49.3	39.4	39.0	80	80
Stream 5	20	52.2	10.4	10.0	20	20
Mass balance across main-dewatering unit						
Stream 3	100	50.8	50.8	54.0[b]	100[e]	106
Stream 4	90	52.2	47.0	47.0	87	93
Stream 6	10	73.3	7.3	7.0	13	13

a- Taken from Appendix N.1

b & d- Adjusted to get a 100% mass balance

c & e -100 kg DM was taken as the basis for final computation of mass balance

Appendix N.4 Estimation of the annual potentials of deinking sludge generated in Germany by combined anaerobic and calcium carbonate recovery treatments

Potentials \ DS types		Raw DS (*Stream 1*)	Pre-dewatered DS (*Stream 2*)	Main-dewatered DS (*Stream 4*)
DM (Mg/a)		126000[a]	100800[b]	119700[c]
oDM (Mg/a)	Minimum	37296	24797	28249
	Lower quartile	40068	29131	34593
	Median	42084	31248	37346
	Upper quartile	42714	32357	39860
	Maximum	49644	34574	44289
$CaCO_3$ (Mg/a)	Minimum	43218	45662	52189
	Lower quartile	53046	47477	60209
	Median	58212	49694	62483
	Upper quartile	69678	59573	84149
	Maximum	79002	69350	86543
Biogas energy (million MJ/a)	Minimum	247	146	167[d]
	Lower quartile	265	172	204[d]
	Median	279	184	220[d]
	Upper quartile	283	191	235[d]
	Maximum	329	204	261[d]
Biogas energy (million kWh/a)	Minimum	68.6	40.7	46.3[d]
	Lower quartile	73.7	47.8	56.7[d]
	Median	77.4	51.2	61.2[d]
	Upper quartile	78.6	53.1	65.4[d]
	Maximum	91.3	56.7	72.6[d]
Cost of $CaCO_3$ in DS as a supplementary building material (million €/a)	Minimum	1.40	1.48	1.70
	Lower quartile	1.72	1.54	1.96
	Median	1.89	1.62	2.03
	Upper quartile	2.26	1.94	2.73
	Maximum	2.57	2.25	2.81

a-Calculation basis, 126000 Mg of oven-dried DS, which is 42% of the lower bound of the estimated range of DS generated in 2020 (Appendix A.3). 42% was used for a conservative computation as the DS reported by Jung et al. 2014 for the year 2013 in Germany was 42% of the lower bound of DS estimated for 2015.

b-Computed as 80% of Raw DS, c- computed as 95% of Raw DS (Figure 5.35)

d-computed with assumption of same biogas yield with *Stream 2*

The cost of DS and DS-digestate was set at 0.0325 € /Mg. This was computed from 25% of the cost of cement (CEM I 42,5 R) from the average of two different companies (CEMEX, n.d.; Dyckerhoff, n.d.)

Appendix O Optimised design of DS-digestate collection for 100-L Bioreactor

Appendix O.1 Integration of a separate recirculation pump for mixing in the 100-L bioreactor system (similar to comonents of 100-L bioreactors system in Figure 4.4 and Appendix B.6)

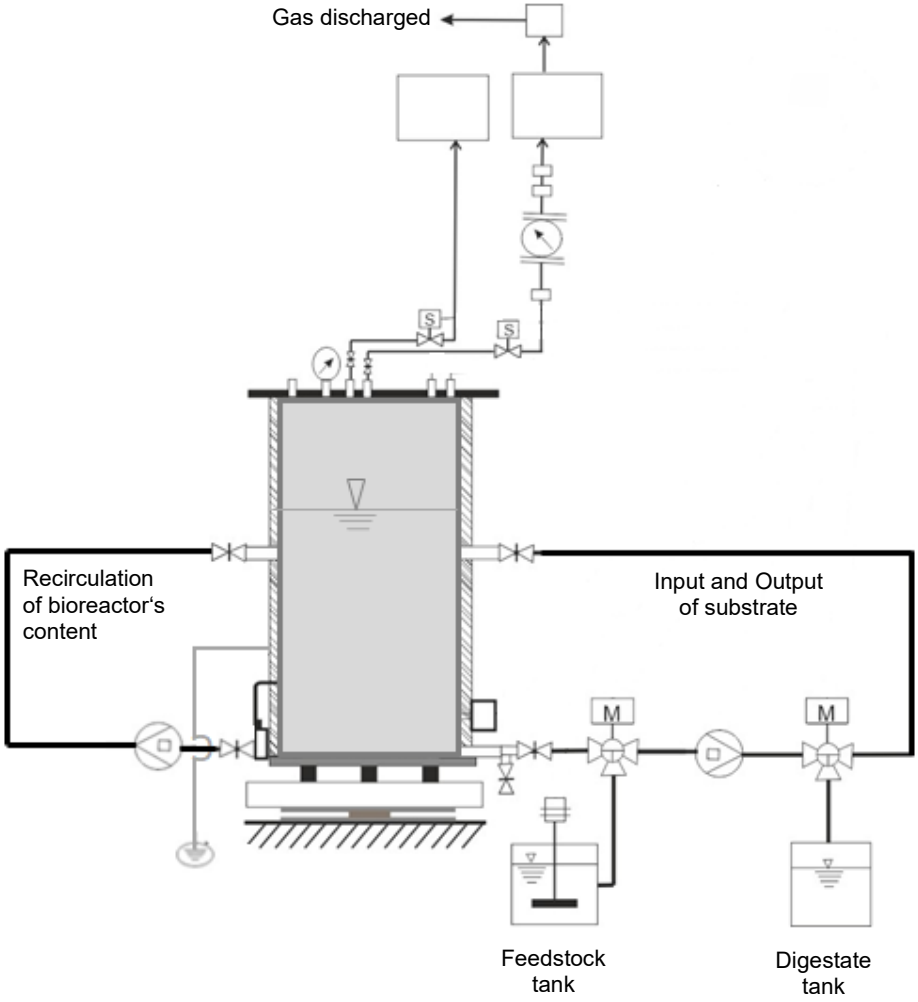

Appendix O.2 Integration of a separate digestate collection system from two different height of bioreactors content in the 100-L bioreactor system (similar to comonents of 100-L bioreactors system in Figure 4.4 and Appendix B.6)